A multifaceted approach to investigate signal transduction at the receptor and post-receptor level focusing on the modulation of the free fatty acid receptor family

Dissertation

zur

Erlangung

des

Doktorgrades (Dr. rer. nat.)

der

Mathematisch-Naturwissenschaftlichen Fakultät

der

Rheinischen Friedrich-Wilhelms-Universität Bonn

vorgelegt von

Manuel Grundmann

aus Aachen

Bonn, 2015

Angefertigt mit Genehmigung der Mathematisch-Naturwissenschaftlichen Fakultät der Rheinischen Friedrich-Wilhelms-Universität Bonn.

Die vorliegende Arbeit wurde in der Zeit von Oktober 2011 bis Juni 2015 am Institut für Pharmazeutische Biologie der Rheinischen Friedrich-Wilhelms-Universität Bonn unter der Leitung von Prof. Dr. Evi Kostenis angefertigt.

1. Gutachter: Prof. Dr. Evi Kostenis

2. Gutachter: Prof. Dr. Klaus Mohr

Tag der Promotion: 27.10.2015

Erscheinungsjahr: 2015

Meinen Eltern

Table of contents

Introduction

Signal transduction - Overview

In physics, the term “signal transduction” means the conversion of energy or information from one form into another and was already used long before it was introduced in biology. The biochemist Martin Rodbell was the first who coined the term “signal transduction” 1980 in a biological sense. He described the principles how cells can regulate their metabolism with GTP and GTP-binding proteins[1].

Signal transduction in biological systems involves a vast number of different molecules and structures. It is therefore helpful to subdivide the signaling complex into larger groups. Hormones are prominent examples of *first messenger* molecules that are characterized by early occurrence in the stream of biological information. In the course of evolution, some species adopted differently to the environment than others, leading to huge biological diversity that might explain interspecies variances in structure, expression levels, constitution and function of signal transduction proteins. The more the need for complex regulation, the more complex the interplay between information and signals, the more diverse is the capacity to generate and process signals differently. One way to fine-tune biological response is the presence of various receptors for the same ligand. Interestingly, although it seems a general rule that the receptors evolved later in the evolution than their ligands (e.g. *first messenger*), some invertebrates do express thyroid and vitamin D receptors, which seemingly undertake highly specialized tasks, but do not express sex or adrenalin receptors, both processing ancient biological stimuli[2,3].

First and second messenger

First messenger are (mostly extracellular) ligands, such as hormones, neurotransmitters, cytokines, lymphokines, growth factors or chemoattractants. Notably, there is considerable functional overlap within types of *first messenger*, demonstrating the evolutionary evolved versatility of organisms and the interdependency within their signaling network structures to code and decode one signal with different informational content[4]. Most of the *first messenger* act from the aqueous extracellular milieu on surface receptors, which process and modulate the signal at this level because biomembranes are semipermeable barriers that interdict the crossing of many *first messenger* due to their hydrophilic structure. But there are also hormones or other *first messenger* that act from intracellular compartments (at receptors or other interaction partners), mainly because they are lipophilic enough to pass the cell membrane such as progesterone and other steroid hormones[5]. However, it is becoming increasingly clear that active transportation of ligands provides an

opportunity to bring even hydrophilic compounds across lipophilic membranes[6]. Thus, considerations about membrane permeability solely based on physicochemical compound parameter fall short.

Transduction of one point to another (be it temporally or spatially in nature) involves a transducer. A possibility that is widely used in biological systems is the concept of receptors. Those signaling proteins process one form of signal (*first messenger*) into other forms of signals (*second messenger). Second messenger* in turn are signal transduction molecules, which carry on the information to further signaling partners, triggering distinct signaling pathways that finally elicit a cellular phenotype[7]. Main devices by which the binding of ligands is converted into a cellular consequence are clusters of phosphorylation/dephosphorylation proteins[8,9]. Prominent *second messenger* are the cyclic nucleotides of adenosine monophosphate and guanosine monophosphate, cAMP and cGMP, respectively, but also inostitolphosphates (e.g. IP3), calcium ions, nitric monoxide or G proteins, such as Ras. These examples make clear that *second messenger* do not share a common structural or physical feature. Furthermore, as the nature of the *first messenger* does not determine the nature of the *second messenger*, the stream of information is rather complexly regulated and subject to extensive modulation.

Among the *second messenger*, the cyclic nucleotides will be described in more detail because members of the family of cyclic nucleotides and G proteins are the key signaling components studied in chapter 6 and chapter 7 of this thesis.

Cyclic adenosine monophosphate (cAMP) acts as a mediator in all pro- and eukaryotic cells[10]. The cell can respond rapidly to a *first messenger* stimulus with changes of intracellular levels of cAMP, which requires the presence of a balanced system of synthesis and breakdown[11]. Prerequisites of *second messenger* function are therefore their specific generation and signal termination but most importantly their biological function. cAMP is generated by membrane-associated (mAC) or soluble forms (sAC) of the enzyme adenylyl cyclase that converts ATP into cyclic AMP. In turn, it is continuously degraded by phosphodiesterases (PDEs), where there are eight isoforms in mammals, which are all regulated by G proteins or calcium ions[12]. In mammals 21 genes encode for PDEs[13], which are expressed throughout the human body with different tissue distribution and different specificity for certain cyclic nucleotides. The balanced process of generation and termination is fine-tuned by other input signals that change the cellular activation state.

The *second messenger* cAMP mediates a variety of cell responses, such as thyroid hormone synthesis, cortisol synthesis, progesterone secretion, glycogen breakdown, bone resorption, increase in heart rate and force of heart contraction, water resorption and triglyceride breakdown[14]. These functions illustrate the variability of signal transduction through the same stimulus that is differently interpreted depending on the cellular setting, such as tissue expression, cellular equipment, metabolic state, temporal rhythm, etc. Most biological effects of cAMP are mediated by the protein

kinase A (PKA), a multienzyme complex consisting of two regulatory and two catalytic subunits. Upon cAMP binding to the regulatory subunits the catalytic subunits dissociate and activate, i.e. phosphorylate, specific target proteins[15]. Interestingly, PKA also phosphorylates and thereby activates adjacent phosphodiesterases, which in turn lead to a rapid decrease of cAMP levels[14]. This provide a means to tightly control cAMP effects in the greater context of signal generation and termination.

Cyclic guanosine monophosphate (cGMP) is a likewise physiologically relevant *second messenger*. It is involved in the process of vision in the retina of vertebrates, the vasodilatation of blood vessels and bronchodilation. cGMP levels are regulated by modules similar to cAMP, such as phosphodiesterases and specific nucleotidyl cyclases, in this case guanylyl cyclases[16]. The pharmacological targeting of signaling units that modulate cAMP and cGMP levels is already clinically exploited. Inhibitors of phosphodiesterase type V are used as drugs against pulmonary arterial hypertension (PAH) and erectile dysfunction, while PDE-IV inhibitors are integrated in the treatment of chronic obstructive pulmonary disease (COPD), whereas stimulators of the soluble guanylyl cyclase (sGC) are used to treat chronic thromboembolic pulmonary hypertension (CTEPH) as well as pulmonary arterial hypertension (PAH). Chapter 6 of this thesis focusses on the exploration of non-canonical cyclic nucleotides, such as cyclic cytidine monophosphate (cCMP) and cyclic uridine monophosphate (cUMP). These molecules are far less studied than cAMP and cGMP but nevertheless fulfill all criteria of *second messenger* and can be considered to undertake a significant job in the regulation of the cellular state[17].

G proteins

Upstream of the *second messenger* are other cellular signaling proteins. Surface receptors were already mentioned but in between we often find so called G proteins that function as molecular switches to control and distribute signaling input not only further downstream but also upstream of the G protein level thus establishing a bidirectional flow of information. G proteins are guanosine triphosphate (GTP)-binding proteins and exist in two states: the active GTP-bound state and the inactive guanosine diphosphate (GDP)-bound state[18–20]. GTPase activity of the G protein degrades GTP to GDP and thus turns the G protein in its inactive state again. Because of this inherent enzyme activity, G proteins also belong to the class of GTPases. Two groups of G proteins can be distinguished: the large or heterotrimeric G proteins, which play a crucial role in the signal transduction triggered by G protein coupled receptors (GPCRs), and the small monomeric G proteins, related to the protein products of the Ras proto-oncogenes. Small G proteins function as regulators of cell motility and cell division and process multiple signaling inputs[3,14].

Heterotrimeric G proteins

Heterotrimeric G proteins consist of three subunits: α, β and γ. The β subunit is tightly associated with the γ subunits so that the βγ subunit behave as a single functional entity[18–22]. The nucleotide binding pocket is located within the α subunits that contacts the β subunit, involving two highly conserved regions, switch I and switch II, as well as its N-terminal helix[18,19]. The whole heterotrimeric protein is anchored to the plasma membrane via lipid modifications at the G protein, one at the N-terminal end of the α subunit and one at the C-terminal end of the γ subunit[20,23] (**Figure 1**).

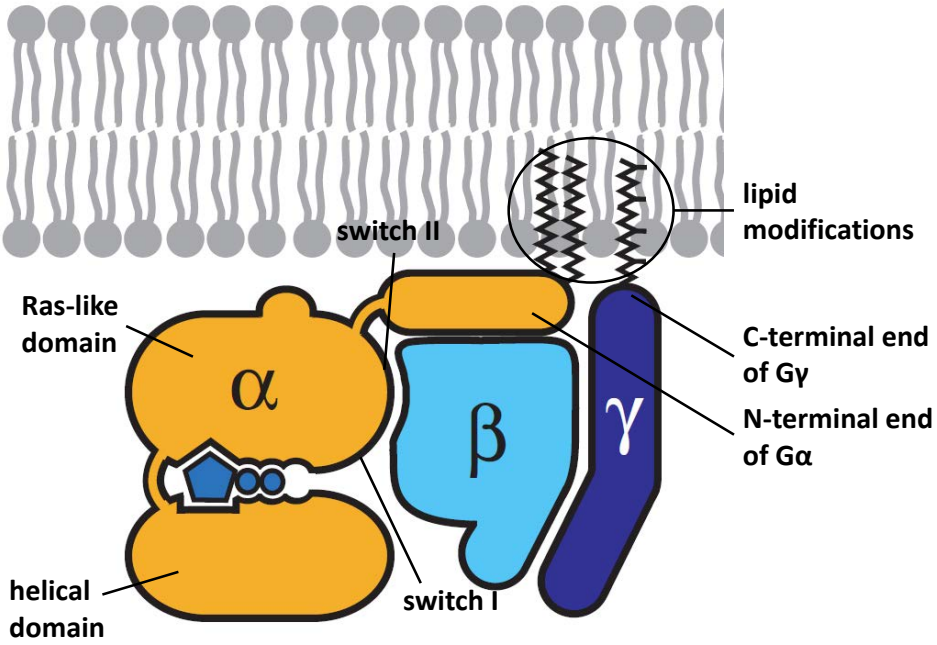

Figure 1 *Schematic of a heterotrimeric G protein consisting of the α- (orange) and the βγ-subunit (blue) and anchored to the plasma membrane by lipid modifications. Key interaction epitopes between α and βγ-subunit are labelled as switch I and II in the Ras-like domain of the α subunit. Depicted is the inactive, GDP-bound, conformation. The nucleotide binding site is located between the Ras-like and the helical domain within the α-subunit. Modified after [24].*

The cycle of G protein activation/deactivation starts and ends in the GDP-bound state. After interaction with a guanine nucleotide-exchange factor (GEF), which can be a GPCR, GDP is released and GTP binds to the α subunit, mainly due to the intracellular excess of GTP compared to GDP[19]. The GDP/GTP exchange is driven by a conformational change within the α subunit[25]. In the GTP-bound, active conformation, the G protein has lower affinity for the interaction with and dissociates from the GEF. It is commonly acknowledged, that upon activation, the α subunit and the βγ subunit dissociate and each are capable to subsequently induce signaling events[26]. GTP is then hydrolyzed to GDP, turning the G protein into the inactive state again, allowing the re-association of α and βγ subunit to the heterotrimeric G protein. The deactivation step is accelerated by GTPase-activating proteins (GAPs) like regulators of G protein signaling (RGS)[27] (**Figure 2**).

G proteins are monostable switches, that means their activation is kinetically regulated, positively by the rate of GDP dissociation and negatively by the rate of GTP hydrolysis. The activation state can thus be approximated by the ratio of the rate constant for GDP dissociation (k_{diss}) and the rate constant for GTP hydrolysis (K_{cat}). Both K_{diss} and K_{cat} can be modulated by proteins that interact with the α subunit[3]. These modulations are allosteric in nature and are already described as the interaction with GEFs, GAPs or RGS proteins[27].

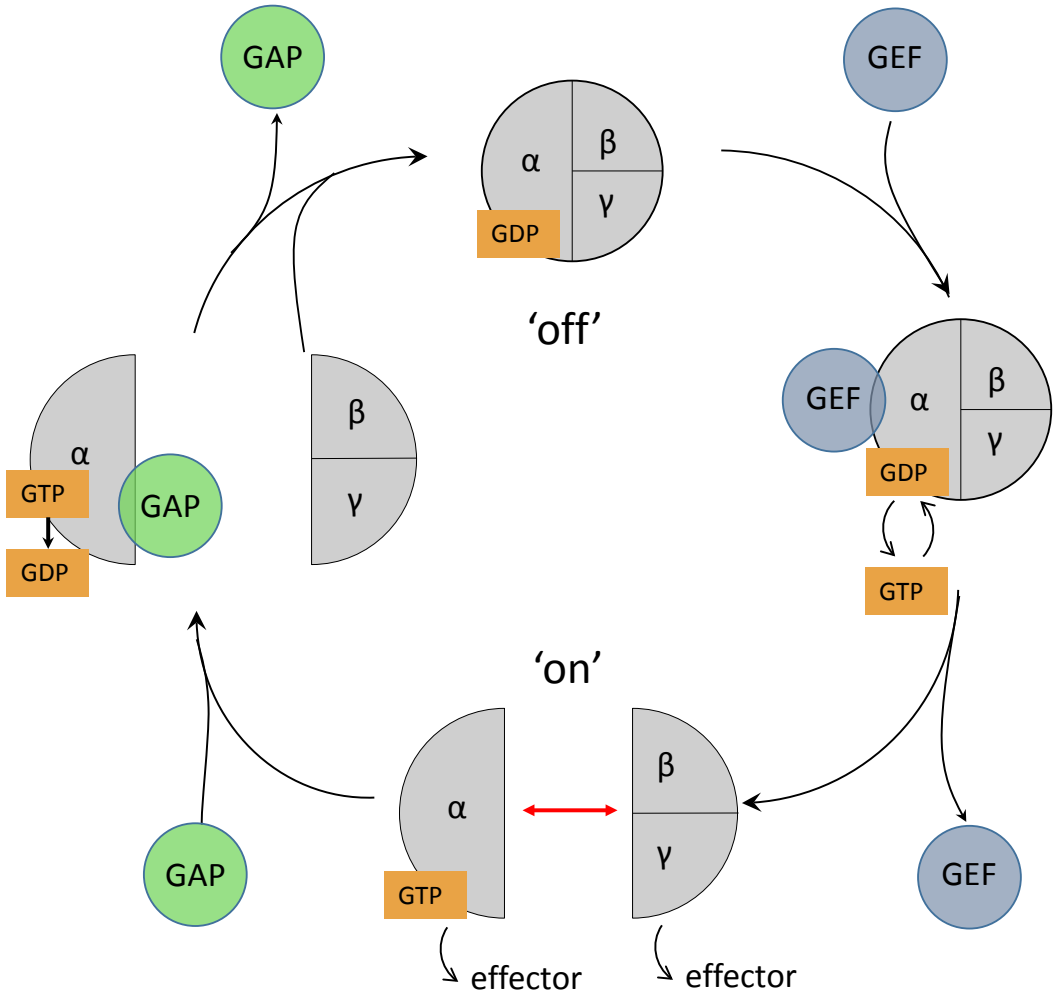

Figure 2 *The G protein activation cycle. In the 'off' state, the G protein rests in the GDP-bound form. Upon activation, e.g. by the interaction with a guanine nucleotide exchange factor (GEF), a conformational change within the G protein induces the release of GDP and the binding of GTP to the α-subunit. This triggers the dissociation of α- and βγ-subunit, both of which in turn can interact with signaling effectors. GTPase-activating proteins (GAPs) enhance the intrinsic GTPase activity of the α-subunit and thus allow the βγ-subunit to re-associate with the GDP-bound α-subunit to form an inactive heterotrimeric G protein again.*

Heterotrimeric G proteins are classified by their α subunits[28]. There are 16 genes encoding for α subunits. Some of them are only found in a specific cell type, such as α_t, α_{olf}, α_{gut} in sensory cells but most are ubiquitously expressed, although α_o shows high levels in neuronal tissue. There are four main classes of Gα subunits: α_s, α_i, α_q and $\alpha_{12/13}$[29]. $G\alpha_s$ proteins stimulate membrane-bound adenylyl

cyclases and thereby increase intracellular cAMP levels. In contrast, $G\alpha_i$ proteins inhibit the adenylyl cyclase leading to a reduction of cAMP level. $G\alpha_q$ subunits activate the phospholipase-Cβ pathway[28,30]. However, not all Gα subunits regulate *second messenger* levels in a narrow sense. $G\alpha_{12/13}$ for example activate a RhoGEF protein that modulates the Ras-related GTPase Rho and thus regulate cell morphology[30].

Five subtypes of β subunits and 12 subtypes of γ subunits expand the variability of possible heterotrimeric G protein assemblies, although not all possible combinations exist in nature[21,31]. It could be shown that the identity of the βγ dimer contributes to the G protein coupling of individual receptors[32–35]. An important modification within the βγ dimer is the attachment of geranylgeranyl or farnesyl groups to the C-terminus of the γ subunit. This extension tethers the γ subunits (and with them the associated β subunits) to the membrane[36]. Furthermore, beside Gα subunits, also the βγ subunits can induce signaling. The effect of Acetylcholine on cardiac output, for example, relies of the opening of K^+ channels by interaction with βγ dimers. Activation of phospholipase A2[37] and some β-isoforms of phospholipase C[38] were also reported to be mediated by an interaction with βγ subunits. In addition, βγ subunits play roles in the localization, coupling and deactivation of α subunits, the regulation of the affinity of the receptors for their activating ligands and are required for certain α subunits to undergo covalent modification by PTX[21,39]. βγ subunits also reduce the tendency of GDP to dissociate from α subunits and thereby stabilize the inactive state[21,39]. **Table 1** summarizes key aspects of heterotrimeric G proteins.

Table 1 *Overview of mammalian heterotrimeric G proteins*

Subunit		Expression	Effects
α_s	α_s	ubiquitous	adenylate cyclase ↑
	α_{olf}	olfactory neurons	
$\alpha_{i/o}$	$\alpha_{i1\text{-}i3}$	ubiquitous	adenylate cyclase ↓
	$\alpha_{o1/2}$	neurons	
	$\alpha_{t1/2}$	photoreceptors	cGMP-PDE ↑
	α_z	neurons, platelets	K^+-channel ↓
	α_{gust}	taste buds	
$\alpha_{q/11}$	$\alpha_{q/11}$	ubiquitous	PLC-β ↑
	$\alpha_{14/15/16}$	hematopoietic cells	
$\alpha_{12/13}$	$\alpha_{12/13}$	ubiquitous	RhoGEF ↕
β/γ	$\beta_{1\text{-}5}$	most cells	PLC-β↑,GIRK-channels↑, Scr↑, Ca^{2+}-channels↑, …
	$\gamma_{1\text{-}12}$	most cells	

Structural considerations on G proteins

The N-terminal sequence of Gα proteins is the site of interaction with the βγ subunits and also subject of myristic acid attachment in the $G\alpha_{i/o}$ protein family[40,41]. The α subunit consists of two independent domains. Because of close similarity to the monomeric GTPase Ras, one is named Ras-like domain, wherein the GDP/GTP exchange takes place. It provides a binding surface for interaction with various interacting proteins, such as the βγ subunit, RGS proteins, receptors and effectors. The second domain is a six-helix bundle and can only be found in heterotrimeric G proteins but not in monomeric G proteins[3].

In contrast to the conserved Ras-like domain, the helical domain is more variable across the α subunits. It covers the GTP-binding pocket and is involved in the nucleotide binding as well as in GTP hydrolysis[20]. Three flexible loops (switch I, II and III) within the Ras-like domain can be found that undergo significant conformational changes upon switching from the GDP-bound to the GTP-bound state[25,42–44]. It is currently not clear, which structural changes within the G protein dictate GDP release but two models are discussed[20] and both imply a significant role of the Gβγ subunit in the process of G protein activation (**Figure 3**). In the first (*lever arm model*), the receptor uses the N-terminal helix of Gα as a lever arm to pull Gβγ away from Gα, enabling GDP release. In the second (*gear shift model*), the receptor uses the N-terminal helix of Gα to force Gβγ into Gα, thereby allowing the N-terminus of Gγ to engage the helical domain of Gα, causing a gap between helical and Ras-like domain and subsequently the GPD exit. After GDP release, a high-affinity state between the empty-pocket conformation of Gα and an active GEF (e.g. receptor) conformation occurs. This state is only intermediate in intact cells since high amounts of guanine nucleotides allow for quick entrance of GTP into the empty pocket and thus induce a conformational change that leads to dissociation of the α subunit from the receptor protein as well as from the βγ subunit[45,46].

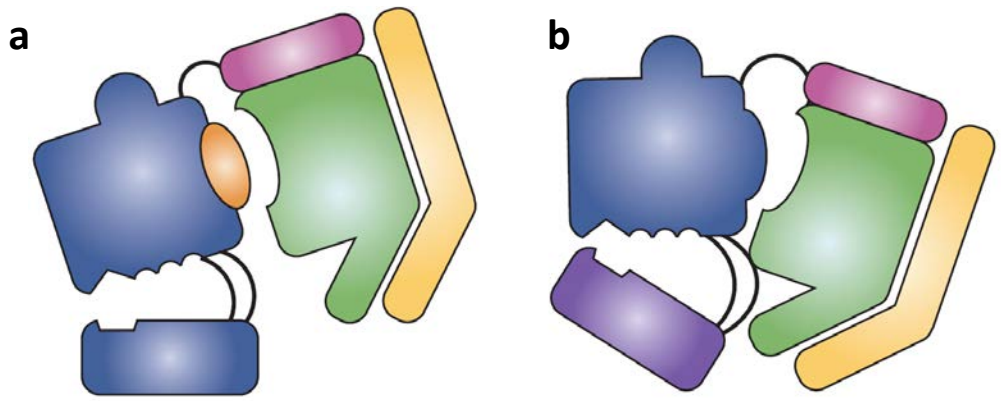

Figure 3 *Proposed model of G protein activation. a) In the lever-arm model, the βγ-subunit (green/yellow) is pulled away from the α-subunit (blue), prying switch II (orange) apart from the nucleotide-binding pocket, leading to GDP release. b) In the gear-shift model, the receptor pushes the βγ-subunit closer to the α helical domain (purple), resulting in a reorientation of the Ras-like and helical domain, which causes the GDP exit. Modified after [20].*

The C-terminal end of Gα subunits dictates the specificity of interaction with the receptor. This is also the site of two important Gα subunit modifications: a) PTX, a toxin from the bacterium *Bordetella pertussis*, ADP-ribosylates a cysteine four residues from the C-terminal end. This modification uncouples the G protein from the receptor, thus freezing the G protein it its GDP-bound state[47,48]. PTX selectively targets the $G\alpha_{i/o}$ protein subfamily with the exception of $G\alpha_z$. PTX emerged as an invaluable tool to dissect G protein signaling. b) Another ADP-ribosylating toxin is produced by the bacterium *Vibrio cholerae* (Cholera toxin, CTX), which targets an arginine residues (R201) situated in close proximity to the γ-phosphate of the bound GTP. As a result of this modification, the G protein turns GTPase deficient and thus remains in an active conformation. Despite the selectivity for $G\alpha_s$ proteins, the use of CTX is limited because it activates rather than inhibits the respective G proteins. Nevertheless, it is used to overstimulate $G\alpha_s$ mediated pathways with the result that no further activation can be detected. Thus, CTX silences $G\alpha_s$ signaling indirectly.

Monomeric G proteins

Monomeric G proteins are also named small GTPases since they bind and hydrolyze GTP like the α subunits of heterotrimeric G proteins. The most well-known members are the Ras proteins, which were discovered as oncogene products. Mutations in the genes encoding Ras proteins frequently lead to the phenotype of cancer. Thus, Ras proteins are products of proto-oncogenes. This also underlines the importance of monomeric G proteins in the regulation of cell proliferation and differentiation[49–52]. Subgroups of the Ras superfamily are Rho, Rab, Ran, Arf and Kir/Rem/Rad. Like in heterotrimeric G proteins also in monomeric GTPases, two switch regions change their conformation in the process of GDP/GTP exchange and are moreover involved in the interaction with effector or regulator molecules[3].

Receptors

Receptors function as mediators between two forms of signals and act like microprocessors decoding and encoding information. The manifestation as a receptor can be multifaceted (see **Table 1**). They can form an integral part of the cellular membrane, such as the group of G protein coupled receptors (GPCRs) (e.g. β-adrenergic receptors) or ligand activated ion channels (e.g. nicotinic acetylcholine receptors). Receptors can be endowed with an intrinsic tyrosine kinase activity (e.g. epidermal growth factor receptors) or with intrinsic serine/threonine kinase activity (e.g. transforming growth factor receptors) and finally those that interact with cytosolic tyrosine kinases or those who are linked to tyrosine kinases (e.g. cytokine receptors). Among the cytokine receptors there are also soluble receptors but they do not constitute the only receptor family that can be found apart from membranes. Nuclear receptors are localized in the cytosol as well and comprise a superfamily of

receptors that are targets of steroid hormones, thyroid hormones, retinoids, vitamin D and other lipids. From the aforementioned receptor types, G protein-coupled receptors constitute by far the largest class of drug targets[53]. They can be found throughout the body of most living forms on earth and play, directly or indirectly, vital roles in nearly every biological process. Therefore, this receptor class will now be described in more detail.

Table 2 *Overview of different receptor classes*

Class	Examples
G protein-couples receptors	β-adrenergic receptors, muscarinic Acetylcholine receptors, Free fatty acid receptors, …
Ionotropic receptors	nicotinic Acetylcholine receptors, $GABA_A$ receptor, NMDA receptors, P2X receptors, …
Kinase-linked receptors	EGFR, Insulin receptors, VEGF receptors, …
Nuclear receptors	PPARγ receptors, Thyroid hormone receptor, Vitamin D receptor, Retinoid X receptor, …

G protein-coupled receptors

G protein-coupled receptors can be divided into five main classes[54,55]. i) the Rhodopsin family (class A), ii) the Secretin family (class B), iii) the Glutamate and GABA family (class C), iv) the frizzled class and v) the adhesion family receptors. They all share a common structural feature, i.e. a single peptide chain that traverses the cell membrane seven times, with the N-terminus projected to the outside and the C-terminus to the cytosolic side[56,57]. That is why G protein-coupled receptors are also named 7TM (7 transmembrane) receptors[58]. Three extracellular (ECLs) and three intracellular loops (ICLs) connect the seven α helices that span the membrane. Most but not all GPCRs activate intracellular G proteins. Common structural and functional features of 7TM receptors in all domains of life suggest a common ancestor, i.e. all 7TM receptors are structurally homologous[59]. With regard to substantial functional and structural differences between each GPCR family, the similarity might arise from convergent rather than divergent evolution. In the human genome there are approximately 800 genes encoding for GPCRs, making up 2 % of the whole human genome and representing the largest group of transmembrane proteins[54,55]. The Rhodopsin family is the largest subfamily with 701 members, of which 460 are olfactory and 241 are non-olfactory[54].

Structural elements of GPCRs

GPCRs can be divided into an extracellular part, consisting of the N-terminus and the three extracellular loops (ECL1-ECL3), a transmembrane (TM) region, consisting of seven α helices (TM1-TM7) and an intracellular part, consisting of three intracellular loops (ICL1-ICL3), an amphipathic helix (H8) and the C-terminus[56,57] (**Figure 4**).

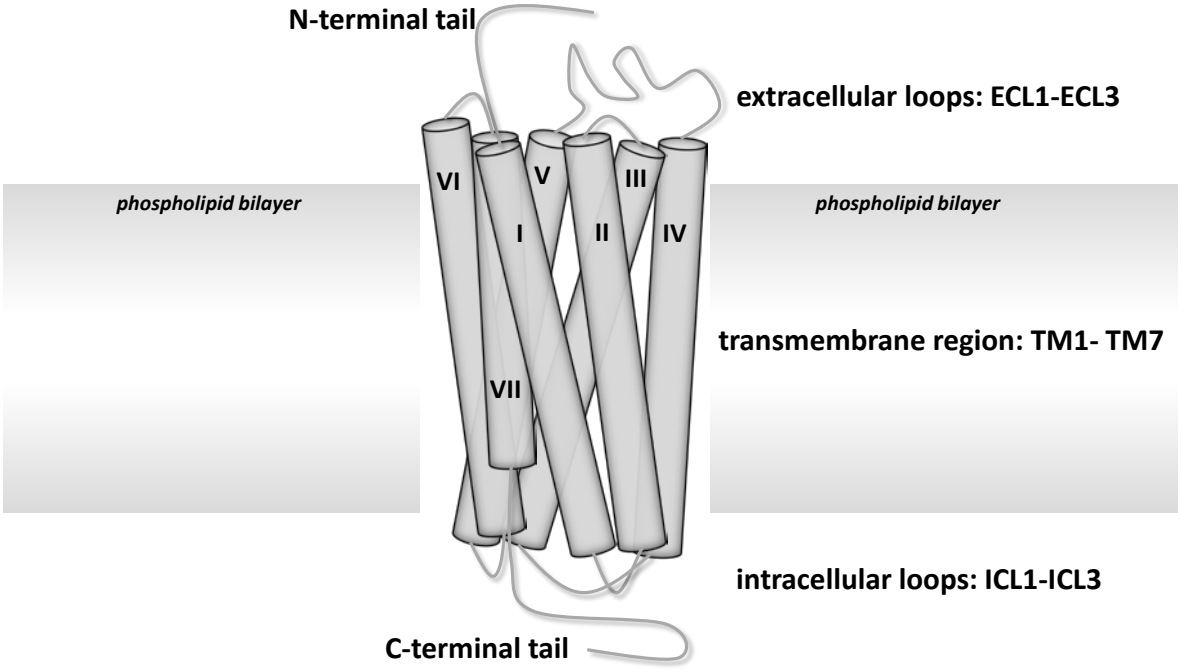

Figure 4 *Structural features common to all class A GPCRs. Seven α helices (TM1-7) spanning the cell membrane constitute the transmembrane region, in which most orthosteric ligands are assumed to bind. The N-terminus of the protein and three extracellular loops (ECL1-3) connecting the transmembrane helices build the outer surface of the receptor, in which many allosteric ligands are expected to bind. The C-terminal tail and three intracellular loops (ICL1-3) form the inner surface and potential binding sites for intracellular signaling molecules, such as G proteins or receptor kinases.*

From crystal structures it is known, that there are two types of extracellular regions. Those who occlude the ligand-binding pocket (like in Rhodopsin[60] or in the sphingosine-1-phosphate receptor[61]) and those who leave the ligand-binding pocket water-accessible. Strikingly, both receptors that show occluded ligand binding-pockets are targeted by hydrophobic ligands that enter the receptor from a transmembrane region of the receptors[61–63], which was also shown for a hydrophobic ligand at the free fatty acid receptor FFA1 by crystallization and subsequent X-ray analysis[64] and discussed for further lipid GPCRs[65–68]. Mainly ECL2 dictates the ligand entry for class A GPCRs and can function as a "lid" obstructing the ligand entry path into the core region of the receptor protein. ECL2 can differ structurally between receptors and might account for different ligand binding selectivity and binding kinetics. Indeed, ECL2 was shown to be involved in the ligand recognition and selectivity of β-adrenergic receptors[69,70] and the binding kinetics at a muscarinic acetylcholine receptor[71]. In chapter 2 of this thesis, the function of ECL2 in the free fatty acid receptor FFA2 and its impact on

receptor activation upon ligand binding is discussed. Another common feature of most GPCRs is a disulphide bridge between TM3 and ECL2 that stabilizes the receptor and limits the extent of conformational changes in this part during activation[57].

The seven α helices in the transmembrane region are stabilized by non-covalent interactions, wherein most ligands are expected to bind. It is this core region where a consensus network of six topographically equivalent amino acids has been identified that directly contribute to ligand recognition[57]. Although the shape and structure of the ligands that target GPCRs vary greatly, four conserved residues in the transmembrane region were found[57], even though binding can occur at different depth within the transmembrane core. TM1 does not seem to be involved in ligand binding. TM1 and TM2, which are within the first parts that are synthesized at the ribosome, are rather thought to be important for correct membrane insertion and protein folding than for more specialized tasks such as ligand recognition[72]. Interestingly, beside the consensus scaffold in class A GPCRs in TM3, TM6 and TM7, water molecules were shown to be indirectly involved in mediating receptor-ligand contact[73–76]. There are three amino acid sequences within the TM segments that are highly conserved and are found across all GPCRs, which points to a common evolutionary origin and a fundamental role in the functioning of the receptor. The *P-I-F-motif* forms an interface between TM3, TM5 and TM6 and was shown to be involved in the formation of active-state conformations of the 5-HT_{1B} receptor[77]. The *D(E)RY motif* at the bottom TM3 is also thought to affect the adaption of active conformations and the regulation of constitutive activity[78]. Finally, the *NPxxY-motif* in TM7 was discovered to be required in the *tyrosine toggle switch*, a microswitch initially studied for Rhodopsin but likely common to most GPCRs[79,80].

The intracellular parts of a GPCR are responsible for binding of downstream effectors such as G proteins, GPCR kinases (GRKs) and arrestins[24,81]. Mutations or phosphorylation of ICL2 has been linked to decreased structural stability and a conformational shift towards the active state[82,83]. The amphipathic helix (H8) was thought to be involved in G protein contact, but crystal structures so far could not corroborate this idea[24]. Among the intracellular parts of a GPCR, ICL3 and the C-terminal tail are rather variable and disordered regions, which typically expose linear peptide motifs that recognize specific binding partners[84,85]. According to the “barcode hypothesis” certain residues in the C-terminal tail are post-translationally modified and serve as a recognition pattern for effector and regulator molecules to modulate receptor activity and internalization from the membrane[86].

Conformational changes during receptor activation

Typically, a GPCR that binds a ligand in the extracellular or upper part of the transmembrane region undergoes a conformational shift from an inactive to an active state, if the binding ligand is an

agonist. The small conformational changes in the direct neighborhood of the ligand binding site translates into a larger structural change deeper within the TM region and finally at the interface of the receptor and the cytosol with several possible signaling transducers present. While X-ray structures - although with unreached precision and fidelity - only allow a snapshot of one possible conformation, several other experimental techniques, such as atomistic molecular dynamics simulations or quantitative mass spectrometry gave insight into intermediate events taking place during receptor activation. For instance, it could be shown for the β_2-adrenergic receptor that the receptor undergoes discrete conformational intermediates[56,86,87]. In general, agonists induce more flexibility in the receptor protein whereas inverse agonists stabilize the receptor[88,89], although the conformation that is finally adopted largely depends on the energy landscape of a specific receptor[90,91]. Furthermore, computational studies showed that ligands with different efficacies induced conformational changes according to their physiological response, which indicates that ligands induce distinct shapes that correspond to the biological effect triggered by the binding event[92].

It is remarkable, that despite the structural diversity of GPCRs and their ligands several conformational changes during the process of receptor activation might be common to all GPCRs. In this context, only three main mechanisms shall be described briefly. The first was already hypothesized by *Schwartz et al.* in 2006 named "*global toggle switch model*"[93]. Newer data from crystal structures confirm the key idea of a toggle movement of TM6 and TM5 at the inner part of the receptor opening a binding cleft for a G protein[57,94]. Beside this global conformational change, microswitches within the transmembrane segments were identified, from which two are described here. Salt bridges within the TM region (in particular with the *D(E)RY motif* at the bottom of TM3) break up upon agonist binding and induce of a *rotamer change* if a G protein is present[24,73,75,95,96]. This underlines the importance of allosteric events that affect the adaption of certain conformations of GPCRs. The second microswitch, the "*ionic lock*", consists of a salt bridge between certain amino acids in TM3 and TM6[97,98]. Although this has only been found for rhodopsin, alternative microswitches based on hydrogen bonds were found in other GPCRs[99,100].

GPCR signaling repertoire

Receptors were long recognized as simple on-off switches but it became increasingly evident that receptors and especially GPCRs can occur in multiple conformations[101,102]. The concept of only one active conformation, which is linked to a single pattern of pathway activation also falls short. Instead, GPCRs can engage various pathways associated to different active conformational states[103,104], whose adaption depends on an wide range of factors, such as the nature of the ligand(s), the nature of the coupling G protein(s) or other interacting proteins, the cellular state and environment or the cellular

and subcellular localization of the receptor to name only a few. Therefore, it is not surprising that signaling via one receptor is multifaceted. The phenomenon of functional selectivity (ligand bias or agonist trafficking) describes the behavior of a receptor to signal via different pathways with different efficacy (multidimensional efficacy)[105]. In this regard, the terms agonist, partial agonist and inverse agonist need to be redefined and understood in its actual context. While being an inverse agonist or partial agonist for one pathway does not exclude the possibility to display full agonism on another pathway[106].

Signaling of GPCRs is canonically linked to the activation of G proteins. As already described above, G proteins are molecular switches that control receptor-dependent but also receptor-independent signaling pathways and occur in several subtypes[29]. $G\alpha_s$ proteins stimulate the adenylyl cyclase, thereby increasing intracellular cAMP levels, whereas $G\alpha_i$ proteins inhibit this enzyme and subsequently lead to a decrease of intracellular cAMP levels. Activation of G proteins of the α_q family activate the phospholipase-Cβ, which in turn hydrolyses phosphatidylinositol-4,5-bisphosphate (PIP_2) into inositoltriphosphate (IP3) and diacylgylcerol (DAG). IP3 can bind to its receptor at the endoplasmic reticulum resulting in an intracellular rise of calcium ions. Together with these, DAG can activate the membranous form of the protein kinase C (PKC). On the other hand, effects of the $G\alpha_{12/13}$ family are largely unknown. They are involved in the rearrangement of the cytoskeletal architecture by activating small GTPases, such as members of the Rho family (see above)[30]. But not only the α subunits induce signaling events, also the βγ subunit was shown to elicit certain biological effects, such as the opening of GIRK channels[107].

To protect the cell from overstimulation, several mechanisms evolved. After prolonged receptor activation, a GPCR is phosphorylated at the inner surface of the protein by G protein receptor kinases (GRKs)[108]. Subsequently, β-arrestin is recruited to the phosphorylated sites and thus blocks interaction with the G protein binding sites by steric hindrance[109,110]. After this first phase of receptor desensitization, β-arrestin leads to receptor internalization via clathrin coated pits[111,112]. Although internalization is long thought to stop signaling via GPCRs, it is now known that this is not true in all cases[113]. Several examples could show that internalized GPCRs continue to signaling to cAMP from endosomes[114–116] (**Figure 5**). β-arrestins seem to play a part (together with Gβγ subunits) in this process as well, thereby linking the ability to target and internalize receptors with the event of signal generation[117].

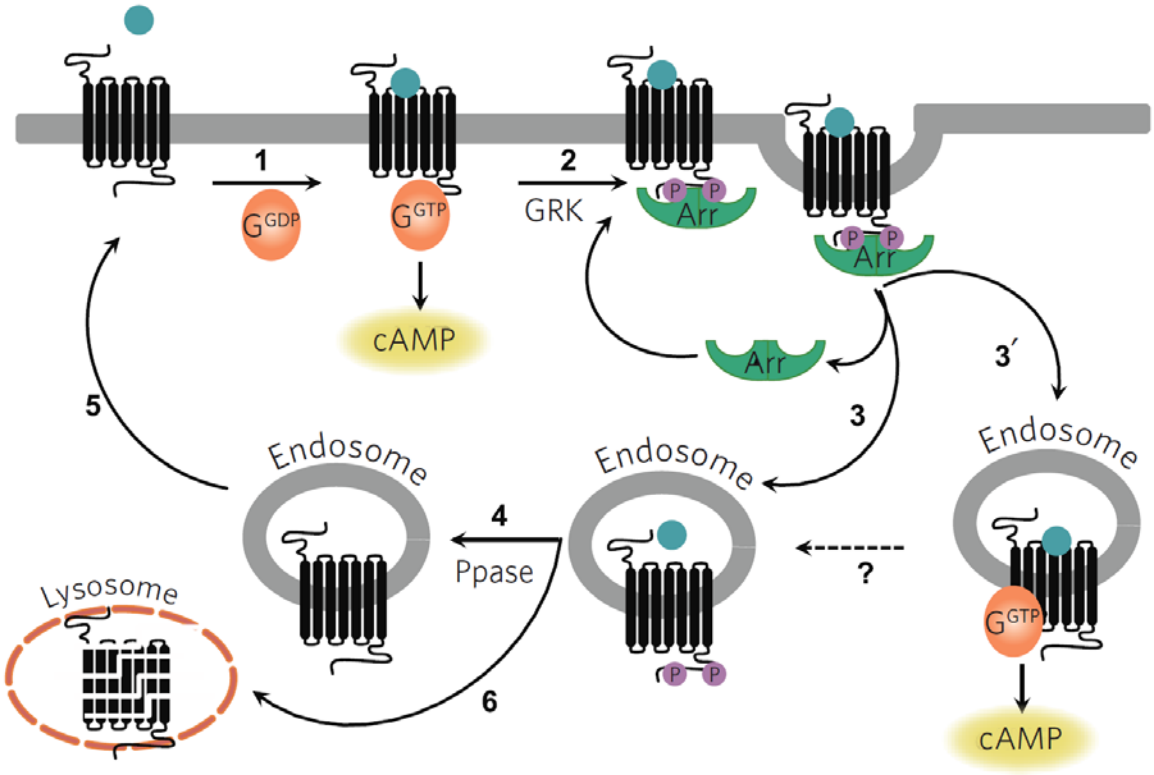

Figure 5 *Classical versus endosomal signaling of a Gα$_s$-coupled model GPCR. Agonist activation leads to cell membrane-originated cAMP signaling (1). After phosphorylation by G protein-coupled receptor kinases (GRKs) (2) β-arrestin can mediate receptor internalization to endosomes (3). Phosphates and ligand are enzymatically removed (4) and endosomal receptors are either recycled to the plasma membrane (5) or degraded by lysosomes (6). In a new model, cAMP signaling can continue after internalization of ligand-GPCR complexes in endosomes (3'). Modified after [118].*

Indeed, there is ample evidence that β-arrestin is capable to signal alongside G protein signaling, such as the activation of the MAPK-pathway[109,119–121]. However, it is also posited that β-arrestins might mediate signaling in a G protein-independent manner. In fact, β-arrestins play a pivotal role as scaffold and might be crucially relevant for some signaling events, but their G protein-independent nature has not been evidenced to date and can be questioned[122]. Since there are no inhibitors for all G proteins available, it is difficult to answer this question satisfactorily. Until specific inhibitors for all subclasses of G proteins are available, the discussion about G protein-independent signaling of GPCRs will go on. These considerations make clear that often made distinctions between G protein-dependent (or canonical) versus G protein-independent (or non-canonical) signaling are artificial and may not have distinct corresponding entities in nature. Pan-G protein inhibitors might serve as a highly desired molecular tool to distinguish between G protein-dependent and G protein-independent signaling of GPCRs. Therefore, the compound BIM-46174 previously reported to act as such inhibitor attracted our interest. Chapter 7 explains our findings that the compound acts as a G protein inhibitor with an unfound molecular mode of action. However, it does not behave as a Pan-G protein inhibitor as proclaimed, which disqualifies its use as a discriminator between G protein-dependent and independent signaling.

Allosterism

Allosterism is a common phenomenon in biochemistry[123]. By binding to an enzyme, the effector often changes the conformation of the enzyme and thus transduces the information into a structural change that might affect binding or response of another effector at another site[124]. Hence, the allosteric effector can enhance or reduce the binding or activity of other effectors at the enzyme, leading to the term of positive and negative cooperativity, respectively. GPCRs function as allosteric modules with several binding sites. Endogenous ligands usually approach the binding site of class GPCRs from the extracellular space and bind within the transmembrane region of the receptor. This binding epitope is designated the "orthosteric" binding site, whereas the "allosteric" binding pocket is spatially distinct and is expected to be situated on top of the orthosteric binding pocket in class A GPCRs. Obviously, this nomenclature is arbitrary and a matter of definition. Thus, the aforementioned cooperativity effects are not unidirectional but reciprocal[125], i.e. the orthosteric ligand allosterically modulates the allosteric ligand to the same degree as the allosteric ligand modulates the orthosteric ligand. An allosteric ligand that enhances the binding and/or efficacy of an orthosteric ligand is called allosteric activator or positive allosteric modulator (PAM), but this effect is also measurable for the opposite direction, i.e. the orthosteric ligand enhances binding and/or efficacy of the allosteric ligand. Concordantly, an allosteric ligand that reduces the binding and/or efficacy of the orthosteric ligand (and *vice versa*) is designated allosteric inhibitor or negative allosteric modulator (NAM). Allosteric ligands that do not change the pharmacological properties of the orthosteric ligand are named neutral allosteric ligands (NALs) or silent allosteric modulator (SAMs)[126–128]. Notably, GPCRs do not only encompass one allosteric site but usually multiple binding sites. The intracellular binding of G proteins to the receptor is also a type of allosterism and affects structure and function of the GPCR with substantial consequences for ligand binding[128]. Meanwhile, other intracellular GPCR ligands were discovered that act as allosteric modulators: G proteins, GPCR-interacting proteins, peptides, lipids and ions[129–131]. Pepducins use this approach on purpose. These lipidated peptides anchor in the plasma membrane and target the receptor intracellularly to modulate the signaling[132].

Allosteric modulation is characterized by four key features. i) Probe dependency: modulatory effects of an allosteric ligand might apply to one orthosteric ligand but not another. The allosteric modulator at the M_4 Acetylcholine receptor LY2033298 enhances the binding affinity of the endogenous ligand Acetylcholine but displays neutral cooperativity against N-methylscopolamin[133]. Probe dependency was also reported for two positive allosteric modulators at the GLP-1 (glucagon-like peptide) receptor. While having only little effect on GLP-1, they greatly potentiated the affinity for the endogenous ligand Oxyntomodulin[134,135]. Moreover, these two allosteric ligands displayed ii) biased

signaling which constitutes another possible characteristic of allosteric ligands. They preferred signaling via cAMP production, β-arrestin recruitment and insulin secretion, but were inactive in terms of intracellular calcium mobilization and ERK phosphorylation[134,135]. iii) Allosteric ligands can have differential effects on efficacy and affinity of an orthosteric ligand. Naphmethonium potentiates the affinity of Pilocarpin but negatively modulates the efficacy of this orthosteric ligand[136]. iv) Finally, allosteric modulation is generally saturable, i.e. the modulatory effect of an allosteric ligand on affinity and/or efficacy of an orthosteric ligand reaches a maximum at complete occupancy of the allosteric binding site. This has beneficial implication for potential allosteric drugs, since these ligands display a "ceiling effect", i.e. the correlation between allosteric drug and side-effects are not linear but are limited by the natural ceiling effect that is reached at saturating concentrations. This lowers the risk of over-dosing[129,137].

Since the allosteric binding site is far less conserved in comparison to the orthosteric binding site, allosteric ligands represent a possibility to design subtype-selective drugs for receptors that are difficult to target with orthosteric ligands. These advantages of allosteric ligands have attracted much attention and efforts to discover and develop allosteric ligands for GPCRs. Despite the benefits of allosteric ligands compared to orthosteric ligands, only a handful of allosteric drugs for class A GPCRs has been approved. This rather low number denotes less the insignificance of allosteric modulation of GPCRs but rather the difficulties that are linked to the drug discovery process of allosteric ligands[138].

Free fatty acid receptor family – Overview

Fatty acids are essential components in biological structures such as membranes but also serve as energy carriers and thus regulate host metabolism as metabolic substrates. Furthermore, they are precursors of several lipid signaling mediators. Fatty acids have long been recognized for their regulatory function in host metabolism but these effects were primarily attributed to their direct function as dietary nutrients or indirectly by their metabolic intermediates[139–141]. They can be classified by their chain length into short-chain fatty acids (SCFA) (C1-C6), medium-chain fatty acids (MCFA) (C7-C12) and long-chain fatty acids (LCFA) (>C12). In 2003, three working groups identified a cell surface receptor that responds to medium- to long-chain fatty acids, and that was subsequently named FFA1 (free fatty acid receptor 1), because the free carboxylic acid group is necessary to activate the receptor[142–144]. The genes for a group of related fatty acids receptors are tandemly located on the chromosomal locus 19q13.1[145] and were formerly named GPR40-43. A study by *Vassilatis et al.* reported on a close phylogenetic relation between this receptor family and the cluster of nucleotide, eicosanoid, protease-activated and lipid class A GPCRs[146]. Formerly identified GPR43 and GPR41 were dubbed FFA2 and FFA3, respectively, recognizing SCFAs as their endogenous

ligands[147–149]. GPR42 was shown to be a gene duplicate of FFA3 (GPR41) with no distinct functionality[147]. Rodents only express one orthologue of the GPR42/GPR41 pair, suggesting that GPR42 indeed represents a gene duplication that occurred since divergence of primate and human lineages[150]. In 2005, GPR120 (FFA4) was reported to respond to unsaturated long-chain fatty acids and its gene was located on the long arm of chromosome 10[151]. Although likewise fatty acid receptors in a wider sense but more distantly encoded and with only minor similarity, there are the hydroxyl carboxylic acid (HCA) receptors GPR81 (HCA1), GPR109A (HCA2) and GPR109B (HCA3) as well as GPR84, which is activated by medium-chain fatty acids and GPR119, activated by the fatty acid derivative oleolylethanolamide. The affinity of FFA receptors for their cognate ligands is overall low (in the micro- to millimolar range), rendering the pharmacological characterization of these receptors difficult. With respect to the low affinity, the physiological relevance of the FFA receptors rely on the local concentrations of the respective ligands. LCFAs can reach blood levels from 0.01 to 10 µM, depending on dietary intake, adipose recycling and hepatic turnover of neutral fats, cholesterol esters and phospholipids[152]. Main source of SCFA is bacterial fermentation of fibers, so that SCFA reach blood levels in the micromolar range (80-180 µM), depending on diet (fiber-rich or fiber-depleted) and microbial composition of the gut[153,154]. Intestinal concentrations of SCFA can even reach millimolar concentration[155]. Hence, ligand concentrations are high enough to be pharmacologically active at FFA receptors.

For the reason of clarity, only the FFA1-3 receptors will be detailed in the following.

Free fatty acid receptor 1 (FFA1)

Saturated and unsaturated long-chain fatty acids are endogenous ligands of the FFA1 but also the FFA4 receptor[142–144,151]. The beneficial effects of polyunsaturated fatty acids such as ω-3 fatty acids have been linked to the presence of FFA receptors, especially to the activation of FFA4[156].

The investigation of the physiological function of FFA1 was primarily guided by high expression levels of FFA1 on pancreatic β-cells[142,144]. FFA1 was further detected in a variety of different cell types, such as osteocytes[157], enteroendocrine cells[158,159], immune cells[160], taste bud cells[161] and brain tissue of primates[162]. The widespread expression pattern needs further validation, since antibody-dependent detection methods of the FFA1 receptor are not faultless (see chapter 4).

LCFA are known to increase glucose-stimulated insulin secretion (GSIS)[163] and were subsequently linked to activation of the FFA1 receptor on β-cells by many studies[144,164–167]. The beneficial effects of LCFA on the metabolic state occur under short-term exposure to LCFA but turn into detrimental effects if LCFA are applied for prolonged periods. Chronically elevated LCFA lead to β-cell death, which coined the term (gluco)lipotoxicity[168]. Although early reports indicated a link between the activation of FFA1 and the adverse LCFA effects[169], further studies disagreed and pointed into a

protective role of the FFA1 receptor against LCFA-mediated lipotoxic effects[165,166,170,171], which is supported by our own studies ([172] and see chapter 4). After discussions about whether FFA1 agonists or antagonists should be developed, evidence for a beneficial role of FFA1 in both acutely and chronically elevated states of fatty acid level entailed the discovery of several small molecule agonists with higher potency and efficacy compared to endogenous agonists as possible drug candidates in the treatment of diabetes type 2 (see chapter 5).

Beside the direct enhancement of GSIS via activation of the FFA1 receptor on β-cells, the indirect FFA1-mediated effects by promoting GLP-1 and GIP (glucose-dependent insulinotropic peptide or gastric inhibitory peptide) production in enteroendocrine cells might contribute to the overall effects of FFA1 stimulation[173]. However, further studies need to show whether this is beneficial or detrimental.

FFA1 is reported to couple to $G\alpha_q$ proteins[144]. The potentiation of GSIS is mediated via direct elevation of intracellular calcium level via the $G\alpha_q$-PLCβ-IP_3-calcium pathway, but also via activation of the DAG-sensitive kinase PKD1 that in turn entails actin depolymerization, a prerequisite for insulin secretion[174]. Although it seems essential for potentiating GSIS, the FFA1 receptor is not restricted to signal via the $G\alpha_q$ pathway. In fact, it was previously demonstrated that FFA1 is also able to promote signaling via $G\alpha_i$ proteins[144,175,176]. However, the significance of this pathway for FFA1-related biological effects is unknown and needs further attention.

Free fatty acid receptor 2 and 3 (FFA2 and FFA3)

FFA2 and FFA3 are often portrayed together because of their overlapping ligand structure and partially overlapping expression pattern. Both receptors are activated by SCFA, making it difficult to distinguish FFA2 from FFA3 mediated effects *in vivo*[177], wherefore chapter 3 is dedicated to this issue. Despite overall low affinity of the endogenous ligands, acetate (C2) has higher prevalence for the human FFA2 than the human FFA3 receptor, whereas valeric (C5) and caproic (C6) acid have higher affinity to FFA3[147–149,178]. There are enormous interspecies differences between ligand recognition for FFA2 and FFA3. While being active at both receptor types in human, propionic acid (C3) selectively activates the mouse FFA3 over the mouse FFA2[179]. The bovine FFA2 receptor shows increased responsiveness to longer chain length compared to the human FFA2, which points to a general difference between these species that may have resulted during evolution from specific adaptations to differences in nutrition and metabolism[177,180]. The FFA2 receptor shows promiscuous G protein coupling via $G\alpha_i$ and $G\alpha_q$ proteins, whereas FFA3 only couples to $G\alpha_i$ proteins[147–149,181].

FFA2 and FFA3 are both expressed on pancreatic islets[182,183] and in adipose tissue[147,148,181,184,185]. While the expression of FFA2 in white adipose tissue seems well evidenced, the expression of FFA3 in

adipose tissue is controversial[181,186,187]. Intestinal L cells (containing GLP-1 and peptide YY) and intestinal I cells (producing cholecystokinin) express FFA2 and FFA3 receptors, thereby linking these receptors with potential roles in the regulation of host metabolism[188–193]. FFA2, but not FFA3, is highly expressed on immune cells such as neutrophils, eosinophils, monocytes and regulatory T cells[147,148,178,184,194,195]. FFA3 on the other hand is expressed on enteric neurons and the sympathetic neuron system[187,196].

The physiological functions of FFA2 and FFA3 are controversial. Since FFA2 and FFA3 are expressed in tissues and cells that are involved in the regulation of metabolic homeostasis, a modulatory effect on host metabolism is plausible. It was shown that a fiber-rich diet is associated with an ameliorated phenotype of obesity and diabetes type 2[197] as well as inflammatory bowel disease[198,199]. The vast majority of physiologically occurring SCFA derive from bacterial fermentation in the digestive system and there is strong evidence for a causal link between the gut microbiome and effects on the metabolic and immune system. Hence, FFA2 and FFA3 emerged as potential mediators of the observed SCFA effects. Indeed, $FFA2^{-/-}$ mice showed exacerbated immune response in inflammatory models of colitis, asthma and arthritis[178], however, others reported that $FFA2^{-/-}$ mice were protected from inflammatory response in a chronic colitis model[200]. Recently, FFA2 was revealed to also play a role in the progression of gout[201]. Amelioration of colitis was entailed to FFA2 effects on regulatory T cells by enhancing their suppressive function, thereby lowering the inflammatory response[195], and on the activation of the macrophage inflammasome complex[199], thereby controlling the inflammatory response.

Under normal chow diet, a positive effect of FFA2 on glucose tolerance was shown by *Tolhurst et al.*[202], whereas *Bjursell et al.* demonstrated under these conditions similar glucose tolerance level for FFA2 wild-type mice compared to $FFA2^{-/-}$ mice[203]. The beneficial effects of FFA2 on the metabolic homeostasis are mainly linked to the increased ability to secrete GLP-1 from enteroendocrine L cells[202,204]. But also a modulatory effect on immunocompetent cells is discussed because in the current understanding of atherogenesis and the pathophysiology of diabetes modulation of immunocompetent cells is involved such as adipose and intimal infiltration with activated monocytes and their differentiation to macrophages.

FFA3 activation on enteroendocrine cells induces the production of peptide YY that reduces transit time and higher energy uptake. Thus $FFA3^{-/-}$ mice under high-fat diet revealed reduced weight gain compared to the wild-type mice[190]. In contrast, *Bellahcene et al.* reported that male, but not female $FFA3^{-/-}$ mice show increased fat mass upon normal and high-fat diet[205]. In conclusion, a role of FFA2 and FFA3 in the regulation of immunological or metabolic disorders is without doubt, however, the direction and the actual extent of their effect is still under debate.

References

1. Rodbell, M. The role of hormone receptors and GTP-regulatory proteins in membrane transduction, *Nature* **284,** 17–22 (1980).
2. Escriva, H. Delaunay, F. & Laudet, V. Ligand binding and nuclear receptor evolution, *Bioessays* **22,** 717–727 (2000).
3. Gomperts, B. D. Kramer, I. M. & Tatham, P. E. R. *Signal transduction.* 2nd ed. (Elsevier Acad. Press, Amsterdam, 2009).
4. Nicoll, C. S. Prolactin and growth hormone: specialists on one hand and mutual mimics on the other, *Perspect. Biol. Med.* **25,** 369–381 (1982).
5. Evans, R. M. The steroid and thyroid hormone receptor superfamily, *Science* **240,** 889–895 (1988).
6. Giacomini, K. M. *et al.* Membrane transporters in drug development, *Nat Rev Drug Discov* **9,** 215–236 (2010).
7. Ashcroft, S. J. Intracellular second messengers, *Adv. Exp. Med. Biol.* **426,** 73–80 (1997).
8. Krebs, E. G. & Fischer, E. H. The phosphorylase b to a converting enzyme of rabbit skeletal muscle, *Biochimica et Biophysica Acta* **20,** 150–157 (1956).
9. Breitkreutz, A. *et al.* A global protein kinase and phosphatase interaction network in yeast, *Science* **328,** 1043–1046 (2010).
10. Serezani, C. H. Ballinger, M. N. Aronoff, D. M. & Peters-Golden, M. Cyclic AMP: master regulator of innate immune cell function, *Am. J. Respir. Cell Mol. Biol.* **39,** 127–132 (2008).
11. Conti, M. Mika, D. & Richter, W. Cyclic AMP compartments and signaling specificity: role of cyclic nucleotide phosphodiesterases, *J. Gen. Physiol.* **143,** 29–38 (2014).
12. Cooper, D. M. F. Regulation and organization of adenylyl cyclases and cAMP, *Biochem. J.* **375,** 517–529 (2003).
13. Conti, M. Phosphodiesterases and cyclic nucleotide signaling in endocrine cells, *Mol. Endocrinol.* **14,** 1317–1327 (2000).
14. Lodish, H. F. *et al. Molecular cell biology* (W.H. Freeman and Company, New York, NY, 2013).
15. Taylor, S. S. *et al.* PKA: a portrait of protein kinase dynamics, *Biochim. Biophys. Acta* **1697,** 259–269 (2004).
16. Francis, S. H. Busch, J. L. Corbin, J. D. & Sibley, D. cGMP-dependent protein kinases and cGMP phosphodiesterases in nitric oxide and cGMP action, *Pharmacol. Rev.* **62,** 525–563 (2010).
17. Seifert, R. cCMP and cUMP: emerging second messengers, *Trends Biochem. Sci.* **40,** 8–15 (2015).
18. Oldham, W. M. van Eps, N. Preininger, A. M. Hubbell, W. L. & Hamm, H. E. Mechanism of the receptor-catalyzed activation of heterotrimeric G proteins, *Nat. Struct. Mol. Biol.* **13,** 772–777 (2006).
19. Oldham, W. M. & Hamm, H. E. Structural basis of function in heterotrimeric G proteins, *Q. Rev. Biophys.* **39,** 117–166 (2006).
20. Oldham, W. M. & Hamm, H. E. Heterotrimeric G protein activation by G-protein-coupled receptors, *Nat. Rev. Mol. Cell Biol.* **9,** 60–71 (2008).

21. Clapham, D. E. & Neer, E. J. G protein beta gamma subunits, *Annu. Rev. Pharmacol. Toxicol.* **37,** 167–203 (1997).

22. Schmidt, C. J. Thomas, T. C. Levine, M. A. & Neer, E. J. Specificity of G protein beta and gamma subunit interactions, *J. Biol. Chem.* **267,** 13807–13810 (1992).

23. Wedegaertner, P. B. Wilson, P. T. & Bourne, H. R. Lipid Modifications of Trimeric G Proteins, *Journal of Biological Chemistry* **270,** 503–506 (1995).

24. Rasmussen, S. G. F. *et al.* Crystal structure of the β2 adrenergic receptor-Gs protein complex, *Nature* **477,** 549–555 (2011).

25. Lambright, D. G. Noel, J. P. Hamm, H. E. & Sigler, P. B. Structural determinants for activation of the alpha-subunit of a heterotrimeric G protein, *Nature* **369,** 621–628 (1994).

26. McCudden, C. R. Hains, M. D. Kimple, R. J. Siderovski, D. P. & Willard, F. S. G-protein signaling: back to the future, *Cell. Mol. Life Sci.* **62,** 551–577 (2005).

27. Siderovski, D. P. The GAPs, GEFs, and GDIs of heterotrimeric G-protein alpha subunits, *Int. J. Biol. Sci.* 51–66 (2005).

28. Simon, M. I. Strathmann, M. P. & Gautam, N. Diversity of G proteins in signal transduction, *Science* **252,** 802–808 (1991).

29. Milligan, G. & Kostenis, E. Heterotrimeric G-proteins: a short history, *Br. J. Pharmacol.* **147 Suppl 1,** S46-55 (2006).

30. Marinissen, M. J. & Gutkind, J. G-protein-coupled receptors and signaling networks. Emerging paradigms, *Trends in Pharmacological Sciences* **22,** 368–376 (2001).

31. Downes, G. B. & Gautam, N. The G protein subunit gene families, *Genomics* **62,** 544–552 (1999).

32. Macrez, N. *et al.* A Dimer Derived from G13 Transduces the Angiotensin AT1 Receptor Signal to Stimulation of Ca2+ Channels in Rat Portal Vein Myocytes, *Journal of Biological Chemistry* **272,** 23180–23185 (1997).

33. Makino, E. R. Handy, J. W. Li, T. & Arshavsky, V. Y. The GTPase activating factor for transducin in rod photoreceptors is the complex between RGS9 and type 5 G protein subunit, *Proceedings of the National Academy of Sciences* **96,** 1947–1952 (1999).

34. Snow, B. E. *et al.* A G protein subunit-like domain shared between RGS11 and other RGS proteins specifies binding to G 5 subunits, *Proceedings of the National Academy of Sciences* **95,** 13307–13312 (1998).

35. Rebois, R. V. & Hébert, T. E. Protein complexes involved in heptahelical receptor-mediated signal transduction, *Recept. Channels* **9,** 169–194 (2003).

36. Zhang, F. L. & Casey, P. J. Protein prenylation: molecular mechanisms and functional consequences, *Annu. Rev. Biochem.* **65,** 241–269 (1996).

37. Jelsema, C. L. & Axelrod, J. Stimulation of phospholipase A2 activity in bovine rod outer segments by the beta gamma subunits of transducin and its inhibition by the alpha subunit, *Proc. Natl. Acad. Sci. U.S.A.* **84,** 3623–3627 (1987).

38. Camps, M. *et al.* Stimulation of phospholipase C by guanine-nucleotide-binding protein beta gamma subunits, *Eur. J. Biochem.* **206,** 821–831 (1992).

39. GRAF, R. *et al.* Studies on the interaction of alpha subunits of GTP-binding proteins with betagamma dimers, *Eur J Biochem* **210,** 609–619 (1992).

40. Smotrys, J. E. & Linder, M. E. Palmitoylation of intracellular signaling proteins: regulation and function, *Annu. Rev. Biochem.* **73,** 559–587 (2004).

41. Chen, C. A. & Manning, D. R. Regulation of G proteins by covalent modification, *Oncogene* **20,** 1643–1652 (2001).

42. Mixon, M. B. *et al.* Tertiary and Quaternary Structural Changes in Gialpha Induced by GTP Hydrolysis, *Science* **270,** 954–960 (1995).

43. Coleman, D. *et al.* Structures of active conformations of Gi alpha 1 and the mechanism of GTP hydrolysis, *Science* **265,** 1405–1412 (1994).

44. Noel, J. P. Hamm, H. E. & Sigler, P. B. The 2.2 A crystal structure of transducin-alpha complexed with GTP gamma S, *Nature* **366,** 654–663 (1993).

45. Abdulaev, N. G. *et al.* The receptor-bound "empty pocket" state of the heterotrimeric G-protein alpha-subunit is conformationally dynamic, *Biochemistry* **45,** 12986–12997 (2006).

46. Schmitz, A.-L. *et al.* A cell-permeable inhibitor to trap Gαq proteins in the empty pocket conformation, *Chem. Biol.* **21,** 890–902 (2014).

47. Burns, D. L. Subunit structure and enzymic activity of pertussis toxin, *Microbiol. Sci.* **5,** 285–287 (1988).

48. Katada, T. Tamura, M. & Ui, M. The A protomer of islet-activating protein, pertussis toxin, as an active peptide catalyzing ADP-ribosylation of a membrane protein, *Archives of Biochemistry and Biophysics* **224,** 290–298 (1983).

49. Seeburg, P. H. Colby, W. W. Capon, D. J. Goeddel, D. V. & Levinson, A. D. Biological properties of human c-Ha-ras1 genes mutated at codon 12, *Nature* **312,** 71–75 (1984).

50. Feramisco, J. R. Gross, M. Kamata, T. Rosenberg, M. & Sweet, R. W. Microinjection of the oncogene form of the human H-ras (t-24) protein results in rapid proliferation of quiescent cells, *Cell* **38,** 109–117 (1984).

51. Mulcahy, L. S. Smith, M. R. & Stacey, D. W. Requirement for ras proto-oncogene function during serum-stimulated growth of NIH 3T3 cells, *Nature* **313,** 241–243 (1985).

52. Bar-Sagi, D. & Feramisco, J. R. Microinjection of the ras oncogene protein into PC12 cells induces morphological differentiation, *Cell* **42,** 841–848 (1985).

53. Overington, J. P. Al-Lazikani, B. & Hopkins, A. L. How many drug targets are there?, *Nat Rev Drug Discov* **5,** 993–996 (2006).

54. Fredriksson, R. Lagerström, M. C. Lundin, L.-G. & Schiöth, H. B. The G-protein-coupled receptors in the human genome form five main families. Phylogenetic analysis, paralogon groups, and fingerprints, *Mol. Pharmacol.* **63,** 1256–1272 (2003).

55. Lagerström, M. C. & Schiöth, H. B. Structural diversity of G protein-coupled receptors and significance for drug discovery, *Nat Rev Drug Discov* **7,** 339–357 (2008).

56. Rosenbaum, D. M. Rasmussen, S. G. F. & Kobilka, B. K. The structure and function of G-protein-coupled receptors, *Nature* **459,** 356–363 (2009).

57. Venkatakrishnan, A. J. *et al.* Molecular signatures of G-protein-coupled receptors, *Nature* **494,** 185–194 (2013).

58. Pierce, K. L. Premont, R. T. & Lefkowitz, R. J. Seven-transmembrane receptors, *Nat. Rev. Mol. Cell Biol.* **3,** 639–650 (2002).

59. Isom, D. G. & Dohlman, H. G. Buried ionizable networks are an ancient hallmark of G protein-coupled receptor activation, *Proc. Natl. Acad. Sci. U.S.A.* **112,** 5702–5707 (2015).

60. Palczewski, K. Crystal Structure of Rhodopsin. A G Protein-Coupled Receptor, *Science* **289,** 739–745 (2000).

61. Hanson, M. A. *et al.* Crystal structure of a lipid G protein-coupled receptor, *Science* **335,** 851–855 (2012).

62. Schadel, S. A. *et al.* Ligand channeling within a G-protein-coupled receptor. The entry and exit of retinals in native opsin, *J. Biol. Chem.* **278,** 24896–24903 (2003).

63. Park, J. H. Scheerer, P. Hofmann, K. P. Choe, H.-W. & Ernst, O. P. Crystal structure of the ligand-free G-protein-coupled receptor opsin, *Nature* **454,** 183–187 (2008).

64. Srivastava, A. *et al.* High-resolution structure of the human GPR40 receptor bound to allosteric agonist TAK-875, *Nature* **513,** 124–127 (2014).

65. Hurst, D. P. *et al.* A lipid pathway for ligand binding is necessary for a cannabinoid G protein-coupled receptor, *J. Biol. Chem.* **285,** 17954–17964 (2010).

66. Pei, Y. *et al.* Ligand-binding architecture of human CB2 cannabinoid receptor: evidence for receptor subtype-specific binding motif and modeling GPCR activation, *Chem. Biol.* **15,** 1207–1219 (2008).

67. Picone, R. P. *et al.* (-)-7'-Isothiocyanato-11-hydroxy-1',1'-dimethylheptylhexahydrocannabinol (AM841), a high-affinity electrophilic ligand, interacts covalently with a cysteine in helix six and activates the CB1 cannabinoid receptor, *Mol. Pharmacol.* **68,** 1623–1635 (2005).

68. Kruijf, P. de *et al.* Identification of a novel allosteric binding site in the CXCR2 chemokine receptor, *Mol. Pharmacol.* **80,** 1108–1118 (2011).

69. Dror, R. O. *et al.* Pathway and mechanism of drug binding to G-protein-coupled receptors, *Proc. Natl. Acad. Sci. U.S.A.* **108,** 13118–13123 (2011).

70. González, A. Perez-Acle, T. Pardo, L. & Deupi, X. Molecular basis of ligand dissociation in β-adrenergic receptors, *PLoS ONE* **6,** e23815 (2011).

71. Kruse, A. C. *et al.* Structure and dynamics of the M3 muscarinic acetylcholine receptor, *Nature* **482,** 552–556 (2012).

72. Schlinkmann, K. M. *et al.* Critical features for biosynthesis, stability, and functionality of a G protein-coupled receptor uncovered by all-versus-all mutations, *Proc. Natl. Acad. Sci. U.S.A.* **109,** 9810–9815 (2012).

73. Lebon, G. *et al.* Agonist-bound adenosine A2A receptor structures reveal common features of GPCR activation, *Nature* **474,** 521–525 (2011).

74. Jaakola, V.-P. *et al.* The 2.6 angstrom crystal structure of a human A2A adenosine receptor bound to an antagonist, *Science* **322,** 1211–1217 (2008).

75. Xu, F. *et al.* Structure of an agonist-bound human A2A adenosine receptor, *Science* **332,** 322–327 (2011).

76. Congreve, M. Langmead, C. J. Mason, J. S. & Marshall, F. H. Progress in structure based drug design for G protein-coupled receptors, *J. Med. Chem.* **54,** 4283–4311 (2011).

77. Wacker, D. *et al.* Structural features for functional selectivity at serotonin receptors, *Science* **340,** 615–619 (2013).

78. Rovati, G. E. Capra, V. & Neubig, R. R. The highly conserved DRY motif of class A G protein-coupled receptors: beyond the ground state, *Mol. Pharmacol.* **71,** 959–964 (2007).

79. Fritze, O. *et al.* Role of the conserved NPxxY(x)5,6F motif in the rhodopsin ground state and during activation, *Proc. Natl. Acad. Sci. U.S.A.* **100,** 2290–2295 (2003).

80. Trzaskowski, B. *et al.* Action of Molecular Switches in GPCRs - Theoretical and Experimental Studies, *CMC* **19,** 1090–1109 (2012).

81. Katritch, V. Cherezov, V. & Stevens, R. C. Diversity and modularity of G protein-coupled receptor structures, *Trends Pharmacol. Sci.* **33,** 17–27 (2012).

82. Warne, T. *et al.* Structure of a beta1-adrenergic G-protein-coupled receptor, *Nature* **454,** 486–491 (2008).

83. Valiquette, M. Parent, S. Loisel, T. P. & Bouvier, M. Mutation of tyrosine-141 inhibits insulin-promoted tyrosine phosphorylation and increased responsiveness of the human beta 2-adrenergic receptor, *EMBO J.* **14,** 5542–5549 (1995).

84. Unal, H. & Karnik, S. S. Domain coupling in GPCRs: the engine for induced conformational changes, *Trends Pharmacol. Sci.* **33,** 79–88 (2012).

85. Babu, M. M. Kriwacki, R. W. & Pappu, R. V. Structural biology. Versatility from protein disorder, *Science* **337,** 1460–1461 (2012).

86. Nobles, K. N. *et al.* Distinct phosphorylation sites on the β(2)-adrenergic receptor establish a barcode that encodes differential functions of β-arrestin, *Sci Signal* **4,** ra51 (2011).

87. Deupi, X. & Standfuss, J. Structural insights into agonist-induced activation of G-protein-coupled receptors, *Curr. Opin. Struct. Biol.* **21,** 541–551 (2011).

88. West, G. M. *et al.* Ligand-dependent perturbation of the conformational ensemble for the GPCR β2 adrenergic receptor revealed by HDX, *Structure* **19,** 1424–1432 (2011).

89. McLean, A. J. Generation and Analysis of Constitutively Active and Physically Destabilized Mutants of the Human beta 1-Adrenoceptor, *Molecular Pharmacology* **62,** 747–755 (2002).

90. Warne, T. *et al.* The structural basis for agonist and partial agonist action on a β(1)-adrenergic receptor, *Nature* **469,** 241–244 (2011).

91. Warne, T. Edwards, P. C. Leslie, A. G. W. & Tate, C. G. Crystal structures of a stabilized β1-adrenoceptor bound to the biased agonists bucindolol and carvedilol, *Structure* **20,** 841–849 (2012).

92. Vaidehi, N. & Kenakin, T. The role of conformational ensembles of seven transmembrane receptors in functional selectivity, *Curr Opin Pharmacol* **10,** 775–781 (2010).

93. Schwartz, T. W. Frimurer, T. M. Holst, B. Rosenkilde, M. M. & Elling, C. E. Molecular mechanism of 7TM receptor activation--a global toggle switch model, *Annu. Rev. Pharmacol. Toxicol.* **46,** 481–519 (2006).

94. Katritch, V. Cherezov, V. & Stevens, R. C. Structure-function of the G protein-coupled receptor superfamily, *Annu. Rev. Pharmacol. Toxicol.* **53,** 531–556 (2013).

95. Rasmussen, S. G. F. *et al.* Structure of a nanobody-stabilized active state of the β(2) adrenoceptor, *Nature* **469,** 175–180 (2011).

96. Shi, L. *et al.* Beta2 adrenergic receptor activation. Modulation of the proline kink in transmembrane 6 by a rotamer toggle switch, *J. Biol. Chem.* **277,** 40989–40996 (2002).

97. Vogel, R. *et al.* Functional role of the "ionic lock"--an interhelical hydrogen-bond network in family A heptahelical receptors, *J. Mol. Biol.* **380,** 648–655 (2008).

98. Yao, X. *et al.* Coupling ligand structure to specific conformational switches in the beta2-adrenoceptor, *Nat. Chem. Biol.* **2,** 417–422 (2006).

99. Wu, H. *et al.* Structure of the human κ-opioid receptor in complex with JDTic, *Nature* **485,** 327–332 (2012).

100. Manglik, A. *et al.* Crystal structure of the μ-opioid receptor bound to a morphinan antagonist, *Nature* **485,** 321–326 (2012).

101. Bockenhauer, S. Fürstenberg, A. Yao, X. J. Kobilka, B. K. & Moerner, W. E. Conformational dynamics of single G protein-coupled receptors in solution, *J Phys Chem B* **115,** 13328–13338 (2011).

102. Kahsai, A. W. *et al.* Multiple ligand-specific conformations of the β2-adrenergic receptor, *Nat. Chem. Biol.* **7,** 692–700 (2011).

103. Malik, R. U. *et al.* Detection of G protein-selective G protein-coupled receptor (GPCR) conformations in live cells, *J. Biol. Chem.* **288,** 17167–17178 (2013).

104. Azzi, M. *et al.* Beta-arrestin-mediated activation of MAPK by inverse agonists reveals distinct active conformations for G protein-coupled receptors, *Proc. Natl. Acad. Sci. U.S.A.* **100,** 11406–11411 (2003).

105. Kenakin, T. Collateral efficacy in drug discovery: taking advantage of the good (allosteric) nature of 7TM receptors, *Trends Pharmacol. Sci.* **28,** 407–415 (2007).

106. Kenakin, T. & Christopoulos, A. Signalling bias in new drug discovery: detection, quantification and therapeutic impact, *Nat Rev Drug Discov* **12,** 205–216 (2013).

107. Smrcka, A. V. Molecular targeting of Gα and Gβγ subunits: a potential approach for cancer therapeutics, *Trends Pharmacol. Sci.* **34,** 290–298 (2013).

108. Pitcher, J. A. *et al.* Feedback Inhibition of G Protein-coupled Receptor Kinase 2 (GRK2) Activity by Extracellular Signal-regulated Kinases, *Journal of Biological Chemistry* **274,** 34531–34534 (1999).

109. DeWire, S. M. Ahn, S. Lefkowitz, R. J. & Shenoy, S. K. Beta-arrestins and cell signaling, *Annu. Rev. Physiol.* **69,** 483–510 (2007).

110. Shukla, A. K. Xiao, K. & Lefkowitz, R. J. Emerging paradigms of β-arrestin-dependent seven transmembrane receptor signaling, *Trends Biochem. Sci.* **36,** 457–469 (2011).

111. Goodman, O. B. *et al.* Beta-arrestin acts as a clathrin adaptor in endocytosis of the beta2-adrenergic receptor, *Nature* **383,** 447–450 (1996).

112. Ferguson, S. S. *et al.* Role of beta-arrestin in mediating agonist-promoted G protein-coupled receptor internalization, *Science* **271,** 363–366 (1996).

113. Calebiro, D. Nikolaev, V. O. Persani, L. & Lohse, M. J. Signaling by internalized G-protein-coupled receptors, *Trends Pharmacol. Sci.* **31,** 221–228 (2010).

114. Ferrandon, S. *et al.* Sustained cyclic AMP production by parathyroid hormone receptor endocytosis, *Nat. Chem. Biol.* **5,** 734–742 (2009).

115. Mullershausen, F. *et al.* Persistent signaling induced by FTY720-phosphate is mediated by internalized S1P1 receptors, *Nat. Chem. Biol.* **5,** 428–434 (2009).

116. Calebiro, D. *et al.* Persistent cAMP-signals triggered by internalized G-protein-coupled receptors, *PLoS Biol.* **7,** e1000172 (2009).

117. Wehbi, V. L. *et al.* Noncanonical GPCR signaling arising from a PTH receptor-arrestin-Gβγ complex, *Proc. Natl. Acad. Sci. U.S.A.* **110,** 1530–1535 (2013).

118. Vilardaga, J.-P. Jean-Alphonse, F. G. & Gardella, T. J. Endosomal generation of cAMP in GPCR signaling, *Nat. Chem. Biol.* **10,** 700–706 (2014).

119. Lefkowitz, R. J. & Shenoy, S. K. Transduction of receptor signals by beta-arrestins, *Science* **308,** 512–517 (2005).

120. Luttrell, L. M. *et al.* Beta-arrestin-dependent formation of beta2 adrenergic receptor-Src protein kinase complexes, *Science* **283,** 655–661 (1999).

121. McDonald, P. H. beta -Arrestin 2. A Receptor-Regulated MAPK Scaffold for the Activation of JNK3, *Science* **290,** 1574–1577 (2000).

122. Saulière, A. *et al.* Deciphering biased-agonism complexity reveals a new active AT1 receptor entity, *Nat. Chem. Biol.* **8,** 622–630 (2012).

123. Changeux, J.-P. The Feedback Control Mechanism of Biosynthetic L-Threonine Deaminase by L-Isoleucine, *Cold Spring Harbor Symposia on Quantitative Biology* **26,** 313–318 (1961).

124. Monod, J. Wyman, J. & Changeux, J.-P. On the nature of allosteric transitions. A plausible model, *Journal of Molecular Biology* **12,** 88–118 (1965).

125. Tränkle, C. Weyand, O. Schröter, A. & Mohr, K. Using a radioalloster to test predictions of the cooperativity model for gallamine binding to the allosteric site of muscarinic acetylcholine M(2) receptors, *Mol. Pharmacol.* **56,** 962–965 (1999).

126. Wootten, D. Christopoulos, A. & Sexton, P. M. Emerging paradigms in GPCR allostery: implications for drug discovery, *Nat Rev Drug Discov* **12,** 630–644 (2013).

127. Christopoulos, A. *et al.* International Union of Basic and Clinical Pharmacology. XC. multisite pharmacology: recommendations for the nomenclature of receptor allosterism and allosteric ligands, *Pharmacol. Rev.* **66,** 918–947 (2014).

128. Kenakin, T. & Miller, L. J. Seven transmembrane receptors as shapeshifting proteins: the impact of allosteric modulation and functional selectivity on new drug discovery, *Pharmacol. Rev.* **62,** 265–304 (2010).

129. May, L. T. Leach, K. Sexton, P. M. & Christopoulos, A. Allosteric modulation of G protein-coupled receptors, *Annu. Rev. Pharmacol. Toxicol.* **47,** 1–51 (2007).

130. Ritter, S. L. & Hall, R. A. Fine-tuning of GPCR activity by receptor-interacting proteins, *Nat. Rev. Mol. Cell Biol.* **10,** 819–830 (2009).

131. Pert, C. B. Pasternak, G. & Snyder, S. H. Opiate agonists and antagonists discriminated by receptor binding in brain, *Science* **182,** 1359–1361 (1973).

132. Covic, L. Gresser, A. L. Talavera, J. Swift, S. & Kuliopulos, A. Activation and inhibition of G protein-coupled receptors by cell-penetrating membrane-tethered peptides, *Proc. Natl. Acad. Sci. U.S.A.* **99,** 643–648 (2002).

133. Valant, C. Felder, C. C. Sexton, P. M. & Christopoulos, A. Probe dependence in the allosteric modulation of a G protein-coupled receptor: implications for detection and validation of allosteric ligand effects, *Mol. Pharmacol.* **81,** 41–52 (2012).

134. Koole, C. *et al.* Allosteric ligands of the glucagon-like peptide 1 receptor (GLP-1R) differentially modulate endogenous and exogenous peptide responses in a pathway-selective manner: implications for drug screening, *Mol. Pharmacol.* **78,** 456–465 (2010).

135. Wootten, D. *et al.* Differential activation and modulation of the glucagon-like peptide-1 receptor by small molecule ligands, *Mol. Pharmacol.* **83,** 822–834 (2013).

136. Jäger, D. *et al.* Allosteric small molecules unveil a role of an extracellular E2/transmembrane helix 7 junction for G protein-coupled receptor activation, *J. Biol. Chem.* **282,** 34968–34976 (2007).

137. Keov, P. Sexton, P. M. & Christopoulos, A. Allosteric modulation of G protein-coupled receptors: a pharmacological perspective, *Neuropharmacology* **60,** 24–35 (2011).

138. Kenakin, T. P. Biased signalling and allosteric machines: new vistas and challenges for drug discovery, *Br. J. Pharmacol.* **165,** 1659–1669 (2012).

139. Crespin, S. R. Greenough, W. B. & Steinberg, D. Stimulation of insulin secretion by infusion of free fatty acids, *J. Clin. Invest.* **48,** 1934–1943 (1969).

140. Stein, D. T. *et al.* Essentiality of circulating fatty acids for glucose-stimulated insulin secretion in the fasted rat, *J. Clin. Invest.* **97,** 2728–2735 (1996).

141. Dobbins, R. L. *et al.* A fatty acid- dependent step is critically important for both glucose- and non-glucose-stimulated insulin secretion, *J. Clin. Invest.* **101,** 2370–2376 (1998).

142. Briscoe, C. P. *et al.* The orphan G protein-coupled receptor GPR40 is activated by medium and long chain fatty acids, *J. Biol. Chem.* **278,** 11303–11311 (2003).

143. Kotarsky, K. Nilsson, N. E. Flodgren, E. Owman, C. & Olde, B. A human cell surface receptor activated by free fatty acids and thiazolidinedione drugs, *Biochemical and Biophysical Research Communications* **301,** 406–410 (2003).

144. Itoh, Y. *et al.* Free fatty acids regulate insulin secretion from pancreatic beta cells through GPR40, *Nature* **422,** 173–176 (2003).

145. Sawzdargo, M. *et al.* A cluster of four novel human G protein-coupled receptor genes occurring in close proximity to CD22 gene on chromosome 19q13.1, *Biochem. Biophys. Res. Commun.* **239,** 543–547 (1997).

146. Vassilatis, D. K. *et al.* The G protein-coupled receptor repertoires of human and mouse, *Proc. Natl. Acad. Sci. U.S.A.* **100,** 4903–4908 (2003).

147. Brown, A. J. *et al.* The Orphan G protein-coupled receptors GPR41 and GPR43 are activated by propionate and other short chain carboxylic acids, *J. Biol. Chem.* **278,** 11312–11319 (2003).

148. Le Poul, E. *et al.* Functional characterization of human receptors for short chain fatty acids and their role in polymorphonuclear cell activation, *J. Biol. Chem.* **278,** 25481–25489 (2003).

149. Nilsson, N. E. Kotarsky, K. Owman, C. & Olde, B. Identification of a free fatty acid receptor, FFA2R, expressed on leukocytes and activated by short-chain fatty acids, *Biochemical and Biophysical Research Communications* **303,** 1047–1052 (2003).

150. Brown, A. J. Jupe, S. & Briscoe, C. P. A family of fatty acid binding receptors, *DNA Cell Biol.* **24,** 54–61 (2005).

151. Hirasawa, A. *et al.* Free fatty acids regulate gut incretin glucagon-like peptide-1 secretion through GPR120, *Nat. Med.* **11,** 90–94 (2005).

152. Spector, A. A. & Hoak, J. C. Letter: Fatty acids, platelets, and microcirculatory obstruction, *Science* **190,** 490–492 (1975).

153. Cummings, J. H. Pomare, E. W. Branch, W. J. Naylor, C. P. & Macfarlane, G. T. Short chain fatty acids in human large intestine, portal, hepatic and venous blood, *Gut* **28,** 1221–1227 (1987).

154. Nilsson, A. C. Östman, E. M. Knudsen, K. E. B. Holst, J. J. & Björck, I. M. E. A cereal-based evening meal rich in indigestible carbohydrates increases plasma butyrate the next morning, *J. Nutr.* **140,** 1932–1936 (2010).

155. Topping, D. L. & Clifton, P. M. Short-chain fatty acids and human colonic function: roles of resistant starch and nonstarch polysaccharides, *Physiol. Rev.* **81,** 1031–1064 (2001).

156. Oh, D. Y. *et al.* GPR120 is an omega-3 fatty acid receptor mediating potent anti-inflammatory and insulin-sensitizing effects, *Cell* **142,** 687–698 (2010).

157. Mieczkowska, A. Baslé, M. F. Chappard, D. & Mabilleau, G. Thiazolidinediones induce osteocyte apoptosis by a G protein-coupled receptor 40-dependent mechanism, *J. Biol. Chem.* **287,** 23517–23526 (2012).

158. Edfalk, S. Steneberg, P. & Edlund, H. Gpr40 is expressed in enteroendocrine cells and mediates free fatty acid stimulation of incretin secretion, *Diabetes* **57,** 2280–2287 (2008).

159. Liou, A. P. *et al.* The G-protein-coupled receptor GPR40 directly mediates long-chain fatty acid-induced secretion of cholecystokinin, *Gastroenterology* **140,** 903–912 (2011).

160. Hirasawa, A. *et al.* Production and characterization of a monoclonal antibody against GPR40 (FFAR1; free fatty acid receptor 1), *Biochem. Biophys. Res. Commun.* **365,** 22–28 (2008).

161. Cartoni, C. *et al.* Taste preference for fatty acids is mediated by GPR40 and GPR120, *J. Neurosci.* **30,** 8376–8382 (2010).

162. Ma, D. *et al.* Expression of free fatty acid receptor GPR40 in the central nervous system of adult monkeys, *Neurosci. Res.* **58,** 394–401 (2007).

163. Stein, D. T. *et al.* The insulinotropic potency of fatty acids is influenced profoundly by their chain length and degree of saturation, *J. Clin. Invest.* **100,** 398–403 (1997).

164. Briscoe, C. P. *et al.* Pharmacological regulation of insulin secretion in MIN6 cells through the fatty acid receptor GPR40: identification of agonist and antagonist small molecules, *Br. J. Pharmacol.* **148,** 619–628 (2006).

165. Latour, M. G. *et al.* GPR40 is necessary but not sufficient for fatty acid stimulation of insulin secretion in vivo, *Diabetes* **56,** 1087–1094 (2007).

166. Kebede, M. *et al.* The fatty acid receptor GPR40 plays a role in insulin secretion in vivo after high-fat feeding, *Diabetes* **57,** 2432–2437 (2008).

167. Nagasumi, K. *et al.* Overexpression of GPR40 in pancreatic beta-cells augments glucose-stimulated insulin secretion and improves glucose tolerance in normal and diabetic mice, *Diabetes* **58,** 1067–1076 (2009).

168. McGarry, J. D. & Dobbins, R. L. Fatty acids, lipotoxicity and insulin secretion, *Diabetologia* **42,** 128–138 (1999).

169. Steneberg, P. Rubins, N. Bartoov-Shifman, R. Walker, M. D. & Edlund, H. The FFA receptor GPR40 links hyperinsulinemia, hepatic steatosis, and impaired glucose homeostasis in mouse, *Cell Metab.* **1,** 245–258 (2005).

170. Tan, C. P. *et al.* Selective small-molecule agonists of G protein-coupled receptor 40 promote glucose-dependent insulin secretion and reduce blood glucose in mice, *Diabetes* **57,** 2211–2219 (2008).

171. Lan, H. *et al.* Lack of FFAR1/GPR40 does not protect mice from high-fat diet-induced metabolic disease, *Diabetes* **57,** 2999–3006 (2008).

172. Wagner, R. *et al.* Reevaluation of fatty acid receptor 1 as a drug target for the stimulation of insulin secretion in humans, *Diabetes* **62,** 2106–2111 (2013).

173. Mancini, A. D. & Poitout, V. The fatty acid receptor FFA1/GPR40 a decade later: how much do we know?, *Trends Endocrinol. Metab.* **24,** 398–407 (2013).

174. Ferdaoussi, M. *et al.* G protein-coupled receptor (GPR)40-dependent potentiation of insulin secretion in mouse islets is mediated by protein kinase D1, *Diabetologia* **55,** 2682–2692 (2012).

175. Schröder, R. *et al.* Deconvolution of complex G protein-coupled receptor signaling in live cells using dynamic mass redistribution measurements, *Nat. Biotechnol.* **28,** 943–949 (2010).

176. Grundmann, M. & Kostenis, E. Label-free biosensor assays in GPCR screening, *Methods Mol. Biol.* **1272,** 199–213 (2015).

177. Offermanns, S. Free fatty acid (FFA) and hydroxy carboxylic acid (HCA) receptors, *Annu. Rev. Pharmacol. Toxicol.* **54,** 407–434 (2014).

178. Maslowski, K. M. *et al.* Regulation of inflammatory responses by gut microbiota and chemoattractant receptor GPR43, *Nature* **461,** 1282–1286 (2009).

179. Hudson, B. D. Tikhonova, I. G. Pandey, S. K. Ulven, T. & Milligan, G. Extracellular ionic locks determine variation in constitutive activity and ligand potency between species orthologs of the free fatty acid receptors FFA2 and FFA3, *J. Biol. Chem.* **287,** 41195–41209 (2012).

180. Hudson, B. D. *et al.* Chemically engineering ligand selectivity at the free fatty acid receptor 2 based on pharmacological variation between species orthologs, *FASEB J.* **26,** 4951–4965 (2012).

181. Hong, Y.-H. *et al.* Acetate and propionate short chain fatty acids stimulate adipogenesis via GPCR43, *Endocrinology* **146,** 5092–5099 (2005).

182. Kebede, M. A. Alquier, T. Latour, M. G. & Poitout, V. Lipid receptors and islet function: therapeutic implications?, *Diabetes Obes Metab* **11 Suppl 4,** 10–20 (2009).

183. Bahar Halpern, K. Veprik, A. Rubins, N. Naaman, O. & Walker, M. D. GPR41 gene expression is mediated by internal ribosome entry site (IRES)-dependent translation of bicistronic mRNA encoding GPR40 and GPR41 proteins, *J. Biol. Chem.* **287,** 20154–20163 (2012).

184. Nilsson, C. Reductions in adipose tissue and skeletal growth in rat adult offspring after prenatal leptin exposure, *Journal of Endocrinology* **176,** 13–21 (2003).

185. Xiong, Y. *et al.* Short-chain fatty acids stimulate leptin production in adipocytes through the G protein-coupled receptor GPR41, *Proc. Natl. Acad. Sci. U.S.A.* **101,** 1045–1050 (2004).

186. Zaibi, M. S. *et al.* Roles of GPR41 and GPR43 in leptin secretory responses of murine adipocytes to short chain fatty acids, *FEBS Lett.* **584,** 2381–2386 (2010).

187. Kimura, I. *et al.* Short-chain fatty acids and ketones directly regulate sympathetic nervous system via G protein-coupled receptor 41 (GPR41), *Proc. Natl. Acad. Sci. U.S.A.* **108,** 8030–8035 (2011).

188. Karaki, S.-i. *et al.* Short-chain fatty acid receptor, GPR43, is expressed by enteroendocrine cells and mucosal mast cells in rat intestine, *Cell Tissue Res.* **324,** 353–360 (2006).

189. Tazoe, H. *et al.* Expression of short-chain fatty acid receptor GPR41 in the human colon, *Biomed. Res.* **30,** 149–156 (2009).

190. Samuel, B. S. *et al.* Effects of the gut microbiota on host adiposity are modulated by the short-chain fatty-acid binding G protein-coupled receptor, Gpr41, *Proc. Natl. Acad. Sci. U.S.A.* **105,** 16767–16772 (2008).

191. Karaki, S.-i. *et al.* Expression of the short-chain fatty acid receptor, GPR43, in the human colon, *J. Mol. Histol.* **39,** 135–142 (2008).

192. Kaji, I. Karaki, S.-i. Tanaka, R. & Kuwahara, A. Density distribution of free fatty acid receptor 2 (FFA2)-expressing and GLP-1-producing enteroendocrine L cells in human and rat lower intestine, and increased cell numbers after ingestion of fructo-oligosaccharide, *J. Mol. Histol.* **42,** 27–38 (2011).

193. Sykaras, A. G. Demenis, C. Case, R. M. McLaughlin, J. T. & Smith, C. P. Duodenal enteroendocrine I-cells contain mRNA transcripts encoding key endocannabinoid and fatty acid receptors, *PLoS ONE* **7,** e42373 (2012).

194. Senga, T. *et al.* LSSIG is a novel murine leukocyte-specific GPCR that is induced by the activation of STAT3, *Blood* **101,** 1185–1187 (2003).

195. Smith, P. M. *et al.* The microbial metabolites, short-chain fatty acids, regulate colonic Treg cell homeostasis, *Science* **341,** 569–573 (2013).

196. Nøhr, M. K. *et al.* GPR41/FFAR3 and GPR43/FFAR2 as cosensors for short-chain fatty acids in enteroendocrine cells vs FFAR3 in enteric neurons and FFAR2 in enteric leukocytes, *Endocrinology* **154,** 3552–3564 (2013).

197. Anderson, J. W. *et al.* Health benefits of dietary fiber, *Nutr. Rev.* **67,** 188–205 (2009).

198. Hou, J. K. Abraham, B. & El-Serag, H. Dietary intake and risk of developing inflammatory bowel disease: a systematic review of the literature, *Am. J. Gastroenterol.* **106,** 563–573 (2011).

199. Macia, L. *et al.* Metabolite-sensing receptors GPR43 and GPR109A facilitate dietary fibre-induced gut homeostasis through regulation of the inflammasome, *Nat Commun* **6,** 6734 (2015).

200. Sina, C. *et al.* G protein-coupled receptor 43 is essential for neutrophil recruitment during intestinal inflammation, *J. Immunol.* **183,** 7514–7522 (2009).

201. Vieira, A. T. *et al.* A role for the gut microbiota and the metabolite sensing receptor GPR43 in a murine model of gout, *Arthritis & rheumatology (Hoboken, N.J.)* (2015).

202. Tolhurst, G. *et al.* Short-chain fatty acids stimulate glucagon-like peptide-1 secretion via the G-protein-coupled receptor FFAR2, *Diabetes* **61,** 364–371 (2012).

203. Bjursell, M. *et al.* Improved glucose control and reduced body fat mass in free fatty acid receptor 2-deficient mice fed a high-fat diet, *Am. J. Physiol. Endocrinol. Metab.* **300,** E211-20 (2011).

204. Lin, H. V. *et al.* Butyrate and propionate protect against diet-induced obesity and regulate gut hormones via free fatty acid receptor 3-independent mechanisms, *PLoS ONE* **7,** e35240 (2012).

205. Bellahcene, M. *et al.* Male mice that lack the G-protein-coupled receptor GPR41 have low energy expenditure and increased body fat content, *Br. J. Nutr.* **109,** 1755–1764 (2013).

Thesis Outline

The purpose of this work is to present main concepts in the exploration of cellular signaling with a special focus on signal transduction related to G protein-coupled receptors. Herein, I will explain the research question entailing context-relevant issues that requires our attentiveness, introduce the tools that are intended to provide the data basis to answer the question, describe the evidence from an experimental approach and highlight implications and consequences of the presented studies.

This thesis is subdivided into four sections.

Section I encompasses a detailed portray of a technology that is key for - or at least an integral part of - all following studies (chapter 1). Dynamic mass redistribution (DMR) represents a recently introduced method to obtain an integrative whole cell readout. The strengths and weaknesses of this novel technique are explained and its possible impact on the process of drug research is delineated.

Grundmann, M., and Kostenis, E. (2015) Label-free biosensor assays in GPCR screening. *Methods Mol. Biol.* 1272, 199–213

Section II elucidates the biology of the free fatty acid receptor 2 (FFA2). In the first publication we report on the disclosure of a new mechanism for modulating receptors using FFA2 as a model GPCR (chapter 2), whereas the second publication describes the pharmacosynthetic approach to generate and characterize a designer receptor of FFA2 to probe FFA2 signaling and physiology (chapter 3).

Grundmann, M., Hudson, B. D., Tikhonova, I. G., Smith, N. J., Sergeev. E., Mohr, K., Ulven, T., Milligan, G., Kenakin, T., Kostenis, E. (2015) A new mechanism for modulating 7TM receptor function: Sequentially activating ligands (SEALs). *Nat. Chem. Biol.* under revision

Hudson, B. D., Christiansen, E., Tikhonova, I. G., Grundmann, M., Kostenis, E., Adams, D. R., Ulven, T., and Milligan, G. (2012) Chemically engineering ligand selectivity at the free fatty acid receptor 2 based on pharmacological variation between species orthologs. *FASEB J.* 26, 4951–4965

Section III reports on the physiological and pathological function of the free fatty acid receptor 1 (FFA1) and methodological concerns about commonly used FFA1 detection techniques (chapter 4). Chapter 5 summarizes the discovery and characterization of potent and selective small molecule FFA1 agonists.

Wagner, R., Kaiser, G., Gerst, F., Christiansen, E., Due-Hansen, M. E., Grundmann, M., Machicao, F., Peter, A., Kostenis, E., Ulven, T., Fritsche, A., Häring, H.-U., and Ullrich, S. (2013) Reevaluation of fatty acid receptor 1 as a drug target for the stimulation of insulin secretion in humans. *Diabetes* 62, 2106–2111

Teutsch, C.-A., Panse, M., Grundmann, M., Kaiser, G., Kostenis, E., Häring, H.-U., and Ullrich, S. (2014) Detection of free fatty acid receptor 1 expression: the critical role of negative and positive controls. *Diabetologia* 57, 776–780

Christiansen, E., Due-Hansen, M. E., Urban, C., Grundmann, M., Schmidt, J., Hansen, S. V. F., Hudson, B. D., Zaibi, M., Markussen, S. B., Hagesaether, E., Milligan, G., Cawthorne, M. A., Kostenis, E., Kassack, M. U., and Ulven, T. (2013) Discovery of a potent and selective free fatty acid receptor 1 agonist with low lipophilicity and high oral bioavailability. *J. Med. Chem.* **56**, 982–992

Christiansen, E., Hansen, S. V. F., Urban, C., Hudson, B. D., Wargent, E. T., Grundmann, M., Jenkins, L., Zaibi, M., Stocker, C. J., Ullrich, S., Kostenis, E., Kassack, M. U., Milligan, G., Cawthorne, M. A., and Ulven, T. (2013) Discovery of TUG-770: A Highly Potent Free Fatty Acid Receptor 1 (FFA1/GPR40) Agonist for Treatment of Type 2 Diabetes. *ACS Med Chem Lett* **4**, 441–445

Christiansen, E., Due-Hansen, M. E., Urban, C., Grundmann, M., Schröder, R., Hudson, B. D., Milligan, G., Cawthorne, M. A., Kostenis, E., Kassack, M. U., and Ulven, T. (2012) Free fatty acid receptor 1 (FFA1/GPR40) agonists: mesylpropoxy appendage lowers lipophilicity and improves ADME properties. *J. Med. Chem.* **55**, 6624–6628

Section IV exemplifies the analysis of signal transduction at a *post-receptor* level. The first publication reveales non-canonical cyclic nucleotides as bona fide *second messenger* (chapter 6), while the second paper discloses the mode-of-action of the first GTP-entry inhibitor for a G protein (chapter7).

Beckert, U., Grundmann, M., Wolter, S., Schwede, F., Rehmann, H., Kaever, V., Kostenis, E., and Seifert, R. (2014) cNMP-AMs mimic and dissect bacterial nucleotidyl cyclase toxin effects. *Biochem. Biophys. Res. Commun.* **451**, 497–502

Schmitz, A.-L., Schrage, R., Gaffal, E., Charpentier, T. H., Wiest, J., Hiltensperger, G., Morschel, J., Hennen, S., Häußler, D., Horn, V., Wenzel, D., Grundmann, M., Büllesbach, K. M., Schröder, R., Brewitz, H. H., Schmidt, J., Gomeza, J., Galés, C., Fleischmann, B. K., Tüting, T., Imhof, D., Tietze, D., Gütschow, M., Holzgrabe, U., Sondek, J., Harden, T. K., Mohr, K., and Kostenis, E. (2014) A cell-permeable inhibitor to trap Gαq proteins in the empty pocket conformation. *Chem. Biol.* **21**, 890–902

Section I

Chapter 1: Dynamic mass redistribution

Prologue

The current or recent-past state in industrial drug research is built on the concept of target-based drug discovery[1,2]. This entails the processing of high-capacity, homogenous assays of cellular signaling endpoints using reconstituted cellular systems overexpressing a receptor (= target) of interest[3]. As a result, huge compound libraries can be screened in a high-throughput manner for prospected effects at the target protein providing reliable and easy to interpret results – representing an important means in the process of decision-making. Much effort has been made to miniaturize and speed up this process resulting in large yet highly cost-efficient screening campaigns. A major drawback of such powerful approaches is the unsatisfactory transferability of the assay results to the pathological situation that should ultimately been addressed. High attrition rates of drug candidates especially in later stages of the drug discovery process have been associated with a lack of knowledge about biological compound behavior derived from early stage data that are generated using artificially engineered cell systems[4]. Introduction of model systems for certain disease states already in early stages of drug discovery represents a diametrically oriented venture to tackle this problem[5–7]. While holding the promise of better predictability, this translational approach imposes high demands on data interpretation because of the multifactorial nature with greater inter- and intra-individual variation in natural biological systems. Provocatively, tissue or organ-based assays were methods of choice before the times of target-based drug discovery and, at the time, enabled the development of several groundbreaking medicines.

These considerations raise the question about the relevance of data from single endpoint assays, especially under the impression of a phenomenon that is increasingly recognized as functional selectivity[8–10]. Functionally selective compounds (= biased ligands) are fueling hopes for fine-tuned pharmacological intervention that specifically enable those signaling events that are beneficial but obviate those that are detrimental[11,12]. However, this requires in-depth insight into the complexity of physiological versus pathological signal transduction and their amalgamation in certain phenotypes, which is difficult to achieve but inextricably linked with basic biomedical research.

Label-free techniques are increasingly engaged in the field of life sciences[13]. The term label-free refers to the absence of any label or marker that is traditionally used to allow the detection of changes in intracellular *second messenger* level, the spatial approximation of certain signaling

partners or the relocation of distinct signaling molecules within cells to name only a few applications[1]. Unfortunately, label-based assays bear the risk of perturbing the outcome by altering the physiological behavior due to the introduced label[9].

One example of a label-free assay is a technology based on dynamic mass redistribution (DMR). Every cell reacts to a stimulus generally with a change in its cellular structure, mostly involving a cytoskeleton rearrangement. This activation is captured as DMR by an optical biosensor[14,15]. In addition to the label-free aspect, the DMR method provides a holistic view on the signal processes in living cells. Because this assay does not restrict the researcher's attention to a single intracellular event (such as the production of a specific *second messenger*), but instead allows the perception of the cellular reaction as a whole, it is ideally suited to explore widely ramified signal transduction networks[9,13,15]. Hence, DMR holds the promise to overcome the above mentioned obstacles by displaying whole cell responses non-invasively and in an unbiased fashion.

Because of deficient understanding about the events underlying the phenomenon of dynamic mass redistribution, this method is often referred to as a "black-box assay" that causes skepticism among decision-makers. Therefore, the DMR technique is rather underexploited and has not found broad application to date[16].

The publication in this chapter gives a comprehensive portray of the label-free DMR technique and provides a step-by-step protocol how to implement this method into laboratory routine experiments. Herein, the prevention of common mistakes and pitfalls that otherwise hamper good quality DMR readouts was emphasized in particular with the aim to reduce skepticism towards a wider deployment of this technology.

References

1. Kenakin, T. P. Cellular assays as portals to seven-transmembrane receptor-based drug discovery, *Nat Rev Drug Discov* **8,** 617–626 (2009).
2. Clark, R. L. *et al.* The Drug Discovery Portal: a resource to enhance drug discovery from academia, *Drug Discov. Today* **15,** 679–683 (2010).
3. Heilker, R. Wolff, M. Tautermann, C. S. & Bieler, M. G-protein-coupled receptor-focused drug discovery using a target class platform approach, *Drug Discov. Today* **14,** 231–240 (2009).
4. Hutchinson, L. & Kirk, R. High drug attrition rates--where are we going wrong?, *Nat Rev Clin Oncol* **8,** 189–190 (2011).
5. Moreno, L. & Pearson, A. D. J. How can attrition rates be reduced in cancer drug discovery?, *Expert Opin Drug Discov* **8,** 363–368 (2013).

6. Dick, E. Rajamohan, D. Ronksley, J. & Denning, C. Evaluating the utility of cardiomyocytes from human pluripotent stem cells for drug screening, *Biochem. Soc. Trans.* **38,** 1037–1045 (2010).
7. McKim, J. M. Building a tiered approach to in vitro predictive toxicity screening: a focus on assays with in vivo relevance, *Comb. Chem. High Throughput Screen.* **13,** 188–206 (2010).
8. Kenakin, T. & Miller, L. J. Seven transmembrane receptors as shapeshifting proteins: the impact of allosteric modulation and functional selectivity on new drug discovery, *Pharmacol. Rev.* **62,** 265–304 (2010).
9. Kenakin, T. A holistic view of GPCR signaling, *Nat. Biotechnol.* **28,** 928–929 (2010).
10. Galandrin, S. Oligny-Longpré, G. & Bouvier, M. The evasive nature of drug efficacy: implications for drug discovery, *Trends Pharmacol. Sci.* **28,** 423–430 (2007).
11. Kenakin, T. Collateral efficacy in drug discovery: taking advantage of the good (allosteric) nature of 7TM receptors, *Trends Pharmacol. Sci.* **28,** 407–415 (2007).
12. Rajagopal, S. Rajagopal, K. & Lefkowitz, R. J. Teaching old receptors new tricks: biasing seven-transmembrane receptors, *Nat Rev Drug Discov* **9,** 373–386 (2010).
13. Scott, C. W. & Peters, M. F. Label-free whole-cell assays: expanding the scope of GPCR screening, *Drug Discov. Today* **15,** 704–716 (2010).
14. Fang, Y. Frutos, A. & Verklereen, R. Label-Free Cell-Based Assays for GPCR Screening, *CCHTS* **11,** 357–369 (2008).
15. Lee, P. H. *et al.* Evaluation of dynamic mass redistribution technology for pharmacological studies of recombinant and endogenously expressed g protein-coupled receptors, *Assay Drug Dev Technol* **6,** 83–94 (2008).
16. Rocheville, M. Martin, J. Jerman, J. & Kostenis, E. Mining the potential of label-free biosensors for seven-transmembrane receptor drug discovery, *Prog Mol Biol Transl Sci* **115,** 123–142 (2013).

Chapter 14

Label-Free Biosensor Assays in GPCR Screening

Manuel Grundmann and Evi Kostenis

Abstract

About one third of currently marketed drugs target G protein-coupled receptors (GPCRs), which form the largest group of transmembrane proteins in the human proteome. GPCRs are ubiquitously expressed throughout the human body and play a pivotal role in a vast number of physiological and pathophysiological processes. Because of their intriguing complexity, their relevance, and yet unexploited potential in the treatment of diseases, GPCRs are studied intensively by both academic and industrial research labs.

Classical biochemical and molecular biology techniques, including traditional second messenger assays, took biomedical research to the next level and represent the fascinating power of in vitro pharmacology. While extremely efficient in capturing one clearly defined cellular readout, those methods do not authentically portray the events taking place in living cells as a whole; hence the process of drug discovery runs the risk to lose sight of a wider context already in early stages. Label-free cell-based assays hold the promise to overcome these shortcomings by considering cellular processes holistically. If combined with diligent assay adjustments, dynamic mass redistribution (DMR) technology is an excellent tool to investigate GPCR signaling. In this article we aim to provide guidance for scientists seeking for information on how to set up and optimize DMR assays with the objective to establish a knowledge base on deciphering integrated cellular readouts. For this reason we focus on a basic DMR protocol for the investigation of the long-chain fatty acid FFA1 receptor as a model family A GPCR and complement it with information that allow a sophisticated approach to more specialized scientific questions with the use of this comparatively novel method.

Key words Dynamic mass redistribution, DMR, Resonant waveguide grating, RWG, G protein-coupled receptor, Optical biosensor, Label-free, FFA1, Holistic readout, Integrated cell response, Real-time assay, Ligand bias

1 Introduction

Optical label-free biosensors based on resonant waveguide grating (RWG), also known as guided-mode grated resonance, arose in the 1990s and were primarily used to detect binding of target molecules to immobilized receptors or, more generally, to determine interaction between molecular partners [1, 2]. The phenomenon underlying the technique can be described as electromagnetic resonance and explained by a simplified design of the biosensor that

Duarte Miguel F. Prazeres and Sofia Aires M. Martins (eds.), *G Protein-Coupled Receptor Screening Assays*,
Methods in Molecular Biology, vol. 1272, DOI 10.1007/978-1-4939-2336-6_14,

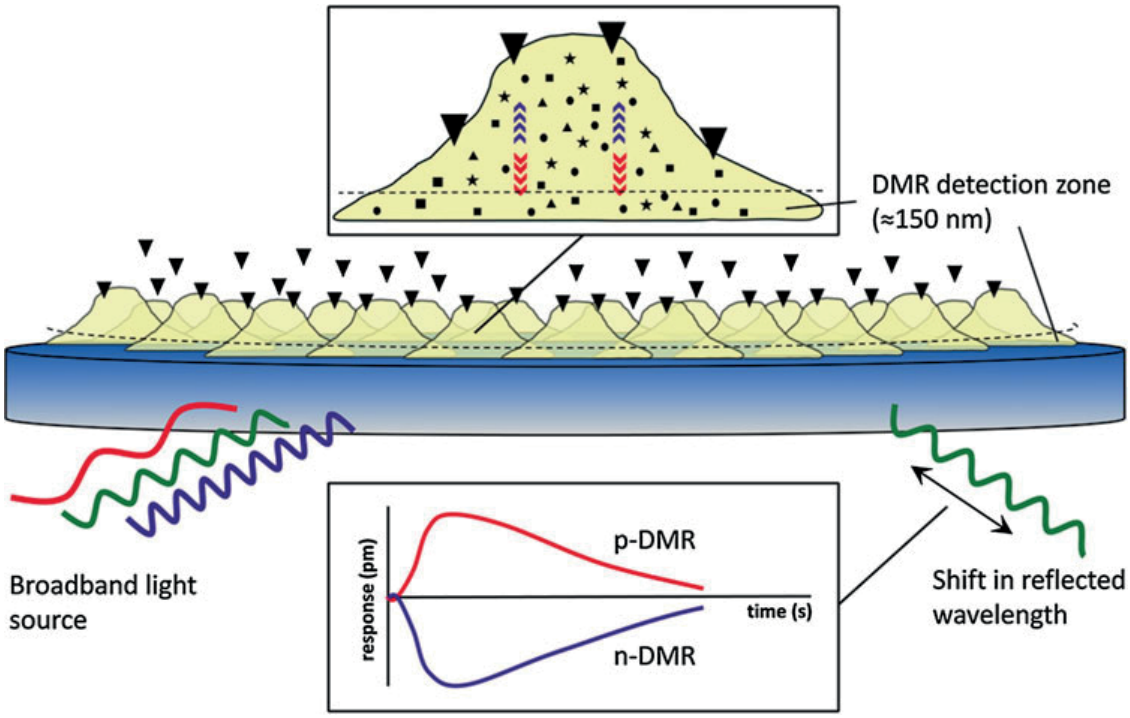

Fig. 1 The structural connection between a planar waveguide and a dielectric diffraction grating allows polarized light to couple in and out when illuminating the sensor under a defined angle. The high efficient coupling wavelength is designated resonance wavelength, whose propagation along the biosensor induces evanescent waves that extend into a zone approximately 150 nm above the sensor. Depending on the optical density of the system (biosensor and adjacent areas above the sensor), a shift of the reflected wavelength (Δpm) can be detected and recorded. In the case of a cell layer above the sensor, changes in optical density can occur by the redistribution of intracellular mass toward or away from the sensor, summarized as dynamic mass redistribution (DMR). Mass movements toward the sensor induce positive wavelength shifts (*p*-DMR), whereas movements away from the surface cause negative shifts of the reflected wavelength (*n*-DMR) at the bottom of the biosensor

contains an optical grating interlocked with a layer of special glass (Fig. 1). More recently, it was recognized that the capabilities of this technology go far beyond analyzing binding events toward a more in-depth understanding of cellular signaling [3–6].

Eukaryotic cells constantly exchange information with their environment. Transmembrane proteins such as G protein-coupled receptors (GPCRs), configured in a unique assembly of signaling pathway components, behave as molecular microprocessors that transduce signals from outside the cell into the cell's interior. For a proper communication, both internally and externally cellular systems need an orchestrated behavior which emerges as morphological transformation. This is often realized by a cytoskeleton-guided transport of molecules. The cellular architecture is controlled by a variety of effector molecules such as calmodulin or protein kinase A, activated by the classical second messenger calcium and cAMP, respectively. Hence, alpha-subunits of heterotrimeric G proteins like $G\alpha_s$, $G\alpha_q$, or $G\alpha_i$ but also $G\alpha_{12/13}$ modulate actin filament

structure within eukaryotic cells. Likewise, small GTPases such as Rho, Rac, or CDC42 and also Gβγ subunits interacting with PH domains (pleckstrin homology domains) are competent to regulate the cytoskeleton [7, 8]. In the field of GPCRs, cell-based assays capturing morphological rearrangement demonstrate the potential of the technology to aid the understanding of receptor biology and compound behavior [9].

The increasing mechanization and automation in drug discovery programs in the past with the aim to accelerate the process from target identification to lead identification raised high hopes for an advent of novel drugs. As a result of an intensified effort to understand the underlying pathophysiology of a given disease, the process of target validation has received much more attention. However, the reductionistic approach of taking a target out of a dysfunctioning context and confining it to a specific readout, often forced by genetic manipulation in an artificial biological environment, enabled researchers to run big screening campaigns testing millions of compounds with hitherto unprecedented efficiency. Despite diligent and rigorous preselection of possible drug candidates in this procedure, high dropout rates in preclinical and clinical stages cannot obscure the fact that these hopes were disappointed. There are various well-argued approaches to that problem [10, 11] and growing consensus about the necessity to investigate compound behavior in a more holistic manner, e.g., reflected in a multiple signaling pathway readout. This becomes even more important when considering the impact of cellular background and altered physiology in disease states on the compound pharmacology and receptor biology [12]. To address the demand for extensive profiling of receptor-modulating ligands, a new approach based on innovative assay designs or combinations of existing assay formats is needed.

The process of drug discovery in particular could benefit from the capabilities of the DMR technique. The label-free and holistic nature of the assay provides more pharmacologically relevant data, thus allows eliminating false-positive results from label-based assays, and improves significance in selectivity screenings. Cellular rearrangement plays a pivotal role as a common cellular phenotype in various diseases such as inflammatory disease, cancer, neurological diseases, and cardiovascular diseases (e.g., cardiac hypertrophy), since many signaling pathways converge at the level of cytoskeleton architecture [13]. Hence, the assay has the potential to detect all cellular events that translate into mass movement, such as (intra) cellular rearrangement or changes in cell morphology, as an integrated cellular response to various inputs. One major advantage of this assay format is the option to investigate test compounds in a native or primary cell setting that is closer to in vivo conditions. Especially the possibility to integrate tissues from patients, reflecting disease relevant conditions holds the promise to stimulate the

field of in vitro translational medicine and thereby addresses the issue of wasting time and money on the production of rather irrelevant data [14].

Furthermore, DMR assays can be automated for HTS purposes or other primary screens [15]. However, the main fields of application most likely are further pharmacological evaluation as an orthogonal assay platform, for example, in hit confirmation or in structure-activity relationship (SAR) studies. By combining the HTS compatibility with the unbiased perspective of dynamic mass redistribution on cell response, the DMR assay facilitates uncovering biased ligands, i.e., functionally selective ligands, more efficiently. A key advantage of this assay is the sensitivity to investigate biased signaling of GPCRs and functional selectivity of their ligands, features that are proposed to deliver more precise therapeutic benefit with reduced amount of side effects [16]. A study including a selection of molecular tool compounds extending the label-free assay allowed the dissection and characterization of all four G protein-mediated pathways and compared them with results from traditional endpoint assays [6].

An interesting possibility opens up by monitoring cellular response in real time. It is becoming increasingly evident that conceiving the spatiotemporal aspect of GPCR signaling solely as one isolated and linear event proves insufficient; in fact, recent data support the idea that signaling via GPCRs rather emerges as multiple signaling waves [17]. Research projects approaching kinetic questions could therefore benefit from this method.

Downside aspects of the technology go along with the unique features of an integrated, holistic view on cellular events. Sometimes referred to as "black box assay," the molecular mechanisms that account for the phenomenon of dynamic mass redistribution remain to be elucidated. As an integrated cell response, unperturbed DMR traces can be composed of on- and off-target effects. It is also possible that positive and negative DMR neutralize each other, and a net null signal would result that can lead to the misinterpretation as an indication of no biological effect. Without the appropriate molecular tools and the effort of different approaches like combining the label-free assay with other biological readouts, it can thus be challenging to decode DMR signatures. Also, high costs of biosensor plates might limit the widespread usability of this technology. Nevertheless, DMR is a powerful, highly versatile, and user-friendly technology platform that is applicable to a vast array of different cell types, ranging from overexpression to native cell systems, and that offers the great advantage of studying target protein behavior in the absence of any labels that may confound protein function. In this protocol, we exemplify the applicability of label-free DMR for analyzing real-time signaling of the long-chain fatty acid FFA1 receptor in different biological contexts.

2 Materials

1. Centrifuge with rotor for microplates.
2. 12-channel pipettor for washing 384-well plates.
3. 8-channel manifold to aspirate liquids from 384-well plates.
4. 75 cm^2 sterile cell culture flasks.
5. Cell line: Flp-In™ T-REx™ 293 cells, stably transfected with the human FFA1 receptor (for more detailed information regarding this cell system, please refer to the manufacturer's manual (http://www.lifetechnologies.com)).
6. Agonists: conjugated linolenic acids (CLA) as long fatty acids and the small molecule TUG-424.
7. FFA1-HEK cell medium: DMEM (Dulbecco's Modified Eagle's Medium), containing 10 % heat-inactivated fetal bovine serum (FBS), 1 % penicillin/streptomycin, 100 µg/mL hygromycin B, and 15 µg/mL blasticidin S.
8. Phosphate buffered saline (PBS): NaCl 8.01 g/L, KCl 0.20 g/L, $Na_2HPO_4 \times 2H_2O$ 1.78 g/L, KH_2PO_4 0.27 g/L, adjusted to pH 7.4 and sterilized.
9. Trypsin/EDTA: 0.05/0.02 % in PBS, sterile filtered.
10. Hank's balanced salt solution (HBSS): $CaCl_2$ 1.4 g/L, $MgCl_2 \times 6H_2O$ 1 g/L, $MgSO_4x7H_2O$ 1 g/L, KCl 4 g/L, KH_2PO_4 0.6 g/l, NaCl 80 g/L, $Na_2HPO_4x7H_2O$ 0.9 g/L, D-glucose 10 g/L.
11. HEPES 2-[4-(2-hydroxyethyl)piperazin-1-yl]ethanesulfonic acid).

2.1 Microplates and Biosensor instruments

1. Corning® Epic® biosensor (Corning).
2. PerkinElmer EnSpire® label-free multimode reader (PerkinElmer).
3. 384-well liquid handling station for compound transfer or for carrying out washing steps.
4. 384-well tips for use with a liquid handling robot.
5. Corning® Epic® biosensor (384-well, fibronectin-coated) microplates (Corning).
6. EnSpire®-LFC (384-well, fibronectin-coated) plate (PerkinElmer).
7. 384-well polypropylene microplate for compound dilutions.

3 Methods

Here, we present our standard protocol for basic investigation of the G protein-coupled receptor FFA1 (free fatty acid receptor 1), formerly described as GPR40 [18, 19], with the help of an optical label-free biosensor platform based on the phenomenon of dynamic mass redistribution (DMR). To this end, we use a HEK293 cell line inducibly expressing the receptor and both conjugated linolenic acids (CLA) as long-chain fatty acids and the selective small molecule TUG-424 as FFA1 agonists [20, 21]. For details about how to apply the DMR technology to decipher GPCR signaling using selective pathway inhibitors, refer to **Note 1**. To study cell lines endogenously expressing the receptor, *see* **Note 2.** In the following steps, all cell culture liquids and the biosensor plate are pre-warmed to 37 °C.

3.1 Preparation of Cells

1. Culture the cells in 75 cm^2 cell culture flasks in 15 mL growth medium. When cells have reached approximately 80 % confluency, aspirate the medium, rinse with 5 mL PBS to remove any residues of growth medium, and aspirate the buffer.
2. Subsequently, detach cells with 1 mL trypsin/EDTA (0.05 %/0.02 %) and count after addition of growth medium to stop trypsin-induced cell detachment.
3. Resuspend in the appropriate amount of growth medium containing 1 μg/mL doxycycline for receptor expression to achieve a cell density of 18,000 cells/30 μL, and seed 30 μL of this suspension into each well of a fibronectin-coated (*see* **Note 3**) 384-well biosensor plate.
4. Spin down the plate for 10 s at 150×*g* to assure cells settle onto the bottom of each well.
5. Let cells adhere for approximately 18 h at 37 °C, 5 % CO_2. Doxycycline will induce receptor expression during that time (for suspension mode *see* **Note 4**).
6. Make sure that cells have reached confluency (*see* **Note 5**) in the biosensor plate before removing the medium.
7. Wash cells twice with 30 μL HBSS (*see* **Note 6**) supplemented with 20 mM HEPES and the appropriate amount of DMSO if needed (*see* below) using a manifold or a liquid handling station. Make sure to adjust the total volume to 30 μL buffer in each well after the last washing step. Caution: When aspirating the washing buffer, avoid detachment of cells by either direct contact or mechanical disintegration of the cellular monolayer.
8. Keep the plate for at least 1 h at measurement temperature for equilibration purpose before starting the assay, preferably in a temperature-controlled DMR reader (*see* **Note 7**). Extend this time period in case of a starvation step (*see* **Note 8**).

3.2 Preparation of Compounds

1. Prepare the compounds to be tested in HBSS buffer (+20 mM HEPES) (*see* **Note 6**) at fourfold concentration. If a compound is solved in DMSO, make sure to adopt the correct DMSO amount in all concentration steps as well as in the washing buffer to avoid any solvent mismatch-induced DMR signals (*see* **Note 9**) when adding the compound solution to the cells during the assay.
2. Transfer 30 μL of compound solution in each well of a 384-well source plate, e.g., in triplicates. The exact amount depends on the geometry of the compound plate and the technical conditions of the liquid handling system.
3. Ensure to include negative controls (vehicle) as well as reliable positive controls to document cell viability, for example, by addressing endogenous receptors (ATP, PGE_1) or other targets (forskolin, FBS) and those to differentiate between on- and off-target effects (*see* **Note 10**).
4. Equilibrate the compound plate at the same temperature as the biosensor plate to avoid temperature-caused shifts in DMR response (*see* **Note 7**).

3.3 DMR Measurement

1. Start the measurement by recording a baseline read over 300 s. It might be necessary to record for a longer time period until the signal is stable, i.e., no or only weak shift in wavelength is detected (*see* **Note 11**).
2. Add 10 μL of compound solution to the biosensor plate using a liquid handling station.
3. Transfer the plate back to the reader and record DMR immediately after addition to capture rapid cell responses.
4. Monitor cellular response as long as needed—e.g., 1 h—then stop the measurement, save the run, and collect the data for further analysis.

3.4 Data Analysis

1. To illustrate cellular response, plot the wavelength shift in picometer (*y*-axis) against the measurement time (*x*-axis) (e.g., in GraphPad Prism®) with scatter for the respective replicates. Throughout this chapter, mean value + s.e.m. is shown.
2. Subtract the buffer trace (i.e., cell response upon addition of vehicle) from compound-induced traces to obtain baseline-corrected DMR traces (*see* **Note 11**).
3. Quantify the DMR response of agonist substances (for antagonist characterization, refer to **Note 12**) by extracting an appropriate parameter, e.g., max Δpm values in a certain time frame (*see* **Note 13**), and plot it against the concentration of compound to generate concentration-response curves by nonlinear regression to determine agonist potency and efficacy (Fig. 2).

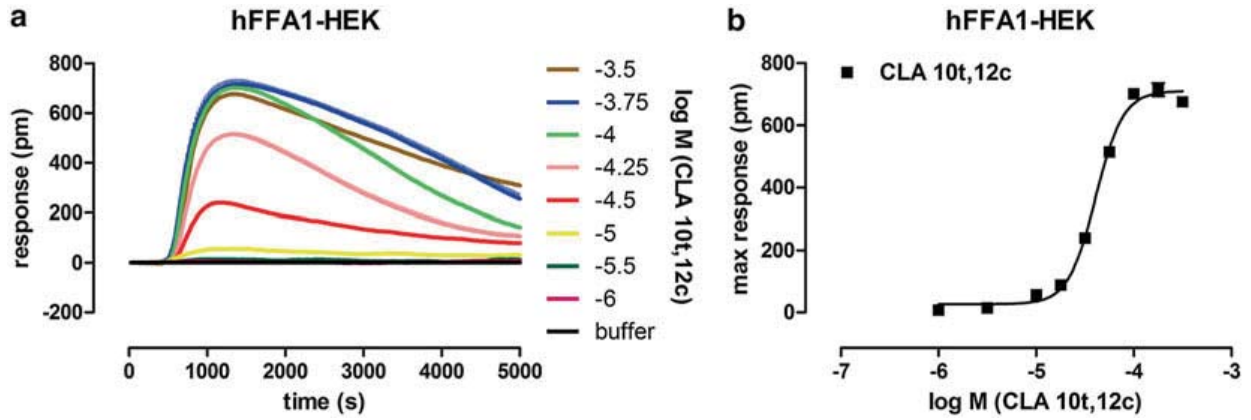

Fig. 2 DMR traces of hFFA1-HEK cells challenged with increasing concentration of the 10t,12c CLA-isomer (**a**). In this case, the maximum Δpm value between 0 and 1,500 s was taken to generate the concentration effect curve (pEC_{50}: 4.39) (**b**). Data from M. Grundmann, redrawn from ref. 20

4 Notes

1. Signal deconvolution: Since most GPCRs do not only signal via one pathway, the holistic readout of a DMR assay enables the researcher to uncover biased compounds, i.e., substances favoring one signaling route over the other. The information-rich DMR trace reflects a signaling fingerprint of the compound-cell interaction. Depending on the research question, it might be relevant to dissect these fingerprints with the help of pathway modulators such as PTX to inhibit $G\alpha_i$ and YM-254890 or FR900359 (=UBO-QIC) to inhibit $G\alpha_q$ proteins [22–24] (http://www.pharmbio.uni-bonn.de/signaltransduktion). The FFA1 receptor is predominantly coupled to $G\alpha_q$ proteins as revealed by FFA1-HEK cells that were pretreated with YM-254890 for 1 h in the biosensor plate before the assay. However, the use of PTX, which is present in the medium during 18–24 h before the assay, also uncovers a substantial contribution of $G\alpha_i$ proteins to the overall cell response upon stimulation with the FFA1 agonist TUG-424 (Fig. 3).
2. Impact of cellular background: As mentioned earlier, the DMR technology entails the advantage to investigate GPCRs in a variety of cell systems including primary, native, and recombinant cell lines. Since the FFA1 receptor is abundantly expressed in pancreatic beta cells, it is possible to use dissociated islets isolated from mouse pancreas and the native rat beta cell line INS-1E endogenously expressing the FFA1 receptor (Fig. 4).
3. Plate coating: Depending on the cellular background, it might be necessary to use extracellular matrix (ECM) or polymer-coated biosensor plates to establish a firm attachment in order to allow for uniform cellular behavior, such as cell movement.

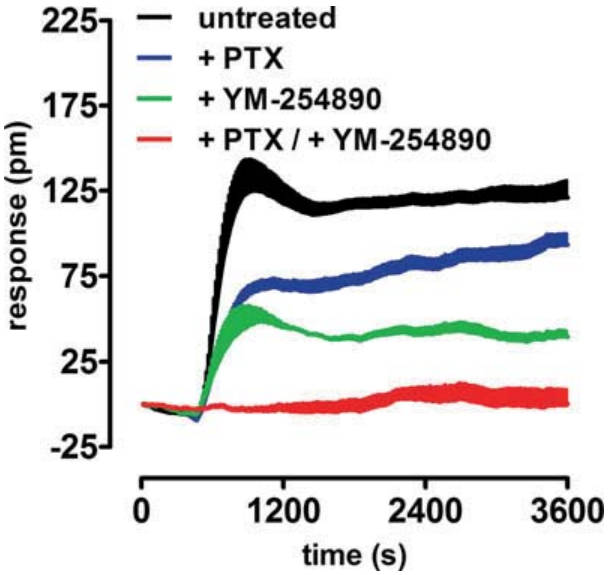

Fig. 3 Dissection of DMR response with pathway inhibitors in FFA1-HEK cells stimulated with 3 μM of FFA1 agonist TUG-424. The overall DMR signal is composed of both $G\alpha_q$ and $G\alpha_i$ proteins as shown by pretreatment with $G\alpha_i$ inhibitor PTX (5 ng/mL) and/or the selective $G\alpha_q$ inhibitor YM-254890 (300 nM), each of which partially reduce the DMR response. The combination of the inhibitors, however, completely abolishes the signal. Redrawn from ref. 6

Matrix coatings are likely to also influence growth, differentiation, and overall cellular function. Preliminary tests and the experience with the particular cell culture will help to decide which coating material and cells will work in harness. Coating or even co-coating plates on your own with the material of your choice is possible, but their suitability has to be determined in each case.

4. Adherent vs. suspension mode: It is also possible to perform DMR experiments in suspension mode, e.g., for nonadherent cells or some primary cells. For this purpose, cells are prepared according to specific protocols for isolation and purification. A higher cell number is required when running the assay in suspension mode (about threefold compared to adherent cells). The appropriate cell number is reconstituted in the assay buffer (e.g., HBSS + 20 mM HEPES), and 30 μL are seeded into each well of a 384-well biosensor plate. The plate is centrifuged subsequently at 150 × *g* for 10 s to assure that cells are positioned in the bottom part of the well, i.e., in close proximity to the biosensor surface. The subsequent steps correspond to the protocol for adherent cells. Depending on the cell system and the coating, interaction between the cells and the coating material might occur which can be displayed in a transient DMR response. This issue is encountered by an extended incubation time. Note that the DMR traces obtained from suspension mode can differ significantly from those in adherent mode

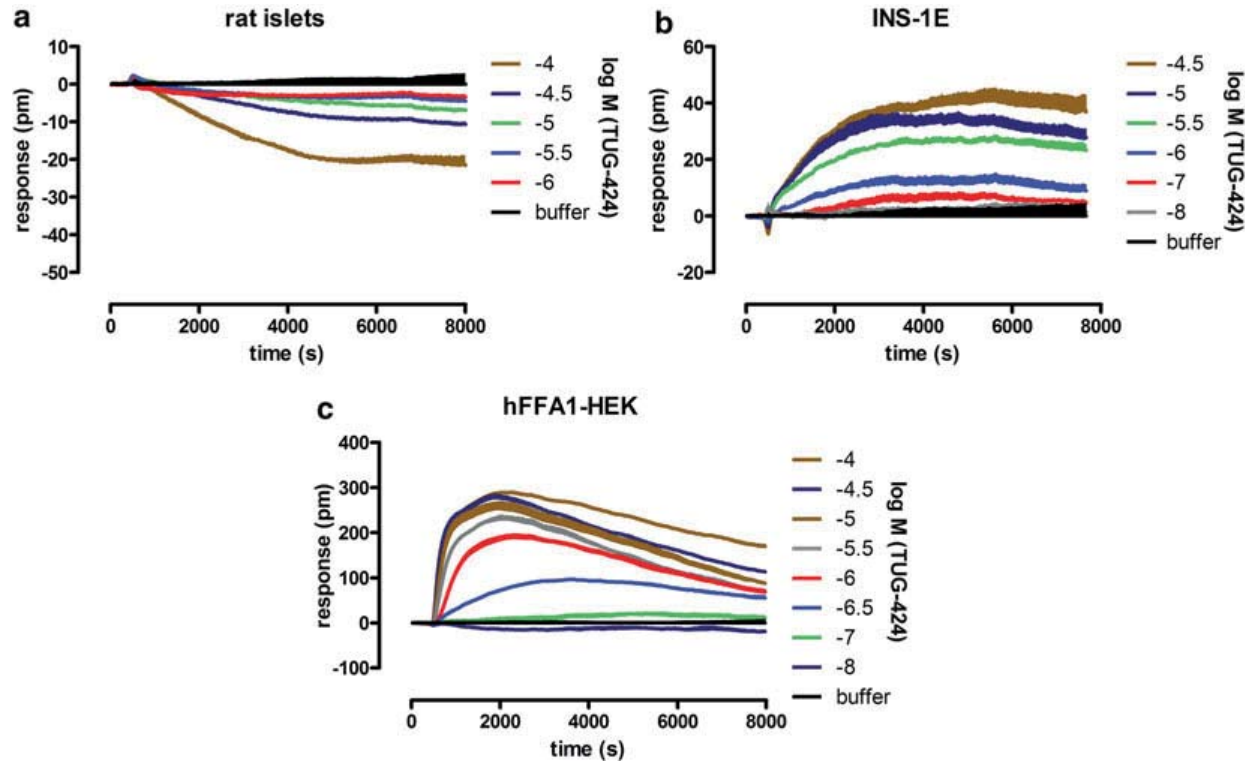

Fig. 4 Primary, native, and recombinant cell lines demonstrate the versatility of the assay platform. Rat islets were dissociated with trypsin and measured 6 days after seeding into the biosensor plate (**a**). INS-1E and FFA1-HEK cells were prepared according to the standard protocol with 30,000 cells/well (INS-1E) (**b**) and 18,000 cells/well (FFA1-HEK) (**c**). The cells were then stimulated with the FFA1 agonist TUG-424 and DMR response was recorded. Different cellular backgrounds can have great impact on the behavior in the assay. Note the different *y*-axis scaling! Data from M. Grundmann, University of Bonn, unpublished observations

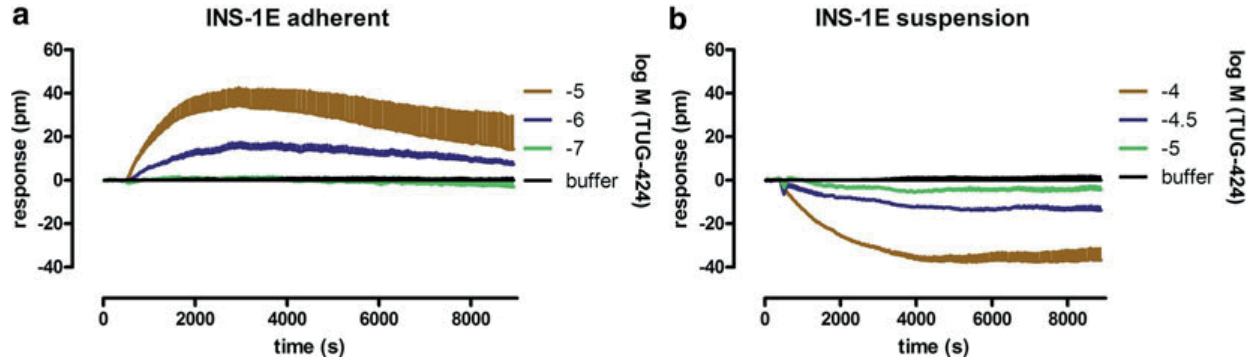

Fig. 5 Rat beta cell line INS-1E endogenously expressing FFA1 and treated with FFA1 agonist TUG-424 shows positive DMR if growing adherent (30,000 cells/well) (**a**) and negative DMR when in suspension mode (90,000 cells/well) (**b**). Data from M. Grundmann, University of Bonn, unpublished observations

(and it might therefore be advisable to choose alternative parameters for data analysis) (Fig. 5).

5. Confluency: Critical steps in optimizing a DMR protocol include growth conditions and cell number in the biosensor plate, because intercellular interaction greatly influences the cell response. As a starting point for assay optimization, always

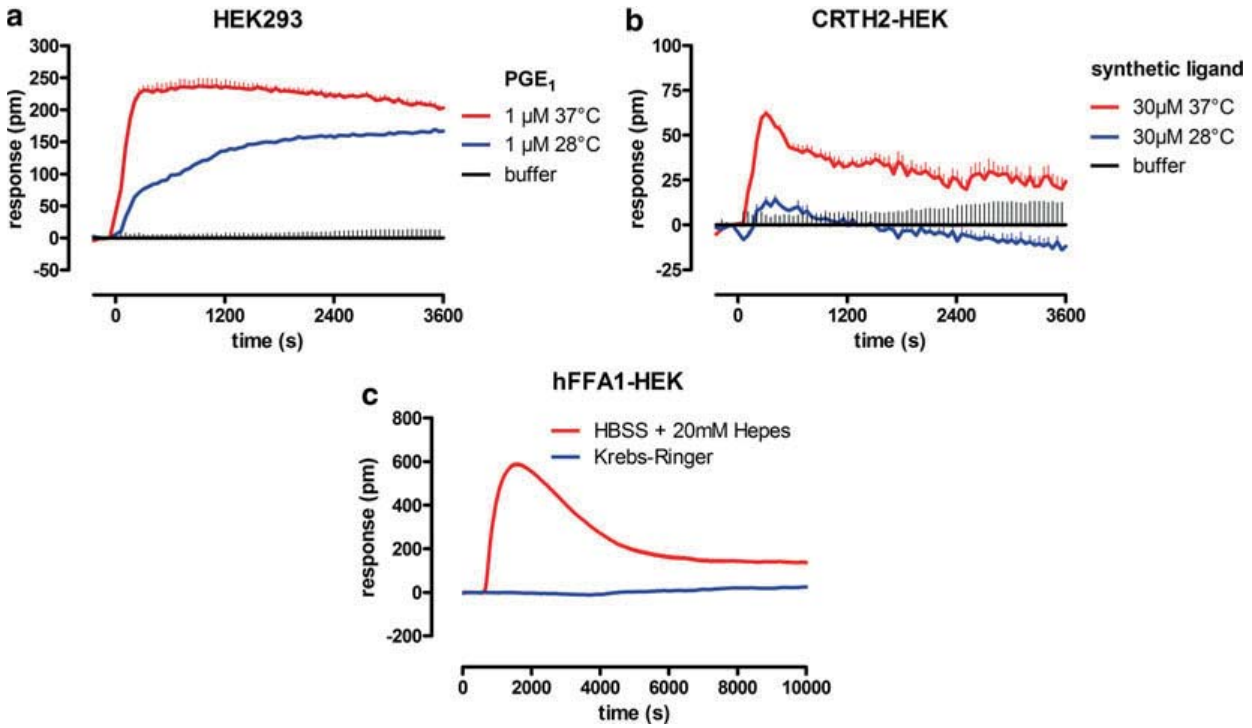

Fig. 6 Influence of temperature and buffer composition on the DMR assay. At higher assay temperatures, DMR signals appear accelerated and with greater amplitude (prostaglandin E1 activating EP2/4 receptors endogenously expressed in HEK293 cells) (**a**). A small molecule CRTH2 agonist induces DMR in HEK cells stably transfected with the CRTH2 receptor at physiological temperature but not at 28°C (**b**). Changing the assay buffer can have great impact on DMR signals by either lowering the cellular responsiveness or limiting the solubility of test compound. Depicted are DMR responses of FFA1-HEK cells stimulated with 100 µM of the 9c,11t CLA-isomer in standard HBSS buffer or Krebs-Ringer buffer (**c**). Data from M. Grundmann and R. Schröder, University of Bonn, unpublished observations

aim for a confluent cellular monolayer with nicely attached cells whose phenotype resembles their usual morphology. To achieve this, it might be necessary to vary growth medium additives, coating material, and especially the cell number.

6. Buffer influence: Changing the assay buffer is possible, but should be made with caution. The system comprising biosensor, cells and compounds might might react differently under modified buffer conditions. Solubility of test compounds can be limited in one buffer and as a result, can greatly affect DMR response (Fig. 6c). However, varying assay buffers is suggested as part of an assay optimization process.
7. Temperature (Fig. 6a, b): Optical density and accordingly the shift in wavelength as the readout of DMR assays are highly sensitive to changes in temperature. It is therefore recommended to assure a uniform temperature throughout the measurement, i.e., minimize temperature differences between test plate and compound plate to be transferred; keep the plates at the same temperature for a sufficient time to ensure temperature equilibration. Otherwise, artifacts such as a wavelength

shift or drift can occur, emerging under negative control conditions such as vehicle addition. Since temperature can be distributed unevenly over the test plate (edge effects), it is recommended to position negative controls randomly over the plate. In addition to system-related effects, temperature has significant impact on overall cellular function as well. Higher temperature generally leads to higher signal amplitude and accelerated kinetics of DMR signals. To some degree, this also implies an extended sensitivity to weak agonists to be detected in a threshold-based screening (Fig. 6b). Note that under different temperature conditions, an expanded cellular repertoire can be displayed that might also complicate interpretation of DMR responses, for example, in signaling pathway decoding.

8. Starvation: Keeping the cells under starvation conditions for varying time periods before the assay (e.g., serum starvation in serum-free medium or in the assay buffer) can also have an impact on cellular response in the DMR assay. Although not generally applicable, especially those experimental setups that suffer from a small assay amplitude may benefit from starvation techniques to gain signal enhancement.
9. DMSO mismatch: DMSO artifacts generally recognized as sharp spikes (up to thousands of Δpm) occur if the DMSO amount in the compound solution is different from that in the assay buffer surrounding the cells. Adjust the DMSO concentration in all assay solutions conscientiously, because the assay is very DMSO sensitive! Avoid DMSO concentrations way above 1.2 %! The DMR technology is less sensitive to other solvents such as ethanol.
10. On- and off-target effects: The holistic nature of the method can make it challenging to differentiate between on- and off-target effects. To trace a given DMR response back to a specific molecular target, it is necessary to include negative controls in the setup. In the described protocol, we could use cells that were not induced with doxycycline and thus do not express our target protein on the cell surface. In the case of primary cells, knockout material would be an appropriate negative control. Another possibility is the use of a target-specific antagonist that is capable of blocking the DMR response of an agonist (*see* **Note 12**). Furthermore—in the absence of suitable pharmacological inhibitors—cross-desensitization or gene silencing methods may be applied to help attribute a DMR signal to a certain cellular event.
11. Buffer control: The course of the buffer signal can give insight into the overall cellular behavior such as detachment from the plate surface as well as temperature effects, which can result in a DMR drift over the time. Normally, these events can be prevented by optimizing cell culture conditions (e.g., cell

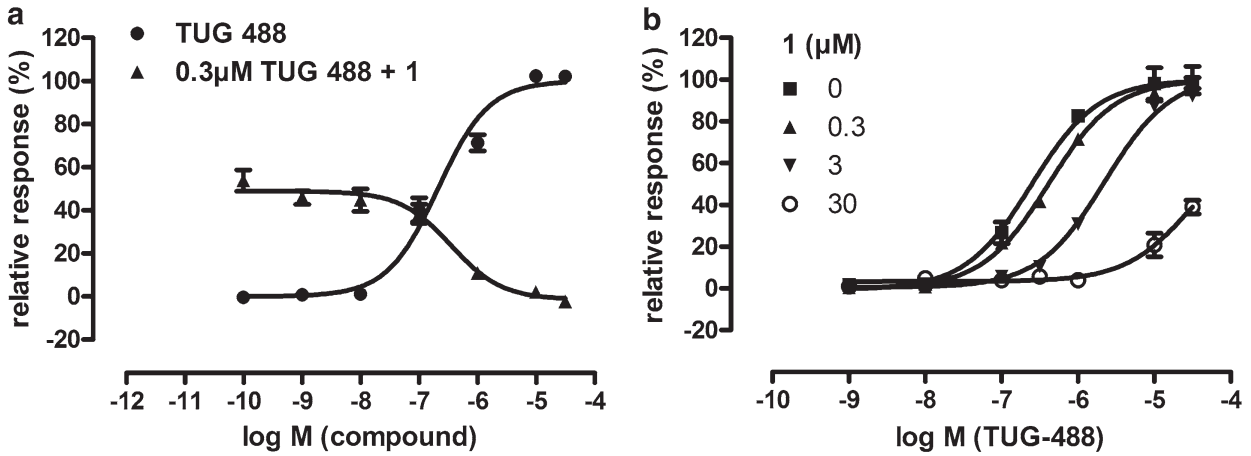

Fig. 7 Analysis of the FFA1 antagonist **1** [26] competing with small molecule FFA1 agonist TUG-488 [27]. A pIC_{50} of 6.45 can be determined for **1** by inhibition curve (**a**); Schild analysis reveals competitive/surmountable antagonism of **1** (**b**). Data from M. Grundmann, unpublished observations

density, plate-coating, media additives, etc.) or measurement options (e.g., temperature equilibration, time, and accuracy).

12. Antagonist mode: The DMR technique is perfectly suited for characterizing antagonists as well. Besides standard determination of IC_{50}-values or the mode of action (competitive, non-competitive, uncompetitive, inverse agonist, partial agonist), it is also possible to describe the kinetic profile of a test substance. Real-time DMR recordings after antagonist addition to agonist-induced cell responses allow the user to gain insight into kinetic features of test compounds or receptors (see, e.g., ref. 25). A basic protocol to determine the mode of action of an antagonist involves a two-step addition. In the first step, after washing the cells, increasing concentrations of antagonist are added, and DMR is recorded to detect any cellular response upon antagonist application. In the second step, after preincubation with antagonist, the agonist is added. After DMR measurement and basic data analysis, an inhibition curve or a Schild regression analysis can be performed to further describe antagonist parameters and mode of action (Fig. 7).
13. Data quantification: Parameters for data quantification range from peak value at a certain time point or within a defined time frame, the area under curve (AUC) between certain time points or steepness of a tangent to the initial DMR trace to capture kinetic compound behavior. In certain cases, the real-time readout enables the researcher to distinguish between multiple phases in cell response. The number, the duration, or the time needed to pass one phase adds to the list of possible quantification parameters. Since the content-rich DMR readout can appear highly complex and multiphasic, we recommend to address the issue of quantification on a case-by-case basis (Fig. 8).

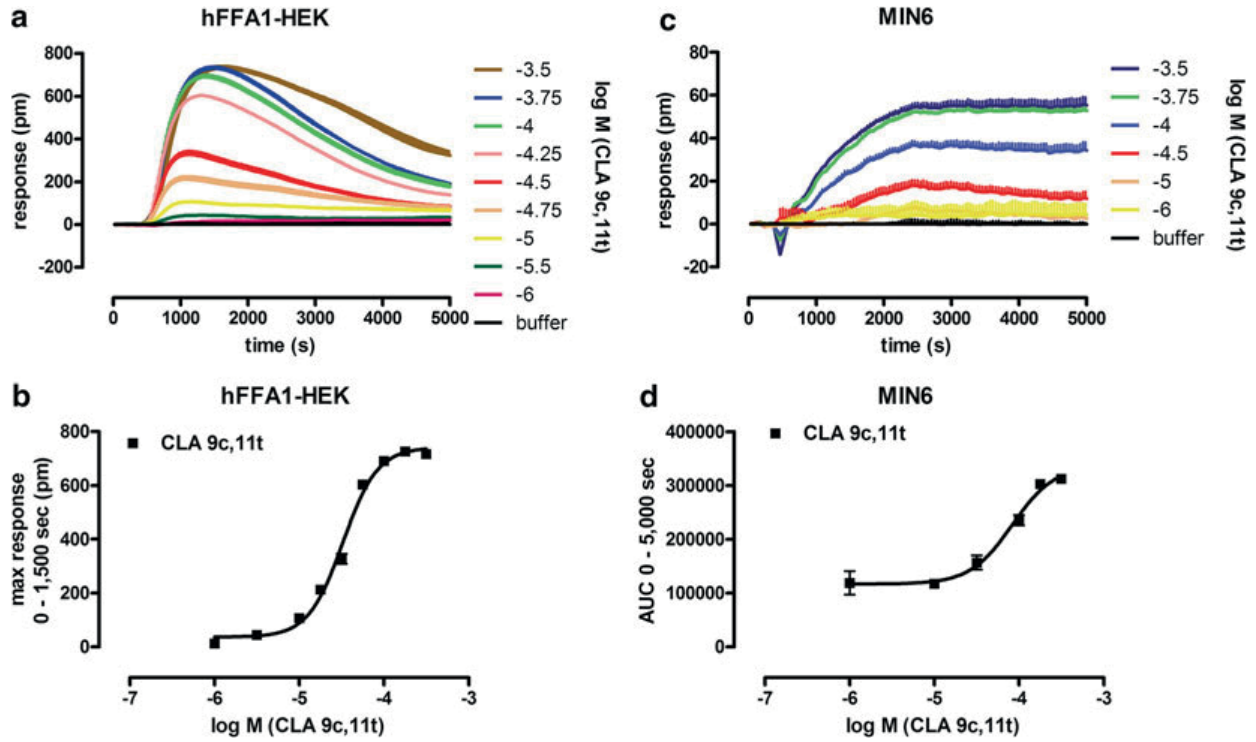

Fig. 8 The parameter used to quantify the cell response depends on the appearance of the DMR traces. One possibility is to calculate the peak Δpm value between 0 and 1,500 s for the HEK cells (18,000 cells/well, pEC_{50}: 4.49) (**a**, **b**) and the AUC between 0 and 5,000 s for the slower response in the MIN6 cell line (20,000 cells/well, pEC_{50}: 4.08) (**c**, **d**). Both cell lines were treated with increasing concentrations of the 9c,11t-isomer of CLA. Data from M. Grundmann, University of Bonn, unpublished observations

References

1. Wang SS, Magnusson R, Bagby JS et al (1990) Guided-mode resonances in planar dielectric-layer diffraction gratings. J Opt Soc Am A 7:1470. doi:10.1364/JOSAA.7.001470
2. Soria S, Katchalski T, Teitelbaum E et al (2004) Enhanced two-photon fluorescence excitation by resonant grating waveguide structures. Opt Lett 29:1989–1991
3. Fang Y, Ferrie AM, Fontaine NH et al (2006) Resonant waveguide grating biosensor for living cell sensing. Biophys J 91:1925–1940. doi:10.1529/biophysj.105.077818
4. Jiang J, Ganesh T, Du Y et al (2010) Neuroprotection by selective allosteric potentiators of the EP2 prostaglandin receptor. Proc Natl Acad Sci U S A 107:2307–2312. doi:10.1073/pnas.0909310107
5. Verrier F, An S, Ferrie AM et al (2011) GPCRs regulate the assembly of a multienzyme complex for purine biosynthesis. Nat Chem Biol 7:909–915. doi:10.1038/nchembio.690
6. Schröder R, Janssen N, Schmidt J et al (2010) Deconvolution of complex G protein–coupled receptor signaling in live cells using dynamic mass redistribution measurements. Nat Biotechnol 28:943–949. doi:10.1038/nbt.1671
7. Seasholtz TM, Majumdar M, Brown JH (1999) Rho as a mediator of G protein-coupled receptor signaling. Mol Pharmacol 55:949–956
8. Touhara K, Inglese J, Pitcher JA et al (1994) Binding of G protein beta gamma-subunits to pleckstrin homology domains. J Biol Chem 269:10217–10220
9. Lee PH, Gao A, van Staden C et al (2008) Evaluation of dynamic mass redistribution technology for pharmacological studies of recombinant and endogenously expressed g protein-coupled receptors. Assay Drug Dev Technol 6:83–94. doi:10.1089/adt.2007.126
10. Butcher EC (2005) Can cell systems biology rescue drug discovery? Nat Rev Drug Discov 4:461–467. doi:10.1038/nrd1754
11. van der Greef J, McBurney RN (2005) Innovation: rescuing drug discovery: in vivo

systems pathology and systems pharmacology. Nat Rev Drug Discov 4:961–967. doi:10.1038/nrd1904

12. Kenakin T (2002) Recombinant roulette versus the apparent virtues of 'natural' cell receptor systems: receptor genotypes versus phenotypes. Trends Pharmacol Sci 23: 403–404
13. Siehler S (2007) G 12/13-dependent signaling of G-protein-coupled receptors: disease context and impact on drug discovery. Expert Opin Drug Discov 2:1591–1604. doi:10.1517/17460441.2.12.1591
14. Goldbard S (2006) Bringing primary cells to mainstream drug development and drug testing. Curr Opin Drug Discov Devel 9(1): 110–116
15. Dodgson K, Gedge L, Murray D et al (2009) A 100K well screen for a muscarinic receptor using the Epic® label-free system – a reflection on the benefits of the label-free approach to screening seven-transmembrane receptors. J Recept Signal Transduct Res 29:163–172. doi:10.1080/10799890903079844
16. Violin JD, Lefkowitz RJ (2007) Beta-arrestin-biased ligands at seven-transmembrane receptors. Trends Pharmacol Sci 28:416–422. doi:10.1016/j.tips.2007.06.006
17. Irannejad R, Tomshine JC, Tomshine JR et al (2013) Conformational biosensors reveal GPCR signalling from endosomes. Nature 495:534–538. doi:10.1038/nature12000
18. Briscoe CP, Tadayyon M, Andrews JL et al (2003) The orphan G protein-coupled receptor GPR40 is activated by medium and long chain fatty acids. J Biol Chem 278:11303–11311. doi:10.1074/jbc.M211495200
19. Itoh Y, Kawamata Y, Harada M et al (2003) Free fatty acids regulate insulin secretion from pancreatic beta cells through GPR40. Nature 422:173–176. doi:10.1038/nature01478
20. Schmidt J, Liebscher K, Merten N et al (2011) Conjugated linoleic acids mediate insulin release through islet G protein-coupled receptor FFA1/GPR40. J Biol Chem 286: 11890–11894. doi:10.1074/jbc.C110.200477
21. Christiansen E, Urban C, Merten N et al (2008) Discovery of potent and selective agonists for the free fatty acid receptor 1 (FFA 1 / GPR40), a potential target for the treatment of type II diabetes. J Med Chem 51:7061–7064. doi:10.1021/jm8010178
22. Takasaki K, Shoun H, Yamaguchi M et al (2004) Fungal ammonia fermentation, a novel metabolic mechanism that couples the dissimilatory and assimilatory pathways of both nitrate and ethanol. Role of acetyl CoA synthetase in anaerobic ATP synthesis. J Biol Chem 279:12414–12420. doi:10.1074/jbc.M313761200
23. Hennen S, Wang H, Peters L et al (2013) Decoding signaling and function of the orphan G protein-coupled receptor GPR17 with a small-molecule agonist. Sci Signal 6:ra93. doi:10.1126/scisignal.2004350
24. Nesterov A, Hong M, Hertel C et al (2010) Screening a plant extract library for inhibitors of cholecystokinin receptor CCK1 pathways. J Biomol Screen 15:518–527. doi:10.1177/1087057110369702
25. Deng H, Wang C, Su M et al (2012) Probing biochemical mechanisms of action of muscarinic M3 receptor antagonists with label-free whole cell assays. Anal Chem 84:8232–8239. doi:10.1021/ac301495n
26. Humphries PS, Benbow JW, Bonin PD et al (2009) Synthesis and SAR of 1,2,3,4-tetrahydroisoquinolin-1-ones as novel G-protein-coupled receptor 40 (GPR40) antagonists. Bioorg Med Chem Lett 19:2400–2403. doi:10.1016/j.bmcl.2009.03.082
27. Christiansen E, Due-Hansen ME, Urban C et al (2013) Discovery of a potent and selective free fatty acid receptor 1 agonist with low lipophilicity and high oral bioavailability. J Med Chem 56:982–992. doi:10.1021/jm301470a

Epilogue

In this chapter, we presented a comprehensive protocol to setup DMR experiments ranging from a basic to an advanced design. Research object was the FFA1 receptor because it is well suited to demonstrate the broad applicability of the DMR method. FFA1 receptor signaling was studied in a recombinant (HEK293) as well as in a native (INS-1E) and a primary (pancreatic rat islets) cell system using both long-chain fatty acids as endogenous ligands as well as synthetic small molecule agonists, thereby reflecting the flexibility of the DMR assay technology. Evidently, taking advantage of the unbiased perspective of the DMR assay, the FFA1 receptor could be classified as promiscuously coupling to both the $G\alpha_q$ and $G\alpha_i$ protein subfamilies. The combination of selective FFA1 agonists and pathway-specific signal transduction inhibitors (selective G protein inhibitors: PTX and FR900359 (= UBO-QIC)) revealed a shared, PTX- and FR900359-sensitive signaling behavior.

Hence, label-free is applicable to a broad set of biological systems and it remains to be seen how this technology integrates into the recent return of phenotypic pharmacology[1,2]. With its holistic approach it fulfills all requirements to play an integral part in translational drug discovery and to shape the process from a reductionist to a holistic analysis of cellular readouts[3]. Since this technology is principally able to capture all facets of cell signaling differences, samples of cells or tissue specimen from patients might also be applicable and could thus stimulate the change of mindset from artificial *in vitro* conditions to a pathologically relevant level of investigation[4,5].

Label-free assays offer broad pathway coverage and delineate an integrated cell response. As a corollary, texture-rich DMR signatures can pose a challenge to analyze. Auspiciously, the DMR technology can generally be hooked up with all kinds of cell manipulating methods such as genetic techniques: *Knock-In*, *Knock-Out* or *Knock-Down*, mutational approaches or pharmacological perturbation, whereby the entire register from reversal, irreversible, competitive or allosteric inhibitors might be employed. Therefore, it is tempting to envision a “developer’s toolkit” to interpret label-free signatures and decipher pathway usage. For the elucidation of GPCR-related signal transduction a starting point could be the availability of compounds that selectively modulate the activation state of G proteins[6]. In this regard, the specific inhibition of certain G protein subfamilies appears particularly attractive to further elucidate G protein-mediated but also putative G protein-independent GPCR-mediated signaling.

Further advantages of label-free assays, that could only be discussed tangentially in the aforementioned publication, are the support of structure-activity-relationship (SAR) studies or mode-of-action (MoA) studies[7], the ability to conduct receptor panning studies to functionally determine which receptors are expressed on certain cells or the possibility to cross-validate a compound of

interest at multiple receptor subtypes and, in particular, check for potential off-target effects. Since the optical biosensor is highly sensitive to changes of optical density directly above the growing surface, the DMR technology can also be used to detect changes in cell adherence and confluence and might therefore applicable for toxicity screens[1,8].

Finally, the capability of the DMR assay to monitor cell response in real time should be emphasized[9]. This label-free readout elegantly provides valuable insight into dynamic aspects of cell activation that would be otherwise arduous to acquire[10,11]. In the following chapter, we profoundly exploit this property to discover a new mechanism of GPCR activation by a small molecule GPCR modulator.

References

1. Rocheville, M. Martin, J. Jerman, J. & Kostenis, E. Mining the potential of label-free biosensors for seven-transmembrane receptor drug discovery, *Prog Mol Biol Transl Sci* **115,** 123–142 (2013).
2. Scott, C. W. & Peters, M. F. Label-free whole-cell assays: expanding the scope of GPCR screening, *Drug Discov. Today* **15,** 704–716 (2010).
3. Kenakin, T. A holistic view of GPCR signaling, *Nat. Biotechnol.* **28,** 928–929 (2010).
4. Martin, J. Addressing attrition in early drug discovery by label-free methodologies: receptor pharmacology in native cells. *Int Drug Discov,* 38–45 (2010).
5. McGuinness, R. Label-free cell-based assays bring greater biorelevance to early drug discovery, *Assay Drug Dev Technol* **7,** 191–193 (2009).
6. Schröder, R. *et al.* Deconvolution of complex G protein-coupled receptor signaling in live cells using dynamic mass redistribution measurements, *Nat. Biotechnol.* **28,** 943–949 (2010).
7. Henstridge, C. M. *et al.* GPR55 ligands promote receptor coupling to multiple signalling pathways, *Br. J. Pharmacol.* **160,** 604–614 (2010).
8. McKim, J. M. Building a tiered approach to in vitro predictive toxicity screening: a focus on assays with in vivo relevance, *Comb. Chem. High Throughput Screen.* **13,** 188–206 (2010).
9. Atienza, J. M. *et al.* Dynamic and label-free cell-based assays using the real-time cell electronic sensing system, *Assay Drug Dev Technol* **4,** 597–607 (2006).
10. Pei, J. Yin, N. Ma, X. & Lai, L. Systems biology brings new dimensions for structure-based drug design, *J. Am. Chem. Soc.* **136,** 11556–11565 (2014).
11. Simpson, P. B. & Wafford, K. A. New directions in kinetic high information content assays, *Drug Discov. Today* **11,** 237–244 (2006).

Section II

Chapter 2: Sequentially activating ligands

Prologue

GPCRs belong to the most successful targets in the history of pharmacological intervention and comprise the largest group of membrane proteins[1–3]. Until very recently, only three groups of ligands did exist for the modulation of GPCRs. These are i) *orthosteric*, ii) *allosteric* and iii) *bitopic ligands*[4–7]. In this chapter we introduce a fourth class of ligands: iv) *Sequentially Activating Ligands (SEALs)*. These ligands are characterized by a stepwise activation mode of the receptor. By binding to multiple binding sites, SEALs initiate signaling from each site and can thus direct temporally coordinated signaling.

The compound 4-CMTB was discovered among several phenylacetamides in a high-throughput-screening to find selective FFA2 ligands and was subsequently characterized as an allosteric ligand, i.e. it modulates orthosterically-mediated FFA2 activation while additionally activating the receptor on its own[8] (ago-PAM). Intriguingly, efforts to optimize the compound by structural variations and to determine the actual binding site at the FFA2 receptor were inconclusive[9–11].

Allosteric ligands are preferred structures to target closely related GPCR subtypes that cannot be selectively targeted with an orthosteric-oriented drug discovery approach[12]. Several positive aspects of allosteric ligands have already been outlined in the introduction but there are also disadvantages of allosteric ligands, of which lack of efficacy in the absence of the orthosteric ligand is a major concern. However, this is only true for pure allosteric ligands but not those who show intrinsic efficacy on their own (e.g. allosteric agonists or ago-PAMs)[13]. This mode-of-action is especially interesting for diseases, in which endogenous agonist tone is low, such as Parkinson's or Alzheimer's disease[14].

Bitopic ligands are ligands that span two spatially separated binding sites at a receptor with one molecule that consists of two bridged pharmacophores[6,7,15]. This construction allows for targeting of two sites at the same time and takes advantage of different compound behavior at these two sites. For example, this could mean a subtype selective targeting by exploiting the structurally less conserved allosteric binding site within a group of closely related receptors and simultaneously inducing receptor activation by binding to the orthosteric binding pocket. By induction of a distinct set of receptor conformations, bitopic ligands might also lead to biased signaling compared to a mono-modal binding ligand[6,16].

Sequentially activating ligands expand the spatially-centered understanding of receptor activation by another dimension, i.e. time. With *SEALs* it might be possible to induce distinct receptor conformations in a time-dependent manner by exploiting all features associated with either orthosteric or allosteric targeting. In this chapter, we describe the concept of *SEALs* in a proof-of-concept study using the FFA2 receptor as a model class A GPCR. By that, we greatly benefit from the real time label-free DMR and impedance-based technology that are capable to monitor the cellular effects of ligands with this new mode-of-action. This information would have been missed by conducting only traditional equilibrium-state GPCR readouts[17]. However, only the direct comparison of classical endpoint assays and innovative label-free assays appropriately describes the process in its entirety and therefore exemplifies a complementation-based approach, which we used to disclose this mechanism.

References

1. Lagerström, M. C. & Schiöth, H. B. Structural diversity of G protein-coupled receptors and significance for drug discovery, *Nat Rev Drug Discov* **7,** 339–357 (2008).
2. Overington, J. P. Al-Lazikani, B. & Hopkins, A. L. How many drug targets are there?, *Nat Rev Drug Discov* **5,** 993–996 (2006).
3. Imming, P. Sinning, C. & Meyer, A. Drugs, their targets and the nature and number of drug targets, *Nat Rev Drug Discov* **5,** 821–834 (2006).
4. Valant, C. *et al.* A novel mechanism of G protein-coupled receptor functional selectivity. Muscarinic partial agonist McN-A-343 as a bitopic orthosteric/allosteric ligand, *J. Biol. Chem.* **283,** 29312–29321 (2008).
5. Antony, J. *et al.* Dualsteric GPCR targeting: a novel route to binding and signaling pathway selectivity, *FASEB J.* **23,** 442–450 (2009).
6. Lane, J. R. Sexton, P. M. & Christopoulos, A. Bridging the gap: bitopic ligands of G-protein-coupled receptors, *Trends Pharmacol. Sci.* **34,** 59–66 (2013).
7. Valant, C. Robert Lane, J. Sexton, P. M. & Christopoulos, A. The best of both worlds? Bitopic orthosteric/allosteric ligands of g protein-coupled receptors, *Annu. Rev. Pharmacol. Toxicol.* **52,** 153–178 (2012).
8. Lee, T. *et al.* Identification and functional characterization of allosteric agonists for the G protein-coupled receptor FFA2, *Mol. Pharmacol.* **74,** 1599–1609 (2008).
9. Wang, Y. *et al.* The first synthetic agonists of FFA2: Discovery and SAR of phenylacetamides as allosteric modulators, *Bioorg. Med. Chem. Lett.* **20,** 493–498 (2010).
10. Swaminath, G. *et al.* Mutational analysis of G-protein coupled receptor--FFA2, *Biochem. Biophys. Res. Commun.* **405,** 122–127 (2011).
11. Smith, N. J. *et al.* Extracellular loop 2 of the free fatty acid receptor 2 mediates allosterism of a phenylacetamide ago-allosteric modulator, *Mol. Pharmacol.* **80,** 163–173 (2011).

12. Kenakin, T. & Miller, L. J. Seven transmembrane receptors as shapeshifting proteins: the impact of allosteric modulation and functional selectivity on new drug discovery, *Pharmacol. Rev.* **62,** 265–304 (2010).

13. Langmead, C. J. & Christopoulos, A. Allosteric agonists of 7TM receptors: expanding the pharmacological toolbox, *Trends Pharmacol. Sci.* **27,** 475–481 (2006).

14. Wootten, D. Christopoulos, A. & Sexton, P. M. Emerging paradigms in GPCR allostery: implications for drug discovery, *Nat Rev Drug Discov* **12,** 630–644 (2013).

15. Mohr, K. *et al.* Rational design of dualsteric GPCR ligands: quests and promise, *Br. J. Pharmacol.* **159,** 997–1008 (2010).

16. Bock, A. & Mohr, K. Dualsteric GPCR targeting and functional selectivity: the paradigmatic M(2) muscarinic acetylcholine receptor, *Drug Discov Today Technol* **10,** e245-52 (2013).

17. Simpson, P. B. & Wafford, K. A. New directions in kinetic high information content assays, *Drug Discov. Today* **11,** 237–244 (2006).

A new mechanism for modulating 7TM receptor function:

Sequentially activating ligands (SEALs)

Manuel Grundmann[1], Brian D. Hudson[2], Irina G. Tikhonova[3], Nicola J. Smith[4], Eugenia Sergeev[2], Klaus Mohr[5], Trond Ulven[6], Graeme Milligan[2], Terry Kenakin[7] & Evi Kostenis[1]**

[1]Molecular-, Cellular- and Pharmacobiology Section, Institute of Pharmaceutical Biology, University of Bonn, Bonn, Germany

[2]Molecular Pharmacology Group, Institute of Molecular, Cell and Systems Biology, College of Medical, Veterinary and Life Sciences, University of Glasgow, Glasgow, Scotland, UK

[3]Molecular Therapeutics, School of Pharmacy, Medical Biology Centre, Queen's University, Belfast, Northern Ireland, UK

[4]Molecular Cardiology Division, Victor Chang Cardiac Research Institute, Faculty of Medicine, University of New South Wales, Sydney, Australia

[5]Pharmacology and Toxicology, University of Bonn, Bonn, Germany

[6]Department of Physics, Chemistry and Pharmacy, University of Southern Denmark, Odense M, Denmark

[7]Department of Pharmacology, University of North Carolina School of Medicine, Chapel Hill, NC, USA

***Correspondence to: E-mail: grundmann@uni-bonn.de and kostenis@uni-bonn.de**

Summary

Ligands targeting seven-transmembrane receptors (7TMR) are currently classified as either orthosteric, allosteric or dualsteric/bitopic. Here, we define a new pharmacological concept for 7TMR functional modulation: sequentially activating ligands (SEALs). A hallmark feature of “SEALs” is the temporary activation of a first receptor site followed by sustained activation via a second topographically distinct site. We identify 4-CMTB, previously classified as a pure allosteric agonist of the free fatty acid receptor FFA2, as the first “SEAL” and corroborate its bifunctionality in living cells by tracking integrated responses with innovative optical- and impedance-based label-free biosensors capable of visualizing multiple signaling inputs in real-time. We validate this unique pharmacology with traditional cellular readouts along with mutational and pharmacological perturbations including molecular modelling, and propose a kinetic model applicable to analysis of SEAL action. Our proof-of-concept study unveils 4-CMTB as prototype of a new class of ligands epitomizing a heretofore-unobserved molecular mechanism of receptor activation.

Introduction

7TM receptors are involved in virtually every (patho)physiological process in mammals and therefore have been the most successful targets for drug development[1,2]. Most drugs act via binding to the orthosteric site, thereby competing with the endogenous ligands that naturally regulate receptor function. During the past years allosteric modulation of 7TM receptors has received considerable interest, and significantly allosteric ligands (that is ligands that bind to a distinct location) are emerging as promising alternatives for therapeutic intervention because they may obviate several of the inherent challenges of orthosteric target-centered approaches[3–6]. First, allosteric ligands may achieve greater receptor subtype selectivity because allosteric epitopes are less well conserved than orthosteric recognition sites, which have stringent evolutionary demands to retain conservation. Second, allosteric ligands may not stimulate the receptor directly but can act to enhance receptor function on a timescale governed by the endogenous agonist. A clear advantage of such "use-dependence" may be the lower propensity for receptor desensitization[7]. If allosteric modulators enhance activity of the physiological agonist, either by altering its affinity or efficacy, they may provide a means to fine-tune cellular signaling by favoring selected signaling routes over others[8]. Third, allosteric modulators are characterized by their saturability of effect on the orthosteric recognition site. This in turn allows preservation of a low-level tone of the endogenous ligand and thus safeguards physiological function even under conditions of full occupancy of the allosteric site[3,5].

To date, allosteric ligands are classified as inhibitors (negative allosteric modulators, NAMs), potentiators (positive allosteric modulators, PAMs), agonists or ago-PAMs, as well as silent or neutral modulators (SAMs/NALs)[3,9,10]. Recently, a novel class of pharmacological agents has become available for modulation of 7TMR function: dualsteric or bitopic ligands[11,12]. These ligands harbor two pharmacophores connected by a linker to concomitantly engage both orthosteric and allosteric receptor binding pockets. Thus, dualsteric/bitopic ligands combine receptor subtype selectivity with the capacity to fine-tune the receptor's natural signaling pattern[13,14].

The purpose of the present study is to introduce a novel mechanism of pharmacological intervention with 7TMR function: *sequentially activating ligands (SEALs)*. This mechanism is posited to explain the differences observed in investigations into the molecular modes of action of two agonists for the free fatty acid receptor 2 (FFA2, formerly GPR43)[15,16]: the short chain fatty acid propionic acid C3 and the small molecule 4-CMTB (phenylacetamide, 2-(4-chlorophenyl)-3-methyl-*N*-(thiazol-2-yl)butanamide). Propionic acid is an endogenous agonist targeting the orthosteric pocket of FFA2[15,16]. 4-CMTB, initially introduced as AMG7703, is a synthetic ligand that was identified in a high-throughput screening campaign in an effort to achieve selective activation of FFA2 over the closely related FFA3 receptor[17]. Interestingly, considerable optimization efforts have failed to provide ligands with significantly higher potency than the initial hit and attempts to map its binding site have been largely inconclusive[18,19]. Nevertheless, of the studies undertaken with 4-CMTB to date, all are indicative of a purely allosteric mode of action[17–21].

Herein, we do confirm allosteric receptor engagement of FFA2 by 4-CMTB but additionally reveal a hitherto unappreciated orthosteric component in its mechanism of action. Intriguingly, this orthosteric activation is only temporary in nature but is followed by sustained activation via the allosteric site. We validate this sequential mode of receptor engagement using a variety of functional assays under kinetic and equilibrium conditions in combination with pharmacological perturbations, receptor mutagenesis and molecular modeling. We also develop a kinetic model applicable to the analysis of SEAL action at 7TMRs.

With the identification of 4-CMTB as the prototype SEAL we not only expand the pharmacological toolbox of 7TM receptor modulators, but moreover present a mechanism of action heretofore unobserved with any other 7TM receptor agonist. We envision that SEALs may allow precise temporal control over receptor signaling dynamics to fine-tune cellular responses, thereby expanding the repertoire of cellular communication via 7TM receptors in space and time.

Results

Label-free techniques unveil different activation modes of C3 versus 4-CMTB

Label-free assays based on the detection of dynamic mass redistribution (DMR) or bioimpedance capture integrated responses in living cells with high temporal resolution and broad signaling pathway coverage[22–25]. They have proven exquisitely suited to visualize cellular activation profiles of signaling-competent proteins such as 7TM receptors[26–28]. We initially set out to compare the cellular reaction to either the endogenous, orthosteric agonist propionic acid (C3) or the synthetic allosteric agonist 4-CMTB in HEK293 cells engineered to stably express the human FFA2 wild-type receptor (hFFA2, hFFA2-wt). Label-free impedance sensing unraveled a striking temporal difference in the signaling patterns triggered by the two receptor ligands. C3 provoked a sharp transient negative peak instantly after compound addition that reversed quickly toward baseline and that was followed by a second gradually descending phase. 4-CMTB largely lacked the first spike but preserved the second phase signal (**Fig. 1a,b**, for magnification of the early timescale see **Supplementary Figure 1**). Comparable results were obtained in optical biosensor-based DMR recordings. C3 generated a uniform signature with a maximal DMR peak at about 1,500 sec, after which it decayed slowly (**Fig. 1c**). 4-CMTB, in contrast, evoked a less pronounced initial increase with a delayed maximal response at approx. 3,000 sec. Yet, overall DMR profiles at later time points were comparable to those generated by C3 (**Fig. 1d**). To consider these temporal differences we quantified concentration-effect relationships for both ligands at early and late time points. This analysis revealed partial agonism of 4-CMTB for the first signaling impulse (**Fig. 1e,f**), but full agonism at later time points (**Fig. 1g,h**, and **Supplementary Table 1**). Acetic acid (C2), another endogenous agonist of hFFA2, induced a phenotypic signaling profile reminiscent to that observed with C3 (**Supplementary Figure 2**). All cell responses in the label-free readouts were specifically mediated via the hFFA2 receptor, since untransfected cells did not react upon compound addition (**Supplementary Figure 3**).

Structural integrity of the orthosteric site has impact on 4-CMTB signaling dynamics

A key residue within the orthosteric binding pocket of hFFA2 is $R255^{7.53}$ in helix 7 (Ballesteros-Weinstein indexing system in superscript), which - if mutated to alanine (hFFA2-R255A) - renders hFFA2 unresponsive to short chain fatty acids despite appropriate surface expression ([29], see methods). Consistent with these findings, C3 was completely inactive on the hFFA2-R255A mutant receptor in both impedance- and optical-based label-free whole cell recordings (**Supplementary Figure 4a,b**). As expected, 4-CMTB retained the capacity to trigger cell activation via the hFFA2-R255A receptor, corroborating its non-orthosteric mode of action. However, we noted that the kinetic profile of 4-CMTB differed significantly from that obtained at the wild-type receptor. Both label-free assays yielded temporal fingerprints for 4-CMTB indicative of impaired early but enhanced late cell responses (**Fig. 1i,j**). Time-dependent quantification of label-free signatures at the hFFA2-R255A receptor revealed loss of function for the orthosteric agonist C3 at all points in time (**Supplementary Figure 4c,d**) as opposed to selective abrogation of 4-CMTB activity for the first signaling impulse (**Fig. 1k,l**). Our mutagenic approach indicates that lack of orthosteric R255 impacts on signaling by 4-CMTB, either because allosteric site signaling requires the integrity of the orthosteric site and/or because 4-CMTB also interacts directly with the orthosteric receptor site. Notably, hFFA2-R255A transfected cells did not lose their ability to react rapidly per se. ATP, acting as an agonist at endogenously expressed P2Y receptors, induced a robust and immediate cell response whose phenotype resembled that of the hFFA2-wt and the untransfected host cell line (**Supplementary Figure 5**). A receptor-independent impairment causing a delay in the signaling kinetics is therefore unlikely.

CATPB serves as a selective orthosteric probe

To provide a complementary view on the biological role of the orthosteric binding site for 4-CMTB signaling, we chose to manipulate hFFA2 function using traditional pharmacological perturbation with CATPB, a small molecule previously reported to competitively antagonize hFFA2-wt receptor function[20] (**Fig. 2a**). We initially verified competitive antagonism of CATPB with C3 using Schild analysis of DMR

recordings at the hFFA2-wt receptor (pA_2: 7.61 ± 0.04, slope: 0.96 ± 0.01) (**Fig. 2b,c**). Competitive inhibition of C3 function by CATPB was further substantiated in ERK1/2 phosphorylation assays (**Supplementary Figure 6a,b**). Moreover, and consistent with previous reports[30], CATPB - in its own right - showed intrinsic activity at hFFA2-wt receptor expressing cells in the DMR assay (**Fig. 2d**). Negative deflection of DMR traces relates to inverse agonism of CATPB at constitutively active hFFA2-wt receptors because CATPB was inactive at the hFFA2-R255A mutant, which lacks constitutive activity (**Fig. 2e,f,** and **Supplementary Figure 6c**). Accordingly, CATPB also lowered basal levels of inositol phosphates (IP) and pERK1/2 in hFFA2-wt receptor expressing cells (**Supplementary Figure 6d,e**). Furthermore, at no time did CATPB affect non-orthosteric 4-CMTB-mediated activation of the hFFA2-R255A mutant in label-free recordings in spite of its capacity to bind to this mutant receptor form (**Fig. 2g,h,i and Supplementary Figure 7**). Thus, data from the current and previous studies suggest occupancy of non-overlapping binding sites by CATPB and 4-CMTB at equilibrium and unambiguously define CATPB as orthosteric probe, competing with C3 for a common site within the orthosteric hFFA2 pocket. Therefore, CATPB can be applied rationally to interrogate the mechanism of 4-CMTB activation at the wild-type hFFA2 receptor.

Attenuation of orthosteric signaling by CATPB remodels the dynamics of 4-CMTB-mediated FFA2 activation

In accordance with an orthosteric mode of action, high concentrations of CATPB completely blocked C3-induced DMR and changes in cellular impedance in hFFA2-wt receptor expressing cells (**Fig. 3a,b**). In contrast, saturating concentrations of CATPB exclusively blunted rapid cell activation, but preserved or even enhanced the second signaling wave mediated by 4-CMTB (**Fig. 3c,d**, for quantification of early and late responses in label-free DMR and impedance assays, respectively, see **Fig. 3e,f**). Of note, CATPB did not affect DMR or impedance responses triggered by endogenously expressed P2Y receptors, confirming the specific nature of hFFA2-wt receptor inhibition (**Supplementary Figure 8**). Thus, pharmacological perturbation of FFA2 signaling by CATPB in conjunction with the orthosteric loss-of-

function mutation (**Fig. 1i,j**) does indeed provide a complementary view on the role of the orthosteric site for 4-CMTB signaling.

Time-specific endpoint assays untangle the kinetics of orthosteric site-driven signaling

To elucidate whether the characteristic temporal inhibition pattern of CATPB on 4-CMTB-induced cell responses is echoed in traditional readouts for 7TM receptor signaling pathways, multiple parallel assays were employed that either capture rapid (mobilization of intracellular Ca^{2+}), delayed (accumulation of IP as well as inhibition of forskolin-mediated cAMP production) or both cell responses (ERK1/2 phosphorylation assays). Indeed, the transient rise of Ca^{2+}, which is detectable within seconds after addition of both C3 and 4-CMTB, is blunted by CATPB (**Fig. 3g,h**; see **Supplementary Figure 9** for real time Ca^{2+} traces). For both ligands, inhibition was complete and entirely consistent with competitive antagonism (**Fig. 3i, Supplementary Table 2**). CATPB did not block Ca^{2+} influx upon stimulation with the calcium ionophore A23187, or carbachol, which activates endogenously expressed muscarinic acetylcholine receptors (**Supplementary Figure 10a,b**), confirming specificity of the inhibitory effect. Second messenger production in IP (**Fig. 3j**) and cAMP accumulation assays (**Fig. 3k**) after 4-CMTB stimulation was fully insensitive to inhibition with CATPB. This is in contrast to complete inhibition that was apparent when C3 was employed as the activating stimulus (**Fig. 3j,k**). Inhibition of early, partial inhibition of intermediate, but lack of CATPB sensitivity at late signaling time points is also recapitulated in ERK1/2 phosphorylation assays examining the time-dependence of interaction between 4-CMTB and CATPB (**Fig. 3l**; see **Supplementary Figure 11a** for unperturbed 4-CMTB pERK1/2 kinetics over time). Inhibition of pERK1/2 levels by CATPB was FFA2 receptor-dependent, since serum-induced controls were unaffected by the antagonist (**Supplementary Figure 11b**). Of note, untransfected cells were nonresponsive to both C3 and 4-CMTB, corroborating FFA2 receptor-specific effects across all second messenger assays (**Supplementary Figure 12**). In summary, with real-time label-free data, second messenger assays provide strong support for the notion that 4-CMTB mediates early cellular responses via transient activation of the orthosteric site.

Mutational analysis unveils dual input control of 4-CMTB signaling at the wild-type receptor

A corollary of orthosteric receptor engagement by 4-CMTB is selective abrogation of early, but not late, cell responses in mutant forms of hFFA2 lacking a functional orthosteric site. To test this prediction, we investigated the temporal signaling pattern of 4-CMTB at the hFFA2-R255A receptor in both Ca^{2+} and second messenger assays. Consistent with our prediction, rapid signaling of transient Ca^{2+} flux upon 4-CMTB stimulation was abolished (**Fig. 3m**) but delayed cell responses in second messenger (**Fig. 3n,o**) and ERK1/2 accumulation assays (**Fig. 3p**) were preserved. Thus, by combining complementary strategies consisting of pharmacological inhibition, receptor mutagenesis along with label-free real-time and canonical endpoint assays, we posit that 4-CMTB dually controls input at the wild-type receptor by sequentially activating the orthosteric followed by the allosteric site, respectively.

An ECL2 swap mutant exaggerates the transient orthosteric action of 4-CMTB

We next chose to investigate the mechanism of receptor activation by 4-CMTB using a chimeric hFFA2 receptor, in which the extracellular loop 2 (ECL2) of hFFA2 was exchanged for the counterpart of the cognate hFFA3 receptor (hereafter hFFA2-ECL). This mutant was designed previously in an effort to understand transmission of allosteric effects by 4-CMTB[18]. Both C3 and 4-CMTB displayed temporal activation patterns in hFFA2-ECL expressing HEK293 cells that were comparable with those observed at the wild-type receptor (**Fig. 4a-d**, compare with **Fig. 1c,d,f,h**). Inhibition of C3 by CATPB remained competitive at the hFFA2-ECL receptor (pA_2: 7.00 ± 0.10; slope: 1.01 ± 0.04; **Supplementary Figure 13a,b**). According to this, saturating concentrations of CATPB completely inhibited C3-induced DMR responses at all times (**Fig. 4e**). Intriguingly, CATPB inhibition of 4-CMTB signaling differed significantly from the pattern observed for the wild-type receptor because both initial and delayed activation of 4-CMTB was largely diminished (**Fig. 4f**, compare with **Fig. 3c**). When we compared CATPB modulation of C3 and 4-CMTB signaling at early time points at the hFFA2-ECL receptor, we observed complete inhibition indistinguishable from competitive antagonism (**Fig. 4g,h**) and reminiscent of the profile at

the wild-type receptor (**Fig. 4i,j**). Quantitative analysis of CATPB IC_{50}-shifts indicates competitive antagonism for both C3 and 4-CMTB and thus strengthens the conclusion of temporary orthosteric receptor activation by 4-CMTB (**Fig. 4k,l, Supplementary Table 3**). Moreover, CATPB remained able to partially inhibit delayed 4-CMTB-induced cell responses at the hFFA2-ECL mutant (**Supplementary Figure 14a,b)**, whereas it gradually turned into enhancement over time at the wild-type receptor (**Supplementary Figure 14c,d;** compare **a** with **c**, and **b** with **d**; for snap-shot quantification of time-dependent modulation by CATPB of 30 µM 4-CMTB see **Fig. 4m**). These data argue for a gatekeeper role of ECL2 in determining the duration of orthosteric first phase agonism by 4-CMTB. To challenge this hypothesis we introduced the Arg255Ala mutation into the hFFA2-ECL receptor resulting in the double mutant hFFA2-R255A-ECL. If 4-CMTB initially adopted an orthosteric pose and provided that adoption of this pose is temporally extended in the hFFA2-ECL construct, then it should be lost in the hFFA2-R255A-ECL mutant and be reflected as a significant impairment of the initial signaling impulse. Indeed, DMR recordings in hFFA2-R255A-ECL expressing cells mirror the traces obtained in hFFA2-ECL cells in the presence of CATPB: DMR signatures indicate loss of the orthosteric contribution ("the fast component") to the overall response but maintenance of the capacity to evoke activation via the allosteric site ("the slow component", **Fig. 4n**). Consistently, Ca^{2+}-ionophore, A23187, but not C3 and 4-CMTB, elicited a calcium transient in hFFA2-R255A-ECL cells (**Fig. 4o**). However, delayed activation via the allosteric site was still detectable for 4-CMTB as evidenced by robust accumulation of inositol phosphates (**Fig. 4p**). These results led us to conclude that concomitant perturbation of the orthosteric binding pocket by Arg255Ala and of the gatekeeper function of ECL2 is well suited to illustrate the sequence of events during receptor activation by 4-CMTB, thereby associating the initial signaling impulse with an orthosteric and the prolonged signaling impulse with an allosteric mechanism.

A single amino acid replacement is sufficient to trap 4-CMTB in an orthosteric pose

The capacity to enhance duration of orthosteric 4-CMTB action in the ECL2 swap mutant prompted us to hypothesize that a similar effect might be achievable by replacement of key residues lining the allosteric FFA2 site by the corresponding FFA3 counterparts. Guided by homology modeling based on

the crystal structure of the related FFA1 receptor we replaced K65$^{2.60}$ by arginine (hFFA2-K65R), a residue which has not been probed previously as determinant of 4-CMTB action (**Fig. 5a,b** and [31]). Both C3 and 4-CMTB robustly activated hFFA2-K65R in DMR assays consistent with the mutated residue being outside the orthosteric area (**Fig. 5c-f**). Most notably, however, and entirely consistent with our hypothesis, both C3 and 4-CMTB were now fully antagonized by CATPB (**Fig. 5g-i**). Similar observations were made in IP accumulation assays: C3 and 4-CMTB induced robust IP production (**Fig. 5j**) and this response was completely ablated by CATPB in a manner compatible with competitive antagonism for both ligands (**Fig. 5k-m, Supplementary table 4**). Thus, at hFFA2-K65R the only mode of interaction available to 4-CMTB is occupancy of epitopes within the orthosteric pocket which manifests as complete sensitivity towards inhibition by CATPB.

Mutational analysis defines orthosteric 4-CMTB topography

To further corroborate transient orthosteric first phase agonism of 4-CMTB, we examined its signaling pattern in mutant forms of hFFA2, in which activation by C3 is either severely impaired (R180$^{5.39}$A) or ablated (R180$^{5.39}$A/R255$^{7.53}$A, H242$^{6.55}$A)[29]. DMR analysis confirms that each mutant lacks key epitopes defining the orthosteric pocket of hFFA2 (**Supplementary Figure 15**). If we assume that these residues are similarly important for shaping 4-CMTB's orthosteric signaling element, then 4-CMTB action should be restricted to exclusive transmission of its allosteric second phase impulse in these mutants. Indeed, in all cases DMR recordings were indicative of selective loss of rapid orthosteric but preservation of delayed allosteric signaling (**Fig. 6a-c**; for quantification of early and late responses see **Supplementary Figure 16**). Consistently, 4-CMTB was unable to induce rapid orthosteric Ca^{2+} flux across all mutants (**Fig. 6d-f**, left panels), yet retained activity in IP accumulation assays capturing the allosteric response (**Fig. 6d-f**, right panels and **Supplementary Figure 17**). C3 was inactive or severely compromised in both Ca^{2+} and IP assays in line with DMR and published data (**Supplementary Figure 15**, and [18,29,32]). Moreover, we also confirmed orthosteric elements of activation for 4-CMTB utilizing an FFA2 mutant designed to mimick the orthosteric site of FFA3: hFFA2-S86G$^{3.29}$-Y90F$^{3.30}$-I145Y$^{4.61}$-E166L^{ECL2}. Because 4-CMTB is selective for FFA2 over FFA3, we predicted the quadruple mutant to specifically lose rapid

orthosteric but preserve allosteric activation. C3, in contrast, should retain functionality in both assays because it is unable to discriminate between FFA2 and FFA3. Indeed, C3 but not 4-CMTB induced intracellular Ca^{2+} flux (**Fig. 6g,** left panel), however, both ligands produced substantial responses in IP accumulation assays (**Fig. 6g,** right panel and **Supplementary Fig. 18**). In agreement with compromised orthosteric but functional allosteric signaling of the quadruple mutant, DMR recordings revealed rapid cell activation exclusively for C3 but delayed signaling that is superimposable for both ligands (**Fig. 6h**). Based on these results, we predicted that combined substitution of a key orthosteric residue together with the allosteric K65R mutation should be sufficient to severely impact, if not ablate, 4-CMTB function. Indeed, complete lack of activation by 4-CMTB of hFFA2-K65R-R255A in DMR assays, despite appropriate surface expression, indicates experimental validation of our prediction (**Fig. 6i** and **Supplementary Fig. 19**). Thus, we demonstrate in a definitive and systematic manner that a single ligand may activate a 7TMR in tandem via two topographically distinct receptor sites (**Fig. 6j-l**), thereby introducing the novel pharmacological concept of sequentially activating ligands (SEALs). A model applicable to mechanisms that involve sequential receptor activation by a single ligand via distinct receptor sites is provided in an Online Appendix.

Discussion

It is common sense that allosteric ligands differ structurally from orthosteric ligands because they address spatially distinct receptor binding sites. In this regard, action of the small molecule 4-CMTB as both orthosteric and allosteric ligand is surprising. In fact, 4-CMTB, which was previously considered to exclusively display allosteric pharmacology[17,18,20,21], may now be classified as a unique bifunctional molecule, competent to sequentially activate both orthosteric and allosteric sites of the FFA2 receptor. This behavior has been inferred from a multifaceted experimental approach based on functional assays under equilibrium and kinetic conditions, label-free DMR and bio-impedance whole cell sensing, pharmacological and mutagenic receptor perturbations along with molecular and mathematical modeling to illustrate and refine the concept, respectively.

Pharmacological targeting of more than one receptor site has to date only been achieved with dualsteric/bitopic ligands[11,12]. This ligand class consists of hybrid molecules, in which orthosteric and allosteric building blocks are bridged by a molecular linker. Thus, dualsteric/bitopic ligands span and simultaneously bind to orthosteric and allosteric receptor sites[33]. Dualsteric pharmacology is a captivating concept that underlies receptor subtype selectivity and may even confer signaling bias[13,14]. 4-CMTB also engages ortho- and allosteric sites, however, this small molecule is distinct from bitopic ligands in that it does not contain individual building blocks that are separated by a defined molecular linker. Rather it achieves activation via targeting of spatially distinct FFA2 receptor sites by altering its signaling competence in a *time-dependent* manner.

Distinction of receptor responses in early and late phases is not unprecedented in the literature, as several ligand-receptor systems are known that change signaling modalities over time such as the control over extracellular signal-regulated kinases ERK1/2[34]. Differential spatial and kinetic patterns of ERK activation have, for example, been observed for angiotensin AT_{1A} receptors in HEK293 cells with G protein-activated ERK peaking after 2 minutes as opposed to β-arrestin-dependent ERK activation that peaks at later time points and is more protracted[35]. Similar mechanistic distinctions were made

for 7TMR-dependent regulation of AKT, a kinase operating downstream of PI3K. AKT activation upon stimulation of protease-activated receptor 1 (PAR1) may be both rapid and sustained and controlled by separate G protein and β-arrestin dependent mechanisms, respectively[36]. While regulation of kinase families by β-arrestin versus G protein-dependent mechanisms are well documented with numerous examples[37], and while engagement of these parallel mechanisms can differ depending on the ligand chosen to stimulate the receptor, a phenomenon referred to as ligand bias, no such study – to the best of our knowledge – has yet linked first and second phase responses to occupancy of topographically distinct sites, which is the key characteristic in the concept of SEALs. We speculate that SEALs may be more frequent than anticipated, yet may have gone unnoticed if ligands were exclusively analyzed in equilibrium assays. Thus it is likely that the SEAL concept described here for 4-CMTB could only be discovered by combining real-time and canonical assays under both non-equilibrium and equilibrium conditions[38].

An intriguing feature of orthosteric-allosteric targeting of FFA2 by 4-CMTB is the chronological order of these events. The structure of class A 7TMRs would suggest that SEALs initiate contact within the allosteric vestibule followed by passage into the transmembrane binding pocket to elicit an orthosteric response[39,40]. 4-CMTB, however, appears to navigate via a different route. We speculate that 4-CMTB achieves sequential orthosteric-allosteric targeting by entering via the lipid bilayer. Such an entry mode differs from the common entrance via the extracellular space but has previously been shown for several class A 7TMR ligands[41–46], particularly for ligands at lipid mediator 7TMRs, such as the ago-allosteric agonist TAK875 (fasiglifam) at the related hFFA1 receptor[31]. Clearly, further studies are needed to investigate the entry mode of 4-CMTB at FFA2 in more detail. Nevertheless, and irrespective of the precise entry mode, 4-CMTB is – to the best of our knowledge - the first 7TMR modulator that conveys sequential activation via two distinct receptor sites.

Our complementary approach identifies 4-CMTB as a small molecule altering its activation mechanism over time. Although compelling experimental evidence is provided in favor of this unique mode of action, we chose to verify the novel concept with a kinetic model to rationalize the sequence of events

on a molecular level (see **Online Appendix**). We propose that two molecules of 4-CMTB bind the receptor at distinct loci with different binding kinetics. Slower binding of one 4-CMTB molecule to the allosteric binding site subsequently results in negative allosteric modulation of the 4-CMTB effect at the orthosteric site. The apparent transient orthosteric signaling phase is therefore rationalized if 4-CMTB functioned as a NAM on its own efficacy at a distinct binding site. The extracellular loop 2 (ECL2) likely contributes to cessation of orthosteric signaling, since the ECL2-swap from the FFA2 receptor to the cognate counterpart of FFA3 substantially enhanced orthosteric elements of activation. Within hFFA2-K65R, however, which lacks a key residue of the allosteric pocket, 4-CMTB was essentially restricted to an orthosteric mechanism, as evidenced by the enhanced sensitivity toward the orthosteric FFA2 antagonist CATPB. In line with these findings, partial agonism of 4-CMTB progressively increased with a rank order of hFFA2-wt < hFFA2-ECL < hFFA2-K65R implying a correlation between residence and efficacy at the orthosteric site. Thus, capacity to switch 4-CMTB pharmacology to orthosteric in mutants lacking key allosteric residues and *vice versa*, i.e. to achieve both orthosteric and allosteric trapping, can only be rationalized by occupancy of two distinct sites by the same molecule, the molecular basis for coining the term SEAL to acknowledge this complex yet unprecedented pharmacological phenotype.

With the assignment of 4-CMTB, previously classified as an ago-allosteric modulator, as the first SEAL, we uncover a heretofore uncharacterized mechanism of 7TMR signaling control. Because SEALs comprise allosteric components of activation, they provide the same potential advantages that are credited to the phenomenon of allosterism, ranging from subtype selectivity and probe dependency to functional selectivity[3,4]. Although much additional work is needed to understand the utility of this novel concept, we anticipate that discovery of the first SEAL will catalyze both identification of additional SEALs among ligands for 7TMRs with defined pharmacology and development of this class of ligands beyond FFA2 to achieve stimulus-specific cell responses to control the multiplicity of 7TMR coupling in space and time.

Acknowledgements

We are grateful to Ulrike Rick for expert technical assistance. We thank Sunil Pandey for the synthesis of CATPB. This work was supported by the Danish Council for Strategic Research (grant 11-11619). The authors declare no conflicts of interest. The authors are grateful to Corning Inc., Perkin Elmer, and Molecular Devices for their support on the dynamic mass redistribution as well as cellular dielectric spectroscopy biosensors.

Author contributions

M.G. conceived the project, designed and performed the experiments, generated receptor mutants and cell lines, performed data analysis and wrote the manuscript. I.G.T. conducted docking and homology modeling. B.D.H. generated receptor mutants. E.S. performed radioligand binding experiments and wrote the corresponding experimental section. T.P.K. contributed to the hypothesis and developed the kinetic model for SEAL action. T.U. supervised chemical synthesis. G.M., B.D.H., N.J.S., T.U., I.G.T., T.P.K., K.M. contributed to discussions and edited the manuscript. M.G. and E.K. developed the hypothesis. E.K. supervised the project and wrote the manuscript.

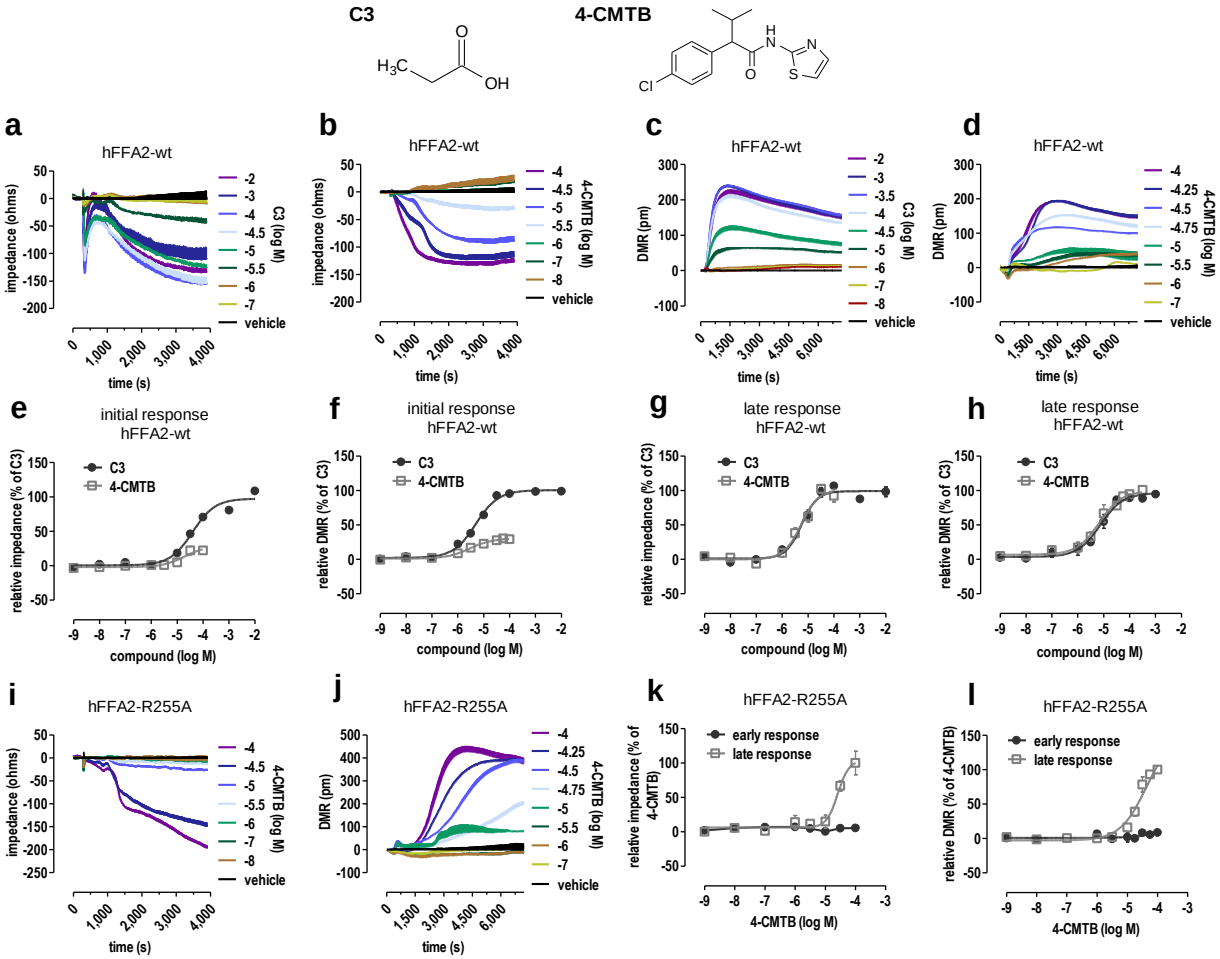

Figure 1. Label-free biosensors disclose unappreciated differences between C3 and 4-CMTB

(a-d) Label-free real-time traces of HEK293 cells stably transfected with the hFFA2-wt receptor stimulated with C3 (a,c) and 4-CMTB (b,d) recorded with the impedance- and optical-based biosensor, respectively. (e-h) Concentration-response-curves (CRC) of FFA2 agonists calculated at early (e,f) and late (g,h) time points from bioimpedance (negative peak within 0 – 600 sec (e) and impedance at 3,600 sec (g)) and DMR recordings (peak within 0 – 800 sec (f) and DMR at 6,000 sec (h)). (i,j) Real-time signatures of 4-CMTB at the hFFA2-R255A construct in the impedance (i) and the DMR assay (j), respectively. (k,l) CRC of 4-CMTB at the hFFA2-R255A receptor calculated from early or late cell responses in the impedance (k) and DMR assay (l), respectively. Label-free signatures are shown as representative traces (mean + s.e.m.), measured in triplicates. CRC are depicted as mean values ± s.e.m from three to six independent experiments.

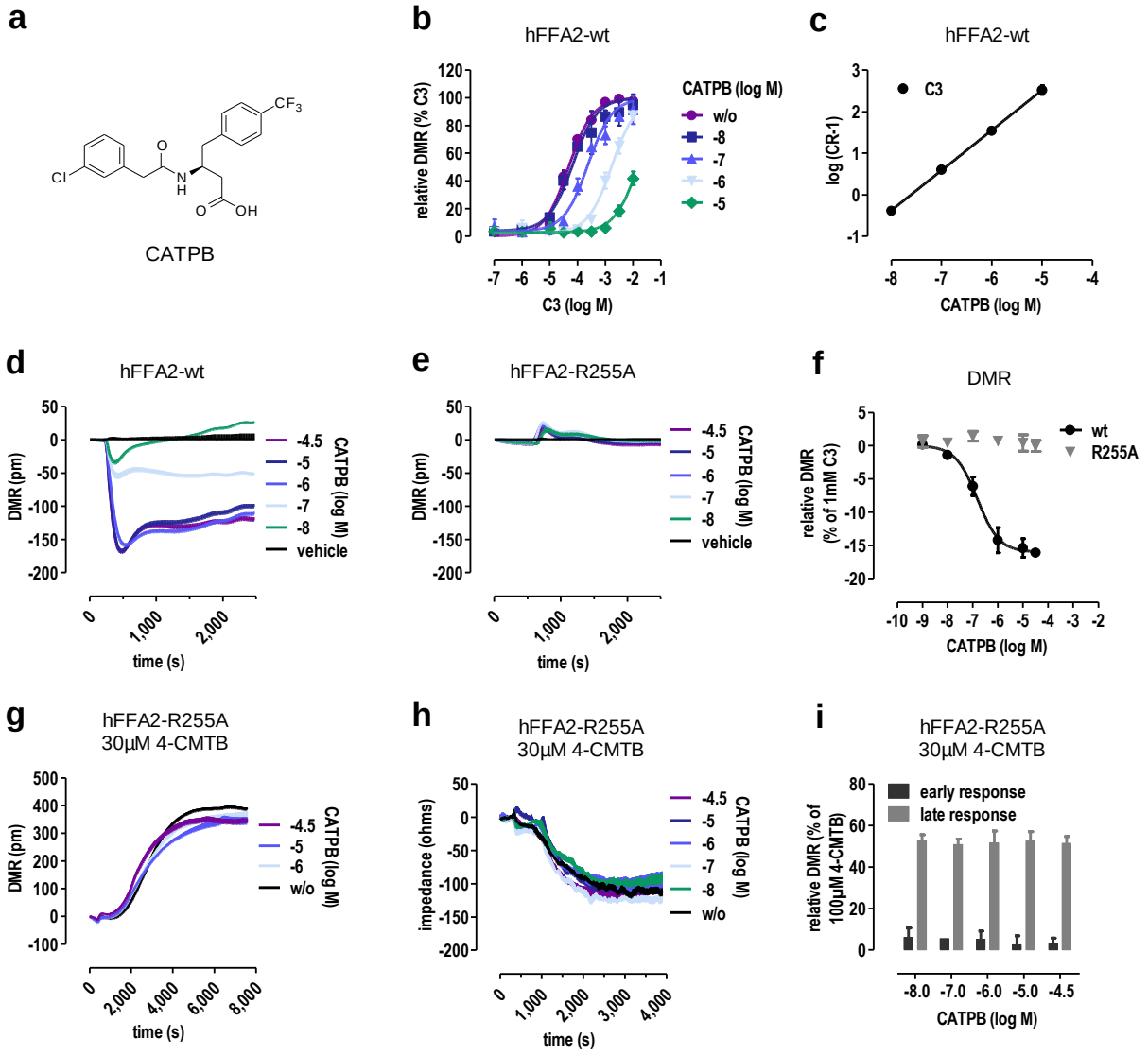

Figure 2. CATPB is an orthosteric inverse agonist at the hFFA2-wt receptor

(a) Chemical structure of CATPB. (b,c) Effect of increasing concentration of CATPB on DMR-derived CRC of C3 at the hFFA2-wt receptor (b) with corresponding Schild plot (c). (d,e) Intrinsic activity of CATPB at hFFA2-wt (d) but not hFFA2-R255A transfected HEK cells (e) captured in the DMR assay. (f) CRC of CATPB at the hFFA2-wt (pIC_{50}: 6.81 ± 0.14) and hFFA2-R255A receptor. (g,h) Effect of CATPB on 4-CMTB (30 µM) signaling at the hFFA2-R255A receptor in the DMR (g) and bioimpedance (h) assay. (i) Analysis of DMR data from panel (g) at different time points (500 sec vs. 6,000 sec.). Real-time recordings are shown as representative traces (mean + s.e.m.), measured in triplicates. Quantified data are shown as mean values ± s.e.m. of three to six independent experiments. Where not shown error bars lie within dimensions of the symbols.

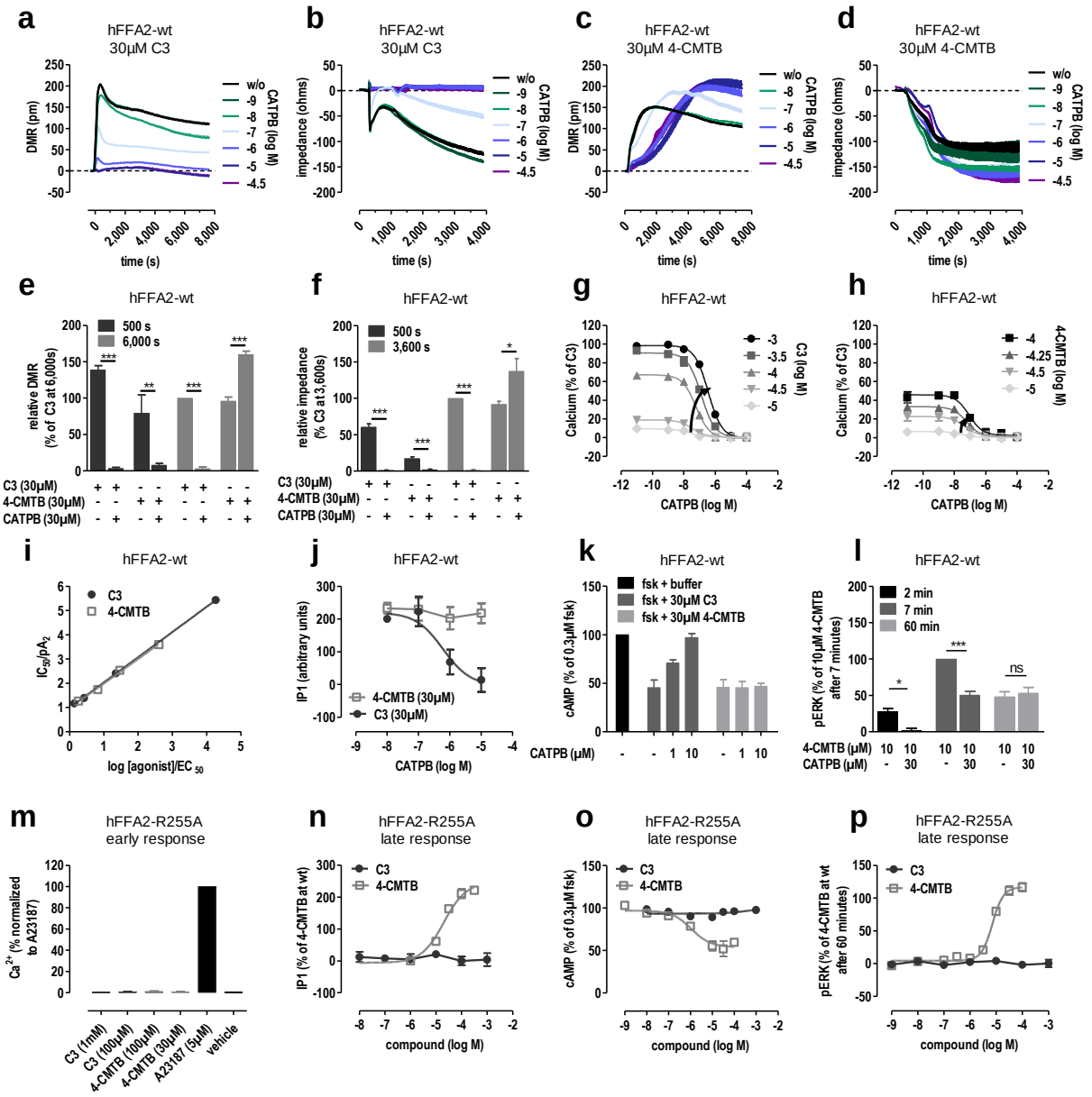

Figure 3. 4-CMTB shows time-dependent sensitivity towards the orthosteric antagonist CATPB and the mutation of a key residue within the orthosteric site.

(a-d) Effect of CATPB on 30 µM C3 (a,b) and 4-CMTB (c,d)-mediated hFFA2-wt receptor activation in the optical- and impedance-based label-free readout, respectively. (e,f) Quantification of FFA2 receptor inhibition by CATPB in the DMR (e) and bioimpedance (f) readout at early (500 sec) and late time points (6,000 sec for DMR; 3,600 sec for impedance). (g,h) Effect of CATPB on hFFA2-wt Ca^{2+} flux evoked by varying concentrations of C3 (g) and 4-CMTB (h). (i) Analysis of IC_{50}-shifts according to Cheng-Prusoff (slope: C3: 1.040 ± 0.024, r^2: 0.9946; 4-CMTB: 1.011 ± 0.045, r^2: 0.9805). (j) CATPB effect on C3 (pIC_{50}: 6.22 ± 0.39) or 4-CMTB-induced IP accumulation at the hFFA2-wt receptor. Data were baseline-corrected to remove the contribution of constitutive activity to IP signaling and CATPB responsiveness. (k) Impact of CATPB on C3 or 4-CMTB-mediated inhibition of 0.3 µM Forskolin-induced cAMP production. (l) Time point-differentiated analysis of CATPB effect on 4-CMTB-mediated ERK1/2 phosphorylation. (m) Ca^{2+} flux in hFFA2-R255A expressing HEK293 cells upon stimulation with FFA2 agonists. Calcium-ionophore A23187 shown as control. (n-p) Equilibrium CRC of C3 and 4-CMTB at the hFFA2-R255A receptor in the IP- (pEC_{50}: 4.70 ± 0.09) (n), the cAMP-(pEC_{50}: 5.96 ± 0.22) (o) and the pERK1/2-assay (pEC_{50}: 5.15 ± 0.04) (p). Label-free signatures are shown as representative traces + s.e.m., measured in triplicates. Bar diagrams and CRC represent mean values ± s.e.m of at least three independent experiments. Statistical significance was analyzed by two-tailed, unpaired Student's *t* test: *p < 0.05, **p < 0.01, ***p < 0.001.

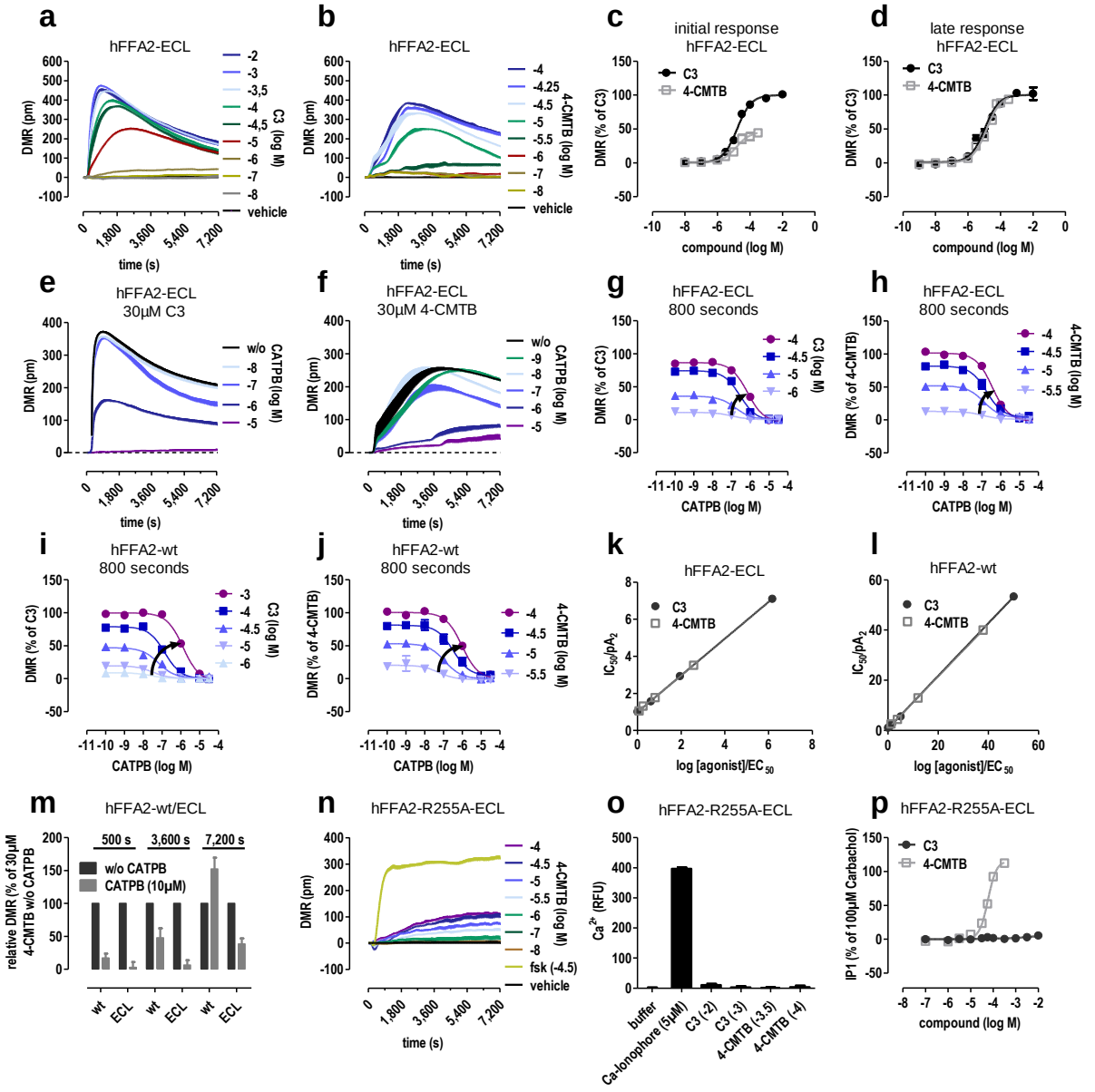

Figure 4. Structural changes within the extracellular receptor region intensify susceptibility of 4-CMTB effect to interrogation at the orthosteric site level

(a,b) DMR traces of HEK293 cells stably transfected with the hFFA2-ECL receptor stimulated with C3 (a) or 4-CMTB (b). (c,d) CRC of FFA2 agonists calculated at early ((c), peak within 0 – 800 sec) and late ((d), DMR at 6,000 sec) time points. (e,f) Effect of increasing concentrations of CATPB on DMR traces of 30 µM C3 (e) and 4-CMTB (f) activating the hFFA2-ECL receptor. (g,h) Comparison of CATPB inhibition at early time points (800 sec) on hFFA2-ECL activation by C3 (g) or 4-CMTB (h). (i,j) Comparison of CATPB inhibition at early time points (800 sec) on hFFA2-wt activation by C3 (i) or 4-CMTB (j). (k,l) Analysis of IC_{50}-shifts according to Cheng-Prusoff at the hFFA2-ECL (slope: C3: 0.992 ± 0.020, r^2: 0.996; 4-CMTB: 0.976 ± 0.046, r^2: 0.978) (k) and hFFA2-wt receptor (slope: C3: 1.049 ± 0.010, r^2: 0.999; 4-CMTB: 1.030 ± 0.029, r^2: 0.992) (l). (m) Temporal quantification of CATPB-sensitivity at the hFFA2-wt and the hFFA2-ECL receptor for 30 µM of 4-CMTB. (n) 4-CMTB effect at the double mutant hFFA2-R255A-ECL in the DMR assay, Forskolin (fsk) is shown as control. (o) Ca^{2+} flux of FFA2 agonists at the hFFA2-R255A-ECL receptor, calcium-ionophore A23187 is shown as control. (p) Assessment of IP levels upon hFFA2-R255A-ECL receptor stimulation with C3 or 4-CMTB (pEC_{50}: 4.23 ± 0.03) under equilibrium conditions. Representative real-time traces are shown as mean + s.e.m., measured in triplicates. Quantified data are depicted as mean values ± s.e.m. of at least three independent experiments.

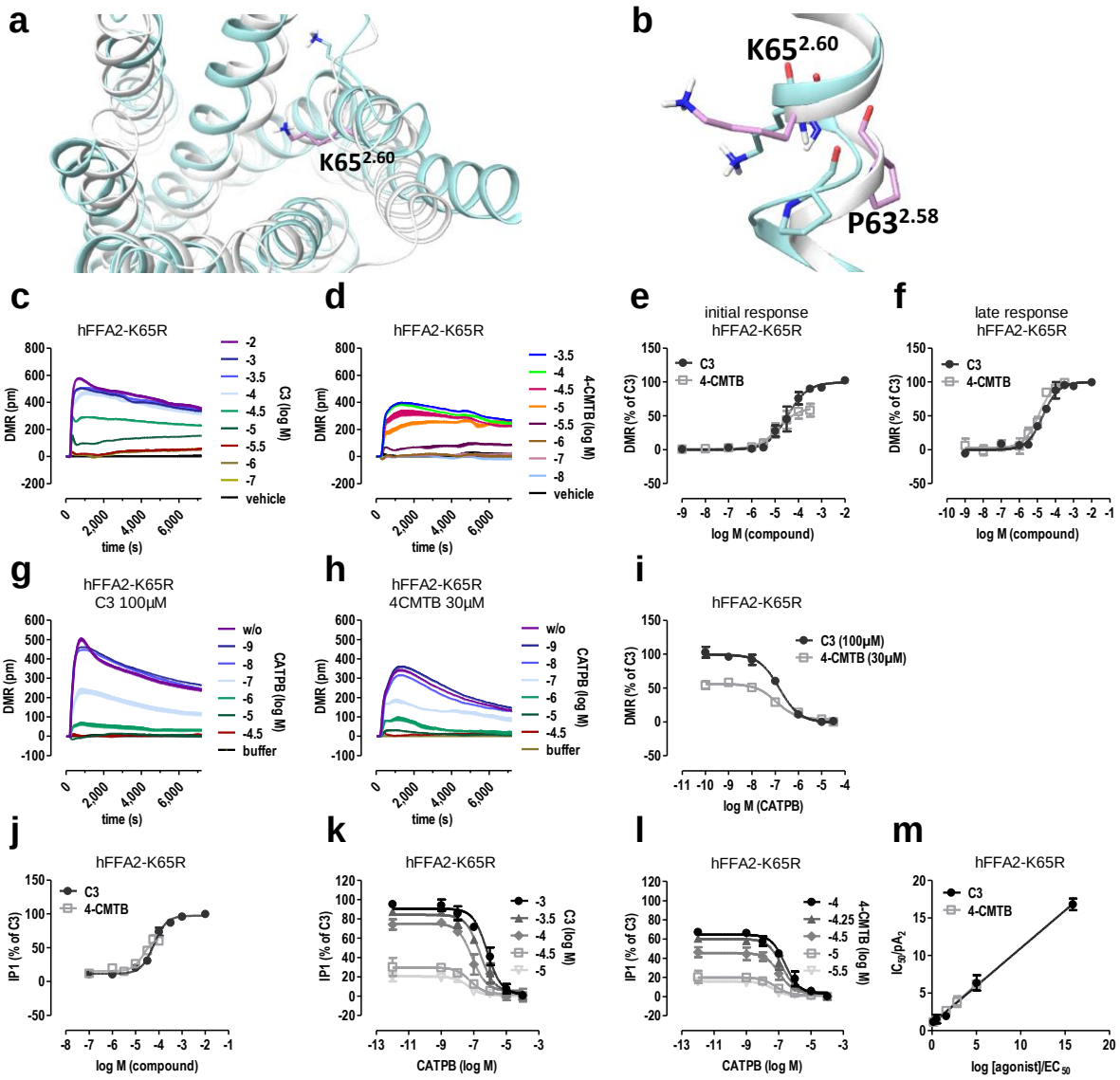

Figure 5. Identification of K65 as a key residue within the allosteric site that controls trapping of 4-CMTB in an orthosteric pose.

(a,b) Superimposition of the FFA2 homology models. K65 is pointed towards the binding cavity in the FFA1-based model (white) due to the proline kink at position 2.58 that unwinds helix 2. This proline kink is conserved in the free fatty acid receptor family but absent in the previously used β2-adrenergic receptor-based model (cyan). (c,d) DMR traces of HEK293 cells stably transfected with the hFFA2-K65R receptor stimulated with C3 (c) or 4-CMTB (d). (e,f) CRC of FFA2 agonists calculated at early ((e), peak within 0 – 800 sec) and late ((f), DMR at 6,000 sec) time points. (g,h) Effect of increasing concentrations of CATPB on DMR signatures of 30 µM C3 (g) and 4-CMTB (h) activating the hFFA2-K65R receptor. (i) CATPB inhibition of hFFA2-K65R receptor-mediated cell activation by C3 (pIC_{50}: 6.82 ± 0.06) or 4-CMTB (pIC_{50}: 6.97 ± 0.10). (j) CRC of FFA2 agonists activating the hFFA2-K65R receptor in the IP assay (pEC_{50}(C3): 4.21 ± 0.05; pEC_{50}(4-CMTB): 4.66 ± 0.12). (k,l) CATPB inhibition of C3 (k) or 4-CMTB (l)-elevated IP levels. (m) Analysis of IC_{50}-shifts according to Cheng-Prusoff (slope: C3: 1.007 ± 0.029, r^2: 0.990; 4-CMTB: 1.033 ± 0.050, r^2: 0.972). Representative real-time traces are shown as mean + s.e.m., measured in triplicates. Quantified data are depicted as mean values ± s.e.m. of three independent experiments.

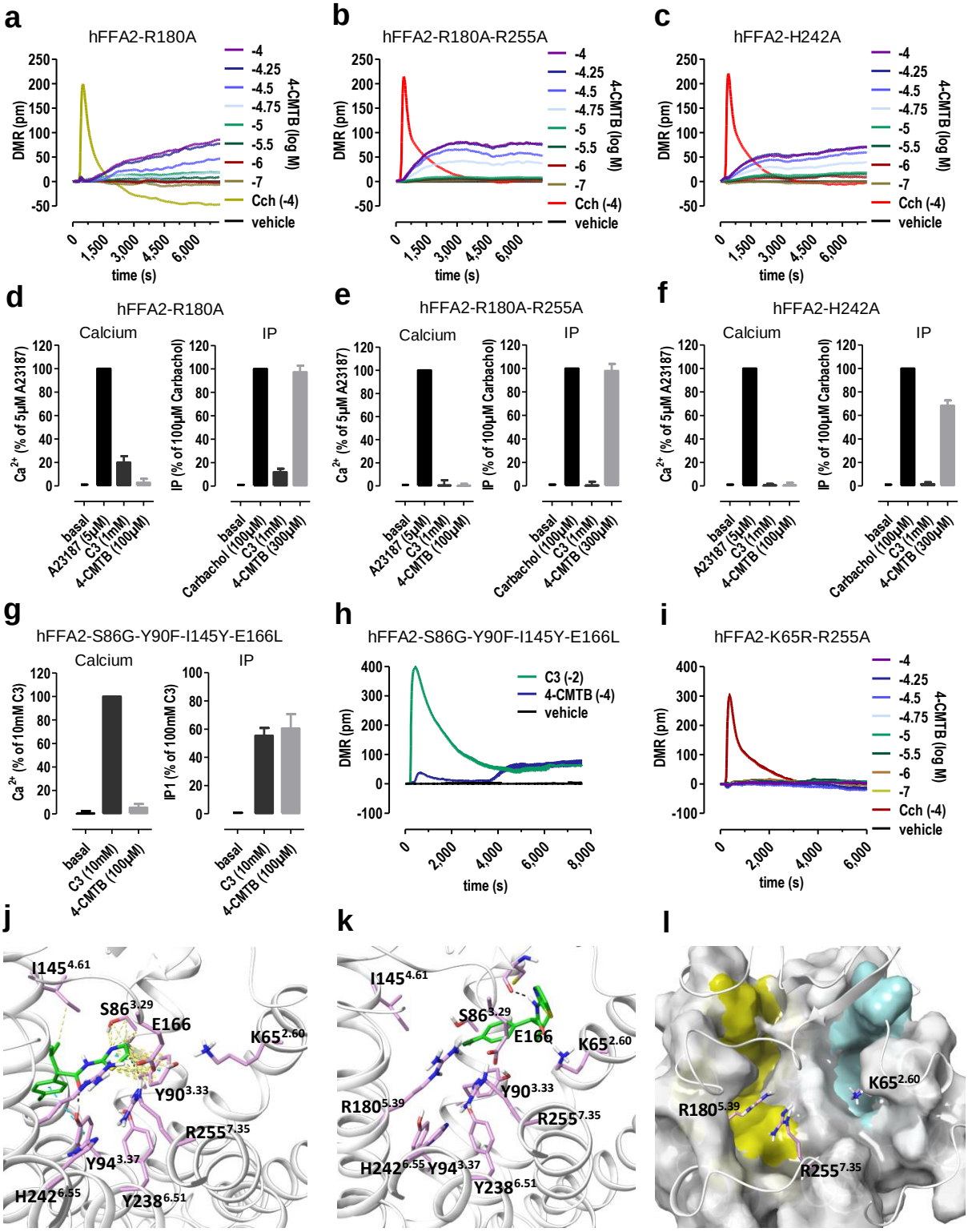

Figure 6. FFA2 receptor mutagenesis delineates two distinct receptor sites that convey 4-CMTB action.

(a-c) DMR traces of 4-CMTB activating HEK293 cells transiently expressing either the hFFA2-R180A (a), the hFFA2-R180A-R255A (b) or the hFFA2-H242A (c) receptor construct, Carbachol is shown as control. (d-f) Ca^{2+}-flux and IP level measurements as traditional endpoint assays capturing early and late cell response to stimulation with FFA2 agonists at the hFFA2-R180A (d), the hFFA2-R180A-R255A (e) and the hFFA2-H242A (f) receptor mutant. (g) Ca^{2+}-flux and IP response after activation with C3 or 4-CMTB at the FFA2 quadruple mutant. (h) DMR traces to C3 and 4-CMTB stimulation of the FFA2 quadruple mutant transfected HEK293 cells. (i) DMR readout of HEK293 cells

transiently expressing the hFFA2-K65R-R255A receptor mutant. Carbachol is shown as control. (j,k) 4-CMTB binding at the FFA2 orthosteric (j) and allosteric site (k). Hydrogen bonding, aromatic and van der Waals interactions are shown in black, cyan and yellow dotted lines, respectively. The binding modes of 4-CMTB were obtained via docking to the FFA1-based homology model of FFA2 and mutagenesis validation. (l) Surface representation of the receptor with coloured orthosteric and allosteric sites in yellow and cyan, respectively. Only anchoring residues, $R180^{5.39}$, $H242^{6.55}$ and $R255^{7.35}$ for the orthosteric site and $K65^{2.60}$ for the allosteric site are visualized. Representative real-time traces are shown as mean values, measured in triplicates. Quantified data are depicted as mean values ± s.e.m. of three independent experiments.

Methods

Chemical compounds

Propionic acid (C3) was purchased from Sigma-Aldrich. *(S)-3-(2-(3-Chlorophenyl)acetamido)-4-(4-(trifluoromethyl)phenyl)butanoic acid* (CATPB) and *2-(4-chlorophenyl)-3-methyl-N-(thiazol-2-yl)butanamide* (4-CMTB) were synthesized as described previously in [30] and [18], respectively.

Plasmids and mutagenesis

Enhanced yellow fluorescent protein (eYFP) was C-terminally fused to FFA2 receptor cDNA and subcloned into pcDNA5/FRT/TO (Invitrogen) as previously reported[29]. C-terminal tagging with eYFP was without effect on receptor functionality as confirmed by holistic label-free readouts (**Supplementary figure 20**). All functional studies were performed with eYFP-fused wt and mutated hFFA2 receptors, either stably (hFFA2-wt, hFFA2-R255A, hFFA2-ECL, hFFA2-R255A-ECL, hFFA2-K65R, hFFA2-S86G-Y90F-I145Y-E166L) or transiently (hFFA2-R180A, hFFA2-R180A-R255A, hFFA2-H242A, hFFA2-K65R-R255A) expressed in HEK293 cells at comparable levels (**Supplementary figure 19**). Fluorescent microscopy images were obtained with cells either induced with 1 µg/mL doxycycline or transiently transfected with respective receptor mutant and subsequently visualized using a 20x objective (Leica DM IL LED Fluo, Leica Microsystems). Site-directed mutagenesis in receptor cDNA in pcDNA5/FRT/TO was carried out following the QuikChange® protocol (Agilent Technologies). DpnI was used to digest template DNA and the mutated constructs were sequenced to confirm correct mutations. ECL2-swap mutant hFFA2-receptor (hFFA2-ECL) was generated as previously described [18].

Cell culture and transfections

To generate stable cell lines inducibly expressing the receptors, Flp-In™ T-REx™ 293 cells (Invitrogen) were cotransfected with pcDNA5/FRT/TO containing the receptor of interest and pOG44 (Invitrogen) in a ratio of 1:9 using a calcium phosphate DNA precipitation method according to manufacturer's instructions. pOG44 drives expression of recombinase, which enables recombination of FRT sites in the

receptor-cDNA carrying plasmid and the host genome of Flp-In™ T-REx™ 293 cells. In consequence, Hygromycin B resistance introduced by pcDNA5/FRT/TO can identify receptor-transfected cells. Stably transfected Flp-In™ T-REx™ 293 cells were cultured in Dulbecco's modified Eagle's medium (DMEM) containing 10% (v/v) fetal bovine serum (FBS), penicillin (100 U/mL), streptomycin (100 µg/mL), Hygromycin B (100 µg/mL) and Blasticidin (15 µg/mL) at 37°C and 5% CO_2. Untransfected Flp-In™ T-REx™ 293 host cells were maintained in DMEM supplemented with 10% (v/v) FBS, penicillin (100 U/mL), streptomycin (100 µg/mL), 100 µg/mL Zeocin and 15 µg/mL Blasticidin at 37°C and 5% CO_2. All experiments were carried out after inducing receptor expression with 1 µg/mL doxycycline for approximately 18 hours.

Dynamic mass redistribution (DMR) assay

DMR measurements were performed using either the Epic® System (Corning) or the EnSpire® System (PerkinElmer) as previously described in detail[26,27]. Briefly, 20,000 cells per well were seeded into a 384 well biosensor plate in culture medium and left to adhere for 4 – 6 hours at 37°C and 5% CO_2. Subsequently, medium was replaced by doxycycline (1 µg/mL) containing culture medium and the plate was incubated at 37°C and 5% CO_2 for approximately 18 hours to drive receptor expression. Cells were then washed at least twice with HBSS (supplemented with 20mM HEPES) and incubated for 1 hour at 37°C on the DMR reader. Compounds were diluted in HBSS (+20 mM HEPES) and added to the biosensor plate after 3 minutes of baseline read with a liquid handling system (CyBi®-SELMA, CyBio). Immediately after compound addition, DMR response was recorded for at least 1.5 hours. Where necessary, cells were preincubated with antagonist for 30 minutes.

Bioimpedance assay

Bioimpedance measurements were performed using the CellKey™ System (MolecularDevices). For this purpose, 15,000 cells were seeded into 384 well poly-D-lysine (PDL)-coated CellKey™ system microplates in culture medium and centrifuged at 150 x *g* for 1 minute. The plate was then incubated for 4 – 6 hours at 37°C and 5% CO_2 to allow cells to adhere to the biosensor plate. Thereafter, medium

was replaced by doxycycline containing (1 µg/mL) culture medium and incubated for approximately 18 hours at 37°C and 5% CO_2. Cells were then washed with HBSS (supplemented with 20 mM HEPES and the appropriate amount of DMSO according to the compound dilutions) three times using a manifold, which leaves 5 µL left in each well. 15 µL of wash buffer was added and the plate was subsequently transferred to the impedance reader and incubated for 1 hour at 37°C. Compounds were diluted in HBSS (containing 20 mM HEPES) and DMSO amount was adjusted in all dilution steps. 25 µL of compound solution was dispensed into a 384 well compound plate and subsequently incubated in the CellKey™ system. A baseline read was then recorded for 5 minutes and compound solutions were added directly onto the biosensor plate. Changes in cellular impedance (ohms) were measured as a result of extracellular current (dZiec) for 1 hour. If needed, cells were preincubated with antagonist for 30 minutes.

Calcium flux assay

Intracellular calcium mobilization was measured using the FLIPR® Calcium 5 Assay Kit in conjunction with the FlexStation® 3 Multimode Benchtop Reader (Molecular Devices). Briefly, cells were seeded into poly-D-lysine coated 96 well microplates at a density of 60,000 cells per well. After 4 – 6 hours the medium was replaced by culture medium supplemented with 1 µg/mL doxycycline and incubated for 18 hours at 37°C and 5% CO_2. Thereafter, cells were loaded with the FLIPR® Calcium 5 dye for 30 minutes at 37°C and subsequently processed according to manufacturer's instructions. Where necessary, cells were preincubated with antagonist for 30 minutes.

IP and cAMP assay

Intracellular levels of the second messenger IP and cAMP were quantified with a Mithras LB 940 multimode reader (Berthold Technologies) using the HTRF®-IP-One kit and the HTRF®-cAMP dynamic kit (CisBio International), respectively, according to the manufacturer's instructions. Briefly, for the IP assay, 10,000 receptor-expressing cells were seeded into a 384 well microplate and incubated for 20 minutes at 37°C. Cells were then stimulated with agonist for 30 minutes and IP levels were quantified

using the HTRF®-IP1 kit. Fr the cAMP assay, 3,000 cells were seeded into a 384 well microplate and incubated for 20 minutes at 37°C. Cells were stimulated with a mixture of agonist and forskolin for 30 minutes and intracellular levels of cAMP were subsequently analyzed using the HTRF®-cAMP dynamic kit. If needed, cells were preincubated with antagonist for 30 minutes.

pERK1/2 assay

Intracellular levels of phosphorylated ERK1/2 were quantified using the HTRF®-Cellul'erk kit (Cisbio International) and the Mithras LB 940 multimode reader (Berthold Technologies) following manufacturer's instructions. Briefly, 80,000 cells were seeded onto poly-D-lysine coated 96 well microplates and incubated for 4 – 6 hours at 37°C. Receptor expression was initiated by adding doxycycline (final concentration 1 µg/mL) and the plate was incubated for 18 hours at 37°C and 5% CO_2. Thereafter medium was replaced by starvation medium, lacking 10% FCS, and incubated for another 4 hours at 37°C and 5% CO_2. Compounds were added and pERK1/2 levels were determined using the HTRF®-Cellul'erk kit at time points as indicated. Where necessary, cells were preincubated with antagonist for 30 minutes.

Radioligand binding assay

The affinity of CATPB at wild type and R255A FFA2 was assessed through equilibrium displacement binding experiments against a radiolabeled form [^{3}H]AZ136821499 of a recently described FFA2 antagonist[47]. Membranes prepared from Flp-In™ T-REx™ 293 cell line induced to express the desired receptor variant were co-incubated in binding buffer (50 mM Tris-HCl, 100 mM NaCl, 10 mM $MgCl_2$, 1 mM EDTA, pH 7.4) with a fixed concentration of [^{3}H]AZ136821499 and increasing concentrations of CATPB for 2 h at 25°C. Membranes were then filtered through glass fiber filter paper and washed with PBS before membrane-bound [^{3}H] was measured by liquid scintillation spectrometry. In order to calculate pK_i values, specific [^{3}H] binding data were fit to a one-site displacement binding equation for which the K_d of [^{3}H]AZ136821499 was constrained to the value obtained for wild type (7.5 ± 0.4 nM) or R255A (13.0 ± 0.5 nM) in saturation binding assays.

Molecular modeling

The FFA1 crystal structure with PDB code 4PHU[31] was used as a template to generate the FFA2 homology model employing the Prime 3.0 program (Schrödinger, LLC, USA) with the default settings. The model was refined using a default energy minimization protocol implemented in Prime 3.0. Docking was conducted using Glide 6.5 (Schrödinger, LLC, USA) with the receptor grid defined by residues at positions 3.37, 4.57, 5.39, 6.51 and 7.53. The standard precision scoring function was used for docking. Modelling figures were generated with Maestro 9.9 (Schrödinger, LLC, USA). Molecular surface was built with probe radius of 0.9 Å.

Curve fitting and data analysis

All calculations were carried out using GraphPad Prism® 5.04 software (GraphPad Software). All label-free data from the DMR and bioimpedance assay were buffer-corrected and quantified as indicated. Calcium response was calculated using the maximal peak fluorescence within 80 seconds.

References

1. Lagerström, M. C. & Schiöth, H. B. Structural diversity of G protein-coupled receptors and significance for drug discovery, *Nature reviews. Drug discovery* **7,** 339–357 (2008).
2. Overington, J. P. Al-Lazikani, B. & Hopkins, A. L. How many drug targets are there?, *Nature reviews. Drug discovery* **5,** 993–996 (2006).
3. Kenakin, T. & Miller, L. J. Seven transmembrane receptors as shapeshifting proteins: the impact of allosteric modulation and functional selectivity on new drug discovery, *Pharmacological reviews* **62,** 265–304 (2010).
4. Wootten, D. Christopoulos, A. & Sexton, P. M. Emerging paradigms in GPCR allostery: implications for drug discovery, *Nature reviews. Drug discovery* **12,** 630–644 (2013).
5. May, L. T. Leach, K. Sexton, P. M. & Christopoulos, A. Allosteric modulation of G protein-coupled receptors, *Annual review of pharmacology and toxicology* **47,** 1–51 (2007).
6. Conn, P. J. Christopoulos, A. & Lindsley, C. W. Allosteric modulators of GPCRs: a novel approach for the treatment of CNS disorders, *Nature reviews. Drug discovery* **8,** 41–54 (2009).
7. Kenakin, T. New concepts in drug discovery: collateral efficacy and permissive antagonism, *Nature reviews. Drug discovery* **4,** 919–927 (2005).
8. Kenakin, T. & Christopoulos, A. Signalling bias in new drug discovery: detection, quantification and therapeutic impact, *Nature reviews. Drug discovery* **12,** 205–216 (2013).
9. Christopoulos, A. Advances in G protein-coupled receptor allostery: from function to structure, *Molecular pharmacology* **86,** 463–478 (2014).
10. Christopoulos, A. *et al.* International union of basic and clinical pharmacology. XC. multisite pharmacology: recommendations for the nomenclature of receptor allosterism and allosteric ligands, *Pharmacological reviews* **66,** 918–947 (2014).
11. Antony, J. *et al.* Dualsteric GPCR targeting: a novel route to binding and signaling pathway selectivity, *FASEB journal : official publication of the Federation of American Societies for Experimental Biology* **23,** 442–450 (2009).
12. Valant, C. *et al.* A novel mechanism of G protein-coupled receptor functional selectivity. Muscarinic partial agonist McN-A-343 as a bitopic orthosteric/allosteric ligand, *The Journal of biological chemistry* **283,** 29312–29321 (2008).
13. Lane, J. R. Sexton, P. M. & Christopoulos, A. Bridging the gap: bitopic ligands of G-protein-coupled receptors, *Trends in pharmacological sciences* **34,** 59–66 (2013).
14. Valant, C. Robert Lane, J. Sexton, P. M. & Christopoulos, A. The best of both worlds? Bitopic orthosteric/allosteric ligands of g protein-coupled receptors, *Annual review of pharmacology and toxicology* **52,** 153–178 (2012).
15. Le Poul, E. *et al.* Functional characterization of human receptors for short chain fatty acids and their role in polymorphonuclear cell activation, *The Journal of biological chemistry* **278,** 25481–25489 (2003).
16. Brown, A. J. *et al.* The Orphan G protein-coupled receptors GPR41 and GPR43 are activated by propionate and other short chain carboxylic acids, *The Journal of biological chemistry* **278,** 11312–11319 (2003).

17. Lee, T. *et al.* Identification and functional characterization of allosteric agonists for the G protein-coupled receptor FFA2, *Molecular pharmacology* **74,** 1599–1609 (2008).

18. Smith, N. J. *et al.* Extracellular loop 2 of the free fatty acid receptor 2 mediates allosterism of a phenylacetamide ago-allosteric modulator, *Molecular pharmacology* **80,** 163–173 (2011).

19. Wang, Y. *et al.* The first synthetic agonists of FFA2: Discovery and SAR of phenylacetamides as allosteric modulators, *Bioorganic & medicinal chemistry letters* **20,** 493–498 (2010).

20. Hudson, B. D. *et al.* Defining the molecular basis for the first potent and selective orthosteric agonists of the FFA2 free fatty acid receptor, *The Journal of biological chemistry* **288,** 17296–17312 (2013).

21. Swaminath, G. *et al.* Mutational analysis of G-protein coupled receptor--FFA2, *Biochemical and biophysical research communications* **405,** 122–127 (2011).

22. Scott, C. W. & Peters, M. F. Label-free whole-cell assays: expanding the scope of GPCR screening, *Drug discovery today* **15,** 704–716 (2010).

23. Verrier, F. *et al.* GPCRs regulate the assembly of a multienzyme complex for purine biosynthesis, *Nature chemical biology* **7,** 909–915 (2011).

24. Kenakin, T. A holistic view of GPCR signaling, *Nature biotechnology* **28,** 928–929 (2010).

25. Kenakin, T. P. Cellular assays as portals to seven-transmembrane receptor-based drug discovery, *Nature reviews. Drug discovery* **8,** 617–626 (2009).

26. Schröder, R. *et al.* Applying label-free dynamic mass redistribution technology to frame signaling of G protein-coupled receptors noninvasively in living cells, *Nat Protoc* **6,** 1748–1760 (2011).

27. Grundmann, M. & Kostenis, E. Label-free biosensor assays in GPCR screening, *Methods in molecular biology (Clifton, N.J.)* **1272,** 199–213 (2015).

28. Schröder, R. *et al.* Deconvolution of complex G protein-coupled receptor signaling in live cells using dynamic mass redistribution measurements, *Nature biotechnology* **28,** 943–949 (2010).

29. Stoddart, L. A. Smith, N. J. Jenkins, L. Brown, A. J. & Milligan, G. Conserved polar residues in transmembrane domains V, VI, and VII of free fatty acid receptor 2 and free fatty acid receptor 3 are required for the binding and function of short chain fatty acids, *The Journal of biological chemistry* **283,** 32913–32924 (2008).

30. Hudson, B. D. Tikhonova, I. G. Pandey, S. K. Ulven, T. & Milligan, G. Extracellular ionic locks determine variation in constitutive activity and ligand potency between species orthologs of the free fatty acid receptors FFA2 and FFA3, *The Journal of biological chemistry* **287,** 41195–41209 (2012).

31. Srivastava, A. *et al.* High-resolution structure of the human GPR40 receptor bound to allosteric agonist TAK-875, *Nature* **513,** 124–127 (2014).

32. Swaminath, G. *et al.* Allosteric rescuing of loss-of-function FFAR2 mutations, *FEBS Lett.* **584,** 4208–4214 (2010).

33. Mohr, K. *et al.* Rational design of dualsteric GPCR ligands: quests and promise, *British journal of pharmacology* **159,** 997–1008 (2010).

34. Lefkowitz, R. J. & Shenoy, S. K. Transduction of receptor signals by beta-arrestins, *Science* **308,** 512–517 (2005).

35. Ahn, S. Shenoy, S. K. Wei, H. & Lefkowitz, R. J. Differential kinetic and spatial patterns of beta-arrestin and G protein-mediated ERK activation by the angiotensin II receptor, *J. Biol. Chem.* **279,** 35518–35525 (2004).

36. Goel, R. Phillips-Mason, P. J. Raben, D. M. & Baldassare, J. J. alpha-Thrombin induces rapid and sustained Akt phosphorylation by beta-arrestin1-dependent and -independent mechanisms, and only the sustained Akt phosphorylation is essential for G1 phase progression, *J. Biol. Chem.* **277,** 18640–18648 (2002).

37. Rajagopal, S. Rajagopal, K. & Lefkowitz, R. J. Teaching old receptors new tricks: biasing seven-transmembrane receptors, *Nat Rev Drug Discov* **9,** 373–386 (2010).

38. Simpson, P. B. & Wafford, K. A. New directions in kinetic high information content assays, *Drug discovery today* **11,** 237–244 (2006).

39. Kruse, A. C. *et al.* Structure and dynamics of the M3 muscarinic acetylcholine receptor, *Nature* **482,** 552–556 (2012).

40. Granier, S. & Kobilka, B. A new era of GPCR structural and chemical biology, *Nature chemical biology* **8,** 670–673 (2012).

41. Kruijf, P. de *et al.* Identification of a novel allosteric binding site in the CXCR2 chemokine receptor, *Molecular pharmacology* **80,** 1108–1118 (2011).

42. Picone, R. P. *et al.* (-)-7'-Isothiocyanato-11-hydroxy-1',1'-dimethylheptylhexahydrocannabinol (AM841), a high-affinity electrophilic ligand, interacts covalently with a cysteine in helix six and activates the CB1 cannabinoid receptor, *Molecular pharmacology* **68,** 1623–1635 (2005).

43. Pei, Y. *et al.* Ligand-binding architecture of human CB2 cannabinoid receptor: evidence for receptor subtype-specific binding motif and modeling GPCR activation, *Chemistry & biology* **15,** 1207–1219 (2008).

44. Hurst, D. P. *et al.* A lipid pathway for ligand binding is necessary for a cannabinoid G protein-coupled receptor, *The Journal of biological chemistry* **285,** 17954–17964 (2010).

45. Hanson, M. A. *et al.* Crystal structure of a lipid G protein-coupled receptor, *Science (New York, N.Y.)* **335,** 851–855 (2012).

46. Schadel, S. A. *et al.* Ligand channeling within a G-protein-coupled receptor. The entry and exit of retinals in native opsin, *The Journal of biological chemistry* **278,** 24896–24903 (2003).

47. Pizzonero, M. *et al.* Discovery and optimization of an azetidine chemical series as a free fatty acid receptor 2 (FFA2) antagonist: from hit to clinic, *J. Med. Chem.* **57,** 10044–10057 (2014).

Appendix

A Kinetic Model for Sequential Agonism at a 7TMR

In vitro, biochemical receptor experiments provide snapshots of agonist activity; label-free technology allows real time to be a variable thereby unveiling kinetic effects. It is useful to model agonist effects in real time assuming first order onset according to:

(1) $$\rho_t = \rho_e\left(1 - e^{-(k_1[A]+k_2)t}\right)$$

where ρ_t is fractional receptor occupancy at time t, k_1 the rate of onset (in s^{-1} M^{-1}), k_2 the rate of offset (in s^{-1}) and ρ_e the receptor occupancy at equilbrium. From the Mass action relationship an equation for the concentration of agonist ([A]) divided by the equilibrium dissociation constant of the agonist receptor complex (K_A) can be derived:

(2) $$\rho = \frac{[A]/K_A}{[A]/K_A + 1} \rightarrow \frac{[A]}{K_A} = \frac{\rho}{1-\rho}$$

Combining equations (1) and (2) yields:

(3) $$\left[\frac{[A]}{K_A}\right]_t = \frac{1 - e^{-(k_{1A}[A]+k_{2A})t}}{\rho^{-1} + e^{-(k_{1A}[A]+k_{2A})t} - 1} = \phi$$

Expressing response according to the Black/Leff operational modelblack[1] and substituting for $[A]/K_A$ for time t (equation (3)) yields an expression for the emergence of response as a function of time:

(4) $$response_t = \frac{\tau_A \phi}{\phi(1+\tau_A)+1}$$

Equation (4) can be used to simulate concentration-response curves to an agonist at various times for agonists of varying rates of onset and offset. **Fig. 1** shows an agonist with relatively slow kinetics ($k_{1A}= 10^3\ M^{-1}\ s^{-1}$, $k_{2A} = 10^{-3}\ s^{-1}$, $K_A= 1\ \mu M$, $\tau_A= 0.1$); it can be seen that a single phase sigmoidal curve is observed at all times. It can also be shown that a series and/or parallel array of fast and slow kinetic stimulus-response functions (seen as forcing functions in **Fig. 1**) that emanate from a single drug-receptor binding interaction will lead to a single-phase sigmoidal function as well.

In contrast, a different pattern emerges for two forcing functions of varying rates when one of the functions modifies the output of the second. Such an array is operative when considering the allosteric nature of receptors and two agonist binding sites utilized in tandem by sequentially activating ligands (SEALs) *vide infra*. As a preface, it is useful to describe the allosteric nature of receptors within the context of molecular dynamics. Seven transmembrane receptors (7TMRs) are nature's prototypic allosteric protein and respond to binding of molecules by changing conformation. All agonists for 7TMRs are allosteric in that they alter the interaction of the receptor with cellular signaling proteins. It is useful to delineate binding loci on 7TMRs as orthosteric, referring to the site utilized by the natural agonist, and allosteric denoting a site distinct from the natural agonist binding site. According to standard allosteric theory, it cannot be assumed that the binding of a molecule to an allosteric site does not alter the interaction of molecules interacting at the orthosteric site and *vice versa*. Sequentially activating ligands are defined as those that demonstrate two kinetically distinct phases of agonism through binding at a first site followed by sustained activation via a second topographically distinct site (herein, site 1 is orthosteric and site 2 is allosteric). This is in

contrast to canonical bitopic ligands which are defined as those that concomitantly engage both receptor sites on 7TMRs[2–4]. Thus, for clarification, the model described here considers a molecule that binds rapidly to the orthosteric site and then more slowly to an allosteric site on the receptor. Such kinetics are consistent with known orthosteric and allosteric ligands when viewed in terms of molecular dynamic models.

Receptors as seen from a molecular dynamic standpoint exist as ensembles of different conformations of similar free energy[5–8]. Under these circumstances there is no reason to assume that an allosteric site will be available for binding at all times, i.e. the site may appear or disappear with dynamic changes in protein conformation. In contrast, the orthosteric site is thought be to be open nearly at all times in view of it's physiological role, i.e. availablity for binding on demand with the natural agonist. This idea has been suggested to account for the relatively rapid enzyme inhibition by orthosteric inhibitors of some p38 mitogen-activated protein (MAP) kinase inhibitors where the rate of onset of allosteric inhibitors is 500 times slower than for orthosteric antagonists[9]. Similarly, allosteric inhibitors of HIV-1 entry have half-times for dissociation from the CCR 5 receptor ranging from 80 to >300 h with correspondingly long times of onset in contrast to the interaction of peptide chemokines binding to the orthosteric site[10]. Thus, in general, it is reasonable to propose binding to the orthosteric site will be more rapid than to the allosteric site of a receptor protein.

A model applicable to mechanisms that involve sequential receptor activation by a single ligand with variation over time is shown in **Fig. 2**. This model assumes that the molecule is an agonist at both sites with an efficacy of τ_A for the orthosteric site and τ_B for the allosteric site. It also alters the affinity for interaction at the orthosteric site by an allosteric factor α and its efficacy by a factor β; these factors reciprocate toward the allosteric site as well as required by standard allosteric models. To accommodate binding to a second allosteric site, a second

kinetic equation for onset to that site is defined just as with the orthosteric onset (equation (3)):

$$\left[\frac{[A]}{K_B}\right]_t = \frac{1-e^{-(k_{1B}[A]+k_{2B})t}}{\rho_e^{-1}+e^{-(k_{1B}[A]+k_{2B})t}-1} = \lambda \quad (5)$$

The equation for the allosteric modification of an orthosteric binding effect is given by the standard functional allosteric model[11–13]:

(6)

$$response = \frac{\tau_A([A]/K_A)_t(1+\alpha\beta([A]/K_B)_t)+\tau_B[A]/K_B}{([A]/K_A)_t(1+\alpha([A]/K_B)_t+\tau_A(1+\alpha\beta([A]/K_B)_t))+([A]K_B)_t(1+\tau_B)+1}$$

where the concentration of the allosteric modulator is [B], K_B the equilibrium dissociation constant of the modulator-receptor complex, α the effect of the modulator on agonist affinity, β the effect of the modulator on agonist efficacy, τ_A and τ_B the intrinsic efficacies of the orthosteric and allosteric agonist, respectively. Substituting the kinetic expressions for $[A]/K_A$ for the orthosteric site (equation (3)) and the allosteric site (equation (5)) yields a kinetic equation for response production for an allosteric system:

$$response_t = \frac{\tau_A\phi(1+\alpha\beta\lambda)+\lambda\tau_B}{\phi(1+\alpha\lambda+\tau_A(1+\alpha\beta\lambda))+\phi+\lambda(1+\lambda_B)+1} \quad (7)$$

The kinetic behavior of a tandem orthosteric-allosteric activation model with a fast rate of onset for the orthosteric site and a slower rate of onset for the allosteric site is shown in **Fig. 3** (for a model with $k_{1A}= 10^5\ M^{-1}s^{-1}$, $k_{2A}= 10^{-1}\ s^{-1}$, $k_{1B}=10^3\ s^{-1}$ and $k_{2B}= 3x10^{-3}\ M^{-1}s^{-1}$ when response is measured at various times). The sequentially activating ligand has an orthosteric

efficacy of τ_A=0.1, an allosteric efficacy of τ_B=10, orthosteric K_A= 1 μM, allosteric K_B= 3 μM , α= 0.01 and β= 3 for reciprocal interaction between the orthosteric and allosteric sites when the ligand is bound to both.

It can be seen that the SEAL model concentration-response curve pattern (**Fig. 3**) differs from the varying rate single binding site model (**Fig. 1**). A single site slow onset is reflected by a single sigmoid characteristic curve with varying location parameters along the concentration axis with time. In contrast a SEAL can produce two distinctly different sigmoid curves at various times reflecting the orthosteric and then orthosteric-allosteric combination with time. It should be noted that the relative locations of the two kinetically distinct curves along the concentration axis depend on a number of parameters including K_A, K_B, α, β, τ_A and τ_B and therefore have no intrinsic meaning to the model.

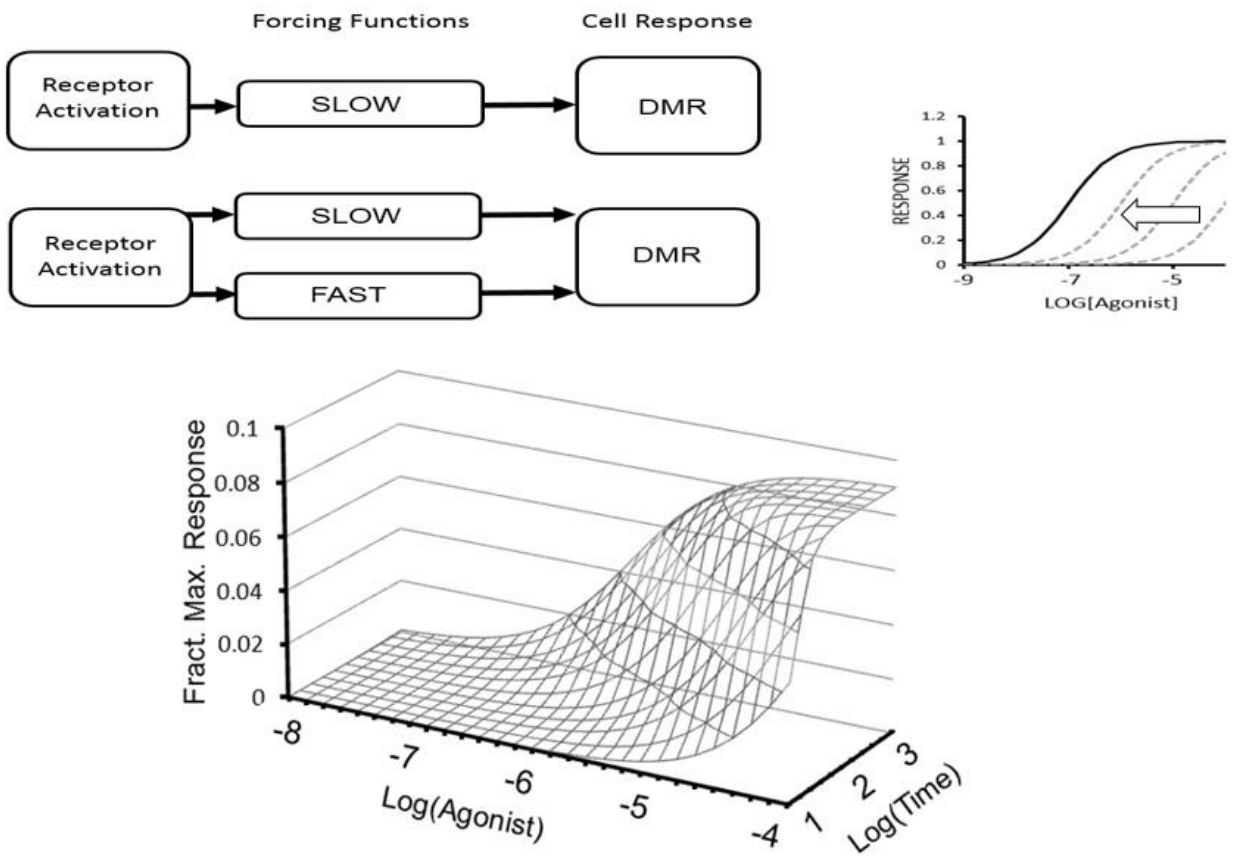

Figure 1. Concentration-response curves to a slow onset orthosteric agonist at various times.

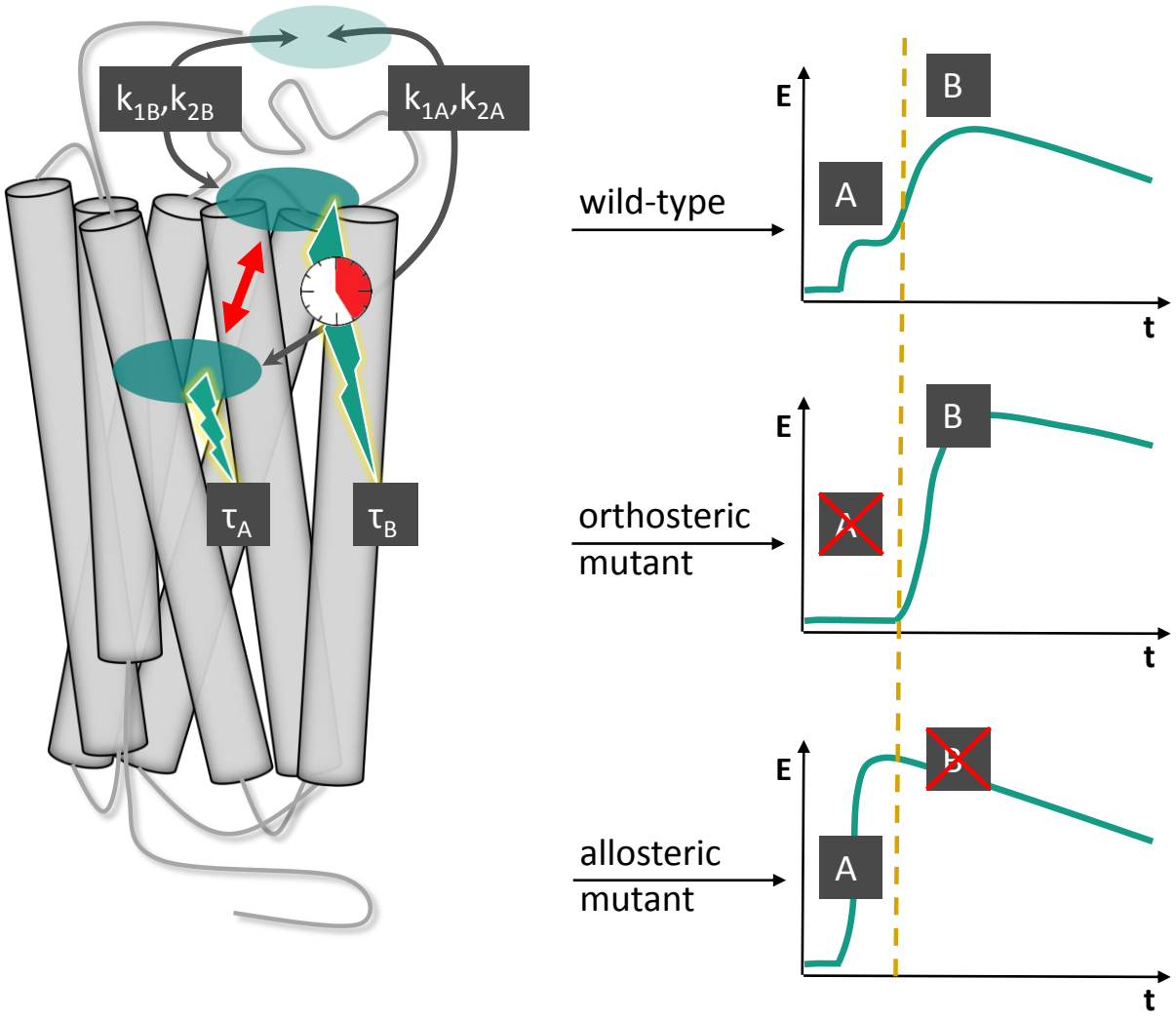

Figure 2. Dual occupancy by a sequentially activating ligand (SEAL) of an orthosteric site with rate of onset k_{1A} and offset k_{2A} and an allosteric site with rate of onset k_{1B} and offset k_{2B} produce a response with an efficacy τ_A for the orthosteric site and τ_B for the allosteric site. According to the allosteric system in the kinetic SEAL model, targeted perturbation of the orthosteric or the allosteric receptor site results in the omission/amplification of initial effect A or delayed effect B, respectively.

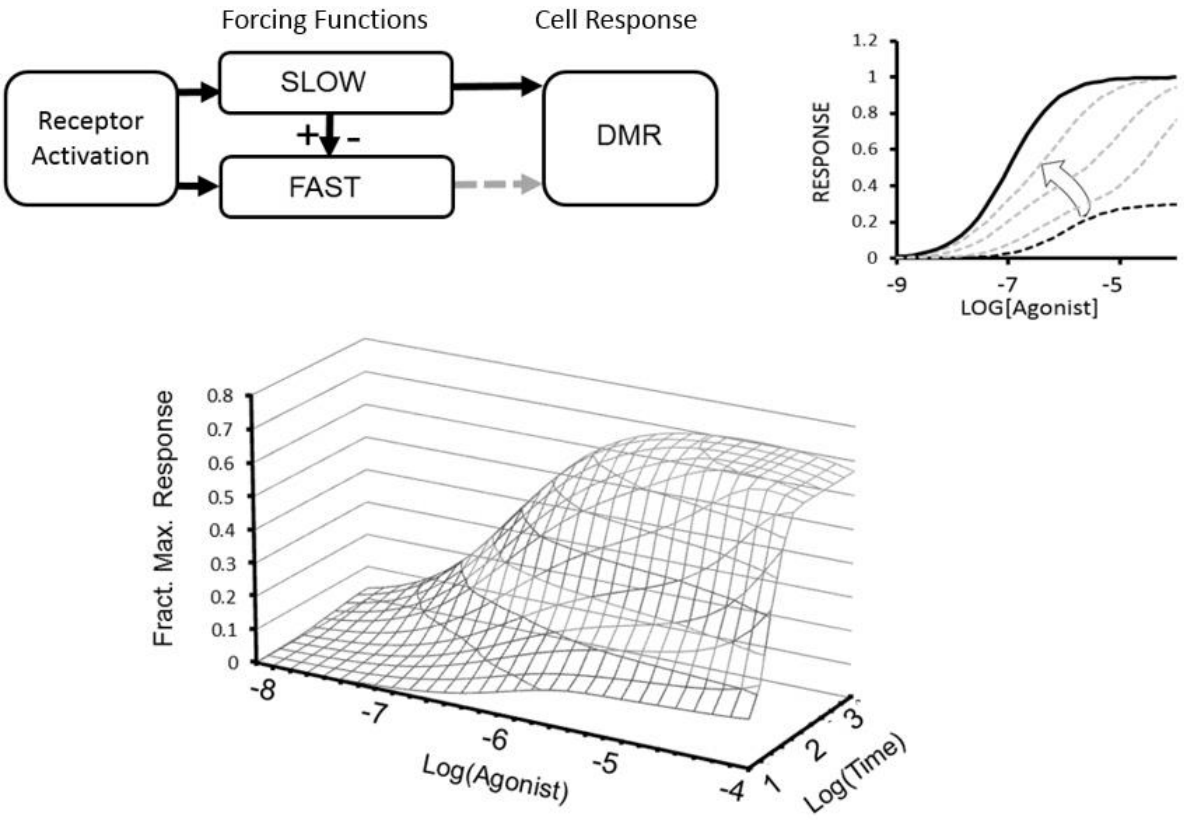

Figure 3. Concentration-response curves to sequentially activating ligands calculated with equation 7 for various times from t=5 to 2000 s.

References

1. Black, J. W. & Leff, P. Operational Models of Pharmacological Agonism, *Proceedings of the Royal Society B: Biological Sciences* **220,** 141–162 (1983).
2. Lane, J. R. Sexton, P. M. & Christopoulos, A. Bridging the gap: bitopic ligands of G-protein-coupled receptors, *Trends in pharmacological sciences* **34,** 59–66 (2013).
3. Keov, P. *et al.* Molecular mechanisms of bitopic ligand engagement with the M1 muscarinic acetylcholine receptor, *J. Biol. Chem.* **289,** 23817–23837 (2014).
4. Valant, C. Robert Lane, J. Sexton, P. M. & Christopoulos, A. The best of both worlds? Bitopic orthosteric/allosteric ligands of g protein-coupled receptors, *Annual review of pharmacology and toxicology* **52,** 153–178 (2012).
5. Hilser, V. J. & Thompson, E. B. Intrinsic disorder as a mechanism to optimize allosteric coupling in proteins, *Proc. Natl. Acad. Sci. U.S.A.* **104,** 8311–8315 (2007).
6. Hilser, V. J. García-Moreno E, B. Oas, T. G. Kapp, G. & Whitten, S. T. A statistical thermodynamic model of the protein ensemble, *Chem. Rev.* **106,** 1545–1558 (2006).
7. Freire, E. Statistical thermodynamic linkage between conformational and binding equilibria, *Adv. Protein Chem.* **51,** 255–279 (1998).
8. Frauenfelder, H. Sligar, S. G. & Wolynes, P. G. The energy landscapes and motions of proteins, *Science* **254,** 1598–1603 (1991).
9. Pargellis, C. *et al.* Inhibition of p38 MAP kinase by utilizing a novel allosteric binding site, *Nat. Struct. Biol.* **9,** 268–272 (2002).
10. Watson, C. Jenkinson, S. Kazmierski, W. & Kenakin, T. The CCR5 receptor-based mechanism of action of 873140, a potent allosteric noncompetitive HIV entry inhibitor, *Mol. Pharmacol.* **67,** 1268–1282 (2005).
11. Price, M. R. *et al.* Allosteric modulation of the cannabinoid CB1 receptor, *Mol. Pharmacol.* **68,** 1484–1495 (2005).
12. Ehlert, F. J. Analysis of allosterism in functional assays, *J. Pharmacol. Exp. Ther.* **315,** 740–754 (2005).
13. Kenakin, T. New concepts in drug discovery: collateral efficacy and permissive antagonism, *Nature reviews. Drug discovery* **4,** 919–927 (2005).

Epilogue

The idea of a ligand-receptor interaction is a long-standing one and was first described by Ehrlich, Langley and Clark[1,2] and was refined ever since then, which is still an ongoing process. In the perception of receptor theory, GPCRs evolved from simple "on-off" switches to highly complex microprocessors for the transduction of cell signaling[3,4]. Indispensable requirements for ligand-receptor interaction are structural determinants. A ligand only binds to a receptor if it "fits" to certain epitopes on the receptor protein. Although large amounts of data pillow the effort (and partial success) to *a priori* predict whether a compound binds to a receptor and how this interaction influences the conformations of the receptor and thus cell signaling, the hurdles seem too high and this yet remains an attempt.

Nonetheless, it is getting clear that GPCR activation upon agonist binding is intrinsically linked with a multistep process[5], which must initially be considered separately from the sequential activation mode introduced in this chapter. On the other hand, binding to several sites of the receptor might in fact induce a set of different conformations that in turn trigger certain signaling events. Several studies could demonstrate that different agonists for the same GPCR induce distinct conformational changes within the receptor protein[4,6,7]. Since active states of GPCRs can be achieved by destabilizing the normal structure of those proteins and increasing their flexibility[8,9], triggering molecular microswitches within GPCRs by their ligands is a well-supported concept of receptor activation[10]. Two of these microswitches are already described in the introductory section and should only be mentioned briefly here. i) The *Rotamer Toggle Switch* in TM6[11–14] and ii) an *Ionic Lock* between TM3 and TM6[15,16]. An increase in the destabilization of the GPCR structure by engagement of these and other microswitches has been associated with graded efficacy of agonists[17]. Since variations in the set of induced conformational changes have been attributed to different signaling behaviors, it could further be envisaged that those microswitches play a substantial role in the generation of signaling bias. Studies on peptide-binding at the neurokinin receptor for example revealed that a rapid binding component was associated with a calcium response, whereas a slow binding event was linked to a cAMP response[18]. Hence, although multistep agonist binding as delineated above and the concept of sequentially activating ligands are distinct phenomena with regard to cell signaling, the underlying structural rearrangements may be overlapping.

A distinctive feature of 4-CMTB is the order of signaling events. An initial orthosteric activation is followed by an allosteric site-mediated signaling impulse. Since the orthosteric binding site is assumed to be situated deeper in the transmembrane region of the receptor protein, whereas the allosteric epitope is expected to be located in the extracellular vestibule of the receptor[10], we

proposed an entry mode for 4-CMTB from the lipid bilayer. This mode-of-action is not unprecedented in the literature and is especially discussed for other lipid-recognizing receptors[19–23].

As mentioned in the prologue, ligands that show intrinsic activity and allosteric modulating features at the same time are attractive compounds for certain diseases[24]. Moreover, ago-allosteric ligands are not only therapeutically interesting but also mechanistically, since their mode-of-action still remains largely elusive[25]. A bitopic binding mode for ago-allosteric ligands has been discussed and some reports indicate that several previously recognized "pure" allosteric ligands might actually bind in a bitopic manner[26–30]. Although bitopic binding or binding to overlapping binding sites is not intuitively compatible with allosteric modulation between the allosteric and the orthosteric compound, *Schwartz et al.* proposed three possible binding scenarios for ago-allosteric ligands at GPCRs that involve a bitopic binding mode in a broader sense[28]. i) The ago-allosteric ligand could interconvert between two binding poses. In the absence of an orthosteric ligand, the ago-allosteric ligand would bind to the orthosteric receptor site (maybe overlapping with an allosteric epitope), whereas it would bind to an allosteric site in the presence of an orthosteric probe, presumably in another orientation. This mechanism would explain both the intrinsic activity of the ago-allosteric ligand and the allosteric modulating character of the compound. Furthermore, in this model the ago-allosteric ligand blocks the exit of the agonist, which is in line with the classic expectation of allosteric ligands inhibiting the dissociation of the orthosteric ligand. ii) "Time-resolved allostery", where the ago-allosteric and the orthosteric ligand bind to partially the same binding site, i.e. the ago-allosteric ligand binds to a site, that shows considerable overlap with the orthosteric binding site. Orthosteric and ago-allosteric ligand bind to distinct active receptor conformations that slowly interconvert into each other. Thus binding of each ligand occurs at different points in time. This scenario, however, would not explain the inhibition of orthosteric agonist dissociation by the allosteric compound. Notably, this scenario also implies a "bitopic" binding mode of the ago-allosteric ligand to both the classical allosteric and the orthosteric binding site. iii) In a dimeric binding mode, the ago-allosteric ligand might bind to an "allosteric" protomer, maybe in a bitopic fashion, whereas the endogenous ligand binds to the orthosteric protomer. This mechanism has recently been confirmed for the dopamine D_2 receptor[31].

However, none of these mechanistic proposals can fully explain the behavior of the ago-allosteric ligand 4-CMTB. Hence, in the here presented study, 4-CMTB emerged as the prototype of a hitherto unknown class of GPCR ligands, for which we coined the term "*sequentially activating ligands*". The ago-allosteric nature of 4-CMTB is explained by a sequential binding mechanism, wherein each interaction step is associated with distinct signaling impulses.

References

1. Maehle, A.-H. A binding question: the evolution of the receptor concept, *Endeavour* **33,** 135–140 (2009).
2. Maehle, A.-H. Prüll, C.-R. & Halliwell, R. F. The emergence of the drug receptor theory, *Nat Rev Drug Discov* **1,** 637–641 (2002).
3. Kenakin, T. P. Biased signalling and allosteric machines: new vistas and challenges for drug discovery, *Br. J. Pharmacol.* **165,** 1659–1669 (2012).
4. Kenakin, T. & Miller, L. J. Seven transmembrane receptors as shapeshifting proteins: the impact of allosteric modulation and functional selectivity on new drug discovery, *Pharmacol. Rev.* **62,** 265–304 (2010).
5. Kobilka, B. Agonist binding: a multistep process, *Mol. Pharmacol.* **65,** 1060–1062 (2004).
6. Vaidehi, N. & Kenakin, T. The role of conformational ensembles of seven transmembrane receptors in functional selectivity, *Curr Opin Pharmacol* **10,** 775–781 (2010).
7. Ghanouni, P. *et al.* Functionally different agonists induce distinct conformations in the G protein coupling domain of the beta 2 adrenergic receptor, *J. Biol. Chem.* **276,** 24433–24436 (2001).
8. West, G. M. *et al.* Ligand-dependent perturbation of the conformational ensemble for the GPCR β2 adrenergic receptor revealed by HDX, *Structure* **19,** 1424–1432 (2011).
9. McLean, A. J. Generation and Analysis of Constitutively Active and Physically Destabilized Mutants of the Human beta 1-Adrenoceptor, *Molecular Pharmacology* **62,** 747–755 (2002).
10. Venkatakrishnan, A. J. *et al.* Molecular signatures of G-protein-coupled receptors, *Nature* **494,** 185–194 (2013).
11. Rasmussen, S. G. F. *et al.* Crystal structure of the β2 adrenergic receptor-Gs protein complex, *Nature* **477,** 549–555 (2011).
12. Rasmussen, S. G. F. *et al.* Structure of a nanobody-stabilized active state of the β(2) adrenoceptor, *Nature* **469,** 175–180 (2011).
13. Xu, F. *et al.* Structure of an agonist-bound human A2A adenosine receptor, *Science* **332,** 322–327 (2011).
14. Shi, L. *et al.* Beta2 adrenergic receptor activation. Modulation of the proline kink in transmembrane 6 by a rotamer toggle switch, *J. Biol. Chem.* **277,** 40989–40996 (2002).
15. Vogel, R. *et al.* Functional role of the "ionic lock"--an interhelical hydrogen-bond network in family A heptahelical receptors, *J. Mol. Biol.* **380,** 648–655 (2008).
16. Yao, X. *et al.* Coupling ligand structure to specific conformational switches in the beta2-adrenoceptor, *Nat. Chem. Biol.* **2,** 417–422 (2006).
17. Warne, T. *et al.* The structural basis for agonist and partial agonist action on a β(1)-adrenergic receptor, *Nature* **469,** 241–244 (2011).
18. Palanche, T. *et al.* The neurokinin A receptor activates calcium and cAMP responses through distinct conformational states, *J. Biol. Chem.* **276,** 34853–34861 (2001).
19. Picone, R. P. *et al.* (-)-7'-Isothiocyanato-11-hydroxy-1',1'-dimethylheptylhexahydrocannabinol (AM841), a high-affinity electrophilic ligand, interacts covalently with a cysteine in helix six and activates the CB1 cannabinoid receptor, *Mol. Pharmacol.* **68,** 1623–1635 (2005).
20. Schadel, S. A. *et al.* Ligand channeling within a G-protein-coupled receptor. The entry and exit of retinals in native opsin, *J. Biol. Chem.* **278,** 24896–24903 (2003).

21. Pei, Y. *et al.* Ligand-binding architecture of human CB2 cannabinoid receptor: evidence for receptor subtype-specific binding motif and modeling GPCR activation, *Chem. Biol.* **15,** 1207–1219 (2008).

22. Kruijf, P. de *et al.* Identification of a novel allosteric binding site in the CXCR2 chemokine receptor, *Mol. Pharmacol.* **80,** 1108–1118 (2011).

23. Hanson, M. A. *et al.* Crystal structure of a lipid G protein-coupled receptor, *Science* **335,** 851–855 (2012).

24. Wootten, D. Christopoulos, A. & Sexton, P. M. Emerging paradigms in GPCR allostery: implications for drug discovery, *Nat Rev Drug Discov* **12,** 630–644 (2013).

25. Langmead, C. J. & Christopoulos, A. Allosteric agonists of 7TM receptors: expanding the pharmacological toolbox, *Trends Pharmacol. Sci.* **27,** 475–481 (2006).

26. Feighner, S. D. *et al.* Structural requirements for the activation of the human growth hormone secretagogue receptor by peptide and nonpeptide secretagogues, *Mol. Endocrinol.* **12,** 137–145 (1998).

27. Spalding, T. A. *et al.* Structural requirements of transmembrane domain 3 for activation by the M1 muscarinic receptor agonists AC-42, AC-260584, clozapine, and N-desmethylclozapine: evidence for three distinct modes of receptor activation, *Mol. Pharmacol.* **70,** 1974–1983 (2006).

28. Schwartz, T. W. & Holst, B. Allosteric enhancers, allosteric agonists and ago-allosteric modulators: where do they bind and how do they act?, *Trends Pharmacol. Sci.* **28,** 366–373 (2007).

29. Holst, B. *et al.* Overlapping binding site for the endogenous agonist, small-molecule agonists, and ago-allosteric modulators on the ghrelin receptor, *Mol. Pharmacol.* **75,** 44–59 (2009).

30. Holst, B. Brandt, E. Bach, A. Heding, A. & Schwartz, T. W. Nonpeptide and peptide growth hormone secretagogues act both as ghrelin receptor agonist and as positive or negative allosteric modulators of ghrelin signaling, *Mol. Endocrinol.* **19,** 2400–2411 (2005).

31. Lane, J. R. *et al.* A new mechanism of allostery in a G protein-coupled receptor dimer, *Nat. Chem. Biol.* **10,** 745–752 (2014).

Chapter 3: Designer FFA2 receptor

Prologue

Discovery of potent agonists that selectively target one member of a closely related receptor family constitutes a great challenge. Traditionally, lead discovery focused on the disclosure of compounds that engage the site of the receptor that is used by the endogenous ligand, also referred to as the orthosteric binding pocket. However, this approach is not suited to selectively target receptors that show greater sequence homology within this receptor epitope such as subtypes in a receptor family that share the same endogenous agonist[1,2]. This applies also to the family of free fatty acid receptors[3].

In the case of the free fatty acid receptor FFA2 the endogenous ligands comprise the short-chain fatty acids (SCFAs), primarily C1 to C5 with a rank order of potency: C2=C3>C4>C5=C1[4]. The overall potency of the endogenous ligands is in the mid micromolar range and thus relatively low. The most obvious problem, however, is the overlap in ligand recognition between FFA2 and the closely related FFA3 receptor[3,4]. This in turn explains why SCFAs as agonists cannot distinguish between these two receptors. Although there is a slight difference in the rank order of potency for SCFAs at FFA2 compared to FFA3, this difference does not suffice to selectively activate FFA2 over FFA3. To circumvent the obstacle of closely related structural realities in the orthosteric binding pocket, targeting sites distinct from the endogenous ligand binding site attracted much interest in the past[1]. These allosteric receptor epitopes are evolutionary less conserved and thus represent a possibility to selectively target receptor subtypes. Recently a structurally diverse series of ligands has been studied and found to be selective for activation of FFA2 over FFA3[5]. 4-CMTB as the most potent and studied agonist from this compound series was already subject of intense research as detailed in the aforementioned chapter and previous publications[6–8]. This compound acts as both agonist and allosteric modulator at the FFA2 receptor and selectively activates FFA2. However, due to the allosteric aspect in the mode of action, 4-CMTB might be subjected to agonist-trafficking, which means that it could engage functionally different cellular outcomes compared to endogenous ligand-stimulated FFA2 signaling. Thus, 4-CMTB data under physiological conditions ought to be treated with caution.

Recently, a series of ligands from the patent literature were identified as orthosteric FFA2-selective agonists[9,10]. However, the exact mechanism of receptor activation remains to be elucidated. These compounds for example lost allosteric cooperativity with 4-CMTB, which can only be explained by the phenomenon of probe dependency or overlapping binding modes between the synthetic orthosteric ligands and 4-CMTB. The latter explanation seems reasonable because the lead structure

TUG-800 shares both an acidic function responsible for orthosteric recognition but also the prominent thiazolyl residue, which is common in the phenylacetamides that are believed to address an allosteric receptor epitope. Hence, a bitopic orientation of TUG-800 and related structures from that series is well conceivable. The uncertainty about these mechanistic fundamentals of receptor activation restricts the significance of the conclusions drawn from experiments with these ligands.

Receptors solely activated by synthetic ligands (RASSLs) represent another opportunity to investigate receptor behavior in the context of closely related and often co-expressed receptors[11,12]. The RASSL concept relies on the structural modification within the wild-type receptor that alters the ligand recognition capabilities of the receptor. While the endogenous ligands lose their activity at a RASSL, a synthetic ligand that has no affinity to the wild-type receptor now activates the modified receptor[13]. This phenomenon might be used to investigate the physiological function of FFA2 because FFA2-mediated biological effects can be explored independently of the presence of SCFAs as endogenous lipid ligands that interfere not only with FFA2 but also with FFA3 and a variety of other targets, which impedes the correct assignment of a cell response to a specific receptor[11,14,15].

In this chapter, we introduce a RASSL form of FFA2, which does not recognize the endogenous agonists but the small molecule sorbic acid, which has no effect at the wild-type receptor. While most designer receptors are discovered by random screening, this approach is of limited use to rationally design receptors[16–18]. In the following publication, we introduce the first FFA2 RASSL, which was carefully considered and reasonably developed based on species orthologue variations of FFA2 and thus followed a rational design path.

The advantages of designer receptors are the elucidation of physiological receptor function by mimicking the endogenous receptor without the drawback of insufficient selectivity and off target effects[11]. This concept could ultimately be used to therapeutically treat diseases by introduction of designer receptors in the affected tissue or cells using genetic techniques[19]. Furthermore, RASSLs could be used to modulate previously non-druggable cellular populations[19] and, finally, to generate synthetically encoded behavior *in vivo* to gain insight into the significance of a specific receptor signaling in a certain disease context.

References

1. Kenakin, T. & Miller, L. J. Seven transmembrane receptors as shapeshifting proteins: the impact of allosteric modulation and functional selectivity on new drug discovery, *Pharmacol. Rev.* **62,** 265–304 (2010).
2. Wootten, D. Christopoulos, A. & Sexton, P. M. Emerging paradigms in GPCR allostery: implications for drug discovery, *Nat Rev Drug Discov* **12,** 630–644 (2013).

3. Stoddart, L. A. Smith, N. J. & Milligan, G. International Union of Pharmacology. LXXI. Free fatty acid receptors FFA1, -2, and -3: pharmacology and pathophysiological functions, *Pharmacol. Rev.* **60,** 405–417 (2008).
4. Milligan, G. Stoddart, L. A. & Smith, N. J. Agonism and allosterism: the pharmacology of the free fatty acid receptors FFA2 and FFA3, *Br. J. Pharmacol.* **158,** 146–153 (2009).
5. Lee, T. *et al.* Identification and functional characterization of allosteric agonists for the G protein-coupled receptor FFA2, *Mol. Pharmacol.* **74,** 1599–1609 (2008).
6. Smith, N. J. *et al.* Extracellular loop 2 of the free fatty acid receptor 2 mediates allosterism of a phenylacetamide ago-allosteric modulator, *Mol. Pharmacol.* **80,** 163–173 (2011).
7. Swaminath, G. *et al.* Mutational analysis of G-protein coupled receptor--FFA2, *Biochem. Biophys. Res. Commun.* **405,** 122–127 (2011).
8. Wang, Y. *et al.* The first synthetic agonists of FFA2: Discovery and SAR of phenylacetamides as allosteric modulators, *Bioorg. Med. Chem. Lett.* **20,** 493–498 (2010).
9. Hoveyda H. Brantis C.E. Dutheuil G. Zoute L. Schils D. Bernard J. *Compounds, pharmaceutical composition and methods for use in treating metabolic disorders ,*
10. Hudson, B. D. *et al.* Defining the molecular basis for the first potent and selective orthosteric agonists of the FFA2 free fatty acid receptor, *J. Biol. Chem.* **288,** 17296–17312 (2013).
11. Wess, J. Nakajima, K. & Jain, S. Novel designer receptors to probe GPCR signaling and physiology, *Trends Pharmacol. Sci.* **34,** 385–392 (2013).
12. Conklin, B. R. *et al.* Engineering GPCR signaling pathways with RASSLs, *Nat. Methods* **5,** 673–678 (2008).
13. Alvarez-Curto, E. *et al.* Developing chemical genetic approaches to explore G protein-coupled receptor function: validation of the use of a receptor activated solely by synthetic ligand (RASSL), *Mol. Pharmacol.* **80,** 1033–1046 (2011).
14. Guettier, J.-M. *et al.* A chemical-genetic approach to study G protein regulation of beta cell function in vivo, *Proc. Natl. Acad. Sci. U.S.A.* **106,** 19197–19202 (2009).
15. Sasaki, K. *et al.* Pharmacogenetic modulation of orexin neurons alters sleep/wakefulness states in mice, *PLoS ONE* **6,** e20360 (2011).
16. Claeysen, S. Joubert, L. Sebben, M. Bockaert, J. & Dumuis, A. A single mutation in the 5-HT4 receptor (5-HT4-R D100(3.32)A) generates a Gs-coupled receptor activated exclusively by synthetic ligands (RASSL), *J. Biol. Chem.* **278,** 699–702 (2003).
17. Armbruster, B. N. Li, X. Pausch, M. H. Herlitze, S. & Roth, B. L. Evolving the lock to fit the key to create a family of G protein-coupled receptors potently activated by an inert ligand, *Proc. Natl. Acad. Sci. U.S.A.* **104,** 5163–5168 (2007).
18. Nakajima, K.-i. & Wess, J. Design and functional characterization of a novel, arrestin-biased designer G protein-coupled receptor, *Mol. Pharmacol.* **82,** 575–582 (2012).
19. Farrell, M. S. & Roth, B. L. Pharmacosynthetics: Reimagining the pharmacogenetic approach, *Brain Res.* **1511,** 6–20 (2013).

Chemically engineering ligand selectivity at the free fatty acid receptor 2 based on pharmacological variation between species orthologs

Brian D. Hudson,* Elisabeth Christiansen,† Irina G. Tikhonova,‡ Manuel Grundmann,§ Evi Kostenis,§ David R. Adams,‖ Trond Ulven,† and Graeme Milligan*,[1]

*Molecular Pharmacology Group, Institute of Molecular, Cell, and Systems Biology, College of Medical, Veterinary, and Life Sciences, University of Glasgow, Glasgow, UK; †Department of Physics, Chemistry, and Pharmacy, University of Southern Denmark, Odense, Denmark; ‡School of Pharmacy, Medical Biology Centre, Queen's University Belfast, Belfast, UK; §Molecular, Cellular, and Pharmacobiology Section, Institute of Pharmaceutical Biology, University of Bonn, Bonn, Germany; ‖Department of Chemistry, School of Engineering and Physical Sciences, Heriot-Watt University, Edinburgh, UK

ABSTRACT **When it is difficult to develop selective ligands within a family of related G-protein-coupled receptors (GPCRs), chemically engineered receptors activated solely by synthetic ligands (RASSLs) are useful alternatives for probing receptor function. In the present work, we explored whether a RASSL of the free fatty acid receptor 2 (FFA2) could be developed on the basis of pharmacological variation between species orthologs. For this, bovine FFA2 was characterized, revealing distinct ligand selectivity compared with human FFA2. Homology modeling and mutational analysis demonstrated a single mutation in human FFA2 of C4.57G resulted in a human FFA2 receptor with ligand selectivity similar to the bovine receptor. This was exploited to generate human FFA2-RASSL by the addition of a second mutation at a known orthosteric ligand interaction site, H6.55Q. The resulting FFA2-RASSL displayed a >100-fold loss of activity to endogenous ligands, while responding to the distinct ligand sorbic acid with pEC_{50} values for inhibition of cAMP, 5.83 ± 0.11; Ca^{2+} mobilization, 4.63 ± 0.05; ERK phosphorylation, 5.61 ± 0.06; and dynamic mass redistribution, 5.35 ± 0.06. This FFA2-RASSL will be useful in future studies on this receptor and demonstrates that exploitation of pharmacological variation between species orthologs is a powerful method to generate novel chemically engineered GPCRs.—Hudson, B. D., Christiansen, E., Tikhonova, I. G., Grundmann, M., Kostenis, E., Adams, D. R., Ulven, T., Milligan, G. Chemically engineering ligand selectivity at the free fatty acid receptor 2 based on pharmacological variation between species orthologs. *FASEB J.* 26, 4951–4965 (2012). www.fasebj.org**

Key Words: GPCR · RASSL

In recent times, it has become apparent that a series of molecules previously considered only as metabolic intermediates are actually able to mediate at least a number of their functions *via* activation of members of the G-protein-coupled receptor (GPCR) superfamily. These include intermediates of the tricarboxylic acid cycle, such as succinate (1), and molecules such as lactate (2) and β-hydroxybutyrate (3), involved in glucogenic and ketogenic control of metabolism. A further group of such intermediates are the free fatty acids. It is now known that three related GPCRs, free fatty acid receptors 1–3 (FFA1, FFA2, and FFA3; previously designated GPR40, GPR43, and GPR41, respectively; ref. 4), respond to either medium- and longer-chain (FFA1) or short-chain, C1-C5, (FFA2 and FFA3) free fatty acids. There is considerable interest in the physiological roles of FFA2, in particular (5, 6), and whether this receptor might be useful as a novel therapeutic target in areas ranging from diabetes and adiposity to satiety and inflammation (7, 8). In the absence of

Abbreviations: bFFA2, bovine free fatty acid receptor 2; bFFA3, bovine free fatty acid receptor 3; BRET, bioluminescence resonance energy transfer; DMEM, Dulbecco's modified Eagle's medium; DMR, dynamic mass redistribution; DREADD, designer receptor exclusively activated by designed drug; ERK, extracellular signal-regulated kinase; eYFP, enhanced yellow fluorescent protein; HBSS, Hanks' balanced salt solution; hFFA2, human free fatty acid receptor 2; FFA1, free fatty acid receptor 1; FFA2, free fatty acid receptor 2; FFA3, free fatty acid receptor 3; GPCR, G-protein-coupled receptor; RASSL, receptor activated solely by synthetic ligand; Rluc, *Renilla* luciferase; SAR, structure-activity relationship; SCA, small carboxylic acid; SCFA, short-chain fatty acid

[1] Correspondence: Wolfson Link Bldg. 253, University of Glasgow, Glasgow G12 8QQ, Scotland, U.K. E-mail: graeme.milligan@glasgow.ac.uk

doi: 10.1096/fj.12-213314

This article includes supplemental data. Please visit *http://www.fasebj.org* to obtain this information.

synthetic ligands that bind to the same region of the receptor as the short-chain fatty acids (SCFAs) and that have reasonable potency and substantial selectivity between FFA2 and FFA3, the marked overlap of potency of C1–C5 fatty acids at FFA2 and FFA3 makes efforts to interpret selective activation of FFA2 *vs.* FFA3 impractical without more detailed analyses involving knockout or knockdown studies (9–11). It would, therefore, be of considerable value to develop chemically engineered forms of these receptors with unique ligand responsiveness.

Such modified GPCRs have been developed for several other receptors and are often described as either designer receptors exclusively activated by designed drugs (DREADDs) or as receptors activated solely by synthetic ligands (RASSLs) (12–15). To date, two general approaches have been employed to generate these chemically engineered GPCRs (16). The first involves site-directed mutagenesis of known ligand interaction sites in the GPCR followed by screening ligands for activity at the resulting mutant receptors (17), while the second method takes the opposite approach, generating thousands of randomly mutated forms of the receptor and screening these against a candidate synthetic ligand (13). Although each of these approaches has found some success, both rely largely on random screening. Considering this, in the present work, we have explored whether a more direct approach could be taken to develop chemically engineered forms of human FFA2 (hFFA2), based on the variation between species orthologs of this receptor.

Mammalian species orthologs of GPCRs are anticipated to respond to the same endogenously produced agonists. However, the potency and affinity of such agonist ligands may vary depending on the physiology of individual species, and where such receptors respond to a number of related ligands (as in the case of FFA2 and the SCFAs; refs. 4, 18), the rank order of function may differ. Although such variation is likely to be limited for GPCRs that coordinate the responses of ancient hormone and transmitter systems, such as the catecholamines, that underpin key physiological processes, including heart rate and intraneural communication, such differences may be substantially greater for GPCRs that play more modulatory roles, or in cases where the receptor is likely to be exposed to vastly different concentrations of ligand between different species. Because SCFAs are primarily produced by the fermentation of nondigestible carbohydrates by the microflora in the gut (6), it could be hypothesized that FFA2 will show significant ortholog variation between species that have greatly different dietary levels of nondigestible carbohydrates and, therefore, different levels of endogenous SCFA ligands. Considering this, in the present work, the bovine ortholog was chosen as the basis for producing chemically engineered forms of hFFA2, since ruminants, such as bovines, are well known to rely heavily on nondigestible carbohydrates.

MATERIALS AND METHODS

Cell culture, transfection, and production of stably expressing cell lines

HEK293 cells were maintained in Dulbecco's modified Eagle's medium (DMEM) supplemented with 10% FBS at 37°C and 5% CO_2. For experiments utilizing transiently transfected HEK293 cells, transfections were carried out using polyethylenimine, and experiments were conducted 48 h post-transfection. For experiments in which stable cell lines were produced and used, the Flp-In T-REx system (Life Technologies, Paisley, UK) was used to generate HEK293 cells with tetracycline-inducible expression of the receptor of interest. To generate these cell lines, Flp-In T-REx HEK293 cells were cotransfected with the pOG44 vector and the receptor of interest in pcDNA5/FRT/TO. Transfection with pOG44 drives expression of Flp recombinase, which, in turn, allows for recombination between FRT sites in pcDNA5/FRT/TO and in the genome of the Flp-In T-REx HEK293 cells, thus allowing stable inducible cells for the receptor of interest to be generated by appropriate antibiotic selection.

DNA constructs

Constructs for the human orthologs of FFA2 and FFA3 fused at their C-terminal with enhanced yellow fluorescent protein (eYFP) were as reported previously (19). To clone the bovine orthologs, the coding sequences of bovine FFA2 and FFA3 (bFFA2 and bFFA3) were amplified without their stop codons from commercially available bovine genomic DNA by PCR. The PCR product was then ligated upstream and in-frame with the eYFP sequence present in a pcDNA5/FRT/TO expression vector (Life Technologies, Carlsbad, CA, USA). Mutagenesis of human and bovine orthologs of FFA2 was carried out according to the QuickChange method (Stratagene, Santa Clara, CA, USA).

Compounds

Formic acid (compound C1), acetic acid (compound C2), propionic acid (compound C3), butyric acid (compound C4), valeric acid (compound C5), caproic acid (compound C6), heptanoic acid (compound C7), caprylic acid (compound C8), pelargonic acid (compound C9), methylthioacetic acid (compound 1), 3-methylbutyric acid (compound 2), pivalic acid (compound 3), 2-methylbutyric acid (compound 4), cyclopropylcarboxylic acid (compound 5), cyclobutylcarboxylic acid (compound 6), 1-methylcyclopropanecarboxylic acid (compound 7), vinylacetic acid (compound 9), 3-pentenoic acid (compound 12), acrylic acid (compound 13), propiolic acid (compound 14), 2-butynoic acid (compound 15), *trans*-crotonic acid (compound 16), 2-methylacrylic acid (compound 18), 3-methylcrotonic acid (compound 19), *trans*-2-methylcrotonic acid (compound 20), *trans*-2-pentenoic acid (compound 22), *trans*-2-hexenoic acid (compound 23), 2,4-pentadienoic acid (compound 24), sorbic acid (compound 25), 4,4,4-trifluoro-3-methyl-2-butenoic acid (compound 26), 1-cyclopentenecarboxylic acid (compound 27), *trans*-cinnamic acid (compound 28), and 1-cyclohexene-1-carboxylic acid (compound 29) were all purchased from Sigma-Aldrich (Dorset, UK). Angelic acid (compound 21) was obtained from ABCR (Karlsruhe, Germany). Cyclopropylacetic acid (compound 8) was purchased from Alfa Aesar (Heysham, UK). 3-Butynoic acid (compound 10) was synthesized as described previously (20). The identity and purity of all compounds were confirmed by ^{1}H and ^{13}C NMR.

β-Arrestin-2 interaction assay

A bioluminescence resonance energy transfer (BRET)-based approach was used to measure β-arrestin-2 recruitment to human and bovine forms of FFA2. Briefly, a plasmid encoding an eYFP-tagged form of the receptor to be assayed was cotransfected in a 4:1 ratio with a β-arrestin-2 *Renilla* luciferase (Rluc) plasmid. Cells were transferred into white 96-well plates at 24 h post-transfection. Then, at 48 h post-transfection, cells were washed, and the culture medium was replaced with Hanks' balanced salt solution (HBSS) immediately prior to conducting the assay. To measure β-arrestin-2 recruitment, the Rluc substrate coelenterazine h was added to a final concentration of 5 μM; then, cells were incubated for 10 min at 37°C, test compounds were next added, and cells were incubated for a further 5 min at 37°C. BRET, resulting from FFA2 receptor-β-arrestin-2 interaction, was then assessed by measuring the ratio of luminescence at 535 and 475 nm using a Pherastar FS fitted with the BRET1 optic module (BMG Labtech, Aylesbury, UK).

Extracellular signal-regulated kinase (ERK) 1/2 phosphorylation assay

All ERK phosphorylation experiments were carried out using Flp-In T-REx stable-inducible cell lines for the human or bovine forms of FFA2 to be assayed. Briefly, 80,000 cells/well were seeded in a 96-well plate and then allowed to attach for 3–6 h before the addition of doxycycline (100 ng/ml) to induce expression of the receptor. After incubating overnight, the culture medium was replaced with serum-free DMEM-containing doxycycline (100 ng/ml), and cells were then incubated for a further 5 or 6 h prior to the assay. For the assay, test compounds were added to the cells and incubated at 37°C for 5 min before the cells were lysed and assayed for phospho-ERK using an Alphascreen-based detection kit (Perkin Elmer, Waltham, MA, USA), according to the manufacturer's protocol.

Ca^{2+} mobilization assay

All Ca^{2+} experiments were carried out using Flp-In T-REx stable-inducible cell lines for the human or bovine forms of FFA2 to be studied. Cells were plated at 80,000 cells/well in black 96-well plates with clear bottoms and then allowed to adhere for 3–6 h. Doxycycline was then added (100 ng/ml) to induce expression of the receptor of interest, and cells were maintained in culture overnight. Prior to the assay, cells were labeled for 45 min with the calcium-sensitive dye Fura-2 AM; then they were washed and maintained in HBSS. Fura-2 fluorescent emission at 510 nm resulting from 340- or 380-nm excitation was then monitored using a Flexstation plate reader (Molecular Devices, Sunnyvale, CA, USA). Basal fluorescence was measured for 16 s, test compounds were then added, and fluorescence was measured for an additional 74 s. The maximum difference in 340/380 ratios obtained before and after compound addition was then used to plot concentration-response data.

cAMP assay

All cAMP experiments were carried out using Flp-In T-REx stable-inducible cell lines for the forms of FFA2 to be studied. These experiments were carried out using a homogenous time-resolved FRET-based detection kit (CisBio Bioassays; CisBio, Codolet, France) according to the manufacturer's protocol. Cells were plated at 2000 cells/well in low-volume 384-well plates, and the inhibition of 1 μM forskolin-stimulated cAMP production was assessed following a 30-min coincubation with test compounds.

[^{35}S]GTPγS incorporation assay

Total cell membranes were prepared from stable, doxycycline-inducible Flp-In T-REx HEK293 cell lines. [^{35}S]GTPγS binding assays were then carried out in reactions with 5 μg of cell membrane protein preincubated for 15 min at 25°C in assay buffer (50 mM Tris-HCl, pH 7.4; 10 mM $MgCl_2$; 100 mM NaCl; 1 mM EDTA; 1 μM GDP; and 0.5% fatty acid-free BSA) containing the indicated concentrations of ligands. The reaction was initiated with the addition of 50 nCi of [^{35}S]GTPγS to each tube, and the reaction was terminated after 1 h incubation by rapid filtration through GF/C glass filters. Unbound radioligand was washed from filters by 3 washes with ice-cold wash buffer (50 mM Tris-HCl, pH 7.4, and 10 mM $MgCl_2$), and [^{35}S]GTPγS binding was determined by liquid scintillation spectrometry.

Homology modeling

Modeling of hFFA2 was carried out using the β_2-adrenergic receptor structure as a template (20, 21). The bFFA2 homology model was constructed on the basis of this hFFA2 model using the Prime module of Schrödinger software with default options (Schrödinger LLC, New York, NY, USA).

Dynamic mass redistribution (DMR) assays

DMR assays were performed on a beta version of the Corning Epic biosensor (Corning Life Sciences, Corning, NY, USA), as described previously in detail (22, 23). Briefly, stable inducible cell lines expressing the hFFA2 or hFFA2-C4.57G/H6.55Q mutant were grown to confluence for 20–24 h on fibronectin-coated Epic biosensor 384-well microplates. Cells were then washed twice with HBSS containing 20 mM HEPES and kept for 1 h in the Epic reader at 28°C. DMR was monitored before (baseline read) and after the addition of compound solutions for ≥6000 s. Concentration-effect curves were generated from the real-time optical traces using the area under the curve between 0 and 6000 s after ligand addition.

Curve fitting and statistical analysis

All data presented represent means ± SE of ≥3 independent experiments. Data analysis and curve fitting were carried out using the GraphPad Prism 5.0b software package (GraphPad, San Diego, CA, USA). Concentration-response data were fit to 3-parameter sigmoidal concentration-response curves. Statistical analysis of curve fit parameters was carried out by independently fitting the data from triplicate experiments and comparing the resulting curve fit values by *t* test or 1-way ANOVA, as appropriate.

RESULTS

Postactivation assays were established for both the human and bovine orthologs of FFA2. In the first of these, an ortholog of FFA2 to which eYFP had been attached in-frame to the C terminus was cotransfected into HEK 293 cells along with β-arrestin-2 C-terminally modified by the in-frame addition of Rluc. BRET generated between Rluc and eYFP in response to an

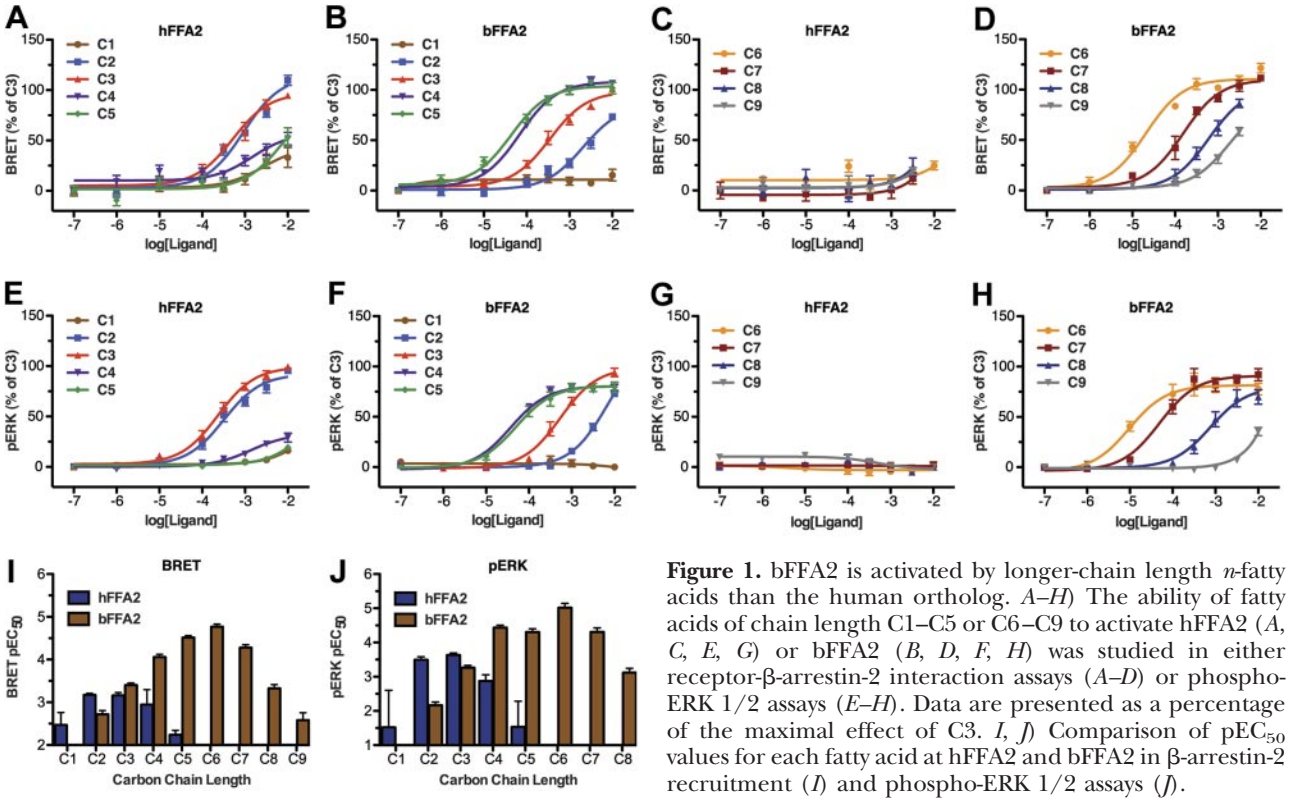

Figure 1. bFFA2 is activated by longer-chain length *n*-fatty acids than the human ortholog. *A–H*) The ability of fatty acids of chain length C1–C5 or C6–C9 to activate hFFA2 (*A*, *C*, *E*, *G*) or bFFA2 (*B*, *D*, *F*, *H*) was studied in either receptor-β-arrestin-2 interaction assays (*A–D*) or phospho-ERK 1/2 assays (*E–H*). Data are presented as a percentage of the maximal effect of C3. *I*, *J*) Comparison of pEC_{50} values for each fatty acid at hFFA2 and bFFA2 in β-arrestin-2 recruitment (*I*) and phospho-ERK 1/2 assays (*J*).

agonist ligand reflects induced interactions between FFA2 and β-arrestin-2. As anticipated from previous studies using a number of different endpoints (19–21), the SCFAs acetic acid (chain length C2) and propionic acid (C3) displayed modest and similar potency at hFFA2 in this assay (**Fig. 1*A***). Although active at hFFA2, *n*-butanoic acid (C4) displayed lower potency (Fig. 1*A*), while both formic acid (C1) and valeric acid (C5) had little effect at concentrations below 10 mM (Fig. 1*A*). When equivalent studies were performed using bFFA2-eYFP, a substantially different structure-activity relationship (SAR) was observed. C1 was without effect, while C2 was significantly ($P<0.05$) less potent than compound C3 (Fig. 1*B*). Furthermore, when exploring the activity of fatty acids of longer chain length than C3, potency significantly increased ($P<0.05$), such that C3 < C4 < C5 (Fig. 1*B*). Because of the increasing potency of *n*-fatty acids with longer chain lengths observed at bFFA2, we examined extended chain lengths from C6 to C9 at both the human and bovine forms of the receptor. While none of the compounds C6–C9 showed appreciable activity at hFFA2 (Fig. 1*C*), all were full agonists at bFFA2, although potency in this case significantly decreased with each additional carbon ($P<0.05$), as chain length increased beyond C6 (Fig. 1*D*). Analysis of the potencies across the complete series of *n*-fatty acids at hFFA2 and bFFA2 (**Table 1**) reveals clearly distinct rank orders of potency, such that for hFFA2, C3 = C2 > C1 = C5, and all other compounds were without effect, while for bFFA2, C6 > C5 > C4 = C7 > C3 = C8 > C2 = C9, and only C1 was without effect.

To ensure that these differences were not limited to measurement at only a β-arrestin recruitment end-

TABLE 1. *Potency values for short-chain fatty acids in various assays at human and bovine orthologs of FFA2 and FFA3*

	FFA2 β-arrestin-2 BRET			FFA2 pERK			FFA3 [^{35}S]GTPγS		
Chain length	Human	Bovine	Selectivity	Human	Bovine	Selectivity	Human	Bovine	Selectivity
C1	2.60 ± 0.40	<2	>0.6	<2	<2		<2	<2	
C2	3.00 ± 0.12	2.69 ± 0.11	0.31	3.50 ± 0.08	2.16 ± 0.10	1.34	2.12 ± 0.34	2.36 ± 0.34	−0.24
C3	3.29 ± 0.10	3.46 ± 0.07	−0.17	3.64 ± 0.06	3.26 ± 0.07	0.38	3.70 ± 0.13	3.81 ± 0.18	−0.11
C4	2.83 ± 0.26	4.16 ± 0.06	−1.33	2.87 ± 0.18	4.43 ± 0.07	−1.56	3.60 ± 0.21	3.58 ± 0.14	0.02
C5	2.15 ± 0.33	4.37 ± 0.09	−2.22	<2	4.30 ± 0.10	<−2.30	4.44 ± 0.24	3.91 ± 0.18	0.53
C6	<2	4.68 ± 0.09	<−2.68	<2	5.01 ± 0.13	<−3.01	3.69 ± 0.33	3.90 ± 0.21	−0.21
C7	<2	3.81 ± 0.09	<−1.81	<2	4.31 ± 0.12	<−2.31	4.16 ± 0.56	3.80 ± 0.61	0.36
C8	<2	3.21 ± 0.11	<−1.21	<2	3.12 ± 0.13	<−1.12	<2	<2	
C9	<2	2.47 ± 0.22	<−0.47	<2	<2		<2	<2	

Selectivity is measured as human pEC_{50} − bovine pEC_{50} for each assay.

point, equivalent studies were performed by measuring phosphorylation of ERK 1/2, and similar results were obtained (Fig. 1*E–H*). In comparing the potencies for the complete series of *n*-fatty acids in β-arrestin-2 recruitment (Fig. 1*I*) and ERK 1/2 phosphorylation (Fig. 1*J*), it is clear that consistently across assays, bFFA2 preferentially responded to longer chain lengths than did hFFA2. By contrast, human and bovine orthologs of the closely related GPCR FFA3 displayed very similar patterns of responsiveness for each of the C1–C9 *n*-fatty acids, as assessed in a [^{35}S]GTPγS assay (chosen because either bFFA3 or hFFA3 did not generate consistent responses in the β-arrestin-2 or ERK 1/2 assays). Unlike bFFA2, bFFA3 displayed no preference for longer chain lengths (Table 1).

We have recently shown that a series of small carboxylic acids (SCAs) can also act as agonists at hFFA2 (20). Considering the marked differences among the *n*-fatty acids at hFFA2 and bFFA2, we next screened these SCAs in the β-arrestin-2 interaction assay to determine whether there were also species differences within this series (**Fig. 2**). A number of the SCAs, including 3-methylbutyric acid (compound 2), cyclopropylacetic acid (compound 8), *trans*-crotonic acid (compound 16), and 3-methylcrotonic acid (compound 19), each with modest potency and/or efficacy at hFFA2 in the β-arrestin-2 interaction assay were ~10- to 100-fold more potent at bFFA2 (**Fig. 3*A–D***). This was, however, not a general reflection that all SCAs were more potent at the bovine ortholog, as propiolic acid (compound 14) and angelic acid (compound 21), although displaying modest efficacy, were both more potent at hFFA2 than bFFA2 (Fig. 3*E, F*). SAR analyses of these results with the SCAs suggest that in addition to its preference for longer-chain fatty acids, bFFA2 also prefers compounds with sp^2 hybridization of the α carbon and those with β-carbon substituents.

On the basis of these SAR observations, we selected a further set of SCAs predicted to have good selectivity for bFFA2 because they contained longer chain lengths (C5 or C6), sp^2 hybridization of the α-carbon, or bulky substitutions at the β-carbon (**Table 2**). Within this series, all compounds were found to be full agonists at bFFA2, while none possessed substantial activity at the human receptor. In particular, it was the C5 and C6 compounds with conjugated double-bond systems that displayed the highest potency at bFFA2. These compounds included *trans*-2-pentenoic acid (compound 22; **Fig. 4*A***), *trans*-2-hexenoic acid (compound 23; Fig. 4*B*), 2,4-pentadienoic acid (compound 24; Fig. 4*C*), and 2,4-hexadienoic acid (sorbic acid; compound 25; Fig. 4*D*). Although some compounds in this series did display weak activity at the human receptor (compounds 22 and 24), all those tested that contained larger β-carbon substituents appeared to be essentially inactive at hFFA2. These included 4,4,4-trifluoro-3-methyl-2-butenoic acid (compound 26; Fig. 4*E*), 1-cyclopentenecarboxylic acid (compound 27; Fig. 4*F*), *trans*-cinnamic acid (compound 28; Fig. 4*G*), and 1-cyclohexene-1-carboxylic acid (compound 29; Fig. 4*H*). In addition, each of these bFFA2-selective ligands was also inactive at the closely related hFFA3 receptor (data not shown).

Having now identified several ligands with very good selectivity for bFFA2 over hFFA2, we next set out to define the molecular basis for this selectivity. In previous studies on hFFA2, sequence alignment with the other members of the free fatty acid receptor family, FFA1 and FFA3, identified 4 key positively charged amino acids within the transmembrane domains. These were arginine residues at positions 5.39 and 7.35 and histidine residues at positions 4.56 and 6.55 (numbering according to the system introduced by Ballesteros and Weinstein; ref. 24) and subsequent mutagenesis demonstrated the importance of particularly R5.39, R7.35, and H6.55 in coordination of the carboxylate group of the SCFAs (19, 21). Alignment of hFFA2 and bFFA2 indicated the presence of equivalent residues in the bovine ortholog. However, in addition to R7.35, the bovine ortholog has an additional arginine at position 7.36, (*i.e.*, the next amino acid in the primary sequence). Each of these residues in bFFA2 was mutated to alanine, and the resulting mutants were screened using the β-arrestin-2 interaction assay to determine what role (if any) these residues had in the selectivity among the identified bFFA2 ligands. The four compounds that were selected for this screen were the most prevalent SCFAs C2 and C3, and the bovine-selective compounds C5 and 19, selected as being the most potent bovine-selective ligands that still had appreciable activity at the human receptor (**Fig. 5*A***; see Supplemental Table S1 for complete mutant screen data). Mutation of R5.39 to alanine resulted in virtual complete loss of function for all four compounds at both the human and bovine forms of FFA2 (Fig. 5*B*). Interestingly, although mutation to generate R7.35A in hFFA2 resulted in complete loss of activity to each ligand, the equivalent mutation in bFFA2 retained some activity to the bovine-selective ligands C5 and 19, although with >100-fold loss of potency (Fig. 5*C*). Mutation of H4.56 to alanine in either hFFA2 or bFFA2 completely eliminated function (Fig. 5*D*), while the H6.55 to alanine mutant retained some activity only in bFFA2 to C5 and 19 (Fig. 5*E*). Mutation of the additional arginine residue present only in bFFA2 to generate R7.36A resulted in large reductions in both efficacy and potency, although the rank-order of potency of 19 > C5 > C3 > C2 was preserved (Fig. 5*F*). To assess the combined role of the two adjacent arginine residues in bFFA2, a double R7.35A/R7.36A mutant was generated, and this essentially failed to respond to any ligand tested (Fig. 5*G*).

To identify residues in bFFA2 that may provide the basis for its greater chain length acceptance and distinct SCA SAR, we aligned the sequence of human, bovine, rat, and murine forms of FFA2 (**Fig. 6*A***) and generated a homology model of bFFA2 (Fig. 6*B*) based on our previous models of the human receptor (20, 21). Nonconserved residues predicted to lie within 8 Å of R5.39 and R7.35 of the orthosteric binding site were

Compound	Structure	hFFA2		bFFA2		Selectivity
		pEC_{50}	E_{Max}	pEC_{50}	E_{Max}	
1	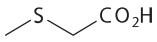	3.39 ± 0.43	69 ± 28	3.85 ± 0.16	56 ± 6	-0.46
2	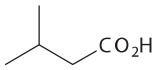	3.38 ± 0.72	38 ± 17	4.82 ± 0.08	100 ± 3	-1.44
3	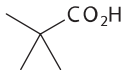	3.50 ± 0.52	45 ± 15	2.95 ± 0.34	136 ± 58	0.55
4	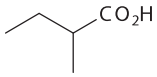	4.03 ± 0.80	36 ± 11	3.82 ± 0.12	106 ± 8	0.21
5	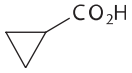	<3		3.42 ± 0.15	121 ± 16	<-1.42
6	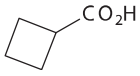	3.63 ± 0.74	40 ± 21	4.11 ± 0.12	97 ± 7	-0.48
7	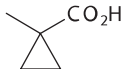	<3		<3		
8	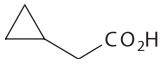	<3.1		4.41 ± 0.12	95 ± 6	<-1.31
9	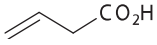	<3.1		4.05 ± 0.13	88 ± 7	<-0.95
10	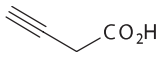	<3		<3		
12	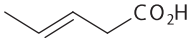	4.62 ± 0.57	21 ± 4	4.12 ± 0.10	102 ± 5	0.50
13	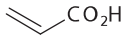	3.39 ± 0.32	104 ± 32	<3		>0.39
14	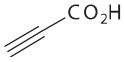	3.74 ± 0.27	144 ± 114	2.93 ± 0.36	88 ± 42	0.81
15	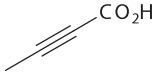	<3		3.65 ± 0.12	93 ± 8	<-0.65
16	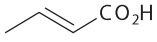	<3		4.68 ± 0.10	109 ±4	<-1.68
18	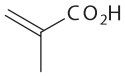	3.16 ± 0.51	104 ± 57	<3		>0.16
19	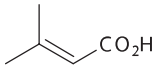	3.10 ± 0.48	90 ± 48	5.38 ± 0.12	112 ±4	-2.28
20	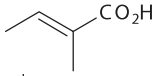	3.87 ± 0.36	68 ± 15	4.45 ± 0.11	107 ± 5	-0.58
21	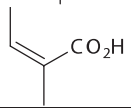	4.06 ± 0.30	43 ± 8	<3		>1.06

Figure 2. SCA concentration-response curve fit parameters in β-arrestin-2 BRET at hFFA2 and bFFA2. Selectivity is expressed as hFFA2 pEC_{50} − bFFA2 pEC_{50}. E_{max} values are reported as a percentage of C3 maximum response at the cognate receptor.

highlighted (Fig. 6*B*). Two of these, human S3.34/bovine G3.34 and human C4.57/bovine G4.57, were selected for mutational analysis. Alteration to generate either human S3.34G or the reciprocal bovine G3.34S forms of FFA2 had limited effects on ligand pharmacology, with each mutant exhibiting the same rank order of potency for the four ligands tested as the corresponding wild-type receptor (Fig. 6*C*). By contrast, mutation to produce hFFA2-C4.57G produced a receptor where although C2 and C3 remained equipotent, the potency of C5 was increased markedly and became significantly ($P<0.01$) more potent than either C2 or

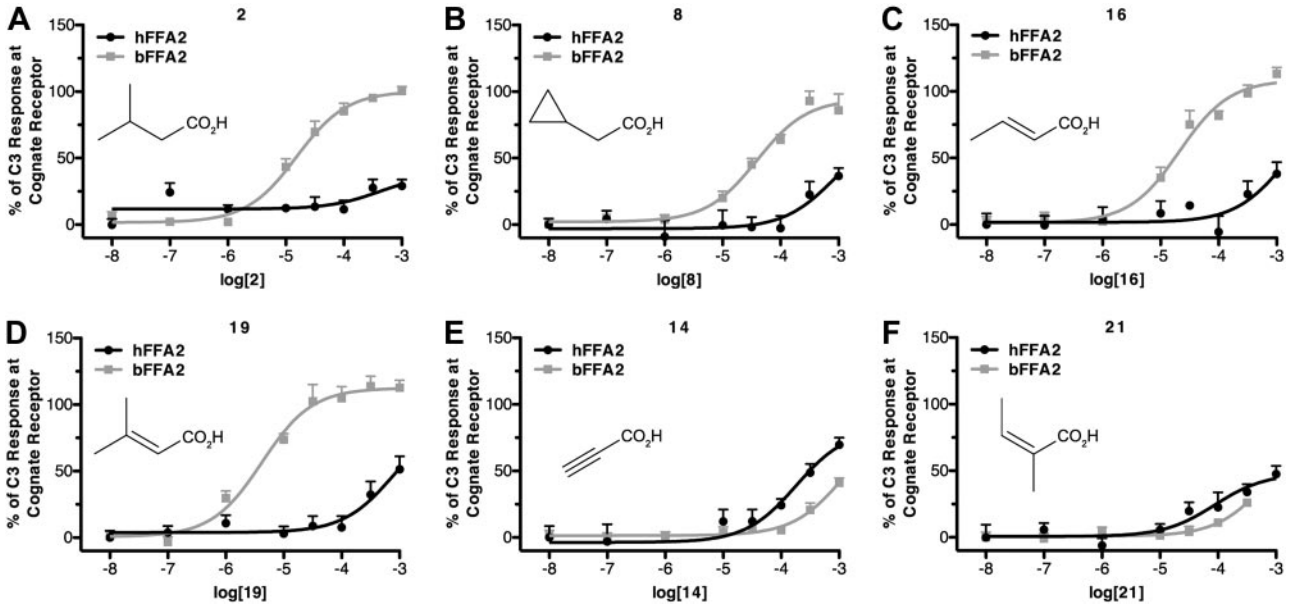

Figure 3. A number of SCAs display marked selectivity for bFFA2. Ability of the noted compounds to promote β-arrestin-2 recruitment at either hFFA2 or bFFA2 is displayed as a percentage of maximally effective concentration of C3 at each species ortholog.

C3 (Fig. 6*D*). Equally, compound 19 was also now substantially more potent than C2 or C3 at this mutant ($P<0.01$) and, as at wild-type bFFA2, was also more potent than C5. To confirm that this observation was not restricted to only the β-arrestin-2 interaction assay, hFFA2-C4.57G was also assessed in ERK 1/2 phosphorylation assays, and similar results were obtained (Fig. 6*E*). The reciprocal mutation G4.57C was also generated in bFFA2 (Fig. 6*D*), and although it did appear that both C5 and 19 had reduced potency relative to C2 and C3, this was difficult to assess accurately, as this variant receptor displayed substantially reduced efficacy in the β-arrestin-2 interaction assay. Therefore, to confirm this observation, bFFA2-G4.57C was also tested in the ERK 1/2 phosphorylation assay, which demonstrated that it did, indeed, lose potency for the bovine-selective compounds C5 and 19 relative to C2 and C3 (Fig. 6*E*).

On the basis of the gain in function we observed for bovine-selective ligands C5 and 19 at hFFA2-C4.57G, we next assessed whether the additional SCFAs and bovine-selective SCAs would also activate this mutant receptor using the β-arrestin-2 interaction assay (**Fig. 7** and **Table 3**). Indeed, C6 and C7 were effective agonists at this variant and now displayed potency akin to that at the bovine ortholog (Fig. 7*A*, *B*). Among the SCAs, particularly compounds with C6 chain lengths, such as compounds 23 and 25, displayed dramatic gain of function at this mutant (Fig. 7*C*, *D*), and indeed, these compounds had equivalent activity at hFFA2-C4.57G, as they do at the bovine receptor. In contrast, although the series of β-carbon-substituted carboxylic acids, including, for example, compounds 26 and 29, also gained function at the C4.57G mutant (Fig. 7*E*, *F*), these compounds were substantially less potent at hFFA2-C4.57G than at bFFA2, suggesting that additional residues besides 4.57 are likely to contribute to this aspect of the bFFA2 ligand SAR.

TABLE 2. *Concentration-response curve-fit parameters for a refined set of SCAs predicted to have high potency and selectivity for bovine FFA2*

	hFFA2		bFFA2		
Compound	pEC_{50}	E_{max}	pEC_{50}	E_{max}	Selectivity
22	<3		5.28 ± 0.08	91 ± 2	>2.28
23	<2		5.40 ± 0.09	104 ± 3	>3.40
24	<3.5		5.00 ± 0.06	104 ± 2	>1.50
25	<2		5.37 ± 0.09	100 ± 3	>3.37
26	<2		4.89 ± 0.06	98 ± 2	>2.89
27	<2		4.96 ± 0.07	102 ± 3	>2.96
28	<2		3.76 ± 0.09	96 ± 6	>1.76
29	<2		4.22 ± 0.06	107 ± 4	>2.22

Selectivity is expressed as bFFA2 pEC_{50} − hFFA2 pEC_{50}. Values of $pEC_{50} < 2$ indicate that no measureable response was obtained. E_{max} values are reported as a percentage of the C3 response at bFFA2.

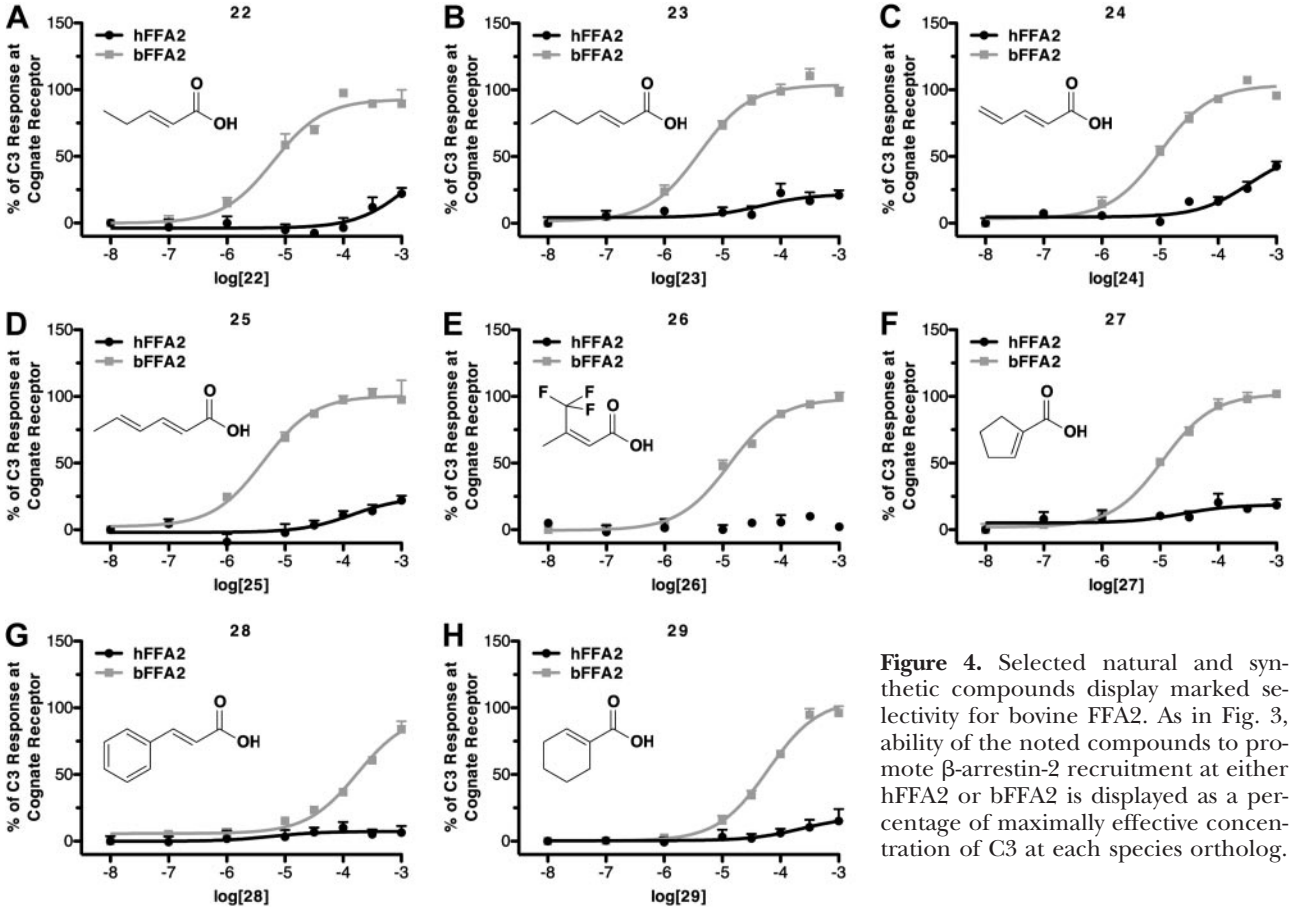

Figure 4. Selected natural and synthetic compounds display marked selectivity for bovine FFA2. As in Fig. 3, ability of the noted compounds to promote β-arrestin-2 recruitment at either hFFA2 or bFFA2 is displayed as a percentage of maximally effective concentration of C3 at each species ortholog.

The substantial gain in function at hFFA2-C4.57G for several ligands that are inactive at wild-type hFFA2 and hFFA3 suggested that this mutant could form the basis of a construct to selectively probe the function of FFA2. However, to be useful in practice, a RASSL form of FFA2 that not only gains function to one or more nonendogenously generated ligands but also loses response to the endogenous ligands is required. Therefore, we used hFFA2-C4.57G as a lead in order to generate a true RASSL form of hFFA2. For this, we returned to the four positively charged residues, R5.39, R7.35, H4.56, and H6.55, previously implicated in SCFA binding to hFFA2 (19). Although our initial studies on the bovine ortholog of FFA2 suggested that mutation to alanine of either R5.39 or H4.56 resulted in a complete loss of function (Fig. 5*B*, *D*), the alanine mutations of both R7.35 or H6.55 each retained some activity for the most potent bovine-selective ligands (Fig. 5*C*, *E*). Because the retained function at R7.35 appeared to result from the presence of an additional arginine at 7.36 in the bovine receptor that is not present in hFFA2, we focused on H6.55. Initially, a H6.55A mutation was incorporated into hFFA2-C4.57G (**Fig. 8*A***). Like bovine H6.55A, this form of hFFA2 also retained some activity to the most potent ligand at the human C4.57G receptor, compound 25, while losing function for the endogenous SCFA C3. However, the potency of compound 25 remained very low at this mutant. Several less extreme mutations were, therefore, also assessed. Replacement by lysine resulted in complete loss of function (Fig. 8*B*). By contrast, introduction of asparagine, which is the residue present at this position in the related long-chain fatty acid receptor FFA1 (25, 26) to generate hFFA2-C4.57G/H6.55N produced a receptor with reasonable potency for compound 25 (Fig. 8*C*), while losing nearly all measurable activity to the endogenous SCFA ligands C1–C5 (Fig. 8*D*). To examine this further, we also generated hFFA2-C4.57G/H6.55Q due to the similarity between asparagine and glutamine. This form of hFFA2 also retained potency for compound 25, which was somewhat improved over hFFA2-C4.57G/H6.55N (Fig. 8*E*) and also showed very little response to each of C1–C5.

Considering the better potency observed for compound 25, we further examined the potential of hFFA2-C4.57G/H6.55Q as a true RASSL form of this receptor. For this, it was tested across multiple functional endpoints, reflective of the range of known signaling pathways FFA2 is able to regulate (27). To assess $G\alpha_{i/o}$ coupling, we compared the effect of C3 at wild-type hFFA2 on inhibition of forskolin-stimulated cAMP production (**Fig. 9*A***) with that of compound 25 at the mutant receptor (Fig. 9*B*). While C3 and C2 were able to inhibit forskolin-stimulated cAMP production *via* wild-type FFA2 (pEC_{50}=4.28±0.19 and 4.60±0.30, respectively), they both had ≥100-fold reduced effect on the mutant receptor. Strikingly, compound 25, although completely inac-

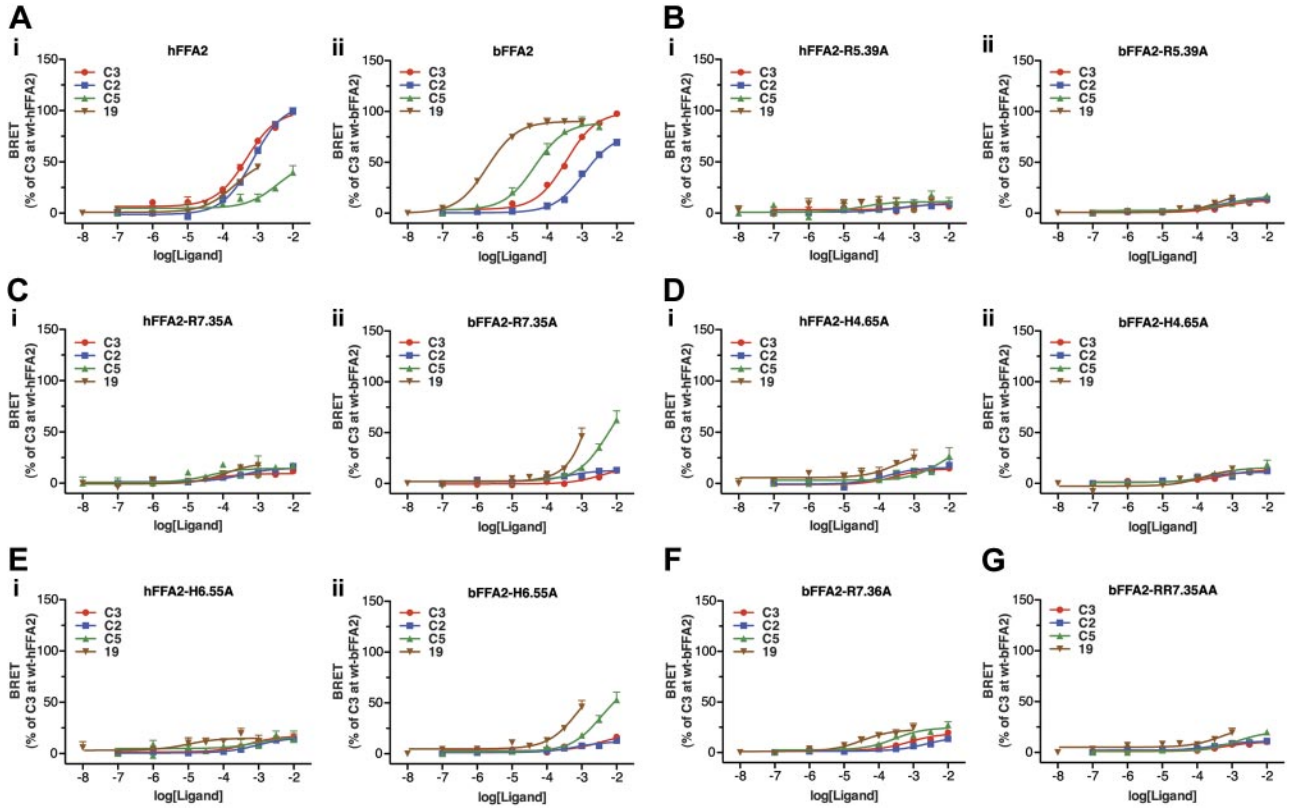

Figure 5. Mutational analysis of the orthosteric binding pocket of bFFA2: comparisons with the human ortholog. *A–E*) Wild-type (*A*) and X-A mutants of residues 5.39 (*B*), 7.35 (*C*), 4.56 (*D*), and 6.55 (*E*) were assessed for β-arrestin-2 recruitment at hFFA2 (*Ai–Ei*) and bFFA2 (*Aii–Eii*) in response to C2, C3, C5, and compound 19. *F, G*) Effects of mutating R7.36 that is present only in bFFA2 to alanine (*F*) and of a double (R7.35A, R7.36A) mutant (*G*) were also assessed.

tive at the wild-type hFFA2 receptor, strongly and potently inhibited forskolin-stimulated cAMP production *via* the mutant (pEC_{50}=5.83±0.11). To assess coupling of hFFA2-C4.57G/H6.55Q to $G\alpha_{q/11}$ pathways, the ability of C3 and compound 25 to stimulate Ca^{2+} mobilization was examined in cells expressing wild-type hFFA2 (Fig. 9*C*) or hFFA2-C4.57G/H6.55Q (Fig. 9*D*). Although C3 and C2 produced an increase in Ca^{2+} *via* wild-type hFFA2 (pEC_{50}=3.21±0.09 and 3.01±0.11, respectively), C3 had no measurable effect at the C4.57G/H6.55Q mutant, while C2 only produced a very small effect at 10 mM. By contrast, compound 25 again had no effect on wild-type hFFA2 but clearly increased Ca^{2+} *via* the mutant receptor (pEC_{50}=4.63±0.05). Comparable experiments were conducted measuring ERK 1/2 phosphorylation by C3 and compound 25 *via* the wild-type (Fig. 9*E*) and C4.57G/H6.55Q (Fig. 9*F*) forms of hFFA2. Again, similar results were obtained: C3 and C2 effectively promoted ERK 1/2 phosphorylation *via* the wild-type receptor (pEC_{50}=4.13±0.09 and 3.94±0.08, respectively) but had little effect on the mutant form, while compound 25 had no effect at the wild type but was active and potent at the mutant form of FFA2 (pEC_{50}=5.61±0.06). Importantly, not only did compound 25 activate hFFA2-C4.57G/H6.55Q in each assay, the rank order of potency for compound 25 at this RASSL form of hFFA2 across the various assays was similar to that for C3 and C2 at the wild-type receptor, such that cAMP > pERK 1/2 > Ca^{2+} > β-arrestin-2, suggesting that the active conformation(s) of hFFA2-C4.57G/H6.55Q induced by compound 25 are very similar to those of the wild-type receptor occupied by C2 or C3. To more directly test this in an unbiased manner, we employed a DMR assay, a method that has been used in the past to broadly measure cellular responses to GPCR activation (20, 22, 23). As in the other assays assessed, C3 and C2 produced DMR responses at hFFA2 (pEC_{50}=4.20±0.11 and 3.85±0.12, respectively), and compound 25 was without effect (Fig. 9*E*), while at hFFA2-C4.57G/H6.55Q, compound 25 produced a good response (pEC_{50}=5.35±0.06), and C3 and C2 had only small effects at the highest concentrations tested (Fig. 9*F*). Finally, DMR time-course experiments were conducted using C3 on hFFA2 (Fig. 9*G*) or compound 25 on hFFA2-C4.57G/H6.55Q (Fig. 9*H*). The resulting DMR responses showed very similar profiles between the two different forms of hFFA2, further supporting the conclusion that the cellular responses of hFFA2-C4.57G/H6.55Q to compound 25 are very similar to those of the wild-type hFFA2 to its endogenous ligands.

In the past, generation of RASSL GPCRs has often resulted in increased levels of ligand-independent constitutive activity in the RASSL receptor (16). Therefore, in addition to confirming that the cellular response to hFFA2-C4.57G/H6.55Q is similar to wild-type hFFA2, it is also important to demonstrate that hFFA2-C4.57G/H6.55Q does not display altered levels of constitutive activity. The Flp-In T-REx cells

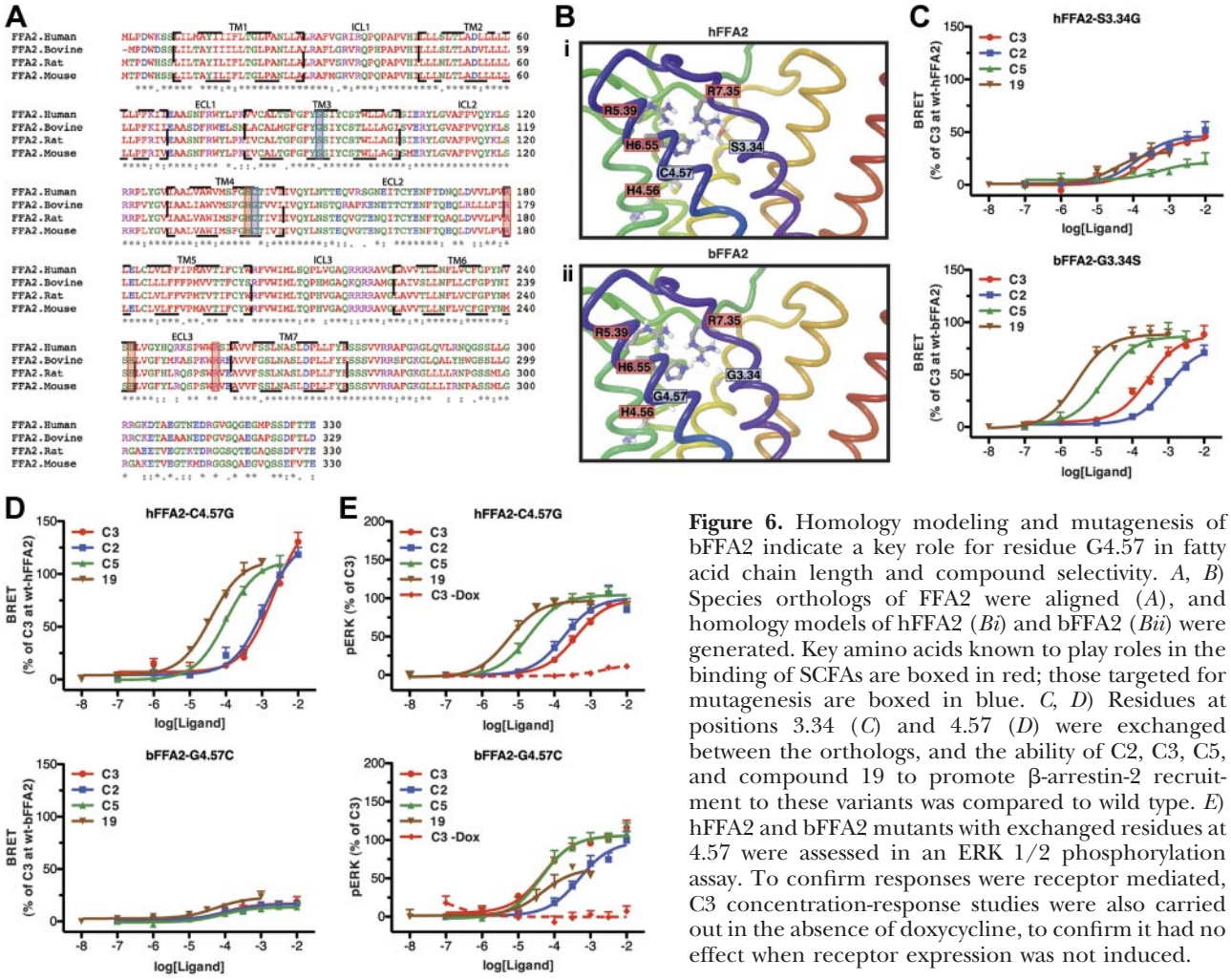

Figure 6. Homology modeling and mutagenesis of bFFA2 indicate a key role for residue G4.57 in fatty acid chain length and compound selectivity. *A*, *B*) Species orthologs of FFA2 were aligned (*A*), and homology models of hFFA2 (*Bi*) and bFFA2 (*Bii*) were generated. Key amino acids known to play roles in the binding of SCFAs are boxed in red; those targeted for mutagenesis are boxed in blue. *C*, *D*) Residues at positions 3.34 (*C*) and 4.57 (*D*) were exchanged between the orthologs, and the ability of C2, C3, C5, and compound 19 to promote β-arrestin-2 recruitment to these variants was compared to wild type. *E*) hFFA2 and bFFA2 mutants with exchanged residues at 4.57 were assessed in an ERK 1/2 phosphorylation assay. To confirm responses were receptor mediated, C3 concentration-response studies were also carried out in the absence of doxycycline, to confirm it had no effect when receptor expression was not induced.

provide an optimal experimental system to examine this, as they allow direct comparison of basal signaling within the same cell line, either with or without induced receptor expression. However, the assays used to describe the signaling properties of hFFA2-C4.57G/H6.55Q, including cAMP, Ca^{2+}, pERK, and DMR, are not well suited to measuring ligand-independent constitutive activity; therefore, we extended our studies to measure incorporation of [^{35}S]GTPγS, an assay that has been widely used previously to study GPCR constitutive activity (28–29). Initially, we demonstrated that hFFA2 activity can be measured in this assay, as C3 (pEC_{50}=4.16±0.11) but not compound 25 stimulated [^{35}S]GTPγS incorporation in membranes induced to express wild-type hFFA2 (**Fig. 10*A***). Similarly, in hFFA2-C4.57G/H6.55Q-expressing membranes, compound 25 promoted incorporation of [^{35}S]GTPγS (pEC_{50}=5.46±0.15), while C3 produced very little response and only at high concentrations (Fig. 10*B*). To examine directly ligand-independent activity, basal [^{35}S]GTPγS incorporation was measured in membranes isolated from either hFFA2 or hFFA2-C4.57G/H6.55Q cells in the absence or presence of doxycycline to induce receptor expression (Fig. 10*C*). In both cases, doxycycline induction resulted in a statistically significant (P<0.001) increase in [^{35}S]GTPγS incorporation. Specifically, induced expression of hFFA2 resulted in a 157 ± 7% increase in basal [^{35}S]GTPγS incorporation, while induced expression of hFFA2-C4.57G/H6.55Q resulted in a similar 156 ± 4% (P>0.05) increase. These findings demonstrate that wild-type hFFA2 displays constitutive activity and that this is unaltered by the alterations to generate hFFA2-C4.57G/H6.55Q.

DISCUSSION

By exploring differences in pharmacology between the human and bovine orthologs of FFA2, the most dissimilar species variants of this receptor that have currently been cloned, then generating homology models and focusing on residues within 8 Å of the predicted ligand-binding site for endogenously produced SCFAs, we have been able to engineer the human ortholog to respond to a novel group of ligands. By so doing, we have provided new insights into the binding pocket of the human ortholog that may allow the design of novel and more potent ligands that target FFA2, a receptor that is a potential therapeutic target in areas including inflammation and metabolic diseases (4, 7, 8). Moreover, the hFFA2-C4.57G/H6.55Q mutant that we generated acts as a RASSL form of this receptor because it

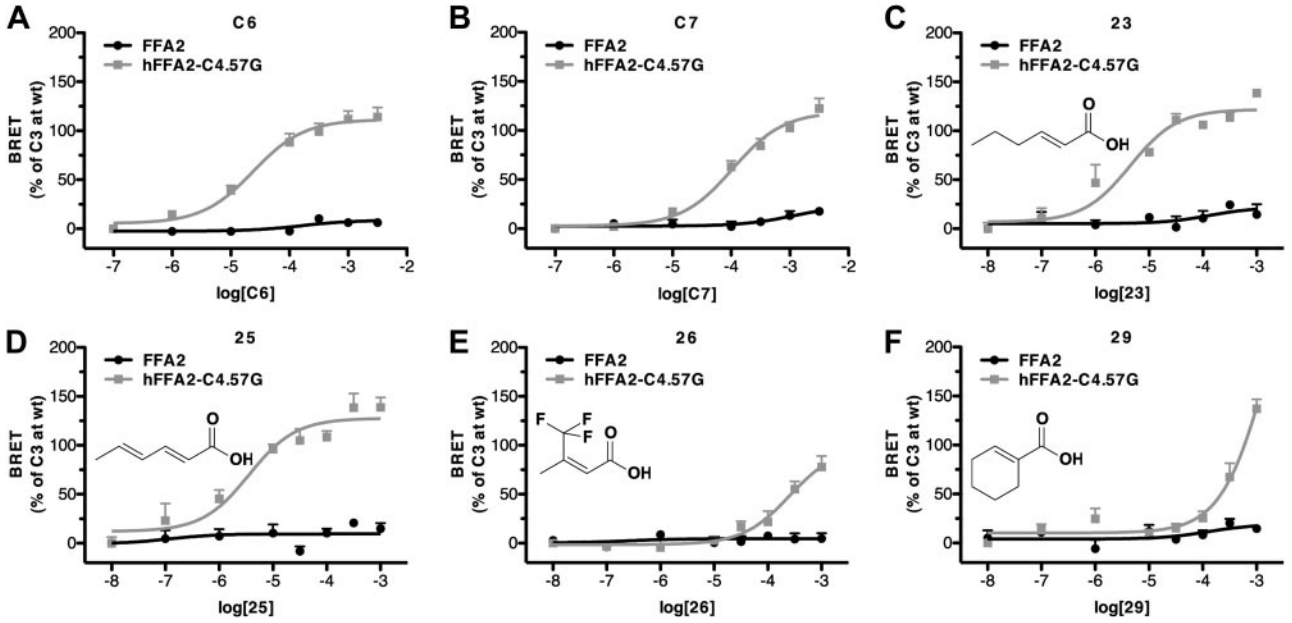

Figure 7. Substitution of C4.57G in hFFA2 generates responses similar to the bovine ortholog. Pharmacology of hFFA2-C4.57G was assessed in β-arrestin-2 recruitment assays with a number of ligands shown earlier to display marked selectivity for bFFA2: C6 (*A*), C7 (*B*), compound 23 (*C*), compound 25 (*D*), compound 26 (*E*), and compound 29 (*F*).

has also lost responsiveness to endogenously produced activators. In this regard, the current studies have similarity to the production of RASSL forms of the muscarinic acetylcholine receptors, which no longer respond with significant potency to acetylcholine but do so instead to the synthetic ligand clozapine *N*-oxide (12, 13). However, unlike the muscarinic receptor RASSLs, where the starting point to evolve the variant forms was random mutagenesis (13), herein, we have taken advantage of the SAR differences in two species orthologs of the FFA2 receptor to the *n*-fatty acids and SCAs. In combination with our previous analysis of the mode of binding and selectivity of SCAs for FFA2 *vs.* the closely related receptor FFA3 (19–21), this has allowed rational design of a RASSL based on homology modeling and sequence alignments. By contrast, rationalization of the basis of the selective binding of clozapine *N*-oxide to a muscarinic RASSL (13) was only possible *post hoc* (12).

A major challenge to understanding the physiological roles of FFA2 is the similarity of the pharmacology of the closely related receptor FFA3, a problem that is compounded by the fact that these two receptors are often coexpressed (30, 31). Although limited variation in potency of C2 between human FFA2 and FFA3 has resulted in its use as a selective FFA2 agonist (32), because C2 does still have activity at FFA3 and has only low potency at FFA2, this is far from ideal. Furthermore, apart from a series of SCAs described by Schmidt *et al.* (20), which, because of their small size, also have poor potency, the only FFA2-selective ligands currently

TABLE 3. *Concentration-response curve parameters for bovine selective SCFAs and SCAs at wild-type and C4.57G human FFA2*

	FFA2-wt		FFA2-C4.57G			
Compound	pEC_{50}	E_{max}	pEC_{50}	E_{max}	*vs.* bFFA2[a]	Selectivity
C6	<2		4.62 ± 0.14	112 ± 4	NS	>2.62
C7	<2		3.98 ± 0.10	119 ± 5	NS	>1.98
C8	<2		2.97 ± 0.13	109 ± 13	NS	>0.97
22	<3		4.48 ± 0.15	107 ± 7	$P < 0.05$	>1.48
23	<2		5.49 ± 0.17	109 ± 4	NS	>3.49
24	<3		4.64 ± 0.14	113 ± 7	$P < 0.01$	>1.64
25	<2		5.34 ± 0.21	113 ± 6	NS	>3.34
26	<2		3.59 ± 0.16	96 ± 12	$P < 0.01$	>1.59
27	<2		4.08 ± 0.09	98 ± 5	$P < 0.01$	>2.08
28	<2		3.41 ± 0.31	93 ± 23	$P < 0.01$	>1.41
29	<2		3.80 ± 0.20	78 ± 11	$P < 0.05$	>1.80

Selectivity is expressed as FFA2-C4.57G pEC_{50} − FFA2-wt pEC_{50}. Values of $pEC_{50} < 2$ indicate that no measureable response was obtained. Values of $pEC_{50} < 3$ indicate that a response was observed; however, the data did not allow for the derivation of accurate curve-fit parameters. E_{max} values are reported as a percentage of the C3 response at wild-type bFF2A. [a]Statistical comparison of pEC_{50} curve-fit data between bFFA2 and hFFA2-C4.57G. NS, not significant.

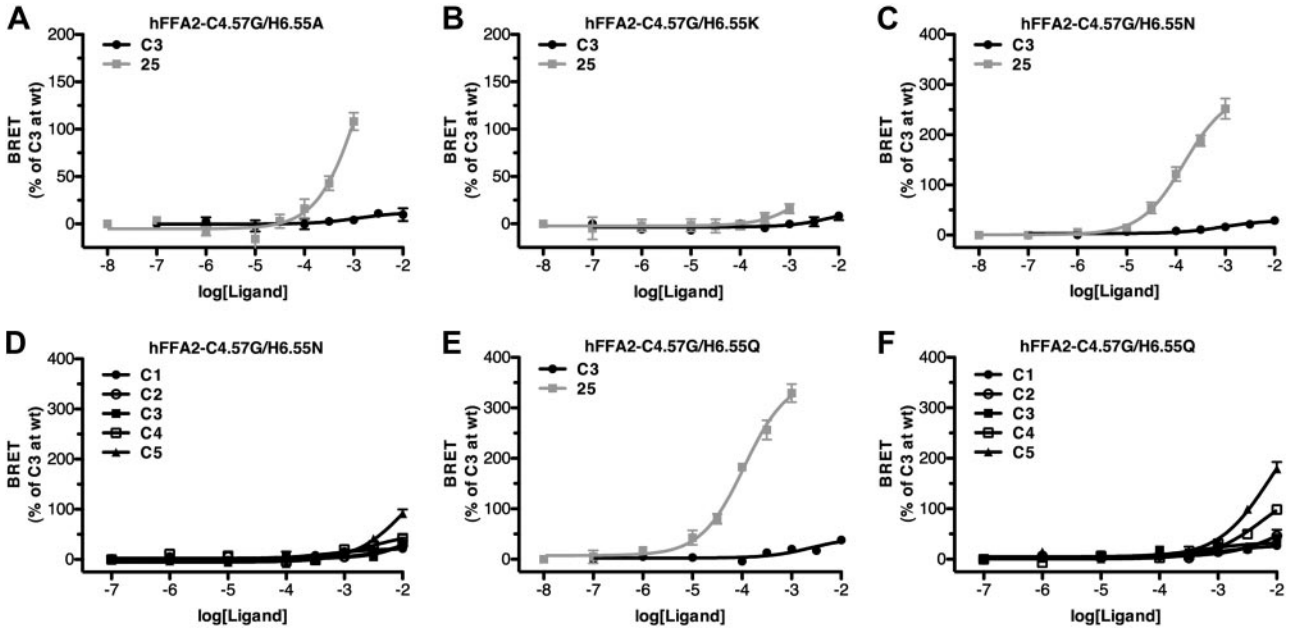

Figure 8. Alterations at residue 6.55 to hFFA2-C4.57G generate a RASSL form of hFFA2. hFFA2-C4.57G was modified further by substitution of H6.55 to alanine (*A*), lysine (*B*), asparagine (*C, D*) or glutamine (*E, F*). Action of either C3 or compound 25 was then assessed in β-arrestin-2 recruitment assays. *D, F*) C1–C5 *n*-fatty acids were tested for activity.

described derive from the phenylacetamide 4-CMTB (21, 33). Although this compound has been used to delineate effects of FFA2 (33, 34), it clearly binds to a site distinct from the SCFAs and acts as a positive allosteric modulator of the action of the SCFAs, as well as a direct agonist (21, 33). With increasing appreciation of the ability of different ligands that bind to overlapping sites on GPCRs to generate different signaling profiles, a feature that is described as either functional selectivity (35) or ligand bias (36, 37), there must be the possibility that agonists that bind to different sites of a GPCR will result in such bias. This issue, although important, remains to be explored for the actions of 4-CMTB and related allosteric ligands at FFA2, and thus, we wished to modify the orthosteric binding pocket of FFA2.

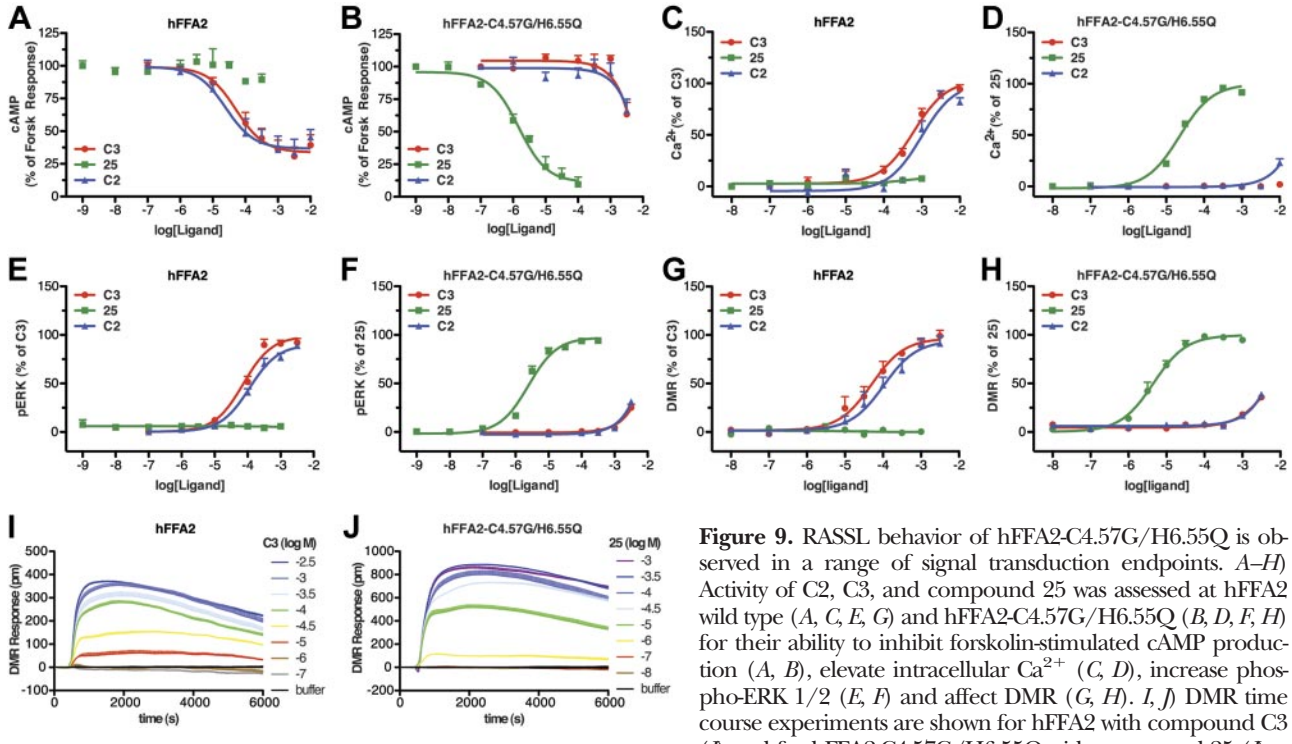

Figure 9. RASSL behavior of hFFA2-C4.57G/H6.55Q is observed in a range of signal transduction endpoints. *A–H*) Activity of C2, C3, and compound 25 was assessed at hFFA2 wild type (*A, C, E, G*) and hFFA2-C4.57G/H6.55Q (*B, D, F, H*) for their ability to inhibit forskolin-stimulated cAMP production (*A, B*), elevate intracellular Ca^{2+} (*C, D*), increase phospho-ERK 1/2 (*E, F*) and affect DMR (*G, H*). *I, J*) DMR time course experiments are shown for hFFA2 with compound C3 (*I*) and for hFFA2-C4.57G/H6.55Q with compound 25 (*J*).

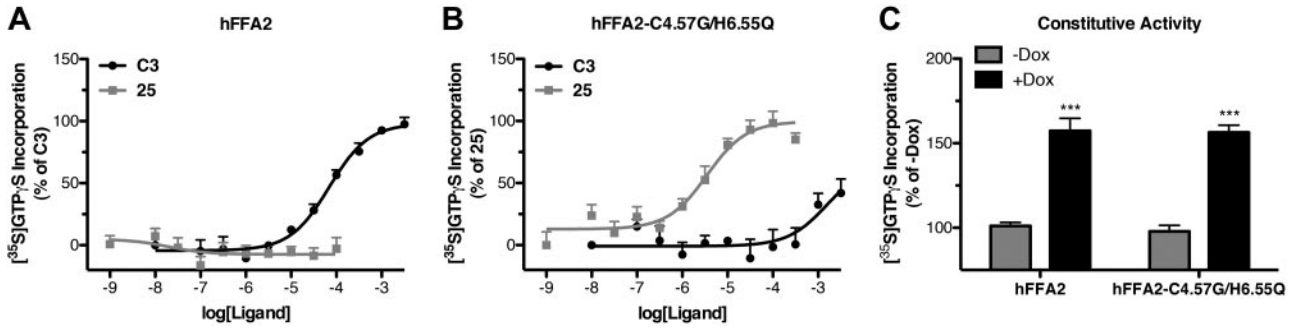

Figure 10. Wild-type hFFA2 and hFFA2-C4.57G/H6.55Q display similar levels of ligand-independent constitutive activity. *A*, *B*) Ability of C3 and compound 25 to stimulate [^{35}S]GTPγS incorporation was assessed in membranes expressing either hFFA2 (*A*) or hFFA2-C4.57G/H6.55Q (*B*). *C*) Basal levels of [^{35}S]GTPγS incorporation were measured in membranes harvested from cells that were either untreated or stimulated with doxycycline (Dox; 100 ng/ml) to induce expression of either hFFA2 or hFFA2-C4.57G/H6.55Q.

An important secondary finding of this work is our demonstration that the pharmacology of bFFA2 is significantly different from that of hFFA2. Although previous work had cloned the bovine SCFA receptors FFA2 and FFA3 (38), little was known about their pharmacology. Our demonstration that bFFA2 responds with a completely different rank order of potency to the SCFAs than does hFFA2 suggests that this receptor may serve different functions in bovines compared with humans, and, clearly, future studies on bFFA2 should take into account its unique ligand selectivity. The bovine ortholog of FFA2 was chosen for this study based on the hypothesis that species, including ruminants, that rely heavily on nondigestible carbohydrates are exposed to significantly higher SCFA concentrations (39) and, therefore, were most likely to have SCFA receptors with distinct pharmacology. Although our findings with bFFA2 appear to support this conclusion, it is also important to consider whether this pharmacology may be preserved in other species with high dietary levels of nondigestible carbohydrates. An alignment of species orthologs of FFA2 (Supplemental Fig. S1) reveals that the only other species with glycine at position 4.57, and, therefore, likely to display similar pharmacology to bFFA2, is the goat, the only other ruminant for which sequencing data are available. Interestingly, the second unique residue that appears to contribute to the pharmacology of bFFA2, R7.36, is also conserved in goat FFA2, indicating that the pharmacology of goat FFA2 is likely to be very similar to bFFA2. Interestingly, the horse ortholog of FFA2 does not appear likely to share pharmacology with bFFA2 on the basis of this sequence alignment (Supplemental Fig. S1), this despite the fact that the horse is also heavily reliant on nondigestible carbohydrates, and, in fact, shows SCFAs concentrations in the digestive tract similar to those observed in ruminants (39). Therefore, it appears that the unique pharmacology of bFFA2 is likely restricted to ruminants and may be related to the fact that FFA2 is expressed in the rumen of these animals (38, 40). Indeed, it is conceivable that the two primary changes that we describe in the pharmacology of bFFA2, namely, a loss of potency to C2 and gain of function to longer chain lengths, may be an evolutionary adaptation designed to maintain dynamic FFA2 function in the high-SCFA-concentration environment of the rumen, where C2, as the predominant SCFA, is present in very high concentrations, but lower levels of longer-chain compounds are also observed (39).

Our initial studies, demonstrating the unique pharmacology of bFFA2, precipitated efforts to understand the molecular basis for this finding. Despite the availability of atomic level structure of a number of GPCRs (41–43), homology modeling remains challenging. This is particularly true for receptors with limited sequence homology to GPCRs of known structure. However, both because the binding sites for fatty acids in FFA1 (25, 26, 44), FFA2 (19), and FFA3 (19) have been explored by mutagenesis and our homology model of FFA1 has been validated by its use in "virtual screening" to identify novel ligands at FFA1 (26), we have been able to model and compare hFFA2 and bFFA2 with some confidence. The models indicated two residues that differ between hFFA2 and bFFA2 that are in proximity to arginine residues, two in the human (5.39 and 7.35), and as we now show, three in the bovine (5.39, 7.35, and 7.36) that coordinate the carboxylate group of the fatty acid ligands. These were, therefore, potential candidates to underpin the species chain-length selectivity. While alteration of position 3.34 in hFFA2 to the bovine sequence had little effect on pharmacology, alteration of the cysteine at position 4.57 in hFFA2 to glycine, which is present in this [1]position of bFFA2, was sufficient to markedly enhance potency to the longer-chain SCFAs C5–C8, as well as to a number of SCAs that we showed to be markedly selective for bFFA2 over hFFA2. To generate a more useful RASSL form of hFFA2, it was also important to develop a receptor that no longer responded to its endogenous SCFA ligands. We achieved this through the addition of a second mutation H6.55Q, one of the positively charged residues previously shown to play a role in SCFA ligand binding (19). Overall, our development of this RASSL form of hFFA2 represents a novel, more rational, approach to chemically engineering ligand

selectivity at a GPCR based on pharmacological differences between species. This is in contrast to approaches based on random mutagenesis and directed molecular evolution used to develop RASSL forms of the muscarinic receptors (13). However, a combination of these two approaches, whereby species differences could be used to rationally identify a RASSL "lead," followed by subsequent molecular evolution to mature an ideal RASSL ligand binding site, may well represent an approach to generate RASSLs with even more favorable properties in the future.

In addition to modifying the RASSL receptor to alter its pharmacology, the selection of an ideal ligand to activate the RASSL is also of critical importance. The ligand chosen to activate the hFFA2-RASSL described here, compound 25, is a natural compound that is widely used as an antifungal preservative in various foodstuffs (45). The compound is essentially nontoxic, with a reported LD_{50} in rodents of 8–10 g/kg (46), suggesting that it could be used *in vivo* without significant side effects. At present, little is known about the bioavailability or tissue distribution of compound 25, and future work will need to address these issues. Interestingly, the compound is approved for use as an additive to cattle feed, and although at least one study has suggested that its use does not affect cattle weight gain (47), future work may well consider what biological effects its use in this context might have, given its ability to activate bFFA2.

Similar RASSLs of muscarinic acetylcholine receptor subtypes have been used to produce transgenic animals to selectively study the functions of individual muscarinic subtypes in a variety of both *ex vivo* and *in vivo* assays (14, 15). Our demonstration that compound 25 has similar signaling properties at the hFFA2-RASSL to those of C3 at the wild receptor across multiple assays indicates that this hFFA2-RASSL would be ideal for these types of studies using knock-in transgenesis. In addition to their use differentiating the actions of closely related GPCRs, RASSLs have also been used as a means to explore selective activation of individual signaling pathways in cells or tissues that have been engineered to express the RASSL (16). Although there are RASSLs described previously for each of the three primary Gα signaling pathways (G_s, G_i, and G_q), the hFFA2-RASSL described in the present work is the first RASSL to selectively coactivate two of these pathways, and thus may represent a novel means to explore combined G_i/G_q activation after its expression *in vitro* or *in vivo*. Furthermore, RASSLs have generated recent interest for their potential use as molecular switches in engineered tissues that could ultimately be used therapeutically in humans (16). The FFA2 RASSL described in the current work may be of particular interest in this respect, given that its ligand is nontoxic and, indeed, already approved for human consumption. Taken together, in the present work, we have described a novel approach to developing chemically engineered GPCRs based on the pharmacological variation between species orthologs, and in doing so, have developed a valuable reagent for the future study of FFA2 function. FJ

These studies were supported by the Wellcome Trust (grant 089600/Z/09/Z to G.M.), the Danish Council for Strategic Research (grant 11-116196 to T.U., G.M., and E.K.), and a Canadian Institutes of Health Research Fellowship (to B.D.H.).

REFERENCES

1. He, W., Miao, F. J., Lin, D. C., Schwandner, R. T., Wang, Z., Gao, J., Chen, J. L., Tian, H., and Ling, L. (2004) Citric acid cycle intermediates as ligands for orphan G-protein-coupled receptors. *Nature* **429,** 188–193
2. Liu, C., Wu, J., Zhu, J., Kuei, C., Yu, J., Shelton, J., Sutton, S. W., Li, X., Yun, S. J., Mirzadegan, T., Mazur, C., Kamme, F., and Lovenberg, T. W. (2009) Lactate inhibits lipolysis in fat cells through activation of an orphan G-protein-coupled receptor, GPR81. *J. Biol. Chem.* **284,** 2811–2822
3. Offermanns, S., Colletti, S. L., Lovenberg, T. W., Semple, G., Wise, A., and IJzerman, A. P. (2011) International Union of Basic and Clinical Pharmacology. LXXXII. Nomenclature and classification of hydroxy-carboxylic acid receptors (GPR81, GPR109A, and GPR109B). *Pharmacol. Rev.* **63,** 269–290
4. Stoddart, L. A., Smith, N. J., and Milligan, G. (2008) International Union of Pharmacology. LXXI. Free fatty acid receptors FFA1, -2, and -3: pharmacology and pathophysiological functions. *Pharmacol. Rev.* **60,** 405–417
5. Hudson, B. D., Smith, N., and Milligan, G. (2011) Experimental challenges to targeting poorly characterized GPCRs: uncovering the therapeutic potential for free fatty acid receptors. *Adv. Pharmacol.* **62,** 175–218
6. Sleeth, M. L., Thompson, E. L., Ford, H. E., Zac-Varghese, S. E., and Frost, G. (2010) Free fatty acid receptor 2 and nutrient sensing: a proposed role for fibre, fermentable carbohydrates and short-chain fatty acids in appetite regulation. *Nutr. Res. Rev.* **23,** 135–145
7. Tiwari, A. (2010) GPR43: an emerging target for the potential treatment of type 2 diabetes, obesity and insulin resistance. *Curr. Opin. Investig. Drugs* **11,** 385–393
8. Swaminath, G. (2008) Fatty acid binding receptors and their physiological role in type 2 diabetes. *Arch. Pharm. (Weinheim)* **341,** 753–761
9. Maslowski, K. M., Vieira, A. T., Ng, A., Kranich, J., Sierro, F., Yu, D., Schilter, H. C., Rolph, M. S., Mackay, F., Artis, D., Xavier, R. J., Teixeira, M. M., and Mackay, C. R. (2009) Regulation of inflammatory responses by gut microbiota and chemoattractant receptor GPR43. *Nature* **461,** 1282–1286
10. Sina, C., Gavrilova, O., Förster, M., Till, A., Derer, S., Hildebrand, F., Raabe, B., Chalaris, A., Scheller, J., Rehmann, A., Franke, A., Ott, S., Häsler, R., Nikolaus, S., Fölsch, U. R., Rose-John, S., Jiang, H. P., Li, J., Schreiber, S., and Rosenstiel, P. (2009) G protein-coupled receptor 43 is essential for neutrophil recruitment during intestinal inflammation. *J. Immunol.* **183,** 7514–7522
11. Zaibi, M. S., Stocker, C. J., O'Dowd, J., Davies, A., Bellahcene, M., Cawthorne, M. A., Brown, A. J., Smith, D. M., and Arch, J. R. (2010) Roles of GPR41 and GPR43 in leptin secretory responses of murine adipocytes to short chain fatty acids. *FEBS Lett.* **584,** 2381–2386
12. Alvarez-Curto, E., Prihandoko, R., Tautermann, C. S., Zwier, J. M., Pediani, J. D., Lohse, M. J., Hoffmann, C., Tobin, A. B., and Milligan, G. (2011) Developing chemical genetic approaches to explore G protein-coupled receptor function—validation of the use of a receptor activated solely by synthetic ligand (RASSL). *Mol. Pharmacol.* **80,** 1033–1046
13. Armbruster, B. N., Li, X., Pausch, M. H., Herlitze, S., and Roth, B. L. (2007) Evolving the lock to fit the key to create a family of G protein-coupled receptors potently activated by an inert ligand. *Proc. Natl. Acad. Sci. U. S. A.* **104,** 5163–5168

14. Guettier, J. M., Gautam, D., Scarselli, M., Ruiz de Azua, I., Li, J. H., Rosemond, E., Ma, X., Gonzalez, F. J., Armbruster, B. N., Lu, H., Roth, B. L., and Wess, J. (2009) A chemical-genetic approach to study G protein regulation of beta cell function in vivo. *Proc. Natl. Acad. Sci. U. S. A.* **106,** 19197–19202
15. Sasaki, K., Suzuki, M., Mieda, M., Tsujino, N., Roth, B., and Sakurai, T. (2011) Pharmacogenetic modulation of orexin neurons alters sleep/wakefulness states in mice. *PLoS One* **6,** e20360
16. Conklin, B. R., Hsiao, E. C., Claeysen, S., Dumuis, A., Srinivasan, S., Forsayeth, J. R., Guettier, J. M., Chang, W. C., Pei, Y., McCarthy, K. D., Nissenson, R. A., Wess, J., Bockaert, J., and Roth, B. L. (2008) Engineering GPCR signalling pathways with RASSLs. *Nat. Methods* **5,** 673–678
17. Claeysen, S., Joubert, L., Sebben, M., Bockaert, J., and Dumuis, A. (2003) A single mutation in the 5-HT4 receptor (5-HT4-R D100(3.32)A) generates a Gs-coupled receptor activated exclusively by synthetic ligands (RASSL). *J. Biol. Chem.* **278,** 699–702
18. Milligan, G., Stoddart, L. And A., Smith, N. J. (2009) Agonism and allosterism: the pharmacology of the free fatty acid receptors FFA2 and FFA3. *Br. J. Pharmacol.* **158**: 146–153
19. Stoddart, L. A., Smith, N. J., Jenkins, L., Brown, A. J., and Milligan, G. (2008) Conserved polar residues in transmembrane domains V, VI and VII of free fatty acid receptor 2 and free fatty acid receptor 3 are required for the binding and function of short chain fatty acids. *J. Biol. Chem.* **283,** 32913–32924
20. Schmidt, J., Smith, N. J., Christiansen, E., Tikhonova, I. G., Grundmann, M., Hudson, B. D., Ward, R. J., Drewke, C., Milligan, G., Kostenis, E., and Ulven, T. (2011) Selective orthosteric free fatty acid receptor 2 (FFA2) agonists: Identification of the structural and chemical requirements for selective activation of FFA2 versus FFA3. *J. Biol. Chem.* **286,** 10628–10640
21. Smith, N. J., Ward, R. J., Stoddart, L. A., Hudson, B. D., Kostenis, E., Ulven, T., Morris, J. C., Trankle, C., Tikhonova, I. G., Adams, D. R., and Milligan, G. (2011) Extracellular loop 2 of the free fatty acid receptor 2 mediates allosterism of a phenylacetamide ago-allosteric modulator. *Mol. Pharmacol.* **80,** 163–173
22. Schröder, R., Janssen, N., Schmidt, J., Kebig, A., Merten, N., Hennen, S., Müller, A., Blättermann, S., Mohr-Andrä, M., Zahn, S., Wenzel, J., Smith, N. J., Gomeza, J., Drewke, C., Milligan, G., Mohr, K., and Kostenis, E. (2010) Deconvolution of complex G protein-coupled receptor signaling in live cells using dynamic mass redistribution measurements. *Nat. Biotechnol.* **28,** 943–949
23. Schröder, R., Schmidt, J., Blättermann, S., Peters, L., Janssen, N., Grundmann, M., Seemann, W., Kaufel, D., Merten, N., Drewke, C., Gomeza, J., Milligan, G., Mohr, K., and Kostenis, E. (2011) Applying label-free dynamic mass redistribution technology to frame signaling of G protein-coupled receptors noninvasively in living cells. *Nat. Protoc.* **6,** 1748–1760
24. Ballesteros, J. A., and Weinstein, H. (1995) Integrated methods for the construction of three-dimensional models and computational probing of structure-function relations in G protein-coupled receptors. *Methods Neurosci.* **25,** 366–428
25. Sum, C. S., Tikhonova, I. G., Neumann, S., Engel, S., Raaka, B. M., Costanzi, S., and Gershengorn, M. C. (2007) Identification of residues important for agonist recognition and activation in GPR40. *J. Biol. Chem.* **282,** 29248–29255
26. Tikhonova, I. G., Sum, C. S., Neumann, S., Engel, S., Raaka, B. M., Costanzi, S., and Gershengorn, M. C. (2008) Discovery of novel agonists and antagonists of the free fatty acid receptor 1 (FFAR1) using virtual screening. *J. Med. Chem.* **51,** 625–633
27. Brown, A. J., Goldsworthy, S. M., Barnes, A. A., Eilert, M. M., Tcheang, L., Daniels, D., Muir, A. I., Wigglesworth, M. J., Kinghorn, I., Fraser, N. J., Pike, N. B., Strum, J. C., Steplewski, K. M., Murdock, P. R., Holder, J. C., Marshall, F. H., Szekeres, P. G., Wilson, S., Ignar, D. M., Foord, S. M., Wise, A., and Dowell, S. J. (2003) The orphan G protein-coupled receptors GPR41 and GPR43 are activated by propionate and other short chain carboxylic acids. *J. Biol. Chem.* **278,** 11312–11319
28. Harrison, C., and Traynor, J. R. (2003) The [^{35}S]GTPγS binding assay: approaches and applications in pharmacology. *Life Sci.* **74,** 489–508
29. Stoddart, L. A., and Milligan, G. (2010) Constitutive activity of GPR40/FFA1 intrinsic or assay dependent? *Methods Enzymol.* **484,** 569–590
30. Le Poul, E., Loison, C., Struyf, J. Y., Lannoy, V., Decobecq, M. E., Brezillon, S., Dupriez, V., Vassart, G., Van Damme, J., Parmentier, M., and Detheux, M. (2003) Functional characterization of human receptors for short chain fatty acids and their role in polymorphonuclear cell activation. *J. Biol. Chem.* **278,** 25481–25489
31. Kebede, M. A., Alquier, T., Latour, M. G., and Poitout, V. (2009) Lipid receptors and islet function: therapeutic implications? *Diabetes Obes. Metab.* **11**(Suppl. 4), 10–20
32. Ge, H., Li, X., Weiszmnn, J., Wang, P., Baribault, H., Che, J. L., Tian, H., and Li, Y. (2008) Activation of G protein-coupled receptor 43 in adipocytes leads to inhibitions of lipolysis and suppression of plasma free fatty acids. *Endocrinology* **149,** 4519–4526
33. Lee, T., Schwandner, R., Swaminath, G., Weiszmann, J., Cardozo, M., Greenberg, J., Jaeckel, P., Ge, H., Wang, Y., Jiao, X., Liu, J., Kayser, F., Tian, H., and Li, Y. (2008) Identification and functional characterization of allosteric agonists for the G protein-coupled receptor FFA2. *Mol. Pharmacol.* **74,** 1599–1609
34. Vinolo, M. A., Ferguson, G. J., Kulkarni, S., Damoulakis, G., Anderson, K., Bohlooly, -Y. M., Stephens, L., Hawkins, P. T., and Curi, R. (2011) SCFAs induce mouse neutrophil chemotaxis through the GPR43 receptor. *PLoS One* **6,** e21205
35. Urban, J. D., Clarke, W. P., von Zastrow, M., Nichols, D. E., Kobilka, B., Weinstein, H., Javitch, J. A., Roth, B. L., Christopoulos, A., Sexton, P. M., Miller, K. J., Spedding, M., and Mailman, R. B. (2007) Functional selectivity and classical concepts of quantitative pharmacology. *J. Pharmacol. Exp. Ther.* **320,** 1–13
36. Kenakin, T. (2007) Functional selectivity through protean and biased agonism: who steers the ship? *Mol. Pharmacol.* **72,** 1393–1401
37. Violin, J. D., and Lefkowitz, R. J. (2007) Beta-arrestin-biased ligands at seven transmembrane receptors. *Trends Pharmacol. Sci.* **28,** 416–422
38. Wang, A., Gu, Z., Heid, B., Akers, R. M., and Jiang, H. (2009) Identification and characterization of the bovine G protein-coupled receptor GPR41 and GPR43 genes. *J. Dairy Sci.* **92,** 2696–2705
39. Bergman, E. N. (1990) Energy contributions of volatile fatty acids from the gastrointestinal tract in various species. *Physiol. Rev.* **70,** 567–590
40. Wang, A., Akers, R. M., and Jiang, H. (2012) Short communication: Presence of G protein-coupled receptors 43 in rumen epithelium but not in the islets of Langerhans in cattle. *J. Dairy Sci.* **95,** 1371–1375
41. Congreve, M., Langmead, C., and Marshall, F. H. (2011) The use of GPCR structures in drug design. *Adv. Pharmacol.* **62,** 1–36
42. Rosenbaum, D. M., Rasmussen, S. G., and Kobilka, B. K. (2009) The structure and function of G-protein-coupled receptors. *Nature* **459,** 356–363
43. Hanson, M. A., Stevens, R. C. (2009) Discovery of new GPCR biology: one receptor structure at a time. *Structure* **17,** 8–14
44. Smith, N. J., Stoddart, L. A., Devine, N. M., Jenkins, L., and Milligan, G. (2009) The action and mode of binding of thiazolidinedione ligands at free fatty acid receptor 1. *J. Biol. Chem.* **284,** 17527–17539
45. Lück, E. (1990) Food applications of sorbic acid and its salts. *Food Addit. Contam.* **7,** 711–715
46. Walker, R. (1990) Toxicology of sorbic acid and sorbates. *Food Addit. Contam.* **7,** 671–676
47. Knický, M., and Spörndly, R. (2009) Sodium benzoate, potassium sorbate and sodium nitrite as silage additives. *J. Sci. Food Agric.* **89,** 2659–2667

Received for publication May 22, 2012.
Accepted for publication August 13, 2012.

Epilogue

We presented an elegant way to generate a RASSL receptor based on variations between the human and the bovine FFA2 receptor. Instead of introducing random mutation, which is a common way to produce RASSL receptors, the interspecies differences were taken as a rational basis for receptor mutation. In a species-specific physiology-oriented approach, the differences in the composition of breakdown products of food constituents explained the variances in the FFA2 receptor structure between the two species[1]. Through the evolutionary process, the different species adapted to the range of diverse nutritive factors, which also function as signaling molecules for example at nutrition sensitive GPCRs[2]. Fatty acids are energy-generating nutrients and play important roles as signaling molecules[3], hence it is not overly surprising that GPCRs targeted by FFAs show considerable adaptive changes in their structure from species to species.

This RASSL form might eventually provide a valuable tool to dissect FFA3- from FFA2-mediated biological effects *in vivo*. However, this would require employing transgenic techniques, e.g. in a *knock-in* fashion. Another manifestation of the RASSL concept are designer receptors exclusively activated by designer drugs (DREADDs)[4]. These receptors were generated from a muscarinic Acetylcholine receptor that does not recognize the endogenous ligand Acetylcholine but the metabolically stable and physiologically inert substance Clozapine-N-oxide (CNO). Since then, DREADDs endowed with coupling specificity for the three main classes of G proteins ($G\alpha_s$, $G\alpha_i$ and $G\alpha_{q/11}$) were generated[4]. CNO is a drug-like small molecule that is extensively characterized and can be recognized as a selective DREADD ligand. Physiological properties of sorbic acid - the synthetic ligand for the FFA2-RASSL - although widely used as antifungal preservative in food, is less well described and off-target effects cannot be ruled out[5–8].

Regardless, the most striking downside of both approaches to designer receptors is the uncertainty about genuine receptor behavior of modified receptors compared to the wild-type receptor. Different ligands at one receptor can generate different signaling patterns or biological effects, since functional selectivity or signaling bias has shown that multiple receptor conformations can induce a plethora of different signal transduction pathways[9,10]. A RASSL or DREADD is per definition activated by another than the endogenous ligand, which implicates the possibility of - although it does not imperatively lead to - distinct biological effects between the synthetic designer drug and the endogenous ligand (i.e. ligand bias). Despite efforts to affirm the coupling behavior of a given receptor, an ample and bona fide characterization of the signaling repertoire is currently beyond the bounds of possibility. It can thus not be ruled out that RASSLs or DREADDs are *a priori* endowed with biased signal transduction capacities if compared to the wild type receptor in its native environment. Especially studies to explore the *in vivo* function of a given receptor are affected by this concern[4,11].

Although a recent study compared the signaling properties of a muscarinic Acetylcholine receptor-derived DREADD with its genuine wild-type receptor and did not find any signaling bias between the DREADD agonist CNO and the endogenous agonist Acetylcholine, this shortcoming cannot be brushed aside[12]. The more so as this study is entirely based on data from cells artificially engineered to express high levels of the DREADD/RASSL, a circumstance, which is known to confound the signaling fidelity and lower the transferability of conclusions drawn from such experiments[13–16]. However, in the here presented publication, we corroborated signaling fidelity of the FFA2-RASSL in comparison to the wild-type form using the holistic DMR readout.

A next step could be to convert the downside of signaling bias into an advantage by using functional selectivity of distinct DREADDs or RASSLs. Generating designer receptors with specific signaling preferences could enable scientists to study the *in vivo* relevance of distinct signaling events. *Nakajima et al.* made a first attempt by constructing a DREADD that is β-arrestin biased[17].

Designer receptors embody a way to explore and modulate receptor biology *in vivo* in an unprecedented fashion. Similar to this, optogenetic methods are used to control and monitor the biological response by introduction of light-sensitive proteins into the cells. Recent developments in the field of optogenetics allow the generation of molecular switches pursuing that goal[18]. Light-switchable receptors can be artificially expressed in living cells to track the consequence of their signaling[19]. There are, however, some differences between these two approaches that are briefly summarized. i) The pharmacosynthetic approach is non-invasive, if transgenic technologies were employed to introduce the designer receptor into the biological system. ii) Optogenetics induce polarization or depolarization in the target cell, whereas DREADDs engage G protein signaling. iii) There is considerable disparity in the signaling nature generated by these two methods. DREADD signaling is under control of physiological relevant parameters like receptor desensitization and internalization or diffusion, clearance and metabolism of the receptor ligand in the biopharmaceutically relevant compartments. On the other side, optogenetic methods directly affect the function of neurons or a neuronal circuit.

Concisely, the difference between a pharmacosynthetic and an optogenetic measurement system is that in the first case the neuronal modulation is analyzed while in the latter case the actual effect on the neuron is measured. However, both technologies will allow to control and follow discrete signaling events and to gain insight into complexly regulated signaling networks.

References

1. Bergman, E. N. Energy contributions of volatile fatty acids from the gastrointestinal tract in various species, *Physiol. Rev.* **70,** 567–590 (1990).
2. Stoddart, L. A. Smith, N. J. & Milligan, G. International Union of Pharmacology. LXXI. Free fatty acid receptors FFA1, -2, and -3: pharmacology and pathophysiological functions, *Pharmacol. Rev.* **60,** 405–417 (2008).
3. Offermanns, S. Free fatty acid (FFA) and hydroxy carboxylic acid (HCA) receptors, *Annu. Rev. Pharmacol. Toxicol.* **54,** 407–434 (2014).
4. Wess, J. Nakajima, K. & Jain, S. Novel designer receptors to probe GPCR signaling and physiology, *Trends Pharmacol. Sci.* **34,** 385–392 (2013).
5. Schiffmann, D. & Schlatter, J. Genotoxicity and cell transformation studies with sorbates in Syrian hamster embryo fibroblasts, *Food Chem. Toxicol.* **30,** 669–672 (1992).
6. Schlatter, J. *et al.* The potential genotoxicity of sorbates: effects on cell cycle in vitro in V79 cells and somatic mutations in Drosophila, *Food Chem. Toxicol.* **30,** 843–851 (1992).
7. Walker, R. Toxicology of sorbic acid and sorbates, *Food Addit Contam* **7,** 671–676 (1990).
8. Lück, E. Food applications of sorbic acid and its salts, *Food Addit Contam* **7,** 711–715 (1990).
9. Kenakin, T. Collateral efficacy in drug discovery: taking advantage of the good (allosteric) nature of 7TM receptors, *Trends Pharmacol. Sci.* **28,** 407–415 (2007).
10. Kenakin, T. P. Biased signalling and allosteric machines: new vistas and challenges for drug discovery, *Br. J. Pharmacol.* **165,** 1659–1669 (2012).
11. Farrell, M. S. & Roth, B. L. Pharmacosynthetics: Reimagining the pharmacogenetic approach, *Brain Res.* **1511,** 6–20 (2013).
12. Alvarez-Curto, E. *et al.* Developing chemical genetic approaches to explore G protein-coupled receptor function: validation of the use of a receptor activated solely by synthetic ligand (RASSL), *Mol. Pharmacol.* **80,** 1033–1046 (2011).
13. Hutchinson, L. & Kirk, R. High drug attrition rates--where are we going wrong?, *Nat Rev Clin Oncol* **8,** 189–190 (2011).
14. Martin, J. Addressing attrition in early drug discovery by label-free methodologies: receptor pharmacology in native cells. *Int Drug Discov,* 38–45 (2010).
15. McKim, J. M. Building a tiered approach to in vitro predictive toxicity screening: a focus on assays with in vivo relevance, *Comb. Chem. High Throughput Screen.* **13,** 188–206 (2010).
16. Moreno, L. & Pearson, A. D. J. How can attrition rates be reduced in cancer drug discovery?, *Expert Opin Drug Discov* **8,** 363–368 (2013).
17. Nakajima, K.-i. & Wess, J. Design and functional characterization of a novel, arrestin-biased designer G protein-coupled receptor, *Mol. Pharmacol.* **82,** 575–582 (2012).
18. Fenno, L. Yizhar, O. & Deisseroth, K. The development and application of optogenetics, *Annu. Rev. Neurosci.* **34,** 389–412 (2011).
19. Levitz, J. *et al.* Optical control of metabotropic glutamate receptors, *Nat. Neurosci.* **16,** 507–516 (2013).

Section III

Chapter 4: Free fatty acid receptor 1

Prologue

As detailed in the introductory section, free fatty acids (FFAs) are lipids and play essential roles as metabolic energy carrier but they also act as components of biological structures such as membranes[1,2]. The physiological effects of FFAs were long reduced to their direct and indirect function in metabolic assembly and dismantling, however, this conception does not explain all effects of FFAs on the host organism. It was found that a group of G protein-coupled receptors is targeted by FFAs, from which the former orphan G protein-coupled receptor GPR40 is activated by medium to long chain fatty acids and was subsequently renamed to FFA1[3–5]. FFA1 is part of the FFA receptor family that to date count four members (FFA1-4) and is abundantly expressed on pancreatic β-cells but was also found on enteroendocrine gut cells, in some brain regions and osteoclasts[6–11]. From these, presence of FFA1 on pancreatic β-cells attracted most interest and was rapidly associated with the previously recognized effect of enhanced glucose-stimulated insulin-secretion (GSIS) in the presence of fatty acids[4]. This resulted in the development of FFA1 receptor small molecule agonists, from which TAK-875/fasiglifam reached late stage clinical trials but was unexpectedly terminated in December 2013 because of unacceptable risk to benefit potential[12–15]. Beside the favorable effects of FFAs, also detrimental effects are frequently reported[16]. While acute elevation of free fatty acid blood levels enhances GSIS, long term elevation causes β-cell dysfunction and is referred to as (gluco)lipotoxicity[6,16]. Although (gluco)lipotoxicity is a well described phenomenon and the link to the presence of high plasma levels of fatty acids is well-established knowledge, the involvement of the FFA1 receptor was subject of intense debate[16]. *Steinberg et al.* proposed that detrimental effects of FFA on pancreatic function is mediated by the FFA1 receptor. By inducing FFA1-mediated insulin hypersecretion, the FFA1 receptor would be responsible for hyperinsulinemia-induced insulin resistance[17]. However, others could demonstrate that the damaging impact of FFA on the host metabolism is not mediated by the FFA1 receptor[18–21].

In the first publication of this chapter, we corroborate the beneficial FFA1-mediated effects of non-esterified fatty acids (NEFA) and strengthen an FFA1-independent mechanism of β-cell death. Furthermore, we report that FFA1 activation counteracts the detrimental effects of NEFAs on β-cell survival. In addition, we explored genetic variations of FFA1 with regard to their influence on insulin secretion to NEFA stimulation.

The second paper focusses on a methodological aspect of FFA1-related research. A prerequisite of meaningful data on physiological function of distinct receptors is the knowledge about their tissue or cellular distribution and the determination of their expression level. Both are frequently studied using antibody-dependent western blotting detection techniques. Although much effort has been made to develop PCR-based methods, protein determination using antibody-relying techniques is still routinely used[22]. Conclusions based on results on defined localization of certain proteins must be correct in order to allow for the generation of accurate working hypotheses. Good-quality techniques and methods are essential prerequisites to drive and develop scientific ideas in general. Therefore, in drug research, more attention should be drawn to the correct evaluation of both the preliminary results (target localization) as well as target characterization such as the investigation of physiological roles of certain targets[23]. Both these factors are highlighted in the two following publications.

While FFA1 expression in β-cells is well described and thoroughly associated with a specific physiological function[4,18–21], the findings of FFA1 on other cell types and tissues must be questioned either because the results are contradictory or their evidential basis is low[2,6]. Some reports rely on the measurement of mRNA level (RT-PCR), which is a mediocre indicator of real expression levels since translation and functional expression is intricately regulated by a variety of cellular systems[22]. However, even the use of "specific" antibodies to detect receptor amounts on a protein level become controvert with the second publication in this chapter. Therein, we checked commonly used and commercially available antibodies against the FFA1 receptor protein for their suitability to detect and determine receptor level, compared the results with RT-PCR data, which is another frequently used method to determine expression, and question the significance of FFA1 receptor expression data derived from immunostaining techniques.

References

1. Stoddart, L. A. Smith, N. J. & Milligan, G. International Union of Pharmacology. LXXI. Free fatty acid receptors FFA1, -2, and -3: pharmacology and pathophysiological functions, *Pharmacol. Rev.* **60,** 405–417 (2008).
2. Offermanns, S. Free fatty acid (FFA) and hydroxy carboxylic acid (HCA) receptors, *Annu. Rev. Pharmacol. Toxicol.* **54,** 407–434 (2014).
3. Briscoe, C. P. *et al.* The orphan G protein-coupled receptor GPR40 is activated by medium and long chain fatty acids, *J. Biol. Chem.* **278,** 11303–11311 (2003).
4. Itoh, Y. *et al.* Free fatty acids regulate insulin secretion from pancreatic beta cells through GPR40, *Nature* **422,** 173–176 (2003).
5. Kotarsky, K. Nilsson, N. E. Flodgren, E. Owman, C. & Olde, B. A human cell surface receptor activated by free fatty acids and thiazolidinedione drugs, *Biochemical and Biophysical Research Communications* **301,** 406–410 (2003).

6. Mancini, A. D. & Poitout, V. The fatty acid receptor FFA1/GPR40 a decade later: how much do we know?, *Trends Endocrinol. Metab.* **24,** 398–407 (2013).

7. Mieczkowska, A. Baslé, M. F. Chappard, D. & Mabilleau, G. Thiazolidinediones induce osteocyte apoptosis by a G protein-coupled receptor 40-dependent mechanism, *J. Biol. Chem.* **287,** 23517–23526 (2012).

8. Edfalk, S. Steneberg, P. & Edlund, H. Gpr40 is expressed in enteroendocrine cells and mediates free fatty acid stimulation of incretin secretion, *Diabetes* **57,** 2280–2287 (2008).

9. Liou, A. P. *et al.* The G-protein-coupled receptor GPR40 directly mediates long-chain fatty acid-induced secretion of cholecystokinin, *Gastroenterology* **140,** 903–912 (2011).

10. Hirasawa, A. *et al.* Production and characterization of a monoclonal antibody against GPR40 (FFAR1; free fatty acid receptor 1), *Biochem. Biophys. Res. Commun.* **365,** 22–28 (2008).

11. Cartoni, C. *et al.* Taste preference for fatty acids is mediated by GPR40 and GPR120, *J. Neurosci.* **30,** 8376–8382 (2010).

12. Burant, C. F. *et al.* TAK-875 versus placebo or glimepiride in type 2 diabetes mellitus. A phase 2, randomised, double-blind, placebo-controlled trial, *The Lancet* **379,** 1403–1411 (2012).

13. Negoro, N. *et al.* Discovery of TAK-875: A Potent, Selective, and Orally Bioavailable GPR40 Agonist, *ACS Med Chem Lett* **1,** 290–294 (2010).

14. Kaku, K. Enya, K. Nakaya, R. Ohira, T. & Matsuno, R. Efficacy and safety of fasiglifam (TAK-875), a G protein-coupled receptor 40 agonist, in Japanese patients with type 2 diabetes inadequately controlled by diet and exercise: a randomized, double-blind, placebo-controlled, phase III trial, *Diabetes Obes Metab* (2015).

15. Lead GPR40 agonist bites the dust, *Nat Rev Drug Discov* **13,** 91 (2014).

16. Poitout, V. *et al.* Glucolipotoxicity of the pancreatic beta cell, *Biochim. Biophys. Acta* **1801,** 289–298 (2010).

17. Steneberg, P. Rubins, N. Bartoov-Shifman, R. Walker, M. D. & Edlund, H. The FFA receptor GPR40 links hyperinsulinemia, hepatic steatosis, and impaired glucose homeostasis in mouse, *Cell Metab.* **1,** 245–258 (2005).

18. Latour, M. G. *et al.* GPR40 is necessary but not sufficient for fatty acid stimulation of insulin secretion in vivo, *Diabetes* **56,** 1087–1094 (2007).

19. Kebede, M. *et al.* The fatty acid receptor GPR40 plays a role in insulin secretion in vivo after high-fat feeding, *Diabetes* **57,** 2432–2437 (2008).

20. Lan, H. *et al.* Lack of FFAR1/GPR40 does not protect mice from high-fat diet-induced metabolic disease, *Diabetes* **57,** 2999–3006 (2008).

21. Tan, C. P. *et al.* Selective small-molecule agonists of G protein-coupled receptor 40 promote glucose-dependent insulin secretion and reduce blood glucose in mice, *Diabetes* **57,** 2211–2219 (2008).

22. Pascal, L. E. *et al.* Correlation of mRNA and protein levels: cell type-specific gene expression of cluster designation antigens in the prostate, *BMC Genomics* **9,** 246 (2008).

23. Smith, C. Drug target validation: Hitting the target, *Nature* **422,** 341, 343, 345 passim (2003).

Reevaluation of Fatty Acid Receptor 1 as a Drug Target for the Stimulation of Insulin Secretion in Humans

Robert Wagner,[1,2] Gabriele Kaiser,[1] Felicia Gerst,[1,2] Elisabeth Christiansen,[4] Maria E. Due-Hansen,[4] Manuel Grundmann,[3] Fausto Machicao,[1,2] Andreas Peter,[1,2] Evi Kostenis,[3] Trond Ulven,[4] Andreas Fritsche,[1,2] Hans-Ulrich Häring,[1,2] and Susanne Ullrich[1,2]

The role of free fatty acid receptor 1 (FFAR1/GPR40) in glucose homeostasis is still incompletely understood. Small receptor agonists stimulating insulin secretion are undergoing investigation for the treatment of type 2 diabetes. Surprisingly, genome-wide association studies did not discover diabetes risk variants in *FFAR1*. We reevaluated the role of FFAR1 in insulin secretion using a specific agonist, FFAR1-knockout mice and human islets. Nondiabetic individuals were metabolically phenotyped and genotyped. In vitro experiments indicated that palmitate and a specific FFAR1 agonist, TUG-469, stimulate glucose-induced insulin secretion through FFAR1. The proapoptotic effect of chronic exposure of β-cells to palmitate was independent of FFAR1. TUG-469 was protective, whereas inhibition of FFAR1 promoted apoptosis. In accordance with the proapoptotic effect of palmitate, in vivo cross-sectional observations demonstrated a negative association between fasting free fatty acids (NEFAs) and insulin secretion. Because NEFAs stimulate secretion through FFAR1, we examined the interaction of genetic variation in *FFAR1* with NEFA and insulin secretion. The inverse association of NEFA and secretion was modulated by rs1573611 and became steeper for carriers of the minor allele. In conclusion, FFAR1 agonists support β-cell function, but variation in *FFAR1* influences NEFA effects on insulin secretion and therefore could affect therapeutic efficacy of FFAR1 agonists. ***Diabetes*** **62:2106–2111, 2013**

Free fatty acids (also called nonesterified fatty acids [NEFAs]) regulate insulin secretion in β-cells. An acute increase in NEFA potentiates glucose-induced insulin secretion, an effect mediated by free fatty acid receptor 1 (FFAR1; formerly G-protein–coupled receptor 40 [GPR40]) (1–3). Targeting FFAR1 with specific agonists is a promising way of enhancing insulin secretion in patients with type 2 diabetes and results from clinical phase 2 trials have already appeared (4).

Previously, we also described small compounds that stimulate insulin secretion as selective FFAR1 agonists (5,6). For this reason, and because of its exceptionally high expression in β-cells, *FFAR1* would be an ideal candidate gene to associate with diabetes and insulin secretion. Surprisingly, from the 53 glycemic trait–related genes hitherto discovered in genome-wide association studies, none is located in or near *FFAR1* (7).

In contrast to the stimulatory effect of an acute increase in NEFA, long-term exposure of insulin-secreting cells to NEFA is believed to cause a reduction in β-cell mass attributable to increased apoptosis (8–10). In humans, several studies demonstrated reduced insulin secretion after prolonged exposure to NEFAs (11,12), but these findings were not unequivocal. The effect seemed to depend on the metabolic status or the individual predisposition of tested individuals (13,14). Animal studies suggested that the deleterious effect of prolonged NEFA elevation is independent of FFAR1 activation, because mice deficient in FFAR1 were not protected against high-fat diet–induced glucose intolerance (15).

The current study uses a translational approach to examine the role of FFAR1 in the Janus-faced effect of NEFAs on β-cell function. First, we analyzed effects of a synthetic FFAR1 agonist (TUG-469) and an antagonist (TUG-761) on insulin secretion and apoptosis. Second, we analyzed a precisely phenotyped human study population to answer the question of how NEFAs relate to insulin secretion and whether it is influenced by common variation in the *FFAR1* gene.

RESEARCH DESIGN AND METHODS

Culture and treatment of islets and insulin-secreting cells. Human islets were cultured in CMRL1066 medium (Biochrom, Berlin, Germany) containing 5.5 mmol/L glucose supplemented with 2 mmol/L L-glutamine, 10 mmol/L Hepes, and 10% FCS (Biochrom). Human islets were provided through the Juvenile Diabetes Research Foundation award 31-2008-413 to the European Consortium for Islet Transplantation (Basic Research program), and their use was approved by the local Ethics Committee of the University Hospital, Tübingen, Germany (533/2010BO2). Preparations of mouse islets from wild-type (WT) and FFAR1 knockout (KO) littermates and preparations of single cells are described in the Supplemental Materials (16). All animal experiments were performed in accordance with the accepted standard of human care of animals and were approved by the local Animal Care and Use Committee. INS-1E cells were cultured as previously described (17).

Isolation of mouse islets and preparation of single islet cells. Islets were isolated from WT and FFAR1 littermates by collagenase digestion (3 mg in 3 mL PBS) at 37°C for 9 min. The islets were collected under a dissecting microscope and were sedimented twice through sterile culture medium and cultured overnight in nonadhesive Petri dishes. Cells were prepared from the islets by digestion with 0.001% trypsin in PBS for 3–6 min. After centrifugation in culture medium, 20-μL drops of the cell suspension were distributed onto culture dishes and, after 1 h of adhesion time, the dish was filled with medium.

Measurement of insulin secretion. Isolated islets, after overnight culture, were preincubated for 1 h in modified Krebs-Ringer bicarbonate buffer containing the following (in mmol/L): 135 NaCl; 4.8 KCl; 1.2 $MgSO_4$; 1.2 NaH_2PO_4; 4.8 Na_2HPO_4; 5 $NaHCO_3$; 2.6 $CaCl_2$; 10 Hepes; 2.8 glucose; and 0.05% (weight/volume)

From the [1]University of Tübingen, Department of Internal Medicine IV, Division of Endocrinology, Diabetology, Vascular Medicine, Nephrology and Clinical Chemistry, Tübingen, Germany; the [2]Institute for Diabetes Research and Metabolic Diseases of the Helmholz Centre Munich at the University of Tübingen, Partner in the German Center for Diabetes Research, Tübingen, Germany; the [3]University of Bonn, Institute for Pharmaceutical Biology, Bonn, Germany; and the [4]University of Southern Denmark, Department of Physics, Chemistry and Pharmacy, Odense M, Denmark.

Corresponding author: Susanne Ullrich, susanne.ullrich@med.uni-tuebingen.de.

Received 11 September 2012 and accepted 28 January 2013.

DOI: 10.2337/db12-1249

This article contains Supplementary Data online at http://diabetes.diabetesjournals.org/lookup/suppl/doi:10.2337/db12-1249/-/DC1.

BSA (fatty acid–free; Sigma-Aldrich). Thereafter, batches of 10 islets/500 μL were incubated for 1 h in Krebs-Ringer bicarbonate buffer supplemented with test substances as indicated. INS-1E cells were cultured as previously described and insulin secretion was measured using the same Krebs-Ringer bicarbonate buffer as for islets (6). Insulin was measured by radioimmunoassay (Linco Research, St. Charles, MO).

Because the stimulation of FFAR1 by the small receptor agonists and by palmitate strongly depends on albumin, experiments with TUG-469 (19) and TUG-761 (5) were performed in the presence of low concentrations of BSA (0.05%) and serum (1.2%) (18). The palmitate concentration was adjusted accordingly. Palmitate (100 mmol/L in DMSO) was merged with FCS at concentrations of 1 and 6 mmol/L when 10% FCS was used. The solutions were further diluted when 1.2% FCS or 0.05% BSA were used.

Measurement of apoptotic cell death in mouse islet cells and INS-1E cells. Apoptosis was quantified by TUNEL staining of isolated mouse and human islet and INS-1E cells after 1–2 days of culture in the presence of test substances using a commercial kit (Roche Diagnostics GmbH, Mannheim, Germany). Nuclei were counterstained with 1 μmol/L TO-PRO3 (Invitrogen GmbH, Karlsruhe, Germany).

Measurement of glycemic traits in humans. We studied 2,110 nondiabetic subjects of European descent from the Tubingen Family Study. All participants gave written informed consent. The study was approved by the local ethics committee. This cross-sectional observational study enrolled individuals with increased risk of type 2 diabetes (positive family history, glucose intolerance, or overweight). All participants underwent an oral glucose tolerance test (OGTT). After an overnight fast, 75 g glucose was ingested at 8:00 A.M.; plasma glucose, insulin, C-peptide, and NEFA concentrations were determined after 0, 30, 60, 90, and 120 min.

Determination of blood parameters. Plasma glucose was determined using a glucose analyzer (glucose oxidase method; Yellow Springs Instruments, Yellow Springs, OH). NEFA concentrations were measured enzymatically (WAKO Chemicals, Neuss, Germany) using the ADVIA 1800 analyzer (Siemens Healthcare Diagnostics, Eschborn, Germany). Insulin and C-peptide were analyzed using the ADVIA Centaur XP immunoassay system.

Selection of tagging single nucleotide polymorphisms in humans. Based on publicly available data of the International HapMap Project derived from the Central European population (release 24, phase II, NCBI B36 assembly), we screened the *FFAR1* gene, located on chromosome 19q13.12, and 5 kb of both flanking regions in silico. Sixteen informative HapMap single nucleotide polymorphisms (SNPs) were present in this range, but only 13 SNPs were present with minor allele frequencies (MAFs) ≥0.05 (HapMap data). Nine SNPs were selected as tagging SNPs covering all other common SNPs within the locus, with $r^2 > 0.8$ (100% coverage) based on Tagger analysis using Haploview software.

Genotyping. DNA was extracted from peripheral blood after cell lysis, protein precipitation, and purification steps. All SNPs were genotyped using the MassARRAY platform from Sequenom (Sequenom, San Diego, CA). Genotype calling was unsuccessful for rs12459138 and Hardy-Weinberg equilibrium was rejected for rs10423648 ($P < 0.05$); therefore, seven SNPs went into analysis. MAFs and P for Hardy-Weinberg equilibrium are provided in Supplementary Table 1.

Calculations and statistics. Insulin sensitivity was assessed from glucose and insulin values during the five-point OGTT with the Matsuda index (19). Area under the curve (AUC) was calculated with the trapezoid method. Insulin secretion was estimated by $AUC_{0–30}$Insulin/$AUC_{0–30}$Glucose and $AUC_{0–30}$C-peptide/$AUC_{0–30}$Glucose. These two parameters, based on independent measurements and representing early insulin secretion, have been shown to provide an excellent assessment of genetically determined β-cell function from OGTT data (20).

To test genotype effects on β-cell function, linear regression models were constructed with parameters of β-cell function as outcome variables. Genotypes were coded as continuous variables with an additive model or with a dominant model in which heterozygous and homozygous carriers of the minor allele were pooled. Sex, age, BMI, and insulin sensitivity were used as covariates. Interaction with NEFA was tested by adding fasting NEFA and the interaction term fasting NEFA × SNP to the model. Variables with skewed distribution were transformed to their natural logarithm before linear regression analyses. To reduce the risk of type I error with multiple testing, the Bonferroni method was used, accepting 0.05/7 = 0.007 as the significance level for α, for which the null hypothesis is rejected. Effect sizes are displayed with the regression coefficient β.

For the insulin-based outcome parameter, the study was sufficiently powered (sensitivity 80%) to detect an effect size of 3.3% in the lowest MAF variant. The needed minimum effect size was 1.7% in the case of the highest MAF variant.

Power analysis was performed with Quanto V1.2.4 (21). All other statistical analyses were conducted with JMP10 (SAS).

RESULTS

A small synthetic agonist of FFAR1 mimics palmitate-induced insulin secretion but antagonizes palmitate-induced β-cell death. Effects of FFAR1 activation were examined with a synthetic receptor agonist, TUG-469. This small molecule concentration-dependently stimulated hGPR40/hFFAR1 (22). TUG-469 maximally stimulated insulin secretion of INS-1E cells at 3 and 10 μmol/L, whereas 1 μmol/L TUG-469 had no effect (Fig. 1*A*, *B*). That TUG-469 exerts insulinotropic effects through FFAR1 was corroborated in islets from FFAR1-deficient mice (Fig. 1*C*, *D*). Whereas glucose stimulated insulin secretion in FFAR1 KO mouse islets as efficiently as in islets of WT mice, the stimulatory effect of TUG-469 (10 μmol/L) was abrogated and the effect of palmitate (50 μmol/L) was significantly reduced in FFAR1-deficient islets compared with WT islets. Finally, in three human islet preparations, TUG-469 (3 μmol/L) robustly augmented insulin secretion (Fig. 1*E*).

Next, we examined whether prolonged exposure to the FFAR1 agonist affects cell survival. Although palmitate (50 μmol/L) for 1 day in culture medium containing 1.2% FCS significantly increased the amount of TUNEL-stained nuclei, TUG-469 (10 μmol/L) was without effect. Moreover, TUG-469 efficiently antagonized palmitate-induced β-cell death (Fig. 1*F*). The FFAR1 antagonist TUG-761 (10 μmol/L) significantly increased the percentage of TUNEL-positive cells. TUG-761, however, did not significantly augment palmitate-induced cell death (Fig. 1*G* and Supplementary Fig. 1). The role of FFAR1 for palmitate-induced β-cell death was further analyzed using WT and FFAR1 KO mice (Fig. 1*H*, *I*). In WT mouse islet cells, increased number of TUNEL-positive nuclei was detected after 2 days of culture in the presence of 10% FCS and 600 μmol/L, but not of 100 μmo/L, palmitate. In islet cell cultures of FFAR1 KO mice, palmitate already maximally induced cell death at 100 μmol/L, supporting the prosurvival role of FFAR1. In accordance, TUG-469 (3 μmol/L) abolished palmitate-induced apoptosis in WT, but not in FFAR1 KO, islet cells (Supplementary Fig. 3). Furthermore, the antagonist TUG-761 (10 μmol/L) increased the percentage of TUNEL-positive cells from WT, but not from FFAR1 KO, mice (Supplementary Fig. 3). Pharmacological efficacy of TUG-761 applied alone can be rationalized with the assumption that FFAR1 displays constitutive activity in vivo, a notion that is corroborated in FFAR1-HEK293 cells (Supplementary Fig. 1). These results suggest that FFAR1 agonists are suitable insulinotropic agents because they stimulate insulin secretion and counter the adverse effects on β-cell survival.

Characteristics of the human cohort and association of fasting NEFA with insulin secretion. Because physiological stimulation of FFAR1 is mediated by NEFA, including the major plasma fatty acids palmitate, stearate, oleate, and linoleate, the correlation of glucose-induced insulin secretion with plasma NEFA was evaluated in the cross-sectional Tubingen Family Study cohort (for basic cohort characteristics, see Table 1). Two independent secretion parameters, $AUC_{0–30}$Insulin/$AUC_{0–30}$Glucose and $AUC_{0–30}$C-peptide/$AUC_{0–30}$Glucose, associated negatively with fasting NEFA after adjustment for sex, age, BMI, and insulin sensitivity ($\beta = -0.12$, $P < 0.0001$, and $\beta = -0.09$, $P < 0.0001$, respectively).

Genetic variation in FFAR1 and its association with insulin secretion in humans. After adjusting for sex, age, BMI, and insulin sensitivity, one of seven tagging SNPs of FFAR1 was associated with either parameter of β-cell

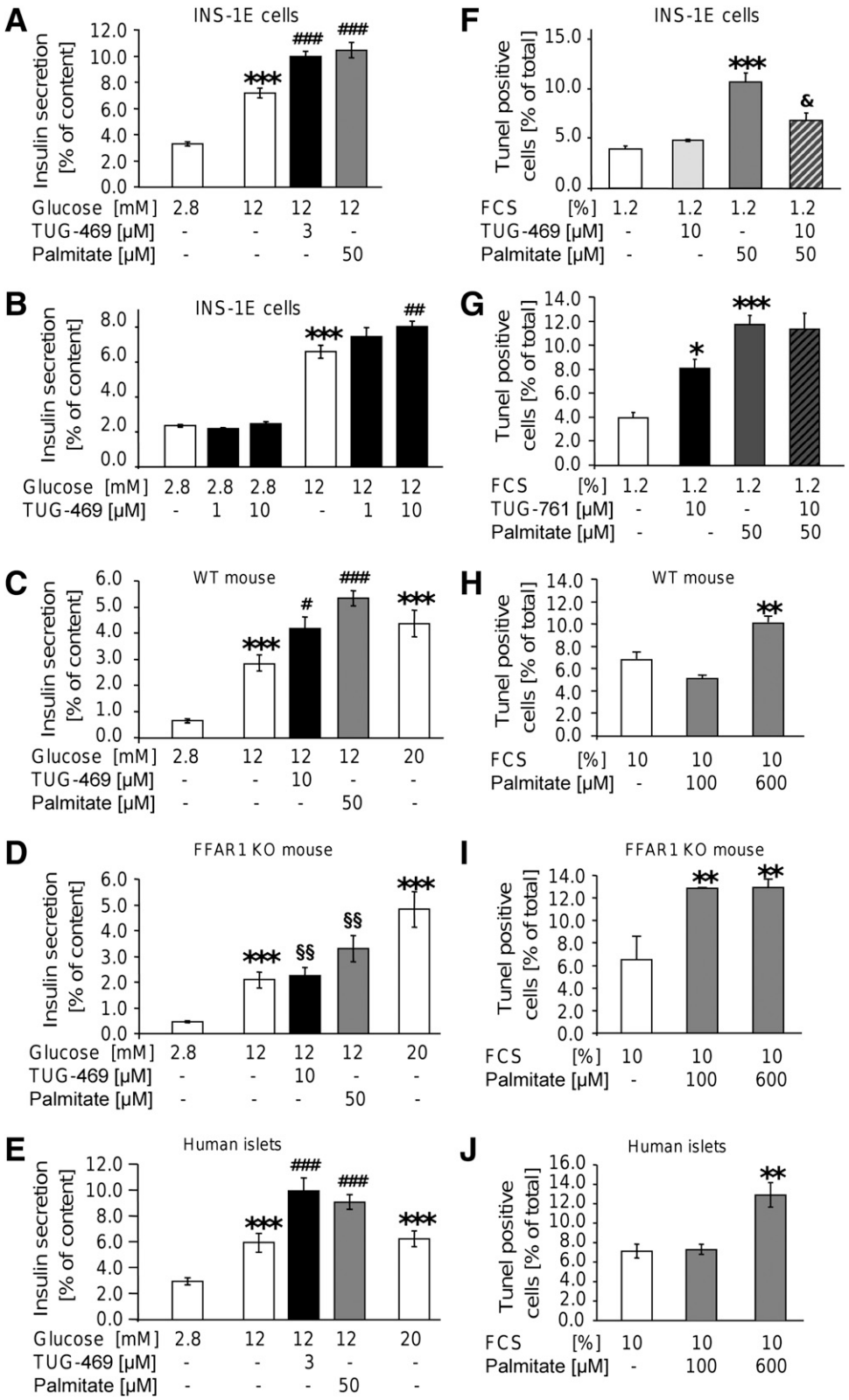

FIG. 1. FFAR1 contributes to palmitate-induced insulin secretion but not palmitate-induced β-cell death. INS-1E cells (*A*, *B*, *F*, *G*), mouse islets (*C*, *D*, *H*, *I*), and human islets (*E*, *J*) were incubated with test substances as indicated and described in RESEARCH DESIGN AND METHODS. Results are expressed as means ± SEM of $n = 4$ independent experiments. Statistical analysis was performed with ANOVA, followed by Newman-Keuls multiple comparison test as post hoc test. *$P < 0.05$, **$P < 0.01$, and ***$P < 0.001$ are significant in controls (first bar of each chart). #$P < 0.05$, ##$P < 0.01$, and ###$P < 0.001$ indicate significance in secretion at 12 mmol/L glucose. §§$P < 0.05$ indicates significance in secretion of WT mouse islets at the same condition. & indicates significance in palmitate-induced apoptosis.

TABLE 1
Basic demographic and metabolic characteristics of the study cohort

N = 1,401/709 (F/M)	Median (IQR)
Age (years)	38 (29–49)
BMI (kg/m^2)	27.8 (23.6–34.5)
Fasting glucose (mmol/L)	5.1 (4.8–5.4)
Postload (2-h) glucose (mmol/L)	6.2 (5.2–7.3)
Insulin sensitivity, Matsuda index (AU)	12.4 (7.3–20.4)
$AUC_{0–30}$Insulin/$AUC_{0–30}$Glucose	36.6 (23.5–56.8)
$AUC_{0–30}$C-peptide/$AUC_{0–30}$Glucose	188.8 (149.2–244.5)
Fasting NEFA (μmol/L)	561.0 (423.0–723.0)

F, female; M, male; AU, arbitrary units.

function, insulin, or C-peptide (Table 2; *P* value for SNP effects).

Given the physiological role of NEFA in the stimulation of insulin secretion through FFAR1, we analyzed the interaction of fasting NEFA and the investigated SNPs on insulin secretion. Significant interactions were found for both the insulin-based and C-peptide–based outcome parameter in rs1573611 (Table 2, first row). This implied that the regression coefficients (β) of the model explaining insulin secretion by NEFA levels were significantly different for each genotype after adjustment for sex, age, BMI, and insulin sensitivity. The negative slope of the regression line between fasting NEFA and $AUC_{0–30}$Insulin/$AUC_{0–30}$Glucose was more pronounced in carriers of the minor allele (Fig. 2; CC: $\beta = -0.061 \pm 0.03$; CT: $\beta = -0.19 \pm 0.04$; TT: $\beta = -0.23 \pm 0.09$). This has the consequence that carriers of the major allele of rs1573611 are protected at least to some extent from the negative effect of NEFAs on insulin secretion.

DISCUSSION

The current study provides evidence that effective stimulation of insulin secretion through FFAR1 in humans requires specific genetic and metabolic predispositions. Previously, a study analyzing two SNPs in *FFAR1* found clues for a possible association between genotypes and insulin secretion (23). However, no association between *FFAR1* and insulin secretion could be shown in genome-wide association studies for the SNPs rs387083, rs2301151, rs12975589, rs12462800, rs417030, and rs1573611 in up to 46,186 individuals (24). In agreement with the genome-wide association studies results, our analysis of seven tagging SNPs in *FFAR1* utilizing OGTT-based insulin secretion parameters could not unravel significant effects on insulin secretion either. Instead, we demonstrated that the inverse association between NEFAs and reduced insulin secretion is modulated by the genetic variation in rs1573611. This interaction was robustly significant and consistent for two independently measured secretion parameters (AUC of insulin and C-peptide). The SNP rs1573611 is located in the *FFAR1* locus, 341 bases upstream from the exon, pointing to a possible effect of the SNP on the modulation of FFAR1 transcription (Supplementary Fig. 2).

Our findings strongly suggest that FFAR1 activation does not mimic proapoptotic effects of palmitate, but that it mediates a protective effect on β cells in addition to the stimulation of insulin secretion. In line with our observation, it has been described previously that the protective effect of oleate is lost in FFAR1-deficient cells (25). Moreover, pharmacological inhibition of FFAR1 by TUG-761 induced apoptosis.

Chronically elevated NEFAs deteriorate insulin secretion in humans (14,26). This is a consequence of FFAR1-independent reduction of β-cell function, which overwhelms FFAR1-mediated stimulation of insulin secretion. The FFAR1-dependent change in the NEFA–insulin secretion regression slope could reflect different stimulatory potentials for NEFA-induced insulin secretion and different grades of β-cell protection against chronic noxious effects of NEFA.

These data also clearly demonstrate that the therapeutic efficacy of specific FFAR1 agonists could be subject to

TABLE 2
Association of common variants in *FFAR1* with insulin secretion and their interaction with fasting NEFA

SNP	Trait*	n		Mean ± SE†		P (SNP)‡	P (SNP × NEFA)§
rs1573611	Insulin	1,061/785/132	45.5 ± 1.02	46.3 ± 1.18	47.5 ± 3.11	0.921	**0.001**
	C-peptide	1,019/760/129	202.1 ± 2.5	208. ± 2.83	202.1 ± 7.61	0.378	**0.001**
rs387083	Insulin	956/826/215	46.4 ± 1.1	46.2 ± 1.25	43.7 ± 2.07	0.431	0.247
	C-peptide	923/795/208	205.5 ± 2.6	203.4 ± 2.8	202.6 ± 5.75	0.837	0.029
rs2301151	Insulin	1,288/614/91	45.9 ± 0.99	46.7 ± 1.32	42.9 ± 2.83	0.757	0.678
	C-peptide	1,243/590/89	204.4 ± 2.26	205.4 ± 3.31	195.6 ± 7.26	0.348	0.080
rs12975589	Insulin	567/997/428	44.7 ± 1.32	46.3 ± 1.09	47. ± 1.85	0.399	0.196
	C-peptide	553/958/410	201.9 ± 3.3	205.9 ± 2.65	203.8 ± 3.75	0.709	0.546
rs12462800	Insulin	1,763/222/7	46.3 ± 0.81	43. ± 2.49	67.2 ± 14.84	0.409	0.597
	C-peptide	1,697/217/7	204.8 ± 1.92	197.8 ± 5.57	273.5 ± 38.59	0.804	0.318
rs10422744	Insulin	690/957/348	47.4 ± 1.44	45.4 ± 1.07	44.9 ± 1.65	0.198	0.708
	C-peptide	668/918/338	205.3 ± 3.11	204.3 ± 2.66	202.3 ± 4.04	0.651	0.303
rs417030	Insulin	1,162/729/104	45.1 ± 0.94	46.4 ± 1.35	53.3 ± 4.25	0.530	0.744
	C-peptide	1,125/697/102	202.8 ± 2.34	205.1 ± 2.99	215.1 ± 8.95	0.622	0.538

*For each gene variation (SNP), an insulin-based ($AUC_{0–30}$Insulin/$AUC_{0–30}$Glucose) and a C-peptide–based ($AUC_{0–30}$C-peptide/$AUC_{0–30}$Glucose) secretion parameter was tested. †Mean of tested glycemic trait ± SE for the genotype with homozygous major allele, heterozygous variant, and homozygous minor allele, respectively. ‡Association of the SNP with insulin secretion. Adjusted for sex, age, BMI, and insulin sensitivity. §Association of the SNP × fasting NEFA interaction term with insulin secretion. Adjusted for sex, age, BMI, insulin sensitivity, and fasting NEFA. Bold values denote statistical significance.

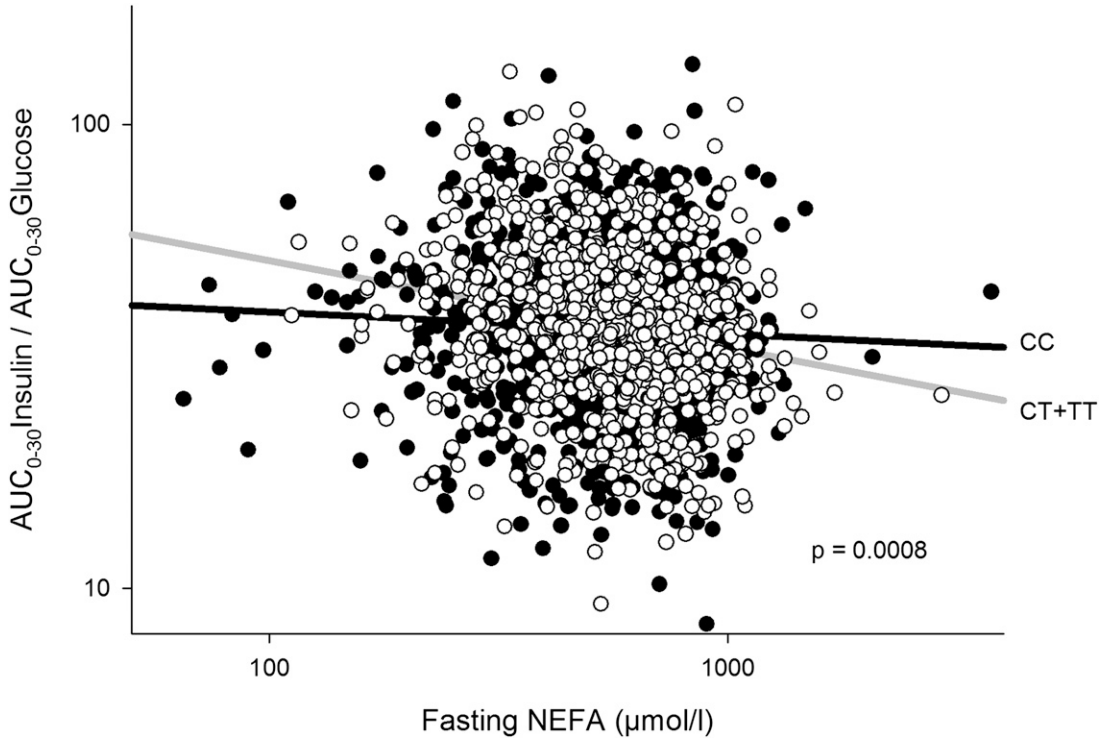

FIG. 2. Interaction of fasting NEFA (in µmol/L) with genotypes of rs1573611 on insulin secretion. Both axes are log-scaled. $AUC_{0–30}$Insulin/ $AUC_{0–30}$Glucose is adjusted for sex, age, BMI, and insulin sensitivity. Filled circles correspond to the CC genotype (homozygous major allele) and empty circles correspond to carriers of the T allele (CT and TT genotypes).

pharmacogenomic interactions. Genotype-dependent dose–response analysis of FFAR1 agonists would provide information about the individual efficacy of FFAR1 agonists in clinical trials.

The demonstration of an interaction between rs1573611 and NEFA shows for the first time that a frequent variant of *FFAR1* has a measurable effect on the biological function of the receptor in humans.

ACKNOWLEDGMENTS

The study was supported by DFG grants UL140/7-2 and GRK1302/1, by the German Federal Ministry of Education and Research (DLR01GI0925), and by the Danish Council for Independent Research, Technology, and Production (grant 09-070364).

No potential conflicts of interest relevant to this article were reported.

R.W. and S.U. researched data and wrote the manuscript. G.K., F.G., E.C., M.E.D.-H., M.G., F.M., A.P., and A.F. researched data and edited the manuscript. E.K., T.U., and H.-U.H. edited the manuscript and contributed to the discussion. R.W. is the guarantor of this work and, as such, had full access to all the data in the study and takes responsibility for the integrity of the data and the accuracy of the data analysis.

Parts of the study were previously presented in poster form at the 71st Scientific Sessions of the American Diabetes Association, San Diego, California, 24–28 June 2011.

The authors thank Sieglinde Haug (German Center for Diabetes Research at the University of Tübingen) and Elisabeth Metzinger (Department of Internal Medicine IV, University of Tübingen) for excellent technical help. The authors thank Claes B. Wollheim (University of Geneva, Switzerland) for providing INS-1E cells.

REFERENCES

1. Briscoe CP, Tadayyon M, Andrews JL, et al. The orphan G protein-coupled receptor GPR40 is activated by medium and long chain fatty acids. J Biol Chem 2003;278:11303–11311
2. Itoh Y, Kawamata Y, Harada M, et al. Free fatty acids regulate insulin secretion from pancreatic beta cells through GPR40. Nature 2003;422:173–176
3. Nolan CJ, Madiraju MS, Delghingaro-Augusto V, Peyot ML, Prentki M. Fatty acid signaling in the beta-cell and insulin secretion. Diabetes 2006;55 (Suppl 2):S16–S23
4. Burant CF, Viswanathan P, Marcinak J, et al. TAK-875 versus placebo or glimepiride in type 2 diabetes mellitus: a phase 2, randomised, double-blind, placebo-controlled trial. Lancet 2012;379:1403–1411
5. Christiansen E, Urban C, Grundmann M, et al. Identification of a potent and selective free fatty acid receptor 1 (FFA1/GPR40) agonist with favorable physicochemical and in vitro ADME properties. J Med Chem 2011; 54:6691–6703
6. Christiansen E, Urban C, Merten N, et al. Discovery of potent and selective agonists for the free fatty acid receptor 1 (FFA(1)/GPR40), a potential target for the treatment of type II diabetes. J Med Chem 2008;51:7061–7064
7. Scott RA, Lagou V, Welch RP, et al; DIAbetes Genetics Replication and Meta-analysis (DIAGRAM) Consortium. Large-scale association analyses identify new loci influencing glycemic traits and provide insight into the underlying biological pathways. Nat Genet 2012;44:991–1005
8. Maedler K, Spinas GA, Dyntar D, Moritz W, Kaiser N, Donath MY. Distinct effects of saturated and monounsaturated fatty acids on beta-cell turnover and function. Diabetes 2001;50:69–76
9. Sargsyan E, Bergsten P. Lipotoxicity is glucose-dependent in INS-1E cells but not in human islets and MIN6 cells. Lipids Health Dis 2011;10:115–121
10. Eitel K, Staiger H, Brendel MD, et al. Different role of saturated and unsaturated fatty acids in beta-cell apoptosis. Biochem Biophys Res Commun 2002;299:853–856
11. Paolisso G, Gambardella A, Amato L, et al. Opposite effects of short- and long-term fatty acid infusion on insulin secretion in healthy subjects. Diabetologia 1995;38:1295–1299

12. Carpentier A, Mittelman SD, Lamarche B, Bergman RN, Giacca A, Lewis GF. Acute enhancement of insulin secretion by FFA in humans is lost with prolonged FFA elevation. Am J Physiol 1999;276:E1055–E1066
13. Carpentier A, Mittelman SD, Bergman RN, Giacca A, Lewis GF. Prolonged elevation of plasma free fatty acids impairs pancreatic beta-cell function in obese nondiabetic humans but not in individuals with type 2 diabetes. Diabetes 2000;49:399–408
14. Kashyap S, Belfort R, Gastaldelli A, et al. A sustained increase in plasma free fatty acids impairs insulin secretion in nondiabetic subjects genetically predisposed to develop type 2 diabetes. Diabetes 2003;52:2461–2474
15. Lan H, Hoos LM, Liu L, et al. Lack of FFAR1/GPR40 does not protect mice from high-fat diet-induced metabolic disease. Diabetes 2008;57:2999–3006
16. Ranta F, Avram D, Berchtold S, et al. Dexamethasone induces cell death in insulin-secreting cells, an effect reversed by exendin-4. Diabetes 2006;55:1380–1390
17. Ullrich S, Berchtold S, Ranta F, et al. Serum- and glucocorticoid-inducible kinase 1 (SGK1) mediates glucocorticoid-induced inhibition of insulin secretion. Diabetes 2005;54:1090–1099
18. Christiansen E, Due-Hansen ME, Urban C, et al. Free fatty acid receptor 1 (FFA1/GPR40) agonists: mesylpropoxy appendage lowers lipophilicity and improves ADME properties. J Med Chem 2012;55:6624–6628
19. Matsuda M, DeFronzo RA. Insulin sensitivity indices obtained from oral glucose tolerance testing: comparison with the euglycemic insulin clamp. Diabetes Care 1999;22:1462–1470
20. Herzberg-Schäfer SA, Staiger H, Heni M, et al. Evaluation of fasting state-/oral glucose tolerance test-derived measures of insulin release for the detection of genetically impaired β-cell function. PLoS ONE 2010;5:e14194
21. Gauderman W, Morrison J. QUANTO 1.1: A computer program for power and sample size calculations for genetic-epidemiology studies. Available at: http://hydra.usc.edu/gxe/
22. Christiansen E, Due-Hansen ME, Urban C, et al. Structure-activity study of dihydrocinnamic acids and discovery of the potent FFA1 (GPR40) agonist TUG-469. ACS Med Chem Lett 2010;1:345–349
23. Kalis M, Levéen P, Lyssenko V, Almgren P, Groop L, Cilio CM. Variants in the FFAR1 gene are associated with beta cell function. PLoS ONE 2007;2:e1090
24. Dupuis J, Langenberg C, Prokopenko I, et al.; DIAGRAM Consortium; GIANT Consortium; Global BPgen Consortium; Anders Hamsten on behalf of Procardis Consortium; MAGIC investigators. New genetic loci implicated in fasting glucose homeostasis and their impact on type 2 diabetes risk. Nat Genet 2010;42:105–116
25. Zhang Y, Xu M, Zhang S, et al. The role of G protein-coupled receptor 40 in lipoapoptosis in mouse beta-cell line NIT-1. J Mol Endocrinol 2007;38:651–661
26. Salgin B, Ong KK, Thankamony A, Emmett P, Wareham NJ, Dunger DB. Higher fasting plasma free fatty acid levels are associated with lower insulin secretion in children and adults and a higher incidence of type 2 diabetes. J Clin Endocrinol Metab 2012;97:3302–3309

SUPPLEMENTARY DATA

Supplementary Table 1. Minor allele frequency (MAF) and p for Hardy-Weinberg equilibrium (HWE p) of genotyped SNPs. The SNP rs10423648 failed Hardy-Weinberg equilibrium, and therefore was not analyzed in the genotype-phenotype association study.

SNP	MAF	HWE (p)
rs1573611	0.27	0.51
rs387083	0.31	0.08
rs2301151	0.20	0.12
rs12975589	0.46	0.71
rs12462800	0.06	0.93
rs10423648	0.06	0.02*
rs10422744	0.41	0.54
rs417030	0.24	0.70

SUPPLEMENTARY DATA

Supplementary Figure 1. Concentration-dependent effects of TUG-469 and TUG-761 in hFFAR1 expressing HEK cells. HEK293 expressing the human FFAR1 receptor were stimulated with the indicated concentrations of FFAR1-agonist TUG-469 and FFAR1-antagonist TUG-761 and accumulation of IP1 (inositol-1-phosphate) as measure of G-protein coupled PLC activity was recorded (for method see ref. S1). Untransfected HEK cells and HEK cells transfected with FFAR2 or FFAR3 respond neither to TUG-469 nor to TUG761 (data not shown). S1. Schmidt J, Smith NJ, Christiansen E, et al. Selective orthosteric free fatty acid receptor 2 (FFA2) agonists: Identification of the structural and chemical requirements for selective activation of FFA2 versus FFA3. J Biol Chem. 2011;286:10628-40.

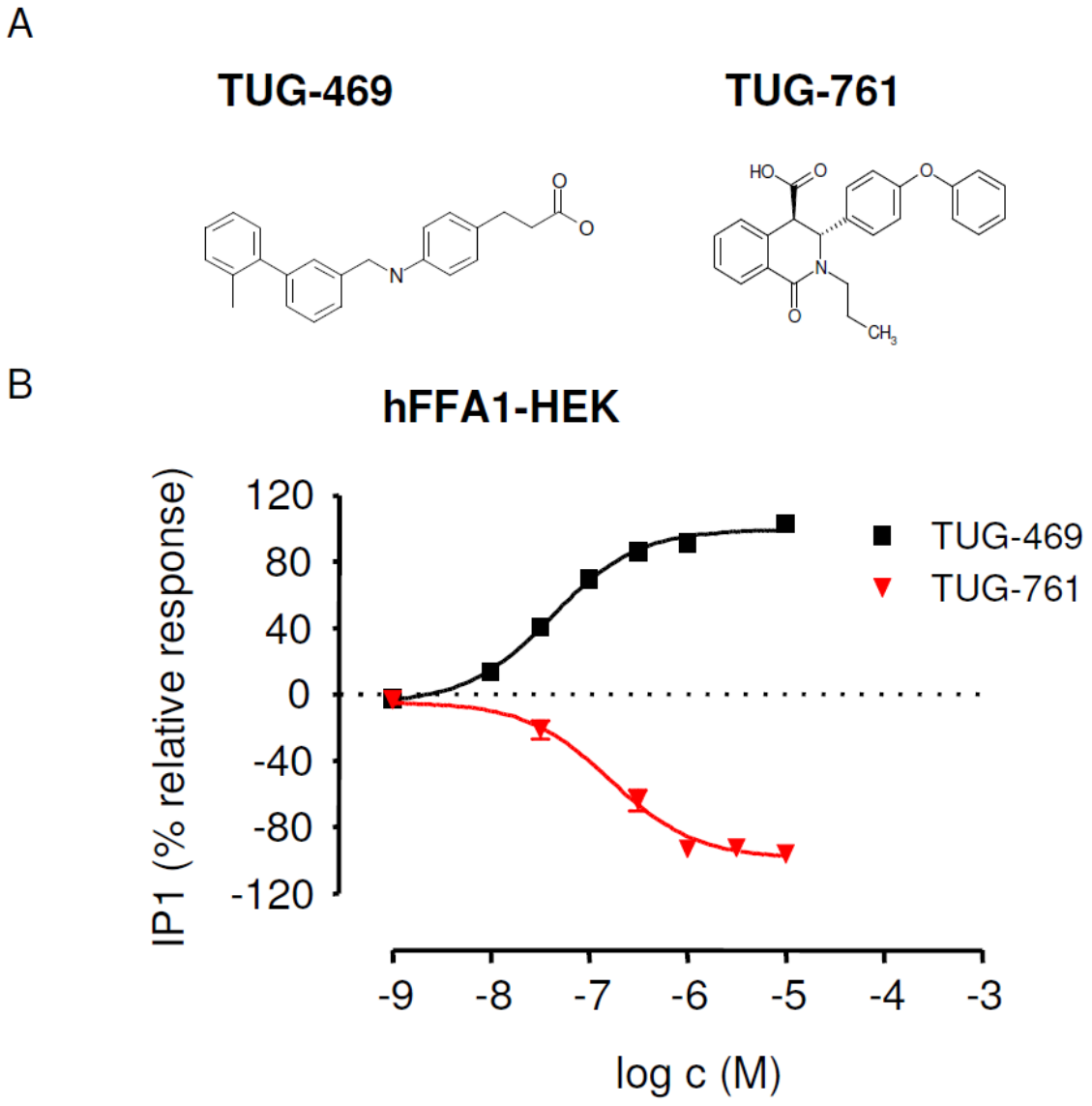

SUPPLEMENTARY DATA

Supplementary Figure 2. Localization of the SNP rs1573611 in the *FFAR1* locus as downloaded from http://genome.ucsc.edu/index.html. ChIP-Seq analyses of transcription-factor binding and digital DNAse hypersensitivity cluster data indicate that rs1573611 is situated amidst an important cis-regulatory region (Encode project consortium, A user's guide to the encyclopedia of DNA elements (ENCODE). PLoS Biol 2011; 9(4):e1001046).

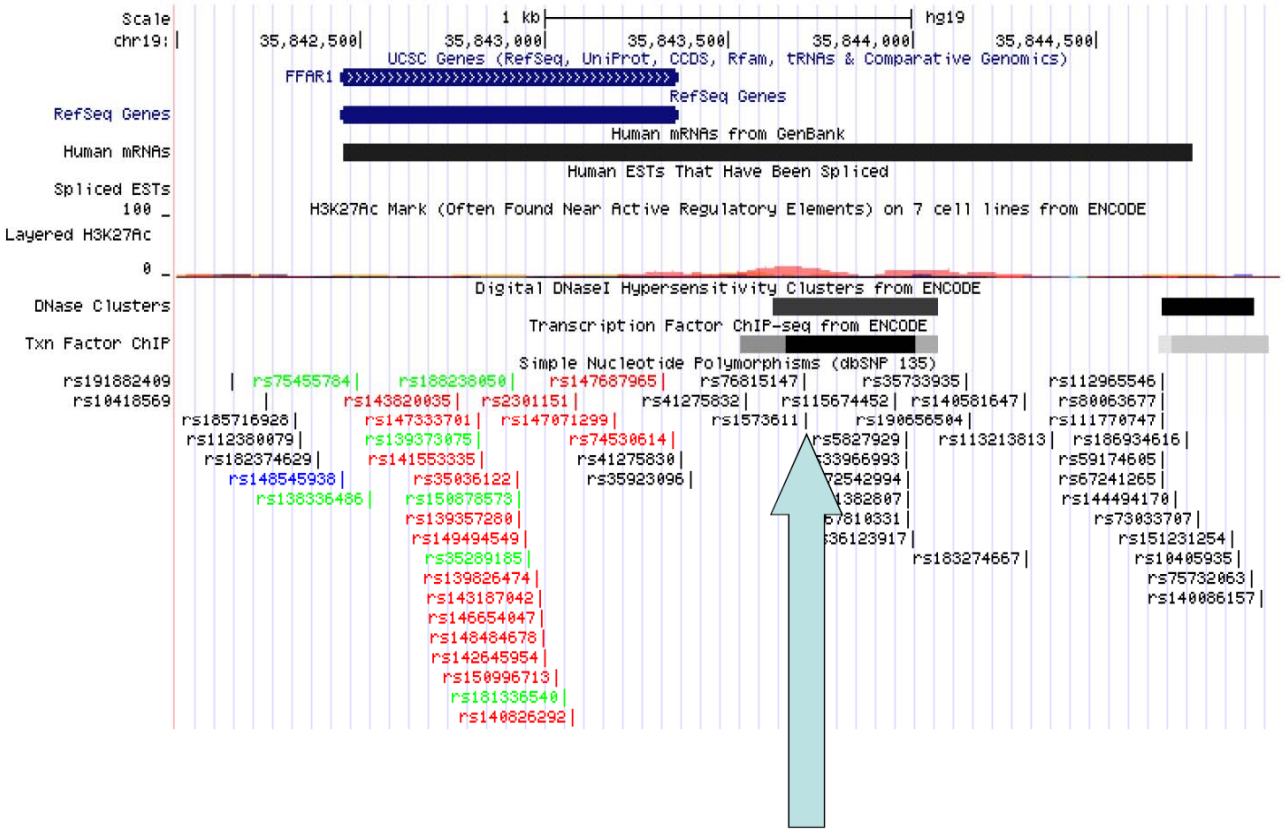

SUPPLEMENTARY DATA

Supplementary Figure 3. FFAR1 protects against palmitate-induced beta-cell death. WT (A) and FFAR1-KO (B) mouse islet cells were incubated with test substances as indicated and described under Research Design and Methods. Results are expressed as means ± SEM of n = 3 - 5 independent experiments. * ($p<0.05$) indicates significance to control culture condition in the presence of 1.2% FCS; § ($p<0.05$) indicates significance to palmitate.

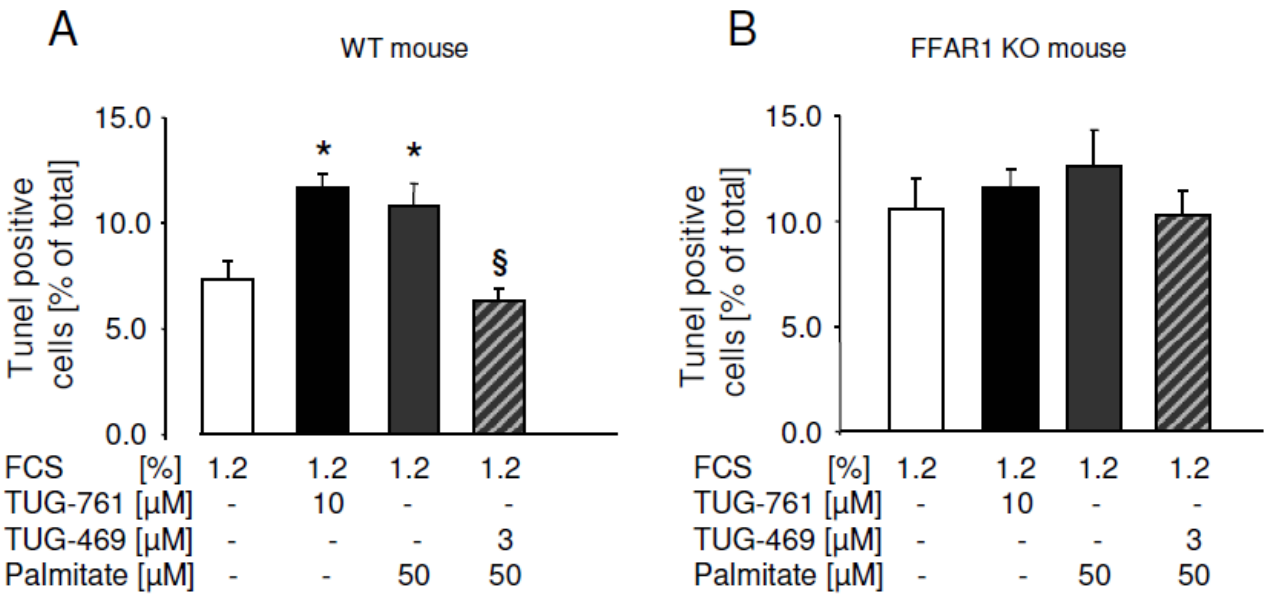

Diabetologia
DOI 10.1007/s00125-014-3161-8

SHORT COMMUNICATION

Detection of free fatty acid receptor 1 expression: the critical role of negative and positive controls

Charlott-Amelie Teutsch · Madhura Panse · Manuel Grundmann · Gabriele Kaiser · Evi Kostenis · Hans-Ulrich Häring · Susanne Ullrich

Received: 14 October 2013 / Accepted: 18 December 2013

Abstract
Aims/hypothesis Adequate evaluation of protein expression is a crucial prerequisite for functional studies. Commonly used strategies comprise detection of proteins by specific antibodies using western blotting and immunohistochemical staining, or detection of mRNA by in situ hybridisation and RT-PCR. We evaluated the tools for the detection of free fatty acid receptor 1 (FFAR1) expression.
Methods Commercially available antibody preparations were used to detect endogenous expression of the FFAR1 receptor and this was compared with cell preparations deficient or overexpressing the mouse or human receptor. Concentrations of mRNA were evaluated by RT-PCR.
Results All insulin-secreting cells, INS-1E, Min6 and mouse islets showed specific expression of *Ffar1* at the mRNA level. However, none of the commercially available antibodies specifically detected rat, mouse or human FFAR1.
Conclusions/interpretation Proper positive and negative controls are an important prerequisite for the evaluation of FFAR1 expression.

Keywords Antibodies · FFAR1/GPR40 · *Ffar1* expression · RT-PCR · Western blotting

Abbreviations

DMR	Dynamic mass redistribution
FFAR1	Free fatty acid receptor 1
GAPDH	Glyceraldehyde-3-phosphate dehydrogenase
HEK	Human embryonic kidney 293
HRP	Horseradish peroxidase
IGF1R	IGF-1 receptor
PKB	Protein kinase B
TBS	TRIS-buffered saline
TUG-488	3-(4-((2-(Cyanomethyl)phenyl)ethynyl) phenyl)propanoic acid
YFP	Yellow fluorescent protein

Introduction

Free fatty acid receptor 1 (FFAR1; also known as G-protein-coupled receptor 40), encoded by *Ffar1*, is differentially expressed in organs, with a particularly high level of expression in the islets of Langerhans, where the receptor plays a stimulatory role in glucose-induced insulin secretion [1]. To understand the role and function of FFAR1, especially during chronic exposure of beta cells to fatty acids, as occurs in obesity, detection of functional receptors at the plasma membrane is an important requirement. Repetitive or continuous stimulation has been found to result in receptor downregulation and internalisation which may impair receptor function [2, 3]. Indeed, receptor desensitisation to agonists after initial

Electronic supplementary material The online version of this article (doi:10.1007/s00125-014-3161-8) contains peer-reviewed but unedited supplementary material, which is available to authorised users.

C.-A. Teutsch · M. Panse · G. Kaiser · H.-U. Häring · S. Ullrich (✉)
Division of Endocrinology, Diabetology, Vascular Medicine, Nephrology and Clinical Chemistry, Department of Internal Medicine IV, University of Tübingen, Otfried-Müller-Str. 10, 72076 Tübingen, Germany
e-mail: susanne.ullrich@med.uni-tuebingen.de

M. Grundmann · E. Kostenis
Institute of Pharmaceutical Biology, University of Bonn, Bonn, Germany

G. Kaiser · H.-U. Häring · S. Ullrich
Institute for Diabetes Research and Metabolic Diseases of the Helmholtz Center Munich at the University of Tübingen (IDM), Partner in the German Center for Diabetes Research (DZD), Tübingen, Germany

Published online: 26 January 2014

stimulation has also been seen for FFAR1 [2]. Consequently, in the case of excessive stimulation, receptor inactivation rather than receptor activation may account for the observed cellular effects. In a recent publication it was suggested that exendin-4 reduced FFAR1 levels using commercially available antibodies against FFAR1 [4]. Previously, another study showed FFAR1 protein expression in mouse brain, although mRNA analysis does not support the idea of *Ffar1* expression in mouse brain [5].

Here, we evaluated the expression of FFAR1 in insulin-secreting cells by RT-PCR and western blotting using commercially available antibodies. We found that all antibodies tested so far are of limited use for FFAR1 protein detection, and appropriate positive and negative controls should be used for evaluation.

Methods

INS-1E cell culture and islet isolation INS-1E cells were kindly provided by C. B. Wollheim (University of Geneva, Geneva, Switzerland). INS-1E and Min6 cells were cultured under standard culture conditions. Mouse islets were isolated by collagenase digestion and cultured overnight under standard conditions [6].

Western blotting Cells and islets were lysed in buffer containing (in mmol/l): 125 NaCl, 10 EDTA, 10 $Na_4P_2O_7$, 10 NaF, 1 Na_2VO_4, 2 phenylmethylsulfonyl fluoride, 25 HEPES, pH 7.3, supplemented with 0.1% SDS, 0.5% sodium deoxycholate, 1% Triton X-100 and protease inhibitors. A soluble and a crude membrane fraction of INS-1E cells were prepared by ultrasonic homogenisation in buffer containing (in mmol/l): 10 TRIS/HCl, pH 7.5, 5 EDTA and protease inhibitors, and subsequent centrifugation (13,000 *g* for 30 min) at 4°C [7]. Protein kinase B (PKB) and IGF-1 receptor (IGF1R) were used as markers for soluble and transmembrane proteins, respectively. Proteins were transferred onto nitrocellulose membranes (Whatman, Dassel, Germany), and unspecific binding was reduced by blocking the membranes for 1 h at room temperature. Blocking solutions contained (in mmol/l):137 NaCl, 20 TRIS and 1.5% Tween-20 supplemented with either 5% milk or 2.5% BSA; alternatively: 150 NaCl, 50 TRIS, 5 EDTA, 0.05% Triton and 0.25% gelatin. After blocking, the membranes were incubated with the primary antibodies overnight at 4°C, and with the secondary antibody for 1 h at room temperature. FFAR1 antibodies (diluted 1:500 and 1:1,000 with TRIS-buffered saline [TBS]–Tween-20 buffer containing 5% BSA) were purchased from Abcam (no. EP4632, Cambridge, UK), Aviva (no. AVARP08008, London, UK) and Santa Cruz (no. 28416, Dallas, TX, USA). Antibodies against PKB and glyceraldehyde-3-phosphate dehydrogenase (GAPDH) were purchased from Cell Signaling (Danvers, MA, USA), and IGF1R antibodies were purchased from Santa Cruz. The horseradish peroxidase (HRP)-conjugated secondary antibodies (diluted 1:2,000 with TBS–Tween-20 buffer containing 5% milk) were purchased from Life Technologies (Carlsbad, CA, USA). HRP activity was detected using a solution containing (in

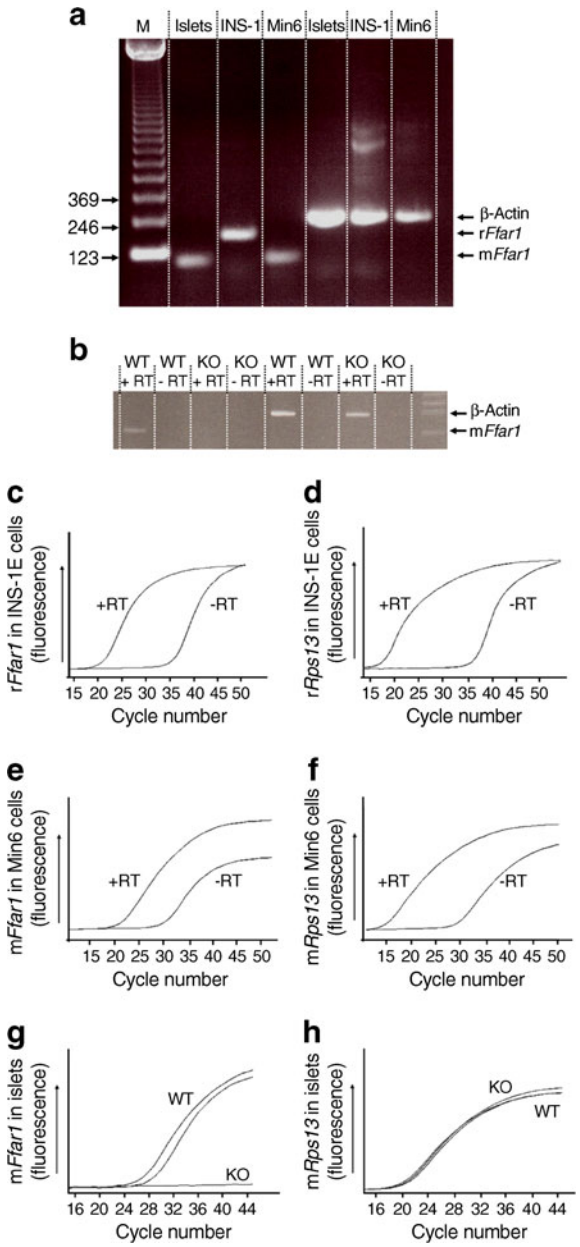

Fig. 1 Detection of rat (r) and mouse (m) *Ffar1* by RT-PCR. (**a**) PCR products of *Ffar1* and β-actin as housekeeping control from mouse islets, INS-1E (INS-1) and Min6 cells. (**b**) PCR products of *Ffar1* and β-actin as housekeeping control from wild-type (WT) and FFAR1-deficient (KO) mice. (**c**–**h**) Amplification curves of semiquantitative RT-PCR of *Ffar1* and *Rps13* as housekeeping control, respectively, for (**c** and **d**) INS-1E, (**e** and **f**) Min6, (**g** and **h**) WT (2 reactions) and KO (1 reaction) mouse islets. (**a**, **g** and **h**) Reactions after RT are shown. (**b**–**f**) Reactions were performed with (+) or without (−) RT. Shown are representative experiments out of three

mmol/l): 4.2 TRIS, 1.4 luminol and 6.7 *p*-hydroxycoumaric acid.

RNA isolation and RT-PCR reactions INS-1E or Min6 cells (5×10^6 cells/600 μl) or purified islets (100 islets/100 μl) were lysed and cellular RNA was isolated using a commercial kit (Qiagen, Hilden, Germany). After DNA digestion, 1 μg RNA was transcribed into cDNA using oligo-dT primers and Moloney murine leukaemia virus reverse transcriptase (MMLV-RT), both purchased from Clontech (Mountain View, CA, USA). PCR was performed with Taq polymerase from peqLab (Erlangen, Germany) using primers from Life Technologies (Carlsbad, CA, USA). Semiquantitative RT-PCR was performed with the LightCycler 480 system (Roche Diagnostics, Basel, Switzerland) using primers from TIB Molbiol (Berlin, Germany). Sequences of all primers are listed in electronic supplementary material [ESM] Table 1.

Functional dynamic mass redistribution measurements Human embryonic kidney 293 (HEK) cells were stably transfected with human or mouse orthologue of FFAR1 receptor using the Flp-In T-REx system according to the manufacturer's instructions (Life Technologies, Carlsbad, CA, USA). The FLAG-tagged human FFAR1 receptor has an expected molecular mass of 32 kDa; the mouse FFAR1 receptor is marked with yellow fluorescent protein (YFP) and therefore has a

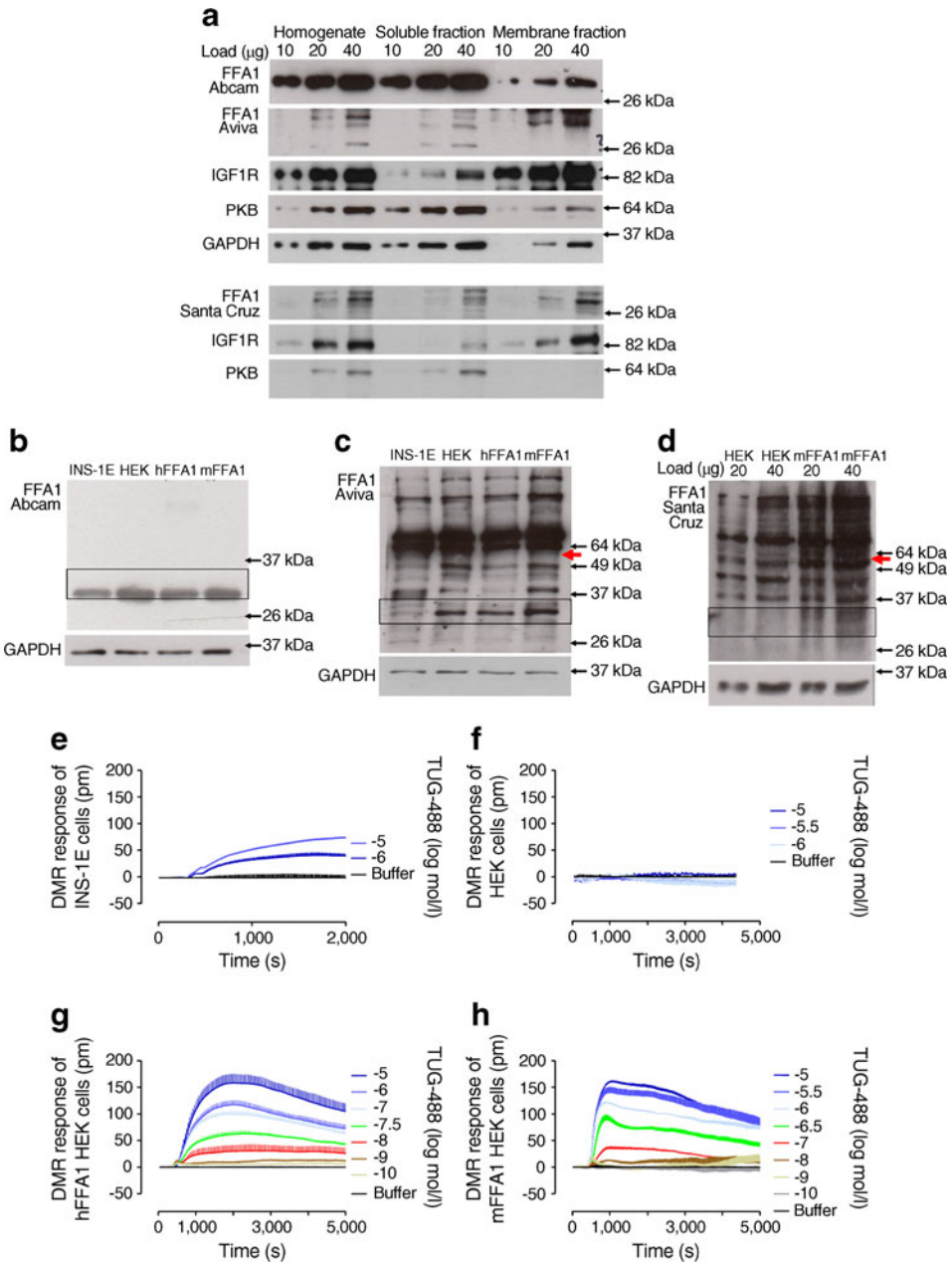

Fig. 2 Detection of rat, mouse (m) and human (h) FFAR1 (FFA1) on western blots. (**a**) INS-1E cell homogenate, a soluble fraction (13,000 *g* supernatant fraction) and a membrane fraction (13,000 *g* pellet) were blotted as indicated. PKB and GAPDH were used as soluble markers and IGF1R as a membrane marker. (**b**–**d**) Homogenates of native HEK cells and HEK cells overexpressing mouse and human FFAR1were probed against FFAR1 antibodies as indicated. Unless otherwise indicated, 20 μg protein was loaded. GAPDH was used as loading control. (**c** and **d**) The red arrow indicates the molecular mass of YFP-tagged mouse FFAR1. (**e**–**h**) DMR response of TUG-488 in (**e**) INS-1E, (**f**) native HEK, (**g**) human FFAR1 HEK, (**h**) mouse FFAR1 HEK cells. DMR response is expressed as picometres (pm); concentrations of TUG-488 are presented in $\log_{10}$

molecular mass of 58 kDa. Cell-based dynamic mass redistribution (DMR) assays were performed, as described previously in detail [8, 9], using DMR readers, the Corning Epic Biosensor (beta version, Corning Incorporated Life Sciences, Tewksbury, MA, USA) or the EnSpire multimode reader (PerkinElmer, Waltham, MA, USA). Cells were seeded at a density of 18,000 cells/well (human FFAR1 HEK, mouse FFAR1 HEK, and HEK) or 30,000 cells/well (INS-1E) on fibronectin-coated biosensor plates and cultivated overnight (37°C, 5% CO_2) to obtain confluent monolayers. After washing the cells with HEPES-buffered salt solution the biosensor plate was incubated for 1 h in the DMR reader. A baseline optical signature was recorded, and compound solutions were transferred onto the biosensor plate and DMR was monitored. Shown are representative traces (+ SEM).

Results and discussion

Detection of Ffar1 expression by RT-PCR Using specific primers, *Ffar1* was detected in mouse islets, INS-1E and Min6 cells (Fig. 1a). As the protein is encoded by a single exon, up- and downstream primers bind to the same exon, which makes it likely that amplicons of cellular DNA contaminate the PCR product. We therefore performed PCR reactions with and without RT. A faint PCR product band was detectable only from samples subjected to RT (Fig. 1b). The reaction was specific, as no amplification product was detected in islets from FFAR1-deficient mice. That RNA was correctly transcribed is suggested by the proper product accumulation for β-actin. Real-time PCR was performed to quantify *Ffar1* mRNA (Fig. 1c–h). Comparison of the results from samples not subjected to RT confirmed a cDNA-dependent amplification of *Ffar1*-specific products in insulin-secreting INS-1E cells, Min6 cells and mouse islets (Fig. 1c, e, g, respectively). Of note, a product accumulated also from RNA without RT but at much later time points. Again, PCR using RNA from islets of FFAR1-deficient mice did not result in accumulation of a specific product, whereas accumulation of the housekeeping gene product was comparable to that of mouse islets expressing the receptor (Fig. 1g, h). The calculated relative mRNA amount, estimated from ΔC_t, suggests a four- to fivefold higher expression of *Ffar1* in INS-1E cells (0.024 AU) compared with Min6 cells (0.006 AU) and mouse islets (0.005 AU). This analysis suggests that mouse islets, INS-1E and Min6 cells express significant amounts of *Ffar1*.

Detection of FFAR1 by western blotting Three commercially available antibody preparations (one monoclonal and two polyclonal) were used to detect FFAR1 protein in insulin-secreting cells. As our INS-1E cell clone expressed the highest amount of the receptor, it was used to optimise the detection procedure. Using INS-1E cell homogenates, a single and prominent protein band between 28 and 31 kDa was stained with one antibody but not with the other two preparations (Fig. 2a; ESM Fig. 1a–c). Exchanging milk for BSA or gelatin did not improve specific staining (ESM Fig. 1d, e). High-speed centrifugation was applied after cell lysis in order to enrich the membrane proteins and reduce background staining. Detection of FFAR1 was performed in the resulting cytosolic and membrane fractions, shown by PKB and IGF1R, respectively, as marker proteins (Fig. 2a). Surprisingly, staining with the Abcam antibody was enriched in the cytosolic fraction together with PKB, while less FFAR1 protein was found in the membrane fraction where IGF1R accumulated. Using the Santa Cruz or Aviva antibody, minor protein bands at 28–31 kDa were detected in the membrane fraction. FFAR1 belongs to the transmembrane proteins and, consequently, its localisation should be restricted to that particular fraction. Thus, the protein detected by the Abcam antibody does not relate to FFAR1.

Finally, FFAR1 detection was performed with homogenates of HEK cells which do not endogenously express the receptor and with HEK cells overexpressing mouse or human FFAR1 (Fig. 2b–d). The results confirm that the Abcam antibody stains an unspecific protein, as the band in HEK cell homogenates was even more pronounced than that detected in INS-1E cells (Fig. 2b). None of the antibodies detected the overexpression. That both mouse and human receptors were functionally overexpressed in HEK cells is shown by the DMR response to the specific full agonist, 3-(4-((2-(cyanomethyl)phenyl)ethynyl)phenyl)propanoic acid (TUG-488) [10], which induced a four- to fivefold higher response in human and mouse FFAR1 HEK cells than in INS-1E cells (Fig. 2e–h). The absence of a DMR response to agonist stimulation in native HEK cells confirms that these cells do not express FFAR1 (Fig. 2f). Since mouse islets expressed lower amounts of receptors than INS-1E cells, the detection of FFAR1 in islet homogenates did not yield satisfactory results (data not shown).

In conclusion, the analysis of FFAR1 protein expression remains a challenge. More studies are needed to understand whether the receptor is functionally expressed at the cell surface, especially after chronic exposure of insulin-secreting cells to fatty acids or agonists.

Acknowledgements We thank S. Haug (University of Tübingen and IDM, Tübingen, Germany) for cell culture maintenance. TUG-488 was kindly provided by T. Ulven (Southern University of Denmark, Odense M, Denmark).

Funding This work was funded by the University of Tübingen, Medical Faculty, through a fellowship to C-AT (IZKF-Promotionskolleg 2012), and was supported by the following three grants: the German Federal Ministry of Education and Research (BMBF) to the German Center for Diabetes Research (DZD), the German Research Foundation (UL140/7-2) and the Danish Council for Independent Research, Technology and Production (grant 09-070364).

Duality of interest The authors declare that there is no duality of interest associated with this manuscript.

Contribution statement This study is part of the MD thesis of C-AT. SU, H-UH and EK were responsible for the study design and the concept. C-AT, MP, MG and GK performed the experiments. C-AT, MP, GK, MG and SU analysed the data. SU, MP, MG and EK drafted the manuscript. GK, C-AT and H-UH critically revised the content. All authors approved the final version.

References

1. Itoh Y, Kawamata Y, Harada M et al (2003) Free fatty acids regulate insulin secretion from pancreatic beta cells through GPR40. Nature 422:173–176
2. Schmidt J, Liebscher K, Merten N et al (2011) Conjugated linoleic acids mediate insulin release through islet G protein coupled receptor FFAR1/GPR40. J Biol Chem 286:11890–11894
3. Millar RP, Newton CL (2010) The year in G protein-coupled receptor research. Mol Endocrinol 24:261–274
4. Natalicchio A, Labarbuta R, Tortosa F et al (2013) Exendin-4 protects pancreatic beta cells from palmitate-induced apoptosis by interfering with GPR40 and the MKK4/7 stress kinase signalling pathway. Diabetologia 56:2456–2466
5. Nakamoto K, Nishinaka T, Matsumoto K et al (2012) Involvement of the long-chain fatty acid receptor GPR40 as a novel pain regulatory system. Brain Res 1432:74–83
6. Wagner R, Kaiser G, Gerst F et al (2013) Reevaluation of fatty acid receptor 1 as a drug target for the stimulation of insulin secretion in humans. Diabetes 62:2106–2111
7. Regazzi R, Ullrich S, Kahn RA, Wollheim CB (1991) Redistribution of ADP-ribosylation factor during stimulation of permeabilized cells with GTP analogues. Biochem J 275:639–644
8. Schröder R, Janssen N, Schmidt J et al (2010) Deconvolution of complex G protein-coupled receptor signaling in live cells using dynamic mass redistribution measurements. Nat Biotechnol 28: 943–949
9. Schröder R, Schmidt J, Blättermann S et al (2011) Applying label-free dynamic mass redistribution technology to frame signaling of G protein-coupled receptors noninvasively in living cells. Nat Protoc 6:1748–1760
10. Christiansen E, Due-Hansen ME, Urban C et al (2013) Discovery of a potent and selective free fatty acid receptor 1 agonist with low lipophilicity and high oral bioavailability. J Med Chem 56:982–992

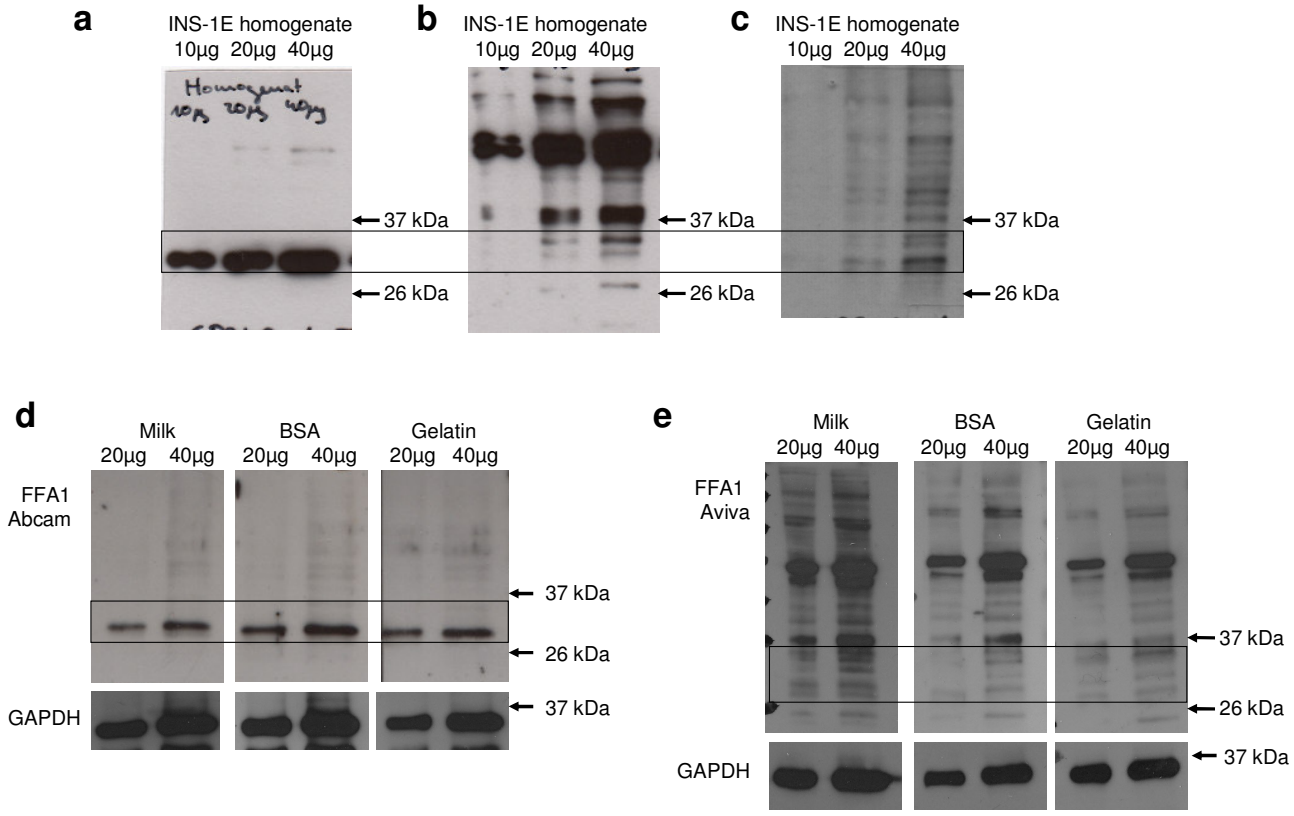

ESM Fig. 1 INS-1E cell homogenates were prepared and subjected to western blotting as described under Methods **(a-c)** Shown are the entire western blots of homogenates from Fig. 2a using **(a)** Abcam, **(b)** Aviva or **(c)** Santa Cruz antibody preparations. **(d, e)** Membranes with 20 or 40 µg/lane of INS-1E homogenates were blocked with three different blocking solutions as indicated. GAPDH was used as loading control.

ESM Table 1 List of Primers used for PCR and real time PCR (Roche Diagnostics, Basel, Switzerland)

Gene	Roche Probe no	Upstream primer	Downstream primer
rat *Ffar1*		5′-CCTTTGGATACCAAGCCATC-3′	5′-GAGCCATTCACGGGTATGTT-3′
rat *β-actin*		5′-TAGCCATCCAGGCTGTGTTG-3′	5′-GGAGCGCGTAACCCTCATAG-3′
mouse *Ffar1*		5′-GGCGCAGTGTCCCACGCTAA-3′	5′-TCCGCCTGCGTAGAGGGGAG-3′
mouse *β-Actin*		5′-CCAGCCTTCCTTCTTGGGTATGGA-3′	5′-ACGCAGCTCAGTAACAGTCCGC-3′
rat *Ffar1*	65	5′-TCATAAACCCGGACTTAGAAGG-3′	5′-TCCAGGCTCCTGTGATGAG-3′
rat *Rps13*	12	5′-CTGACGACGTGAAGGAACAA-3′	5′-TCACAAAACGGACCTGTGC-3′
mouse *Ffar1*	50	5′-CATCACTCTGCCCCTGAAG-3′	5′-AAGGCAAAGACTGGGCAGA-3′
mouse *Rps13*	110	5′-TGCTCCCACCTAATTGGAAA-3′	5′-CTTGTGCACACAACAGCATTT-3′

Epilogue

In the first paper, the role of the FFA1 receptor in the process of insulin secretion and β-cell survival was further elucidated. By using both small molecule ligands and endogenous agonists of the FFA1 receptor, we corroborated the receptor-mediated enhancement of glucose-stimulated insulin secretion (GSIS) and provided further evidence against a role of the FFA1 receptor in mediating NEFA-induced β-cell death. In fact, we could demonstrate that FFA1 activation by both the small molecule TUG-469 and the endogenous ligand palmitate protected β-cells from fatty acid-induced detrimental effects, whereas antagonizing receptor activity with the inverse agonist TUG-761 exacerbated β-cell death provoked by increased NEFA levels.

Furthermore, this publication provides pharmacogenomic insight into the potential modulation of drug action since carrier of genetic receptor variants might react with different drug efficacies[1]. It turned out that people carrying the major allele of a single nucleotide polymorphism (SNP) (rs1573611) in the FFA1 receptor gene might be protected from high-fat diet-induced negative effects of increased NEFA blood levels.

In summary, the role of FFA1 in the context of the metabolic syndrome was reevaluated. While providing further evidence to contradict a role for FFA1 in mediating (gluco)lipotoxicity of high NEFA blood levels, we posited the contrary by attesting that the FFA1 receptor protects against the deleterious effects of NEFAs. The physiological function of the receptor is moreover modulated by SNP genetic variations as shown by *in vivo* cross-sectional observations.

As the results of the second paper indicate, insufficiency of antibody-derived expression data is a largely uncharted problem. Conclusions based on erroneous data mislead the scientific community and can hinder a fruitful research process resulting in the production of rather useless matter (also see chapter 6). Since the exact structure of commercially available antibodies often remain unknown or the characterization of key epitopes kept secret on purpose, a decent knowledge of the factors that account for antibody-dependent detection is problematic to obtain yet desirable.

In the case of the FFA1 receptor, reports on certain tissue-specific expression patterns are argued by other researchers[2,3]. *Flodgren et al.* reported on the expression of FFA1 protein on glucagon producing α-cells in the pancreas[4], whereas *Hirsawa et al.* could not confirm colocalization of FFA1 in glucagon-positive cells[5]. In addition, the potent FFA1 agonist TAK-875 did not reveal a glucagon-modulating effect in studies with patients suffering from diabetes type 2[6]. FFA1 expression in the brain was claimed, although no studies with FFA1$^{-/-}$ mice indicated a significant influence of FFA1 expression in brain tissue, thus doubting the existence of FFA1 at least in mouse brain[2,3,7,8]. FFA1 was found in several diverse cell types, such as osteoblasts and osteoclasts, in mouse brain microvessels,

taste buds and also in a breast cancer cell line[9]. Studies on the functionality in some of these proposed tissues are rare and expression of the receptor itself has never even been unequivocally demonstrated[2,3].

We tested several commercially available antibodies against the FFA1 receptor and checked their capability to reliably detect the FFA1 protein. We therefore used endogenously expressing cell lines as well as artificially overexpressing cell lines in conjunction with RT-PCR methods and functional assays to confirm the cellular presence of the receptor. We demonstrated that all tested antibodies are of limited use to detect either the human or rodent forms of the FFA1 receptor. Some antibodies even detected an unspecific band in native HEK293 cells that do not endogenously express FFA1 protein. Since efforts to study receptor biology such as receptor trafficking demand a reliable technique to determine the correct amount and localization of protein of a cell sample, we conclude that the available FFA1 antibodies do not meet these criteria and therefore raise the question on the significance of data obtained with those antibody-based detection methods.

References

1. Ma, Q. & Lu, A. Y. H. Pharmacogenetics, pharmacogenomics, and individualized medicine, *Pharmacol. Rev.* **63,** 437–459 (2011).
2. Offermanns, S. Free fatty acid (FFA) and hydroxy carboxylic acid (HCA) receptors, *Annu. Rev. Pharmacol. Toxicol.* **54,** 407–434 (2014).
3. Mancini, A. D. & Poitout, V. The fatty acid receptor FFA1/GPR40 a decade later: how much do we know?, *Trends Endocrinol. Metab.* **24,** 398–407 (2013).
4. Flodgren, E. *et al.* GPR40 is expressed in glucagon producing cells and affects glucagon secretion, *Biochem. Biophys. Res. Commun.* **354,** 240–245 (2007).
5. Hirasawa, A. *et al.* Production and characterization of a monoclonal antibody against GPR40 (FFAR1; free fatty acid receptor 1), *Biochem. Biophys. Res. Commun.* **365,** 22–28 (2008).
6. Burant, C. F. *et al.* TAK-875 versus placebo or glimepiride in type 2 diabetes mellitus. A phase 2, randomised, double-blind, placebo-controlled trial, *The Lancet* **379,** 1403–1411 (2012).
7. Briscoe, C. P. *et al.* The orphan G protein-coupled receptor GPR40 is activated by medium and long chain fatty acids, *J. Biol. Chem.* **278,** 11303–11311 (2003).
8. Ma, D. *et al.* Expression of free fatty acid receptor GPR40 in the central nervous system of adult monkeys, *Neurosci. Res.* **58,** 394–401 (2007).
9. Cartoni, C. *et al.* Taste preference for fatty acids is mediated by GPR40 and GPR120, *J. Neurosci.* **30,** 8376–8382 (2010).

Chapter 5: Small molecule FFA1 agonists

Prologue

Targeting free fatty acid (FFA) receptors with endogenous ligands poses a challenge because free fatty acids as the natural agonists for these receptors are lipids and therefore substrates for a multitude of enzyme complexes and biological targets[1–3]. Moreover, since these "off-target" effects are relevant in metabolic homeostasis it is problematic to accurately define the biological role of the FFA receptors in an *in vivo* context[4]. Especially those targets are challenging to study with the endogenous ligands that show a significant overlap in the structural properties of their recognized ligands[5–7]. While this complication has been addressed for the FFA2/FFA3 receptor pair and already discussed in chapter 2 and chapter 3 with the discovery of a selective FFA2 modulator or the invention of a RASSL form of FFA2, this is also evident for the FFA1/FFA4 receptor pair, which are both activated by medium to long-chain fatty acids[8].

Both receptors are crucially involved in the regulation of host metabolism and both have been linked to glucose-stimulated insulin secretion and the pathology of diabetes type 2 and obesity[8]. Some of the beneficial effects of ω-3 fatty acids could be traced back to an interaction with the FFA4 receptor[9]. On the other side conjugated linoleic acids (CLAs) act as agonists on the FFA1 receptor and have been associated with both ameliorating and deteriorating effects on the symptoms of metabolic diseases[10–12]. Thus, the biological effects of polyunsaturated fatty acids cannot be clearly attributed to either a FFA1- or a FFA4-dependent mechanism.

As already mentioned above, FFA1 has attracted considerable interest as a possible target for the treatment of type 2 diabetes, since FFA1 is known to enhance glucose-stimulated insulin secretion (GSIS)[13,14]. To unambiguously put the effects down to an interaction with the FFA1 receptor, selective small molecule agonists for FFA1 are desirable and the search for suitable chemical compounds yielded in a substantial library of structures that show considerable activity with high selectivity for this receptor[15–17]. Since fatty acids were used as a the lead structure for the development of FFA1 selective agonists, literally all found agonists show high lipophilicity, an unwanted compound property because these drug candidates also suffer from high attrition rates in clinical trials. High lipophilicity goes along with lower metabolic stability, less favorable pharmacokinetics, higher toxicity and higher promiscuity but also higher compound potency[18–20]. Consequently, increasing efforts were made to lower compound lipophilicity by largely maintaining ligand potency and efficacy[21–23].

In this chapter, we report on the development of three FFA1 agonists. Inspired by already clinically investigated FFA1 compounds, the following structure-activity relationship (SAR) studies represent a possible way to rationally design and synthesize ligands with more favorable properties.

References

1. Dobbins, R. L. *et al.* A fatty acid- dependent step is critically important for both glucose- and non-glucose-stimulated insulin secretion, *J. Clin. Invest.* **101,** 2370–2376 (1998).
2. Stein, D. T. *et al.* Essentiality of circulating fatty acids for glucose-stimulated insulin secretion in the fasted rat, *J. Clin. Invest.* **97,** 2728–2735 (1996).
3. Crespin, S. R. Greenough, W. B. & Steinberg, D. Stimulation of insulin secretion by infusion of free fatty acids, *J. Clin. Invest.* **48,** 1934–1943 (1969).
4. Hudson, B. D. *et al.* Chemically engineering ligand selectivity at the free fatty acid receptor 2 based on pharmacological variation between species orthologs, *FASEB J.* **26,** 4951–4965 (2012).
5. Smith, C. Drug target validation: Hitting the target, *Nature* **422,** 341, 343, 345 passim (2003).
6. Milligan, G. Stoddart, L. A. & Smith, N. J. Agonism and allosterism: the pharmacology of the free fatty acid receptors FFA2 and FFA3, *Br. J. Pharmacol.* **158,** 146–153 (2009).
7. Stoddart, L. A. Smith, N. J. & Milligan, G. International Union of Pharmacology. LXXI. Free fatty acid receptors FFA1, -2, and -3: pharmacology and pathophysiological functions, *Pharmacol. Rev.* **60,** 405–417 (2008).
8. Offermanns, S. Free fatty acid (FFA) and hydroxy carboxylic acid (HCA) receptors, *Annu. Rev. Pharmacol. Toxicol.* **54,** 407–434 (2014).
9. Oh, D. Y. *et al.* GPR120 is an omega-3 fatty acid receptor mediating potent anti-inflammatory and insulin-sensitizing effects, *Cell* **142,** 687–698 (2010).
10. Ryder, J. W. *et al.* Isomer-Specific Antidiabetic Properties of Conjugated Linoleic Acid. Improved Glucose Tolerance, Skeletal Muscle Insulin Action, and UCP-2 Gene Expression, *Diabetes* **50,** 1149–1157 (2001).
11. Poirier, H. Shapiro, J. S. Kim, R. J. & Lazar, M. A. Nutritional supplementation with trans-10, cis-12-conjugated linoleic acid induces inflammation of white adipose tissue, *Diabetes* **55,** 1634–1641 (2006).
12. Schmidt, J. *et al.* Conjugated linoleic acids mediate insulin release through islet G protein-coupled receptor FFA1/GPR40, *J. Biol. Chem.* **286,** 11890–11894 (2011).
13. Mancini, A. D. & Poitout, V. The fatty acid receptor FFA1/GPR40 a decade later: how much do we know?, *Trends Endocrinol. Metab.* **24,** 398–407 (2013).
14. Itoh, Y. *et al.* Free fatty acids regulate insulin secretion from pancreatic beta cells through GPR40, *Nature* **422,** 173–176 (2003).
15. McKeown, S. C. *et al.* Solid phase synthesis and SAR of small molecule agonists for the GPR40 receptor, *Bioorg. Med. Chem. Lett.* **17,** 1584–1589 (2007).
16. Garrido, D. M. *et al.* Synthesis and activity of small molecule GPR40 agonists, *Bioorg. Med. Chem. Lett.* **16,** 1840–1845 (2006).

17. Briscoe, C. P. *et al.* Pharmacological regulation of insulin secretion in MIN6 cells through the fatty acid receptor GPR40: identification of agonist and antagonist small molecules, *Br. J. Pharmacol.* **148,** 619–628 (2006).

18. Waring, M. J. Lipophilicity in drug discovery, *Expert Opin Drug Discov* **5,** 235–248 (2010).

19. Hann, M. M. Molecular obesity, potency and other addictions in drug discovery, *MEDCHEMCOMM* **2,** 349–355 (2011).

20. Leeson, P. D. & Springthorpe, B. The influence of drug-like concepts on decision-making in medicinal chemistry, *Nat Rev Drug Discov* **6,** 881–890 (2007).

21. Hopkins, A. L. Keserü, G. M. Leeson, P. D. Rees, D. C. & Reynolds, C. H. The role of ligand efficiency metrics in drug discovery, *Nat Rev Drug Discov* **13,** 105–121 (2014).

22. Lipinski, C. A. Lombardo, F. Dominy, B. W. & Feeney, P. J. Experimental and computational approaches to estimate solubility and permeability in drug discovery and development settings1PII of original article. S0169-409X(96)00423-1. The article was originally published in Advanced Drug Delivery Reviews 23 (1997) 3–25.1, *Advanced Drug Delivery Reviews* **46,** 3–26 (2001).

23. Gleeson, M. P. Generation of a set of simple, interpretable ADMET rules of thumb, *J. Med. Chem.* **51,** 817–834 (2008).

Journal of Medicinal Chemistry

Article

pubs.acs.org/jmc

Discovery of a Potent and Selective Free Fatty Acid Receptor 1 Agonist with Low Lipophilicity and High Oral Bioavailability

Elisabeth Christiansen,[†] Maria E. Due-Hansen,[†] Christian Urban,[‡] Manuel Grundmann,[§] Johannes Schmidt,[§] Steffen V. F. Hansen,[†] Brian D. Hudson,[⊥] Mohamed Zaibi,[∥] Stine B. Markussen,[†] Ellen Hagesaether,[†] Graeme Milligan,[⊥] Michael A. Cawthorne,[∥] Evi Kostenis,[§] Matthias U. Kassack,[‡] and Trond Ulven*[,†]

[†]Department of Physics, Chemistry and Pharmacy, University of Southern Denmark, Campusvej 55, DK-5230 Odense M, Denmark,

[‡]Institute of Pharmaceutical and Medicinal Chemistry, University of Düsseldorf, Universitätsstrasse 1, D-40225 Düsseldorf, Germany,

[§]Institute for Pharmaceutical Biology, University of Bonn, Nussallee 6, D-53115 Bonn, Germany,

[⊥]Institute of Molecular, Cell and Systems Biology, College of Medical, Veterinary and Life Sciences, University of Glasgow, Glasgow G12 8QQ, Scotland, U.K.,

[∥]Clore Laboratory, University of Buckingham, Hunter Street, Buckingham MK18 1EG, U.K.

Supporting Information

ABSTRACT: The free fatty acid receptor 1 (FFA1, also known as GPR40) mediates enhancement of glucose-stimulated insulin secretion and is emerging as a new target for the treatment of type 2 diabetes. Several FFA1 agonists are known, but the majority of these suffer from high lipophilicity. We have previously reported the FFA1 agonist **3** (TUG-424). We here describe the continued structure−activity exploration and optimization of this compound series, leading to the discovery of the more potent agonist **40**, a compound with low lipophilicity, excellent in vitro metabolic stability and permeability, complete oral bioavailability, and appreciable efficacy on glucose tolerance in mice.

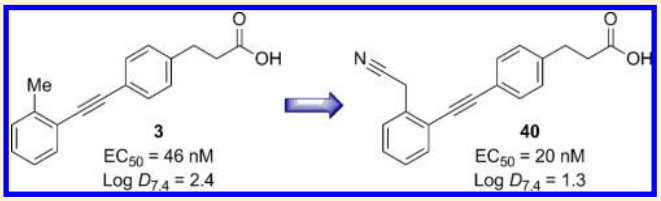

INTRODUCTION

Type 2 diabetes (T2D) is characterized by insulin resistance and insufficient insulin secretion by pancreatic β-cells, leading to dysfunctional control of plasma glucose and numerous long-term health consequences, such as increased risk of heart disease and stroke, kidney failure, blindness, neuropathy, and amputations. The global number of diabetics has now reached 350 million, of which 90% are type 2 diabetics.[1,2] Besides a healthy lifestyle, the most common treatments include insulin, metformin, and sulfonylureas, all of which are associated with problems such as weight gain, risk of hypoglycemia, and lack of sustained efficacy, and there is an urgent need for improved therapeutics.

The long-chain free fatty acid receptor 1 (FFA1, previously known as GPR40) is highly expressed in pancreatic β-cells and enhances glucose-stimulated insulin secretion (GSIS) but does not affect insulin secretion at low glucose levels.[3−6] This mechanism provides the potential for boosting insulin levels of type 2 diabetics without the risk of hypoglycemia associated with sulfonylureas and insulin administration. FFA1 is also expressed in enteroendocrine cells and has been implicated in the secretion of the incretin hormones glucagon-like peptide-1 (GLP-1) and glucose-dependent insulinotropic polypeptide (GIP).[7] Thus, the receptor may potentially enhance insulin secretion at high glucose levels through two independent mechanisms.

A number of synthetic FFA1 agonists have been reported in the literature (Chart 1),[5,8−26] of which the compounds TAK-875 and AMG-837 have reached clinical trials. A general problem with the currently known FFA1 ligands is their relatively high lipophilicity, which is associated with numerous problems, such as poor pharmacokinetic properties, metabolic instability, toxicity, and off-target effects, and correlates with attrition in clinical trials.[27−32] Studies have recommended that ClogP values should not exceed 4−5,[30,33] and ranking functions such as ligand lipophilicity efficiency (LLE) have been suggested to facilitate implementation of lipophilicity concerns in the optimization process.[27]

We previously reported the discovery of the alkyne agonist series with **3** (TUG-424, Chart 1) as the most potent compound.[13] The compound is, however, relatively lipophilic and exhibited only moderate in vitro metabolic stability and is thus not suitable as a drug candidate. We therefore aimed at improving the lipophilicity and metabolic stability of the compound by replacement of the terminal benzene ring by nitrogen-containing heterocycles, which led to the identification

Received: October 10, 2012
Published: January 8, 2013

Chart 1. Representative FFA1 Agonists

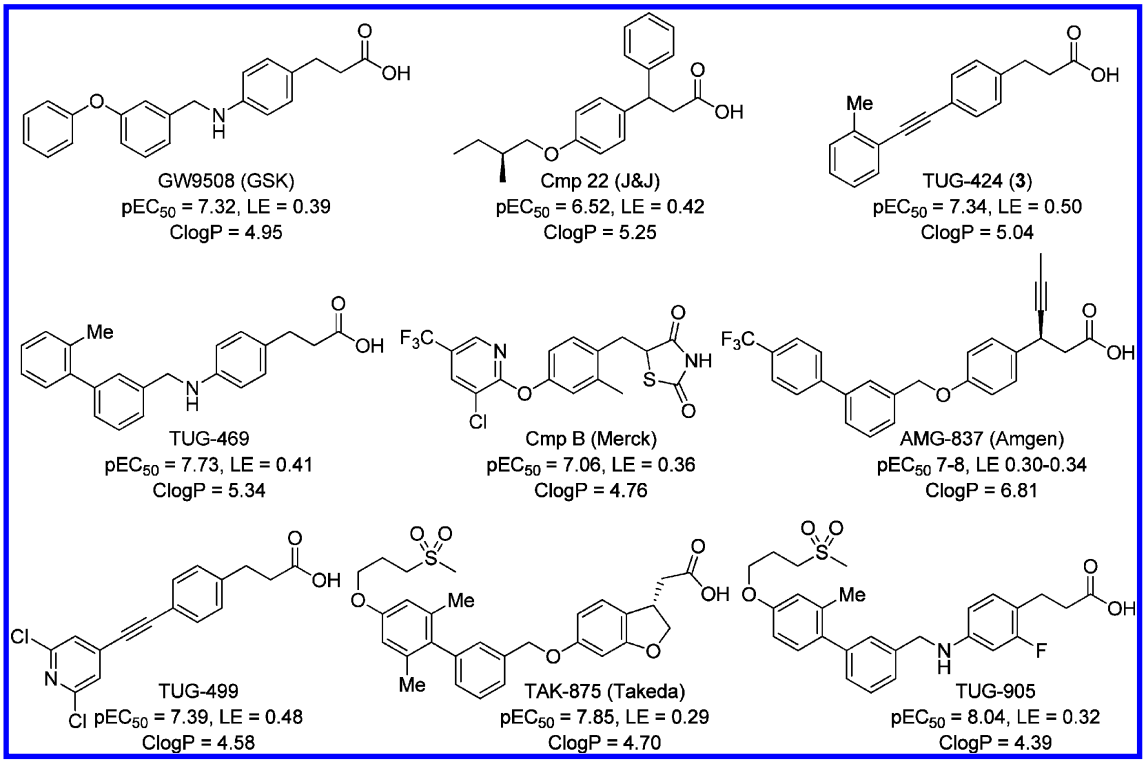

of TUG-499 (Chart 1).[19] Inspired by Takeda's clinical candidate TAK-875 (Chart 1), we recently explored the attachment of a mesylpropoxy appendage on TUG-469 (Chart 1), the previously reported compound from another series, and thereby identified TUG-905 (Chart 1), a compound with significant reduction in lipophilicity.[25] We have also continued the further optimization and exploration of structure–activity relationships (SAR) around **3** with focus on lowering lipophilicity and improving metabolic stability by the introduction of polar substituents. Herein, we report the results from these studies, which led to the identification of **40**, a compound with improved potency, lower lipophilicity than any previously reported FFA1 agonist, high selectivity, excellent in vitro ADME properties, complete bioavailability, and appreciable efficacy on glucose tolerance in mice.

RESULTS AND DISCUSSION

The majority of the alkyne ligands were synthesized directly by Sonogashira cross-coupling between the alkyne intermediate **1** and aryl halides (Scheme 1).[34] As the classical Sonogashira protocol (method A) in most cases works unsatisfactorily with **1**, we screened other methods and found that a method reported by Beller and co-workers (method B) gave improved results.[35] This method however also often gave low yields, especially with aryl iodides. We therefore optimized the method further and found that addition of 10% water (method C) resulted in suppression of Glaser–Hay dimerization of the alkyne and very rapid cross-coupling in high yields with both aryl bromides and iodides.[34] Method C is more convenient and has so far given significantly better results than other methods in all cases where iodo- and bromobenzenes are used as substrates.

The phenylacetic acid (**6**) and 4-phenylbutanoic acid (**7**) analogues were synthesized from the corresponding aryl bromides by Sonogashira coupling with phenylacetylene (Scheme 2). Acrylic acid analogues **8** and **9** were synthesized from 4-bromocinnamic acid via esterification and Sonogashira cross-coupling reactions as for the propionic acids (Scheme 3).

Scheme 1[a]

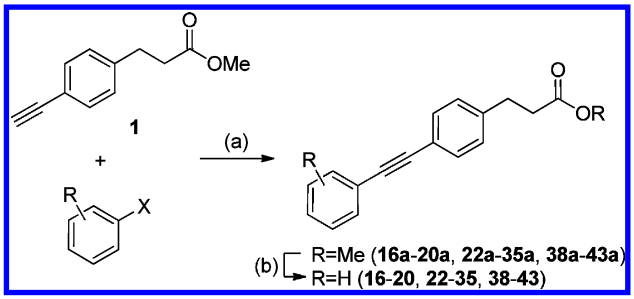

[a]Reagents and conditions: (a) method A, $Pd(PPh_3)_2Cl_2$, CuI, aryl halide, Et_3N, DMF, 50 °C; method B, Na_2PdCl_4, PIntB, CuI, aryl halide, TMEDA, water, 80 °C; method C, Na_2PdCl_4, PIntB, CuI, aryl halide, TMEDA, water, 80 °C. (b) LiOH, THF, water, room temperature.

Scheme 2[a]

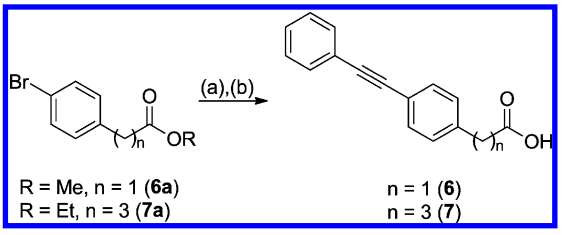

[a]Reagents and conditions: (a) Na_2PdCl_4, PIntB, CuI, phenylacetylene, TMEDA, water, 80 °C (78%). (b) LiOH, THF, water, room temperature (95–99%).

dx.doi.org/10.1021/jm301470a | J. Med. Chem. 2013, 56, 982–992

Scheme 3[a]

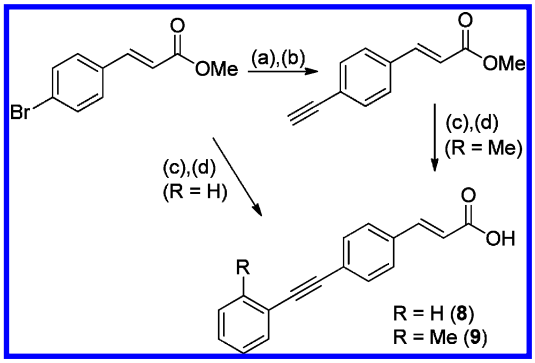

[a]Reagents and conditions: (a) trimethylsilylacetylene, Na_2PdCl_4, PIntB, CuI, TMEDA, water, 80 °C (77%). (b) K_2CO_3, MeOH, room temperature (95%). (c) Na_2PdCl_4, PIntB, CuI, 2-bromotoluene or phenylacetylene, TMEDA, water, 80 °C (68−84%). (d) LiOH, THF, water, room temperature (85−91%).

The *β*-methyl substituted analogue **10** was prepared by a conjugated addition of methyl Gilman reagent to methyl 4-bromocinnamate in the presence of chlorotrimethylsilane (Scheme 4).[36−38] All cyclopropyl analogues are racemic and

Scheme 4[a]

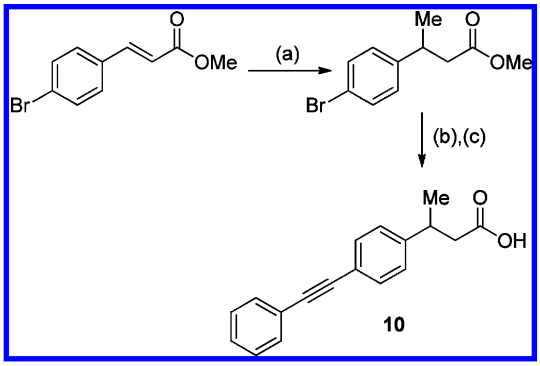

[a]Reagents and conditions: (a) MeMgCl, copper(I) thiophenolate, TMSCl, THF, −78 °C → 0 °C (47%). (b) Na_2PdCl_4, PIntB, CuI, phenylacetylene, TMEDA, water, 80 °C (57%). (c) LiOH, THF, water, room temperature (64%).

were prepared from methyl *trans*-2-(4-iodophenyl)-cyclopropanoate (Scheme 5).[19] The bicyclic alkyne **11** was synthesized from 5-bromodihydroindanone by a Horner−Wadsworth−Emmons reaction with triethyl phosphonoacetate, reduction with triethylsilane and TFA, and Sonogashira coupling with phenylacetylene followed by ester hydrolysis (Scheme 6). Aryl halides used to prepare **27**, **28**, **42**, and **43** were synthesized by alkylation of iodophenols. The methoxymethyl-substituted bromobenzene building blocks for **34** and **35** were synthesized following a $FeSO_4$-promoted ether synthesis of the corresponding bromobenzyl bromides.[39] The biphenylalkyne **21** was synthesized from the methyl ester **23a** by Suzuki cross-coupling (Scheme 7).

The mesylalkoxy-substituted alkynes were prepared from **26a** by a Williamson ether synthesis to form the bromoalkylated intermediate, which was subsequently mesylated by gentle heating with sodium methanesulfinate in PEG-400 (Scheme 8).

Compounds were screened on the human FFA1 in a calcium mobilization assay. Besides overall activity, ligand efficiency

Scheme 5[a]

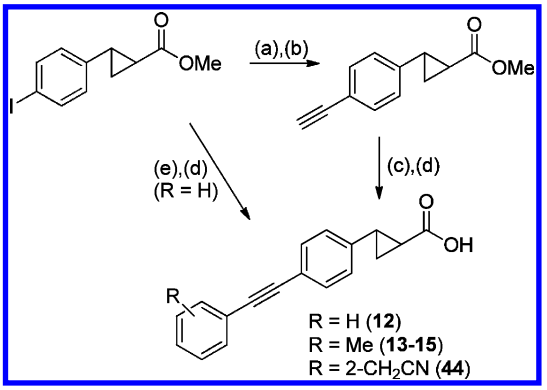

[a]Reagents and conditions: (a) trimethylsilylacetylene, Na_2PdCl_4, PIntB, CuI, TMEDA, water, 80 °C. (b) K_2CO_3, MeOH, room temperature (97% over two steps). (c) Na_2PdCl_4, PIntB, CuI, aryl halide, TMEDA (or TMEDA with 10% water for R = 2-CH_2CN), 80 °C (36−49%). (d) LiOH, THF, water, room temperature (97−99%). (e) $Pd(PPh_3)_2Cl_2$, CuI, phenylacetylene, Et_3N, DMF, 50 °C (53%).

Scheme 6[a]

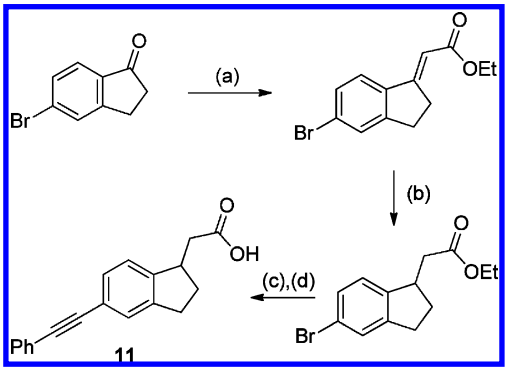

[a]Reagents and conditions: (a) triethyl phosphonoacetate, 60% NaH, toluene, 0 °C → reflux (45%). (b) Et_3SiH, TFA, room temperature → 50 °C (58%). (c) Na_2PdCl_4, PIntB, CuI, phenylacetylene, TMEDA, water, 80 °C (57%). (d) LiOH, THF, water, room temperature (91%).

Scheme 7[a]

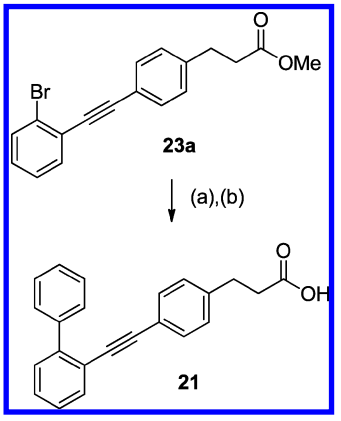

[a]Reagents and conditions: (a) $PhB(OH)_2$, $Pd(OAc)_2$, SPhos, K_3PO_4, toluene, 100 °C (74%). (b) LiOH, THF, water, room temperature (94%).

(LE)[40] and calculated lipophilicity (ClogP), as well as LLE[27] calculated as the difference between pEC_{50} and ClogP, were taken advantage of in the evaluation of analogues. Since the

dx.doi.org/10.1021/jm301470a | J. Med. Chem. 2013, 56, 982−992

Scheme 8[a]

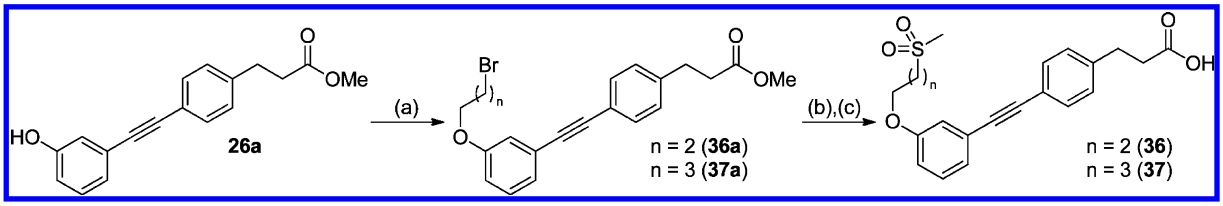

[a]Reagents and conditions: (a) $Br(CH_2)_{n+1}Br$, K_2CO_3, acetone, reflux (79−93%). (b) $MeSO_2Na$, PEG-400, 45 °C (38−51%). (c) LiOH, THF, water, room temperature (58−80%).

Table 1. SAR Exploration of the Propionic Acid Chain

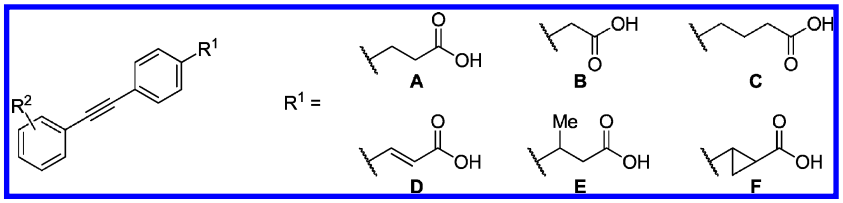

compd	R^1	R^2	FFA1, calcium pEC_{50} (% efficacy)[a]	LE[b]	ClogP[c]	log $D_{7.4}$[d]	LLE[e]
2[f]	A	H	6.70 ± 0.03 (106)	0.48	4.54		2.16
3[f]	A	2-Me	7.34 ± 0.07 (103)	0.50	5.04	2.44 ± 0.01	2.86
4[f]	A	3-Me	7.13 ± 0.05 (97)	0.49	5.04		2.75
5[f]	A	4-Me	6.55 ± 0.04 (109)	0.45	5.04	2.13 ± 0.02	2.17
6	B	H	6.01 ± 0.03 (93)	0.46	4.05		1.96
7	C	H	6.00 ± 0.02 (99)	0.41	4.92		1.08
8[g]	D	H	5.03 ± 0.08 (83)	0.36	4.88		0.15
9	D	2-Me	5.64 ± 0.04 (104)	0.39	5.38		0.26
10	E	H	6.70 ± 0.03 (103)	0.46	4.94		1.76
11	(Scheme 6)		6.46 ± 0.04 (99)	0.42	5.05		1.42
12	F	H	6.84 ± 0.04 (107)	0.47	4.59		2.25
13	F	2-Me	6.86 ± 0.02 (99)	0.45	5.09		1.78
14	F	3-Me	7.03 ± 0.02 (102)	0.46	5.09		1.95
15	F	4-Me	6.51 ± 0.04 (107)	0.42	5.09		1.43

[a]Efficacy is given as percent response relative to 10 μM TUG-20.[18] [b]Ligand efficiencies (LE) were calculated by LE = $RT \ln K_D$, presuming that $EC_{50} \approx K_D$. Values are given in kcal mol^{-1} per non-hydrogen atom.[40] [c]Calculated by BioByte's algorithm as implemented in ChemBioDraw Ultra 12.0 (the "ClogP" option). [d]Determined by the shake flask method.[25] [e]Ligand lipophilicity efficiencies (LLE) were calculated by the formula LLE = pEC_{50} − ClogP.[27] [f]Previously reported.[13] [g]Tested with 0.05% bovine serum albumin (BSA).

ClogP calculation method was used extensively in the optimization, a validation and comparison of alternative methods using related compounds with experimental log $D_{7.4}$ values was performed, and log $D_{7.4}$ values from representative new alkynes were subsequently added to strengthen the validation. Of 11 methods, the ClogP method showed the best correlation with experimental values (R^2 = 0.96; see the Supporting Information).

We have previously reported the discovery of the potent and selective FFA1 agonist **3** (Chart 1) by screening of a focused library of constrained fatty acid analogues and optimization of a 4-(phenylethynyl)phenoxyacetic acid hit.[13] The optimization study revealed the phenylpropanoic acid analogue **2** (Table 1) to be clearly favored over the phenoxyacetic acid of the initial hit and that introduction of methyl substituents at the terminal phenyl showed the 2-position (**3**) was preferred over the 3-position (**4**), while a 4-methyl (**5**) did not result in increased potency relative to the unsubstituted **2**.[25] Shortening or elongating the propionic acid chain by one methylene group (**6** and **7**) resulted in significant decrease in potency. The planar acrylic acid **8** showed a further order of magnitude reduced potency, which to some degree was regained by introduction of the 2-methyl on the terminal phenyl ring (**9**). The introduction of a β-methyl group (**10**) did not affect potency, but is disfavored relative to **2** as it results in lower LE and higher lipophilicity and introduces a chiral center that complicates synthesis. Constraining the propionic acid by connecting the methyl group of **10** back to the benzene ring via a methylene group to form a dihydroindane system (**11**, Scheme 6), in analogy to the structures reported by Takeda,[21] yielded reduced potency. In contrast, connecting the β-methyl to the α-carbon to form a cyclopropyl constraint of the propionic acid chain (**12**) results in a moderate gain of activity. Unfortunately, the gain was not maintained with the introduction of methyl substituents at the terminal benzene ring (**13**−**15**).

Although methyl substituents in both 2- and 3-position resulted in increased potency, the initial studies showed that the 2,3-dimethyl as well as the 3,5-dimethyl pattern gave a compound with lower potency than the corresponding monomethyl analogues.[13] To complete this study, we synthesized the 2,5-dimethyl (**16**), 2,6-dimethyl (**17**), and 4-chloro-2-methyl (**18**) analogues, all of which exhibited reduced activity relative to **3** (Table 2).

We found that **3** had only moderate stability toward human liver microsomes (HLM, see below) and suspected that the 2-

dx.doi.org/10.1021/jm301470a | J. Med. Chem. 2013, 56, 982−992

Table 2. Exploration of Substitution on the Terminal Phenyl Ring

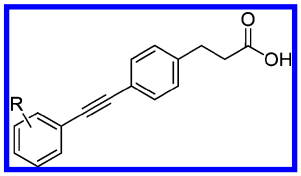

compd	R	FFA1, calcium pEC_{50} (efficacy, %)[a]	LE[b]	ClogP[c]	log $D_{7.4}$[d]	LLE[e]
16	2-Me, 5-Me	6.91 ± 0.06 (102)	0.45	5.54		1.37
17	2-Me, 6-Me	6.38 ± 0.04 (103)	0.42	5.54		0.84
18	2-Me, 4-Cl	6.86 ± 0.02 (103)	0.45	5.75		1.11
19	4-F	6.28 ± 0.05 (96)	0.43	4.68		1.60
20	2-Et	7.05 ± 0.03 (101)	0.46	5.57		1.48
21	2-Ph	6.00 ± 0.02 (91)	0.33	6.43		−0.43
22	2-Cl	6.82 ± 0.04 (107)	0.47	5.25		1.57
23	2-Br	7.08 ± 0.06 (99)	0.49	5.40		1.68
24	2-CF_3	6.47 ± 0.02 (98)	0.39	5.42		1.05
25	2-OH	4.79 ± 0.07 (83)	0.33	3.87		0.92
26	3-OH	6.35 ± 0.04 (103)	0.43	3.87		2.48
27	2-OMe	6.66 ± 0.03 (99)	0.44	4.46		2.20
28	3-OMe	7.15 ± 0.03 (101)	0.47	4.46		2.69
29	2-OCF_3	6.65 ± 0.03 (106)	0.38	5.57	2.66 ± 0.01	1.08
30[f]	3-OCF_3	7.02 ± 0.04 (103)	0.40	5.57	2.83 ± 0.01	1.45
31	2-COMe	6.73 ± 0.04 (101)	0.42	3.98		2.75
32	2-CH_2OH	6.24 ± 0.02 (111)	0.41	3.50		2.74
33	2-C_2H_4OH	5.69 ± 0.02 (106)	0.35	3.73		1.96
34	2-CH_2OMe	7.39 ± 0.03 (108)	0.46	4.34	1.29 ± 0.00	3.05
35	3-CH_2OMe	7.42 ± 0.04 (99)	0.46	4.34	1.43 ± 0.01	3.08
36	3-$O(CH_2)_3Ms$	6.09 ± 0.03 (100)	0.31	3.55		2.55
37	3-$O(CH_2)_4Ms$	6.37 ± 0.03 (106)	0.31	3.33	0.88 ± 0.01	3.04
38	2-CN, 5-Me	6.33 ± 0.02 (103)	0.39	4.47		1.86
39	2-Me, 5-CN	7.40 ± 0.03 (105)	0.45	4.47	1.75 ± 0.01	2.93
40	2-CH_2CN	7.70 ± 0.04 (103)	0.48	3.96	1.28 ± 0.01	3.76
41	3-CH_2CN	6.72 ± 0.04 (98)	0.42	3.96	0.98 ± 0.01	2.76
42	2-OCH_2CN	7.33 ± 0.03 (105)	0.44	3.45		3.89
43	3-OCH_2CN	6.58 ± 0.03 (105)	0.39	3.45		3.14
44	(Scheme 5)	7.45 ± 0.03 (99)	0.45	4.01		3.44

[a]Efficacy is given as percent response relative to 10 μM TUG-20.[18] [b]Ligand efficiencies (LE) were calculated by LE = $RT \ln K_D$, presuming that $EC_{50} \approx K_D$. Values are given in kcal mol^{-1} per non-hydrogen atom.[40] [c]Calculated by ChemBioDraw Ultra 12.0 with the "ClogP" option. [d]Determined by the shake flask method.[25] [e]Calculated by the formula LLE = pEC_{50} − ClogP.[27] [f]Tested with 0.05% BSA.

methyl group might be implicated. A 4-fluoro substituent on the terminal phenyl ring (**19**) to stabilize the terminal phenyl ring toward oxidation came with a penalty in terms of lower potency. Increasing the steric bulk of the 2-methyl group of **3** by replacement with ethyl (**20**) or phenyl (**21**) resulted in reduced potency. These analogues also had increased lipophilicity and were unlikely to improve the HLM stability. Replacement of the 2-methyl by metabolically stable chloro (**22**), bromo (**23**), or trifluoromethyl (**24**) substituents did not preserve potency, while lipophilicity was increased in all cases.

It is well-known that lipophilicity generally correlates with poor metabolic stability, a consequence of the increased tendency of more lipophilic molecules to seek out of the aqueous phase and into the active sites of the metabolic enzymes. We have previously described our efforts to optimize **3** by replacing the terminal phenyl group with hydrophilic heterocycles,[19] and we recently described the effects of introducing a polar substituent on an FFA1 agonist, resulting in reduced lipophilicity and higher HLM stability together with preserved potency.[25] Although initial attempts to introduce polar substituents on the terminal phenyl ring of **3** had resulted in compounds with low or no activity,[13] we decided to continue the exploration of this strategy. Introduction of a hydroxyl group in the 2-position (**25**) resulted in a 2 orders of magnitude erosion of activity. A 3-hydroxy substituent (**26**) gave a moderate reduction in potency relative to **2**, but a higher LLE. It is thus clear that the positioning of a polar group is critical. A rationale for this was provided by the modeling study below. Methoxy groups in the 2- and 3-positions (**27**, **28**) improved the situation significantly compared to the hydroxyls. In the case of the 3-MeO analogue **28**, the reduction in lipophilicity compensated for the lower potency and gave the compound an LLE of 2.69 based on ClogP, compared to 2.86 for **3**. As methoxy substituents imply a risk of metabolic instability, the more stable trifluoromethoxy group was explored in the same positions (**29**, **30**). The activities of **29** and **30** paralleled those of methoxy analogues **27** and **28**, but the increased lipophilicity and decreased LE and LLE made the compounds less attractive. Continuing the screen for more polar substituents, the 2-acetyl (**31**) turned out equipotent with the unsubstituted **2**, but significantly less potent than **3**. Fishing for hydrogen-bond interactions further away from the scaffold,

dx.doi.org/10.1021/jm301470a | J. Med. Chem. 2013, 56, 982−992

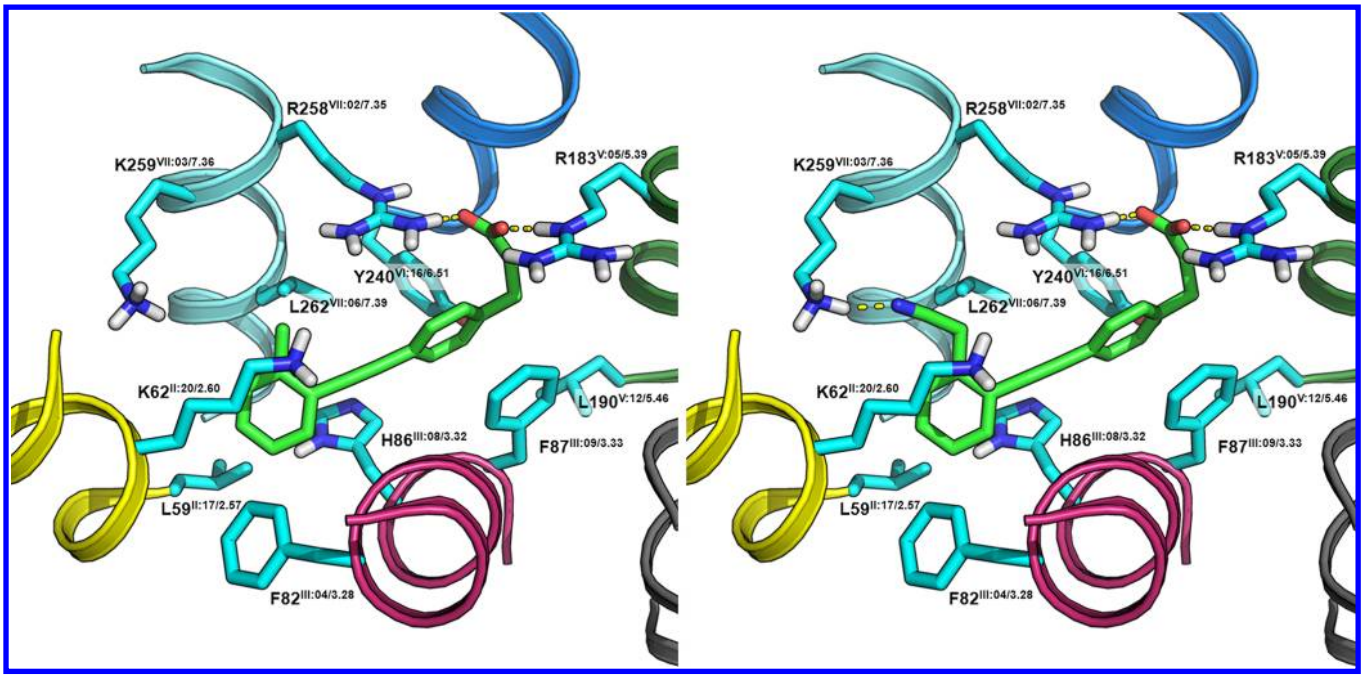

Figure 1. Complex of **3** (left) and **40** (right) with a homology model of the human FFA1. Residues situated close to the ligands are labeled with sequence number, and Schwartz–Baldwin[41] and Ballesteros–Weinstein[42] notations are given as superscripts.

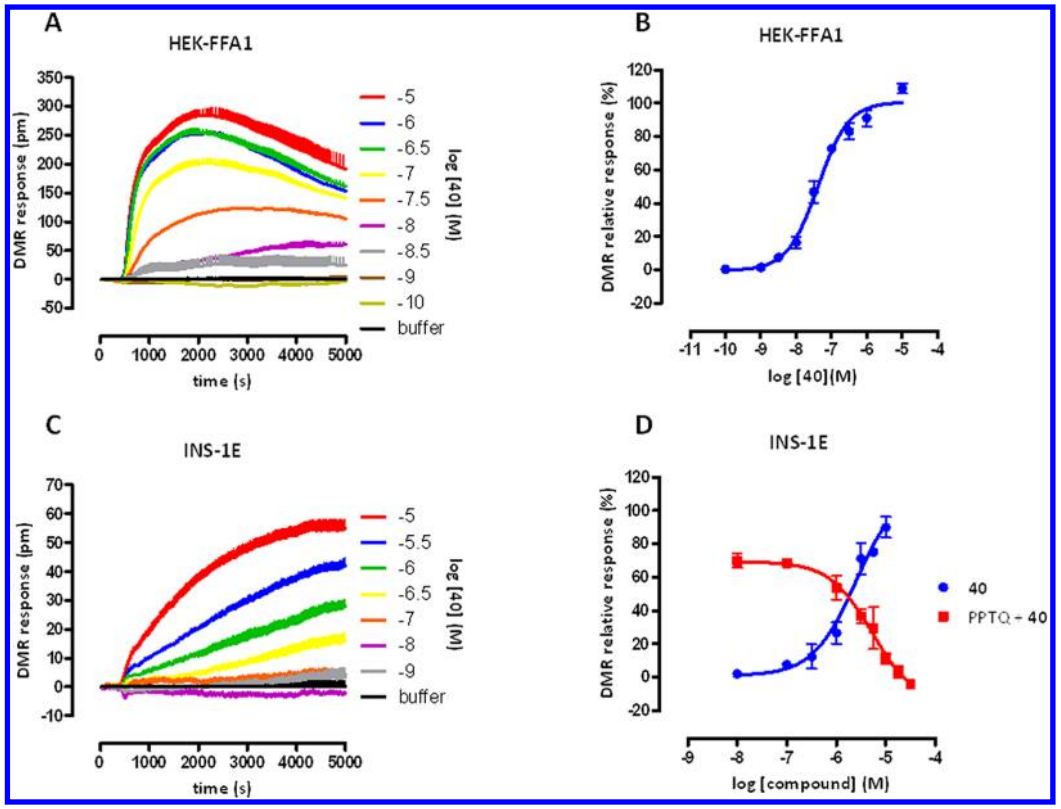

Figure 2. Activity of **40** on FFA1-transfected HEK-293 cells and in the rat β-cell line INS-1E that endogenously expresses FFA1. (A) Representative traces from the dynamic mass redistribution (DMR) assay of **40** on HEK-FFA1 cells. (B) Concentration–response curves of **40** in FFA1-HEK cells from the DMR assay (pEC_{50} = 7.4 ± 0.05, n = 3). (C) Traces from the DMR assay of **40** in INS-1E cells. (D) Concentration–response curve of **40** in INS-1E cells (pEC_{50} = 5.6 ± 0.16, n = 5) and inhibition of **40** (3 μM) by the FFA1 antagonist PPTQ (pIC_{50} = 5.3 ± 0.13, n = 3).

the 2-hydroxymethyl (**32**) and 2-hydroxyethyl (**33**) analogues were investigated, but these did not display sufficient potency. The methoxymethyl substituent in the 2- or 3-position (**34**, **35**), however, brought the activity up to the same level as **3** while lower lipophilicity was maintained, thus increasing LLE. Mesylalkoxy substituents, successfully applied on another compound series,[25] were investigated with various chain lengths (**36**, **37**). The 3-mesylbutoxy substituent (**37**) resulted in a

dx.doi.org/10.1021/jm301470a | J. Med. Chem. 2013, 56, 982–992

small decrease in activity relative to **2** but more than an order of magnitude reduced lipophilicity, and thereby a significantly increased LLE relative to both **2** and **3**. The concept of introducing mesylalkoxy substituents to lower lipophilicity while potency was maintained thus seems to work well, although the potencies of these analogues were too low to place them among the preferred compounds.

The introduction of a polar cyano substituent on the terminal ring together with a methyl group (**38**, **39**) resulted in **39** being equipotent with **3** with somewhat reduced lipophilicity. Gratifyingly, combining the cyano and the methyl into a 2-cyanomethyl substituent (**40**) produced a significant increase in potency and a pronounced reduction in lipophilicity relative to **3**. The 3-cyanomethyl analogue (**41**) turned out an order of magnitude less potent. Thus, the substituent position is important, as for the hydroxyl analogues **25** and **26**, but the favored position is reversed. Extending the substituent to cyanomethoxy (**42**, **43**) led to reduced potency to the same degree in both the 2- and 3-postion together with further reduced lipophilicity. The preference for the 2-position is thus in agreement with the methyl (**3**, **4**) and cyanomethyl (**40**, **41**) analogues, but reversed in comparison to the other analogues where oxygen is attached directly to the phenyl ring (**25**−**29**). A combination of 2-cyanomethyl with the cyclopropyl constraint of the propionic acid chain (**44**) resulted in a drop in potency, as for the methyl substituents. Altogether, **40** remained the preferred compound, despite the slightly higher LLE of **42**.

A molecular modeling study was performed to explore the basis for the interesting effects observed with the different substituent positions. The complex of **3** and **40** with a homology model of hFFA1 was generated as described previously.[19] The carboxylic acid of the compounds interacts with the two arginine residues Arg183 and Arg258 and the diphenylacetylene part extends toward TM2 (Figure 1). The benzene rings are twisted with almost 90° between them, as also observed in the crystal structure of **3**,[13] which favors interaction between the central ring and Phe87 and places the methyl group in a small hydrophobic cavity created by Leu262. This hydrophobic cavity provides a rationale for the preference of the 2-methyl substituent (**3**) over the 3-methyl (**4**) and the unsubstituted compound (**2**), and for the highly disfavored interaction with the 2-hydroxy-substituted **25** compared to the 3-hydroxy analogue **26**. Likewise, the lower potency of the 2-cyano-5-methyl-substituted **38** compared to the 5-cyano-2-methyl-substituted **39** can be rationalized by the disfavored polar ortho-substituent. The 2-cyanomethyl moiety of **40** fit well into the hydrophobic cavity and, in addition, provides a hydrogen bond acceptor that is perfectly situated to form a hydrogen bond interaction with Lys259 (distance ∼ 2.0 Å) with Lys62 as an alternative interaction point, thus providing a rationale for the high potency of this compound.

The 2-cyanomethyl analogue **40** was the most potent agonist by good margin and also had lower lipophilicity and was thus chosen for further examination. The compound was evaluated using a dynamic mass redistribution (DMR) assay, which monitors real-time protein activity in the living cell without the need of labeling.[43] Potent activity in HEK293 cells transfected with hFFA1 was confirmed [Figures 2 and S1 (Supporting Information)]. Further testing of **40** with the insulin-secreting rat β-cell line INS-1E endogenously expressing FFA1 showed a concentration-dependent effect that was confirmed to be FFA1-mediated by treatment with the FFA1 antagonist *trans*-1-oxo-3-(4-phenoxyphenyl)-2-propyl-1,2,3,4-tetrahydroisoquinoline-4-carboxylic acid (PPTQ).[44]

Counterscreens demonstrated >100-fold selectivity for FFA1 over FFA2 (GPR43, $pEC_{50} < 5$), FFA3 (GPR41, $pEC_{50} < 5$), GPR120 ($pEC_{50} = 5.32 \pm 0.03$), PPARγ ($pEC_{50} < 5$), and 55 other receptors, enzymes, and transporters (see the Supporting Information). Physicochemical and in vitro ADME properties of **40** were obtained for a full comparison with the lead compound **3** (Table 3). Both **3** and **40** have good solubility and demonstrated excellent chemical stability. The experimental lipophilicity of **40** as measured by log $D_{7.4}$ was reduced by an order of magnitude relative to **3**. Stability toward HLM was drastically improved, supporting that the 2-methyl group was involved in the insufficient stability observed with **3** and demonstrating that reduction of lipophilicity is an efficient means for mending unsatisfactory metabolic stability. No significant cell toxicity or inhibition of the most important CYP enzymes or P-glycoprotein (P-gp) was found. Both compounds exhibited high permeability in Caco-2 cells. The permeability of **40** was also examined on the mucus-secreting cell-line HT29-MTX,[45] an improved model system for the intestinal epithelium, and was found to be significantly higher [$P_{app} = (2.54 \pm 0.07) \times 10^{-5}$ cm/s, 78% recovered] than the readily absorbed drug ketoprofen [$P_{app} = (1.51 \pm 0.05) \times 10^{-5}$ cm/s, 80% recovered].

Table 3. Physicochemical and in Vitro ADME Properties of 3 and 40

assay	3	40
aqueous solubility (PBS, pH 7.4)[a]	174 μM	188 μM
chemical stab. (PBS, 37 °C, 12 days)	99.9%	99.8%
log D (*n*-octanol/PBS, pH 7.4)[b]	2.44 (2.34)	1.28 (1.32)
plasma protein binding (human)[c]	97.7%	>99.9%
metabolic stability (HLM)[a]	26%	81%
CYP inhibition (10 μM)[a]		
CYP1A2	−8%	−3%
CYP2C9	−25%	11%
CYP2C19	−1%	−2%
CYP2D6	0%	5%
CYP3A4	−4%	8%
P-gp inhibition (% @ 30/100 μM)[a]	6.6/23.3	−4.0/−1.8
Caco-2 (A to B, TC7, pH 6.5/7.4)[a]	87×10^{-6} cm/s	91×10^{-6} cm/s

[a]Determined at Cerep Inc. [b]Determined by the shake-flask method.[25] The values given in parentheses were determined at Cerep Inc. [c]Determined by equilibrium dialysis at Cerep Inc.

Pharmacokinetic investigations of **3** and **40** in mice revealed rapid and complete absorption of both compounds after oral dosing (Table 4). The half-life in mice is as expected rather short, but **40** showed a somewhat longer half-life than **3**. The exposure of **40** after oral dosing was 3.5-fold higher than for **3**. The relatively low volume of distribution for **40** can be rationalized by the high plasma protein binding and contributes to **40** having a half-life only moderately longer than **3** despite higher metabolic stability. A low clearance was confirmed with **40** compared to a quite high clearance for **3**, corresponding to approximately 15% and 60% of the hepatic blood flow in mice, respectively. Both compounds were well-tolerated by the mice in acute exposures up to 250 mg/kg po. A satisfactory overall pharmacokinetic profile was found for **40**.

The effects of **3** and **40** on glucose tolerance in normal mice after oral administration 30 min prior to glucose challenge were

dx.doi.org/10.1021/jm301470a | J. Med. Chem. 2013, 56, 982−992

Table 4. Pharmacokinetic Profiles of 3 and 40 in Mice[a]

	3	40
Intravenous		
C_{max} (ng/mL)	2284	5071
t_{max} (min)	5	5
$t_{1/2}$ (min)	10	17
$AUC_{0-\infty}$ (μg/mL·min)	47	174
V_d (L/kg)	0.80	0.35
CL_{total} (mL/min/kg)	53	14
Oral		
C_{max} (ng/mL)	2591	7757
t_{max} (min)	30	30
$t_{1/2}$ (min)	48	50
$AUC_{0-\infty}$ (μg/mL·min)	205	732
F (%)	109	105

[a]Data are mean concentrations in mouse plasma (n = 3) following a single 2.5 mg/kg intravenous dose or 10 mg/kg oral dose.

studied. **3** showed a significant improvement in glucose tolerance at a 50 mg/kg dose (Figure 3), similar to the effect of the oral antihyperglycemic DPP-4 inhibitor sitagliptin (10 mg/kg), a compound on the market for treatment of T2D. **40** exhibited a dose-dependent response with a significant effect similar to that of sitagliptin at 10 mg/kg and a maximal effect reached at 50 mg/kg, sustained at 250 mg/kg (Figure 3). Compound **40** is confirmed to be a full agonist also of the murine FFA1, but with an order of magnitude lower potency (pEC_{50} = 6.40 on mFFA1) than on the human orthologue. The considerable difference in efficacy and to some degree potency between the two compounds in the glucose tolerance test can thus be ascribed mainly to the improved pharmacokinetic properties of **40**.

CONCLUSION

In the continued SAR exploration of the alkyne series of FFA1 agonists represented by **3**, we focused especially on lowering the lipophilicity of the compounds. Introduction of polar substituents on the terminal phenyl ring led to the discovery of **40**, a compound with significantly improved potency and reduced lipophilicity relative to **3** (EC_{50} = 20 vs 46 nM, log $D_{7.4}$ 1.3 vs 2.4). Compound **40** exhibited high selectivity over a panel of enzymes, receptors, and transporters, and in vitro ADME-tox studies indicated high absorption, good metabolic stability, and no inhibition of enzymes implicated in drug−drug interactions. Pharmacokinetic evaluation in mice indicated complete bioavailability and >3-fold higher exposure of **40** compared to **3**. The effect of **40** in a glucose tolerance test in mice indicated an effect comparable to sitagliptin at 10 mg/kg after oral administration and maximal effect reached at 50 mg/kg. Altogether, **40** appears as a promising candidate for more advanced animal studies and further development of improved therapeutics for T2D.

EXPERIMENTAL SECTION

All commercial starting materials and solvents were used without further purification, unless otherwise stated. THF was freshly distilled from sodium/benzophenone. Purification by flash chromatography was carried out using silica gel 60 (0.040−0.063 mm, Merck). TLC analysis was performed on silica gel 60 F_{254} plates. ^{1}H and ^{13}C NMR spectra were calibrated relative to TMS internal standard or residual solvent peak. High-resolution mass spectra (HRMS) were obtained on Thermo Finnigan TSQ 700 using electrospray ionization (ESI) or

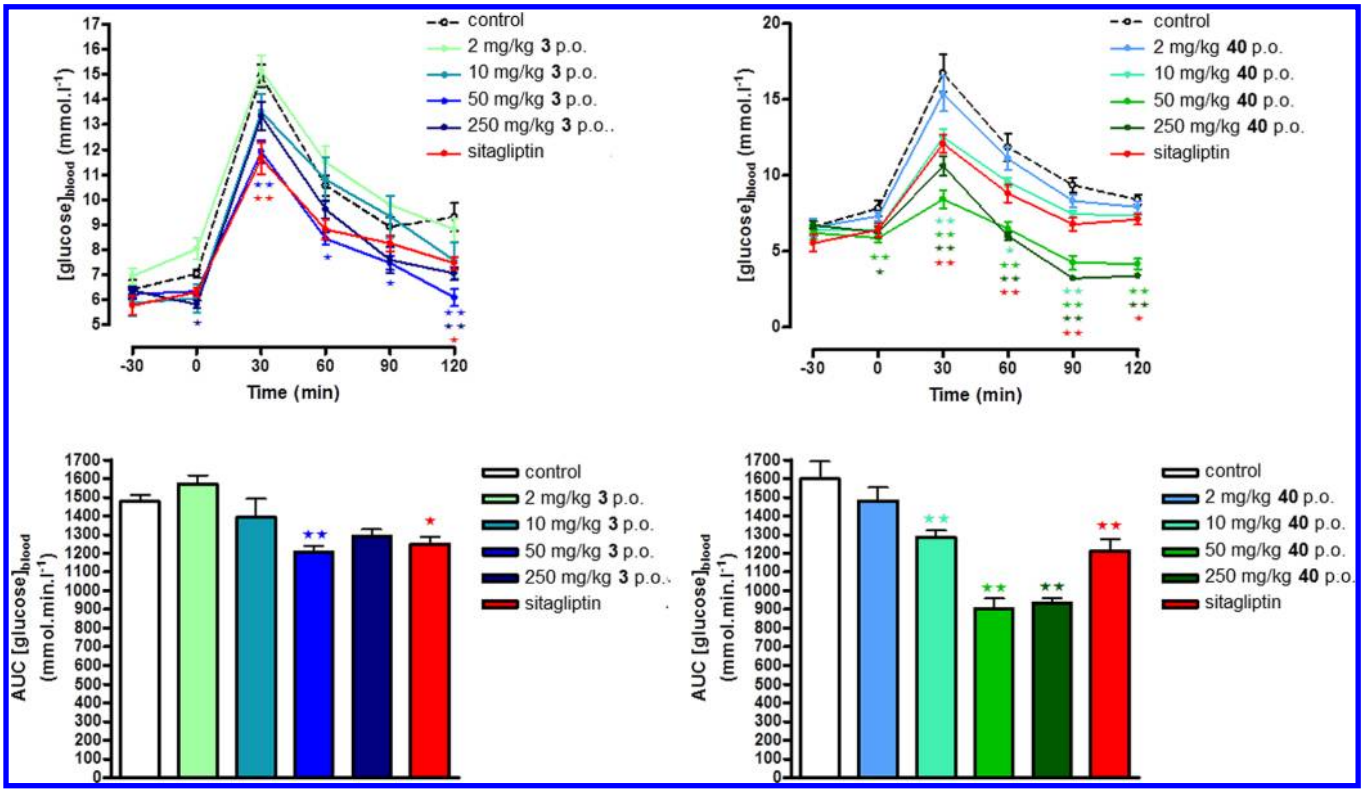

Figure 3. Effect of **3** and **40** on glucose tolerance in normal mice. Male C57Bl/6 mice were dosed po with test compound, vehicle, or positive control (sitagliptin, 10 mg/kg) 30 min prior to a 2 g/kg glucose challenge. Top panels show plasma glucose concentration curves as a function of time, and bottom panels show areas under the curves. Means ± standard errors (n = 6) are shown (*, $p < 0.05$; **, $p < 0.01$).

dx.doi.org/10.1021/jm301470a | J. Med. Chem. 2013, 56, 982−992

Bruker micrOTOF-Q II (ESI). Purity was determined by HPLC and confirmed by inspection of NMR spectra. HPLC analysis was performed using a Dionex 120 C18 column (5 μm, 4.6 × 150 mm) with 10% acetonitrile in water (0−1 min), 10−100% acetonitrile in water (1−10 min), 100% acetonitrile (11−15 min), with both solvents containing 0.05% TFA as modifier; a flow of 1 mL/min; and UV detection at 230 and 254 nm. All test compounds were of ≥95% purity unless otherwise stated.

General Procedure I: Sonogashira Coupling. A Schlenk flask charged with Na_2PdCl_4 (1 mol %), 2-(di-*tert*-butylphosphino)-*N*-phenylindole (PIntB, 2 mol %), CuI (2 mol %), alkyne (1 equiv), aryl halide (1.1−1.5 equiv), H_2O (0.2 mL/mmol), and TMEDA (1.8 mL/mmol) was evacuated and back-filled with argon three times and then heated to 80 °C. After consumption of the alkyne, the reaction was cooled to room temperature, water was added, and the mixture was extracted with EtOAc (×3). The organic phases were combined, washed with brine, dried over $MgSO_4$, and concentrated under vacuum. The residue was purified by flash chromatography and dried under vacuum to give the desired product.

General Procedure II: Ester Hydrolysis. A solution of $LiOH·H_2O$ (2−3 equiv) in H_2O (~2 mL/mmol ester) was added to the ester dissolved in THF (~5 mL/mmol ester). The reaction was stirred at room temperature until complete consumption of the starting material as indicated by TLC, typically after 1−12 h. The reaction had water added, was acidified with 3% HCl until pH <1, and was extracted with EtOAc (×3). The combined extracts were washed with brine, dried over $MgSO_4$, and concentrated under vacuum.

*3-(4-((3-(Methoxymethyl)phenyl)ethynyl)phenyl)propanoic Acid (**35**). Step 1.* **35a** was prepared from **1**[34] (93 mg, 0.49 mmol) and 1-bromo-3-(methoxymethyl)benzene (99 mg, 0.49 mmol) according to the general procedure I to give 96 mg (64%) of a clear oily product after purification by flash chromatography (SiO_2, EtOAc:petroleum ether, 1:10): R_f = 0.22 (EtOAc:petroleum ether, 1:4); ^{1}H NMR ($CDCl_3$) δ 7.51 (s, 1H), 7.47−7.42 (m, 3H), 7.36−7.27 (m, 2H), 7.21−7.16 (m, 2H), 4.45 (s, 2H), 3.67 (s, 3H), 3.40 (s, 3H), 2.96 (t, J = 7.7 Hz, 2H), 2.64 (t, J = 7.8 Hz, 2H); ^{13}C NMR ($CDCl_3$) δ 173.1, 140.9, 138.5, 131.8, 130.8, 128.44, 128.36, 127.5, 123.5, 121.2, 89.4, 89.0, 74.2, 58.2, 51.7, 35.4, 30.8.

Step 2. **35** was prepared from **35a** (76 mg, 0.25 mmol) according to the general procedure II to give 61 mg (84%) of a white solid (t_R = 11.96, purity 98.7% by HPLC); ^{1}H NMR (acetone-d_6) δ 7.55−7.43 (m, 4H), 7.42−7.29 (m, 4H), 4.46 (s, 2H), 3.36 (s, 3H), 2.95 (t, J = 7.6 Hz, 2H), 2.65 (t, J = 7.6 Hz, 2H); ^{13}C NMR (acetone-d_6) δ 173.8, 142.9, 140.3, 132.4, 131.19, 131.15, 129.6, 129.4, 128.3, 124.1, 121.7, 90.0, 89.6, 74.3, 58.2, 35.5, 31.4; ESI-HRMS calcd for $C_{19}H_{18}O_3Na$ (M + Na^+) 317.1148, found 317.1159.

*3-(4-((5-Cyano-2-methylphenyl)ethynyl)phenyl)propanoic Acid (**39**). Step 1.* **39a** was prepared from **1**[34] (98 mg, 0.52 mmol) and 3-iodo-4-methylbenzonitrile (136 mg, 0.56 mmol) according to the general procedure I to give 104 mg (68%) of a clear oily product after purification by flash chromatography (SiO_2, EtOAc:petroleum ether, 1:10): R_f = 0.20 (EtOAc:petroleum ether, 1:5); ^{1}H NMR ($CDCl_3$) δ 7.75 (d, J = 1.7 Hz, 1H), 7.49 (d, J = 1.7 Hz, 1H), 7.48−7.44 (m, 2H), 7.33 (d, J = 8.0 Hz, 1H), 7.24−7.18 (m, 2H), 3.68 (s, 3H), 2.98 (t, J = 7.7 Hz, 2H), 2.65 (t, J = 7.7 Hz, 2H), 2.56 (s, 3H); ^{13}C NMR ($CDCl_3$) δ 173.0, 145.5, 141.7, 135.1, 131.8, 131.2, 130.3, 128.5, 124.8, 120.5, 118.4, 110.0, 95.6, 85.7, 51.7, 35.3, 30.9, 21.2; ESI-MS m/z 326.1 (M + Na^+).

Step 2. **39** was prepared from **39a** (91 mg, 0.30 mmol) according to the general procedure II to give 83 mg (96%) of a white solid (t_R = 12.08, purity: 99% by HPLC); ^{1}H NMR ($CDCl_3$) δ 11.20 (s, 1H), 7.75 (d, J = 1.7 Hz, 1H), 7.52−7.44 (m, 3H), 7.33 (d, J = 8.0 Hz, 1H), 7.23 (d, J = 8.3 Hz, 2H), 2.99 (t, J = 7.6 Hz, 2H), 2.71 (t, J = 7.7 Hz, 2H), 2.56 (s, 3H); ^{13}C NMR ($CDCl_3$) δ 178.3, 145.5, 141.3, 135.1, 131.9, 131.2, 130.4, 128.5, 124.8, 120.6, 118.4, 110.0, 95.5, 85.8, 35.2, 30.5, 21.2; ESI-HRMS calcd for $C_{19}H_{15}NO_2Na$ (M + Na^+) 312.0996, found 312.0983.

*3-(4-((2-(Cyanomethyl)phenyl)ethynyl)phenyl)propanoic Acid (**40**). Step 1.* **40a** was prepared from **1**[34] (250 mg, 1.33 mmol) and 2-(2-iodophenyl)acetonitrile (354 mg, 1.45 mmol) according to the general procedure I to give 312 mg (77%) of a white solid after purification by flash chromatography (SiO_2, EtOAc:petroleum ether, 1:4): R_f = 0.08 (EtOAc:petroleum ether, 1:4); ^{1}H NMR ($CDCl_3$) δ 7.55−7.46 (m, 4H), 7.37−7.34 (m, 2H), 7.21 (d, J = 8.4 Hz, 2H), 3.96 (s, 2H), 3.67 (s, 3H), 2.97 (t, J = 7.7 Hz, 2H), 2.64 (t, J = 7.5 Hz, 2H); ^{13}C NMR ($CDCl_3$) δ 173.0, 141.6, 132.3, 131.7, 131.6, 128.9, 128.5, 128.1, 122.9, 120.4, 117.4, 95.6, 85.7, 51.7, 35.3, 30.8, 22.7; ESI-MS m/z 326.1 (M + Na^+).

Step 2. **40** was prepared from **40a** (292 mg, 0.96 mmol) according to the general procedure II to give 216 mg (77%) of a white solid (t_R = 11.44, purity: 99.9% by HPLC) after purification by flash chromatography [SiO_2, EtOAc (with 1% AcOH):petroleum ether, 1:2]; ^{1}H NMR (DMSO-d_6) δ 11.87 (br s, OH), 7.31−7.21 (m, 4H), 7.16−7.12 (m, 2H), 7.03−7.00 (m, 2H), 3.87 (s, 2H), 2.57 (t, J = 7.5 Hz, 2H), 2.27 (t, J = 7.5 Hz, 2H); ^{13}C NMR (DMSO-d_6) δ 173.6, 142.3, 132.8, 132.0, 131.4, 129.3, 128.9, 128.7, 128.3, 122.2, 119.6, 118.4, 95.3, 85.9, 34.8, 30.3, 22.1; ESI-HRMS calcd for $C_{19}H_{15}NO_2Na$ (M + Na^+) 312.0996, found 312.1002.

■ ASSOCIATED CONTENT

Ⓢ Supporting Information

Synthetic procedures and compound characterization, evaluation of log *P* calculation methods, and biological assays. This material is available free of charge via the Internet at http://pubs.acs.org.

■ AUTHOR INFORMATION

Corresponding Author

*Tel: +45 6550 2568. Fax: +45 6615 8780. E-mail: ulven@sdu.dk.

Notes

The authors declare no competing financial interest.

■ ACKNOWLEDGMENTS

We thank Lone Overgaard Storm for excellent technical assistance and the Danish Council for Independent Researchl Technology and Production (grant 09-070364) and the Danish Council for Strategic Research (grant 11-116196) for financial support.

■ ABBREVIATIONS USED

DMR, dynamic mass redistribution; DPP-4, dipeptidyl peptidase 4; FFA1, free fatty acid receptor 1 (GPR40); FFA2, free fatty acid receptor 2 (GPR43); FFA3, free fatty acid receptor 3 (GPR41); GSIS, glucose-stimulated insulin secretion; HLM, human liver microsomes; LLE, ligand lipophilicity efficiency; PIntB, 2-(di-*tert*-butylphosphino)-1-phenylindole; SPhos, 2-dicyclohexylphosphino-2′,6′-dimethoxybiphenyl; T2D, type 2 diabetes.

■ REFERENCES

(1) Danaei, G.; Finucane, M. M.; Lu, Y.; Singh, G. M.; Cowan, M. J.; Paciorek, C. J.; Lin, J. K.; Farzadfar, F.; Khang, Y.-H.; Stevens, G. A.; Rao, M.; Ali, M. K.; Riley, L. M.; Robinson, C. A.; Ezzati, M. National, regional, and global trends in fasting plasma glucose and diabetes prevalence since 1980: Systematic analysis of health examination surveys and epidemiological studies with 370 country-years and 2.7 million participants. *Lancet* **2011**, *378*, 31−40.

(2) WHO, Diabetes, Fact Sheet No. 312, August 2011.

(3) Itoh, Y.; Kawamata, Y.; Harada, M.; Kobayashi, M.; Fujii, R.; Fukusumi, S.; Ogi, K.; Hosoya, M.; Tanaka, Y.; Uejima, H.; Tanaka, H.; Maruyama, M.; Satoh, R.; Okubo, S.; Kizawa, H.; Komatsu, H.; Matsumura, F.; Noguchi, Y.; Shinobara, T.; Hinuma, S.; Fujisawa, Y.; Fujino, M. Free fatty acids regulate insulin secretion from pancreatic beta cells through GPR40. *Nature* **2003**, *422*, 173−176.

(4) Briscoe, C. P.; Tadayyon, M.; Andrews, J. L.; Benson, W. G.; Chambers, J. K.; Eilert, M. M.; Ellis, C.; Elshourbagy, N. A.; Goetz, A. S.; Minnick, D. T.; Murdock, P. R.; Sauls, H. R.; Shabon, U.; Spinage, L. D.; Strum, J. C.; Szekeres, P. G.; Tan, K. B.; Way, J. M.; Ignar, D. M.; Wilson, S.; Muir, A. I. The orphan G protein-coupled receptor GPR40 is activated by medium and long chain fatty acids. *J. Biol. Chem.* **2003**, *278*, 11303−11311.
(5) Kotarsky, K.; Nilsson, N. E.; Flodgren, E.; Owman, C.; Olde, B. A human cell surface receptor activated by free fatty acids and thiazolidinedione drugs. *Biochem. Biophys. Res. Commun.* **2003**, *301*, 406−410.
(6) Stoddart, L. A.; Smith, N. J.; Milligan, G. International union of pharmacology. LXXI. Free fatty acid receptors FFA1,-2, and-3: Pharmacology and pathophysiological functions. *Pharmacol. Rev.* **2008**, *60*, 405−417.
(7) Edfalk, S.; Steneberg, P.; Edlund, H. Gpr40 is expressed in enteroendocrine cells and mediates free fatty acid stimulation of incretin secretion. *Diabetes* **2008**, *57*, 2280−2287.
(8) Holliday, N. D.; Watson, S. J.; Brown, A. J. Drug discovery opportunities and challenges at G protein coupled receptors for long chain free fatty acids. *Front. Endocrinol.* **2011**, *2*, 112.
(9) Briscoe, C. P.; Peat, A. J.; McKeown, S. C.; Corbett, D. F.; Goetz, A. S.; Littleton, T. R.; McCoy, D. C.; Kenakin, T. P.; Andrews, J. L.; Ammala, C.; Fornwald, J. A.; Ignar, D. M.; Jenkinson, S. Pharmacological regulation of insulin secretion in MIN6 cells through the fatty acid receptor GPR40: Identification of agonist and antagonist small molecules. *Br. J. Pharmacol.* **2006**, *148*, 619−628.
(10) Garrido, D. M.; Corbett, D. F.; Dwornik, K. A.; Goetz, A. S.; Littleton, T. R.; McKeown, S. C.; Mills, W. Y.; Smalley, T. L.; Briscoe, C. P.; Peat, A. J. Synthesis and activity of small molecule GPR40 agonists. *Bioorg. Med. Chem. Lett.* **2006**, *16*, 1840−1845.
(11) McKeown, S. C.; Corbett, D. F.; Goetz, A. S.; Littleton, T. R.; Bigham, E.; Briscoe, C. P.; Peat, A. J.; Watson, S. P.; Hickey, D. M. B. Solid phase synthesis and SAR of small molecule agonists for the GPR40 receptor. *Bioorg. Med. Chem. Lett.* **2007**, *17*, 1584−1589.
(12) Song, F. B.; Lu, S. F.; Gunnet, J.; Xu, J. Z.; Wines, P.; Proost, J.; Liang, Y.; Baumann, C.; Lenhard, J.; Murray, W. V.; Demarest, K. T.; Kuo, G. H. Synthesis and biological evaluation of 3-aryl-3-(4-phenoxy)-propionic acid as a novel series of G protein-coupled receptor 40 agonists. *J. Med. Chem.* **2007**, *50*, 2807−2817.
(13) Christiansen, E.; Urban, C.; Merten, N.; Liebscher, K.; Karlsen, K. K.; Hamacher, A.; Spinrath, A.; Bond, A. D.; Drewke, C.; Ullrich, S.; Kassack, M. U.; Kostenis, E.; Ulven, T. Discovery of potent and selective agonists for the free fatty acid receptor 1 (FFA1/GPR40), a potential target for the treatment of type II diabetes. *J. Med. Chem.* **2008**, *51*, 7061−7064.
(14) Tikhonova, I. G.; Sum, C. S.; Neumann, S.; Engel, S.; Raaka, B. M.; Costanzi, S.; Gershengorn, M. C. Discovery of novel agonists and antagonists of the free fatty acid receptor 1 (FFAR1) using virtual screening. *J. Med. Chem.* **2008**, *51*, 625−633.
(15) Humphries, P. S.; Benbow, J. W.; Bonin, P. D.; Boyer, D.; Doran, S. D.; Frisbie, R. K.; Piotrowski, D. W.; Balan, G.; Bechle, B. M.; Conn, E. L.; Dirico, K. J.; Oliver, R. M.; Soeller, W. C.; Southers, J. A.; Yang, X. J. Synthesis and SAR of 1,2,3,4-tetrahydroisoquinolin-1-ones as novel G-protein-coupled receptor 40 (GPR40) antagonists. *Bioorg. Med. Chem. Lett.* **2009**, *19*, 2400−2403.
(16) Tan, C. P.; Feng, Y.; Zhou, Y. P.; Eiermann, G. J.; Petrov, A.; Zhou, C. Y.; Lin, S. N.; Salituro, G.; Meinke, P.; Mosley, R.; Akiyama, T. E.; Einstein, M.; Kumar, S.; Berger, J. P.; Mills, S. G.; Thornberry, N. A.; Yang, L. H.; Howard, A. D. Selective small-molecule agonists of G protein-coupled receptor 40 promote glucose-dependent insulin secretion and reduce blood glucose in mice. *Diabetes* **2008**, *57*, 2211−2219.
(17) Negoro, N.; Sasaki, S.; Mikami, S.; Ito, M.; Suzuki, M.; Tsujihata, Y.; Ito, R.; Harada, A.; Takeuchi, K.; Suzuki, N.; Miyazaki, J.; Santou, T.; Odani, T.; Kanzaki, N.; Funami, M.; Tanaka, T.; Kogame, A.; Matsunaga, S.; Yasuma, T.; Momose, Y. Discovery of TAK-875: A potent, selective, and orally bioavailable GPR40 agonist. *ACS Med. Chem. Lett.* **2010**, *1*, 290−294.
(18) Christiansen, E.; Due-Hansen, M. E.; Urban, C.; Merten, N.; Pfleiderer, M.; Karlsen, K. K.; Rasmussen, S. S.; Steensgaard, M.; Hamacher, A.; Schmidt, J.; Drewke, C.; Petersen, R. K.; Kristiansen, K.; Ullrich, S.; Kostenis, E.; Kassack, M. U.; Ulven, T. Structure−activity study of dihydrocinnamic acids and discovery of the potent FFA1 (GPR40) agonist TUG-469. *ACS Med. Chem. Lett.* **2010**, *1*, 345−349.
(19) Christiansen, E.; Urban, C.; Grundmann, M.; Due-Hansen, M. E.; Hagesaether, E.; Schmidt, J.; Pardo, L.; Ullrich, S.; Kostenis, E.; Kassack, M. U.; Ulven, T. Identification of a potent and selective free fatty acid receptor 1 (FFA1/GPR40) agonist with favorable physicochemical and in vitro ADME properties. *J. Med. Chem.* **2011**, *54*, 6691−6703.
(20) Sasaki, S.; Kitamura, S.; Negoro, N.; Suzuki, M.; Tsujihata, Y.; Suzuki, N.; Santou, T.; Kanzaki, N.; Harada, M.; Tanaka, Y.; Kobayashi, M.; Tada, N.; Funami, M.; Tanaka, T.; Yamamoto, Y.; Fukatsu, K.; Yasuma, T.; Momose, Y. Design, synthesis, and biological activity of potent and orally available G protein-coupled receptor 40 agonists. *J. Med. Chem.* **2011**, *54*, 1365−1378.
(21) Negoro, N.; Sasaki, S.; Ito, M.; Kitamura, S.; Tsujihata, Y.; Ito, R.; Suzuki, M.; Takeuchi, K.; Suzuki, N.; Miyazaki, J.; Santou, T.; Odani, T.; Kanzaki, N.; Funami, M.; Tanaka, T.; Yasuma, T.; Momose, Y. Identification of fused-ring alkanoic acids with improved pharmacokinetic profiles that act as G protein-coupled receptor 40/free fatty acid recptor 1 agonists. *J. Med. Chem.* **2012**, *55*, 1538−1552.
(22) Mikami, S.; Kitamura, S.; Negoro, N.; Sasaki, S.; Suzuki, M.; Tsujihata, Y.; Miyazaki, T.; Ito, R.; Suzuki, N.; Miyazaki, J.; Santou, T.; Kanzaki, N.; Funami, M.; Tanaka, T.; Yasuma, T.; Momose, Y. Discovery of phenylpropanoic acid derivatives containing polar functionalities as potent and orally bioavailable G protein-coupled receptor 40 agonists for the treatment of type 2 diabetes. *J. Med. Chem.* **2012**, *55*, 3756−3776.
(23) Negoro, N.; Sasaki, S.; Mikami, S.; Ito, M.; Tsujihata, Y.; Ito, R.; Suzuki, M.; Takeuchi, K.; Suzuki, N.; Miyazaki, J.; Santou, T.; Odani, T.; Kanzaki, N.; Funami, M.; Morohashi, A.; Nonaka, M.; Matsunaga, S.; Yasuma, T.; Momose, Y. Optimization of (2,3-dihydro-1-benzofuran-3-yl)acetic acids: Discovery of a non-free fatty acid-like, highly bioavailable G protein-coupled receptor 40/free fatty acid receptor 1 agonist as a glucose-dependent insulinotropic agent. *J. Med. Chem.* **2012**, *55*, 3960−3974.
(24) Houze, J. B.; Zhu, L.; Sun, Y.; Akerman, M.; Qiu, W.; Zhang, A. J.; Sharma, R.; Schmitt, M.; Wang, Y.; Liu, J.; Liu, J.; Medina, J. C.; Reagan, J. D.; Luo, J.; Tonn, G.; Zhang, J.; Lu, J. Y.-L.; Chen, M.; Lopez, E.; Nguyen, K.; Yang, L.; Tang, L.; Tian, H.; Shuttleworth, S. J.; Lin, D. C. H. AMG 837: A potent, orally bioavailable GPR40 agonist. *Bioorg. Med. Chem. Lett.* **2012**, *22*, 1267−1270.
(25) Christiansen, E.; Due-Hansen, M. E.; Urban, C.; Grundmann, M.; Schroder, R.; Hudson, B. D.; Milligan, G.; Cawthorne, M. A.; Kostenis, E.; Kassack, M. U.; Ulven, T. Free fatty acid receptor 1 (FFA1/GPR40) agonists: Mesylpropoxy appendage lowers lipophilicity and improves ADME properties. *J. Med. Chem.* **2012**, *55*, 6624−6628.
(26) Brown, S. P.; Dransfield, P. J.; Vimolratana, M.; Jiao, X.; Zhu, L.; Pattaropong, V.; Sun, Y.; Liu, J.; Luo, J.; Zhang, J.; Wong, S.; Zhuang, R.; Guo, Q.; Li, F.; Medina, J. C.; Swaminath, G.; Lin, D. C. H.; Houze, J. B. Discovery of AM-1638: A potent and orally bioavailable GPR40/FFA1 full agonist. *ACS Med. Chem. Lett.* **2012**, *3*, 726−730.
(27) Leeson, P. D.; Springthorpe, B. The influence of drug-like concepts on decision-making in medicinal chemistry. *Nat. Rev. Drug Discovery* **2007**, *6*, 881−890.
(28) Hann, M. M. Molecular obesity, potency and other addictions in drug discovery. *MedChemComm* **2011**, *2*, 349−355.
(29) Waring, M. J. Lipophilicity in drug discovery. *Expert Opin. Drug Discovery* **2010**, *5*, 235−248.
(30) Gleeson, M. P. Generation of a set of simple, interpretable ADMET rules of thumb. *J. Med. Chem.* **2008**, *51*, 817−834.
(31) Walters, W. P.; Green, J.; Weiss, J. R.; Murcko, M. A. What do medicinal chemists actually make? A 50-year retrospective. *J. Med. Chem.* **2011**, *54*, 6405−6416.

(32) Tarcsay, A.; Nyiri, K.; Keseru, G. M. The impact of lipophilic efficiency on compound quality. *J. Med. Chem.* **2012**, *55*, 1252−1260.
(33) Lipinski, C. A.; Lombardo, F.; Dominy, B. W.; Feeney, P. J. Experimental and computational approaches to estimate solubility and permeability in drug discovery and development settings. *Adv. Drug Delivery Rev.* **1997**, *23*, 3−25.
(34) Christiansen, E.; Due-Hansen, M. E.; Ulven, T. A rapid and efficient Sonogashira protocol and improved synthesis of free fatty acid 1 (FFA1) receptor agonists. *J. Org. Chem.* **2010**, *75*, 1301−1304.
(35) Torborg, C.; Zapf, A.; Beller, M. Palladium catalysts for highly selective Sonogashira reactions of aryl and heteroaryl bromides. *ChemSusChem* **2008**, *1*, 91−96.
(36) Rai, R.; Katzenellenbogen, J. A. Guanidinophenyl-substituted enol lactones as selective, mechanism-based inhibitors of trypsin-like serine proteases. *J. Med. Chem.* **1992**, *35*, 4150−4159.
(37) Posner, G. H.; Whitten, C. E.; Sterling, J. J. New class of mixed cuprate(I) reagents, Het(R)Culi, which allow selective alkyl group transfer. *J. Am. Chem. Soc.* **1973**, *95*, 7788−7800.
(38) Alexakis, A.; Berlan, J.; Besace, Y. Organocopper conjugate addition-reaction in the presence of trimethylchlorosilane. *Tetrahedron Lett.* **1986**, *27*, 1047−1050.
(39) Joshi, G.; Adimurthy, S. New method for the synthesis of benzyl alkyl ethers mediated by $FeSO_4$. *Synth. Commun.* **2011**, *41*, 720−728.
(40) Hopkins, A. L.; Groom, C. R.; Alex, A. Ligand efficiency: A useful metric for lead selection. *Drug Discov. Today* **2004**, *9*, 430−431.
(41) Rosenkilde, M. M.; Benned-Jensen, T.; Frimurer, T. M.; Schwartz, T. W. The minor binding pocket: A major player in 7TM receptor activation. *Trends Pharmacol. Sci.* **2010**, *31*, 567−574.
(42) Ballesteros, J. A.; Weinstein, H. W. Integrated methods for the construction of three-dimensional models and computational probing of structure-function relations in G-protein coupled receptors. In *Methods in Neuroscience*; Sealfon, S. C., Conn, P. M., Eds.; Academic Press: San Diego, CA, 1995; Vol. *25*, pp 366−428.
(43) Schroder, R.; Janssen, N.; Schmidt, J.; Kebig, A.; Merten, N.; Hennen, S.; Muller, A.; Blattermann, S.; Mohr-Andra, M.; Zahn, S.; Wenzel, J.; Smith, N. J.; Gomeza, J.; Drewke, C.; Milligan, G.; Mohr, K.; Kostenis, E. Deconvolution of complex G protein-coupled receptor signaling in live cells using dynamic mass redistribution measurements. *Nat. Biotechnol.* **2010**, *28*, 943−950.
(44) Schmidt, J.; Liebscher, K.; Merten, N.; Grundmann, M.; Mielenz, M.; Sauerwein, H.; Christiansen, E.; Due-Hansen, M. E.; Ulven, T.; Ullrich, S.; Gomeza, J.; Drewke, C.; Kostenis, E. Conjugated linoleic acids mediate insulin release through islet G protein-coupled receptor FFA1/GPR40. *J. Biol. Chem.* **2011**, *286*, 11890−11894.
(45) Pontier, C.; Pachot, J.; Botham, R.; Lenfant, B.; Arnaud, P. HT29-MTX and Caco-2/TC7 monolayers as predictive models for human intestinal absorption: Role of the mucus layer. *J. Pharm. Sci.* **2001**, *90*, 1608−1619.

ACS Medicinal Chemistry Letters

Letter

pubs.acs.org/acsmedchemlett

Discovery of TUG-770: A Highly Potent Free Fatty Acid Receptor 1 (FFA1/GPR40) Agonist for Treatment of Type 2 Diabetes

Elisabeth Christiansen,[†] Steffen V. F. Hansen,[†] Christian Urban,[‡] Brian D. Hudson,[§] Edward T. Wargent,[∥] Manuel Grundmann,[⊥] Laura Jenkins,[§] Mohamed Zaibi,[∥] Claire J. Stocker,[∥] Susanne Ullrich,[#] Evi Kostenis,[⊥] Matthias U. Kassack,[‡] Graeme Milligan,[§] Michael A. Cawthorne,[∥] and Trond Ulven*[,†]

[†]Department of Physics, Chemistry and Pharmacy, University of Southern Denmark, Campusvej 55, DK-5230 Odense M, Denmark

[‡]Institute of Pharmaceutical and Medicinal Chemistry, University of Düsseldorf, Universitätsstrasse 1, D-40225 Düsseldorf, Germany

[§]Institute of Molecular, Cell and Systems Biology, College of Medical, Veterinary and Life Sciences, University of Glasgow, Glasgow G12 8QQ, Scotland, U.K.

[∥]Clore Laboratory, University of Buckingham, Hunter Street, Buckingham MK18 1EG, U.K.

[⊥]Institute of Pharmaceutical Biology, University of Bonn, Nussallee 6, D-53115 Bonn, Germany

[#]Department of Internal Medicine IV, Division of Endocrinology, Diabetology, Vascular Medicine, Nephrology and Clinical Chemistry, University of Tübingen, Otfried-Müller-Str. 10, 72076 Tübingen, Germany

Supporting Information

ABSTRACT: Free fatty acid receptor 1 (FFA1 or GPR40) enhances glucose-stimulated insulin secretion from pancreatic β-cells and currently attracts high interest as a new target for the treatment of type 2 diabetes. We here report the discovery of a highly potent FFA1 agonist with favorable physicochemical and pharmacokinetic properties. The compound efficiently normalizes glucose tolerance in diet-induced obese mice, an effect that is fully sustained after 29 days of chronic dosing.

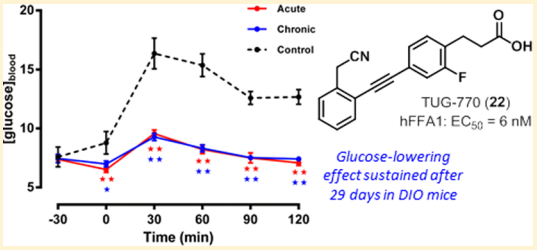

KEYWORDS: *Type 2 diabetes, free fatty acid receptor, TUG-770, insulin secretagogue, FFA1 agonist, GPR40 agonist*

The free fatty acid receptor 1 (FFA1, previously known as GPR40) has, since its deorphanization in 2003, received considerable attention as a new potential target for treatment of type 2 diabetes (T2D).[1−3] Activation of FFA1 increases glucose-stimulated insulin secretion but does not affect insulin secretion at low glucose levels, providing a potentially safe and efficient strategy for enhancing insulin levels in patients suffering from T2D. Accordingly, the interest in FFA1 as a new drug target has been high, and several potent agonists for the receptor have been disclosed.[4−6] Of these, TAK-875 is most advanced with highly encouraging results from phase II clinical trials.[7] Being a fatty acid receptor, FFA1 has a natural preference for relatively lipophilic compounds. This property has been reflected in the majority of the reported synthetic agonists, which mostly have been at the high end of the generally recommended lipophilicity range. We have previously reported a series of alkyne FFA1 agonists[8] and have subsequently directed our efforts toward lowering the lipophilicity of these compounds.[9,10] Herein, we report the further optimization of this compound series, leading to a highly potent FFA1 agonist with excellent physicochemical and pharmacokinetic properties and sustained glucose lowering capability in diet-induced obese (DIO) mice after acute and chronic dosing.

The alkyne ligands with either pyridine or fluoro-substituted benzene as the central ring were synthesized from the corresponding 4-bromoaldehydes (Scheme 1). Initially, a Wittig reaction with the phosphonium ylide, formed in situ from ethyl bromoacetate and triphenylphosphine, provided the corresponding cinnamic esters. The double bond was reduced by $NaBH_4$ in the presence of catalytic $CoCl_2$.[11] Subsequently, Sonogashira coupling with phenylacetylene followed by a base promoted hydrolysis provided the alkyne ligands.[12]

The 2-fluoro substituted ligands were synthesized from the central intermediate **2**, prepared from aryl bromide **1** by an initial Sonogashira coupling with trimethylsilylacetylene and subsequent removal of the TMS-group (Scheme 2). A second Sonogashira coupling of **2** with various aryl halides followed by ester hydrolysis gave the alkyne ligands in moderate to high yields.

We set out to investigate modifications in the central ring of the alkyne ligands (Table 1). Compounds were tested on the human FFA1 in a calcium mobilization assay and counterscreened on the human FFA4 (previously GPR120)[13] because of the selectivity issues frequently observed for these receptors.[14] The central benzene ring was replaced by pyridine due to its marked lipophilicity lowering effect. The 2-pyridyl

Received: February 17, 2013
Accepted: April 8, 2013
Published: April 8, 2013

   dx.doi.org/10.1021/ml4000673 | ACS Med. Chem. Lett. 2013, 4, 441−445

Scheme 1[a]

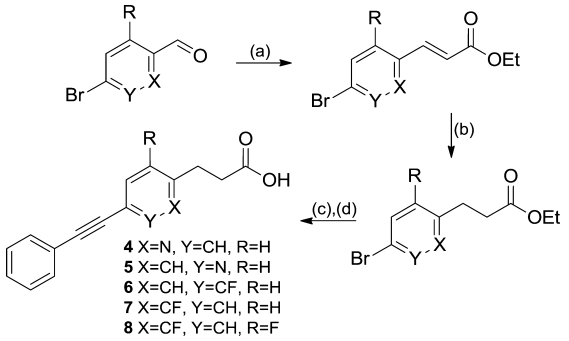

[a]Reagents and conditions: (a) ethyl bromoacetate, PPh_3, $NaHCO_3$, water, EtOAc, room temp, 18 h, 87−96%; (b) $CoCl_2 \cdot 6H_2O$, $NaBH_4$, MeOH, 0 °C → room temp, 3 h, 59−87%; (c) PhCCH, Na_2PdCl_4, 2-(di-*tert*-butylphosphino)-1-phenylindole (PIntB), CuI, TMEDA, water, 70 → 80 °C, 0.5−4.5 h, 56−86%; (d) LiOH, THF, water, room temp, 12 h, 79−97%.

Scheme 2[a]

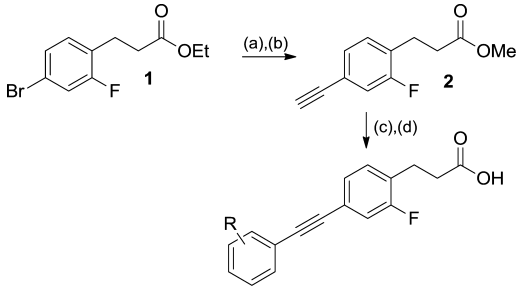

[a]Reagents and conditions: (a) trimethylsilylacetylene, Na_2PdCl_4, PIntB, CuI, TMEDA, water, 70 → 80 °C, 10 min; (b) K_2CO_3, MeOH, room temp, 2 h, 74% over two steps; (c) aryl halide, Na_2PdCl_4, PIntB, CuI, TMEDA, water, 80 °C, 1−4 h, 52−70%; (d) LiOH, THF, water, room temp, 12 h, 69−100%.

(**4**) and 3-pyridyl (**5**) analogues turned out to be twice as potent as previously reported ligands with pyridines as the terminal ring[9] but, nevertheless, resulted in >20-fold decrease in potency compared to **3**. Aromatic fluoro-substituents often result in higher metabolic stability and have been applied with success in the corresponding ring of other compound series.[15,16] Thus, we selected three mono- and difluoro-substituted analogues for synthesis and testing. The 3-fluoro analogue (**6**) showed maintained potency and only a small increase in ClogP compared to **3**. The 2-fluoro analogue (**7**) resulted in a 5-fold increased potency and the highest ligand efficiency (LE)[17] and ligand lipophilicity efficiency (LLE)[18] values and, moreover, the highest selectivity over FFA4 (>200-fold). Introduction of a second *ortho*-fluoro substituent (**8**) led to a reduction of potency back to the level of **6** and **3**.

With **7** showing high potency and LE, we decided to focus on the 2-fluoro scaffold in the exploration of the terminal ring in analogy with our previous studies (Table 2). Introduction of a corresponding 2-fluoro substituent in the lead structure TUG-424 (**9**) to give **10** resulted in increased potency but less so than for the terminally unsubstituted pair **3** and **7** (ΔpEC_{50} = 0.14 vs 0.78). Moving the methyl of the terminal ring to the *meta*-position (**11**) gave a further increase in potency. The order of potency is thus reversed relative to the analogues lacking the 2-fluoro substituent,[8] implying that previous SAR information is not directly transferrable to the 2-fluoro series.

Table 1. SAR Investigations of the Central Ring

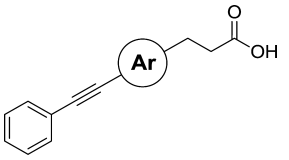

	Ar	hFFA1[a] pEC$_{50}$ (efficacy, %)	hFFA4[b] pEC$_{50}$ (efficacy, %)	ClogP[c]	LE / LLE[d]
3		6.70 ± 0.03 (106)	5.07 ± 0.08 (91)	4.54	0.48 2.16
4		5.67 ± 0.03 (92)	n.a.	3.04	0.41 2.63
5		5.60 ± 0.03 (99)	4.04 ± 0.03 (41)	3.04	0.40 2.56
6		6.84 ± 0.02 (100)	5.24 ± 0.03 (117)	4.68	0.47 2.16
7		7.48 ± 0.05 (100)	5.10 ± 0.01 (107)	4.68	0.51 2.80
8		6.85 ± 0.02 (108)	5.08 ± 0.02 (112)	4.83	0.45 2.02

[a]Efficacy is given as % response relative to 10 μM TUG-20.[19] [b]Efficacy is given as % response relative to **9**; n.a. = no activity (pEC_{50} < 4).[14] [c]Calculated by BioByte's algorithm as implemented in ChemBioDraw Ultra 12.0 (ClogP option). [d]LE = RTln K_D, presuming that $EC_{50} \approx K_D$. Values are given in kcal mol^{-1} per non-hydrogen atom.[17] LLE = pEC_{50} − ClogP.[18]

Introduction of a cyano-substituent on **10** to give the 2-methyl-5-cyano analogue (**12**) resulted in reduced ClogP together with doubled potency and increased selectivity over FFA4. The difluoromethyl analogue (**13**) was found to be more potent than **10** but only equipotent with **12**, despite its higher lipophilicity. The 3,5-dichloro analogue (**14**) was synthesized to mimic the previously published chloro-substituted pyridine alkyne TUG-499[9] but turned out only equipotent with TUG-499, despite its high lipophilicity.

Extension of the *ortho*- and *meta*-methyl with the hydrophilic mesyl group was explored (**15** and **16**) and resulted in significantly reduced ClogP values and improved LLE but unfortunately also markedly reduced potency. Methoxymethyl substituents on the terminal ring have previously shown good potency and significantly reduced lipophilicity in the alkyne series.[10] When adding larger substituents on the terminal ring of the alkyne ligands, the *meta*-substituted compounds (**18** and **20**) were found to be favored over the *ortho* analogues (**17** and **19**). Although all four analogues exhibited high selectivity over FFA4, the potency was found to be rather low (EC_{50} = 0.3−0.7 μM).

We then directed our attention to the cyanomethyl alkyne TUG-488 (**21**).[10] The corresponding 2-fluoro analogue **22** (TUG-770) showed a pronounced increase in potency on FFA1 (ΔpEC_{50} = 0.51) with EC_{50} = 6 nM and 150-fold selectivity over FFA4. Moving the cyanomethyl to the *meta*-position (**23**), which had been beneficial for the methyl analogue (**11**), led to 12-fold erosion of potency. Finally, homologation to the

dx.doi.org/10.1021/ml4000673 | ACS Med. Chem. Lett. 2013, 4, 441−445

Table 2. Structure–Activity Investigations of the 2-Fluoro Alkyne Agonists

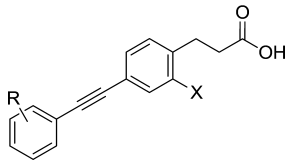

			pEC$_{50}$ (efficacy, %)				
compd	R^1	X	hFFA1, calcium[a]	hFFA4, BRET[b]	ClogP[c]	LE[d]	LLE[e]
9	2-Me	H	7.34 ± 0.07 (103)	5.84 ± 0.01 (103)	5.04	0.50	2.30
10	2-Me	F	7.48 ± 0.03 (107)	5.80 ± 0.03 (98)	5.18	0.49	2.30
11	3-Me	F	7.65 ± 0.03 (100)	5.41 ± 0.07 (124)	5.18	0.50	2.47
12	2-Me, 5-CN	F	7.77 ± 0.03 (104)	5.02 ± 0.04 (123)	4.62	0.46	3.15
13	2-CF_2H, 5-F	F	7.74 ± 0.04 (97)	5.93 ± 0.04 (117)	5.02	0.44	2.72
14	3,5-Cl	F	7.42 ± 0.07 (99)	5.50 ± 0.25 (90)	6.11	0.46	1.31
15	2-CH_2Ms	F	5.84 ± 0.02 (97)	n.a.	2.67	0.33	3.17
16	3-CH_2Ms	F	5.71 ± 0.02 (104)	4.19 ± 0.06 (26)	2.67	0.33	3.04
17	2-$CH_2O(CH_2)_2$Ms	F	6.21 ± 0.03 (94)	n.a.	3.33	0.31	2.88
18	3-$CH_2O(CH_2)_2$Ms	F	6.44 ± 0.03 (93)	n.a.	3.33	0.33	3.11
19	2-$CH_2O(CH_2)_3$Ms	F	6.14 ± 0.04 (92)	n.a.	3.59	0.30	2.55
20	3-$CH_2O(CH_2)_3$Ms	F	6.43 ± 0.04 (83)	n.a.	3.59	0.31	2.84
21	2-CH_2CN	H	7.70 ± 0.04 (103)	6.11 ± 0.06 (99)	3.96	0.48	3.76
22	2-CH_2CN	F	8.21 ± 0.03 (102)	6.03 ± 0.06 (98)	4.11	0.49	4.10
23	3-CH_2CN	F	7.13 ± 0.03 (104)	5.41 ± 0.07 (115)	4.11	0.42	3.02
24	2-CH_2CH_2CN	F	7.74 ± 0.04 (97)	5.86 ± 0.00 (114)	4.25	0.44	3.50

[a]Efficacy is given as % response relative to 10 μM TUG-20.[19] [b]Efficacy is given as % response relative to **9**; n.a. = no activity (pEC$_{50}$ < 4).[14] [c]Calculated by BioByte's algorithm as implemented in ChemBioDraw Ultra 12.0 (ClogP option). [d]LE = RTln K_D, presuming that EC$_{50}$ ≈ K_D. Values are given in kcal mol^{-1} per non-hydrogen atom.[17] [e]LLE = pEC$_{50}$ − ClogP.[18]

corresponding cyanoethyl (**24**) resulted in good potency but the compound could not compete with **22**.

With **22** being the clearly superior agonist in terms of potency and LLE, as well as displaying significantly higher potency (EC$_{50}$ = 6 vs 14 nM), lower lipophilicity (log $D_{7.4}$ = 1.41 vs 2.24) and higher ligand efficiency (LE = 0.49 vs 0.29) compared to the most advanced compound in the field TAK-875,[20] we set out to evaluate the compound further using our previously preferred compound **21** as reference (Table 3). Compound **22** displayed excellent physicochemical and in vitro ADME properties, with good aqueous solubility, good chemical stability, low lipophilicity, and decreased plasma protein binding (PPB). In support of the lower PPB, **21** showed significantly decreased activity on hFFA1 in a BRET assay in the presence of 0.1% BSA (from 7.16 ± 0.09 to 6.62 ± 0.05, p = 0.0024), whereas the corresponding reduction of activity for **22** was insignificant (from 7.64 ± 0.09 to 7.58 ± 0.06, p = 0.5635). Compound **22** furthermore showed excellent stability toward human liver microsomes (HLM), no inhibition of selected CYP-enzymes implicated in drug–drug interactions, no P-glycoprotein (P-gp) inhibition, and good permeability in the Caco-2 cell assay. Pharmacokinetic studies in mice showed a fast oral absorption, higher plasma concentration, a longer half-life, lower clearance, and increased bioavailability, overall giving a markedly improved pharmacokinetic profile compared to **21**. No cytotoxicity was observed in vitro in up to 100 μM concentration (see the Supporting Information), and no adverse effects were seen in mice after four weeks of daily oral treatment of 20 mg/kg and acute treatment in doses up to 250 mg/kg.

In addition to the counterscreen on FFA4, **22** showed a high selectivity over FFA2, FFA3, PPARγ, and 54 diverse receptors, transporters, and enzymes (see the Supporting Information). The compound exhibited lower potency on the rodent orthologs (mFFA1, pEC$_{50}$ = 6.83 ± 0.07 (n = 3); rFFA1, pEC$_{50}$ = 6.49 ± 0.05 (n = 2)). The effect of **22** was initially evaluated in vitro in

Table 3. Physicochemical Properties, in Vitro ADME, and Pharmacokinetics of 21 and 22

physicochemical properties	**21**	**22**
aqueous solubility (PBS, pH 7.4)[a]	196 μM	197 μM
chemical stab. (PBS, 37 °C, 12 days)	99.8%	99.1%
log D (n-octanol/PBS, pH 7.4)[b]	1.28 (1.32)	1.35 (1.44)
in vitro ADME properties[c]		
PPB (human)	>99.9%	97.3%
metabolic stability (HLM)	81%	87%
CYP inhibition (10 μM)		
CYP1A2	−3%	−10%
CYP2C9	11%	−33%
CYP2C19	−2%	−5%
CYP2D6	5%	−1%
CYP3A4	8%	−1%
P-gp inhibition (% @ 30/100 μM)	−4.0/−1.8	−4.4/−3.6
Caco-2 (A to B, TC7, pH 6.5/7.4)	91 × 10^{-6} cm/s	72 × 10^{-6} cm/s
pharmacokinetic properties[d]	**21**	**22**
Intravenous		
C_{max} (ng/mL)	5071	7811
t_{max} (min)	5	5
$t_{1/2}$ (min)	17	119
AUC$_{0-\infty}$ (μg/mL·min)	174	809
V_d (L/kg)	0.35	0.53
CL_{total} (mL/min/kg)	14	3.1
Oral		
C_{max}(ng/mL)	7757	12340
t_{max} (min)	30	15
$t_{1/2}$ (min)	50	355
AUC$_{0-\infty}$ (μg/mL·min)	732	4388
F (%)	105	136

[a]The maximum concentration of the assay is 200 μM. [b]Determined by shake-flask method.[16] The values given in parentheses were determined at Cerep Inc. [c]Determined at Cerep Inc. [d]Data are mean concentrations in mouse plasma (n = 3) following a single 2.5 mg/kg intravenous dose or 10 mg/kg oral dose.

dx.doi.org/10.1021/ml4000673 | ACS Med. Chem. Lett. 2013, 4, 441–445

the rat INS-1E cell line, performed as previously reported,[9] where the compound caused significantly increased insulin secretion (10.75 ± 0.74% of total content with 10 μM **22** vs 8.74 ± 0.54 with vehicle, $p < 0.05$) at high glucose concentration (12.4 mM) and, as expected, no effect (4.14 ± 0.15% of total content with 10 μM **22** vs 4.02 ± 0.08 with vehicle) at low glucose concentration (2.8 mM).

In vivo examination of **22** in an acute intraperitoneal glucose tolerance test (IPGTT) in normal mice revealed a good dose dependent response with maximal reduction in glucose level reached at 50 mg/kg (Figure 1). The study was followed up by

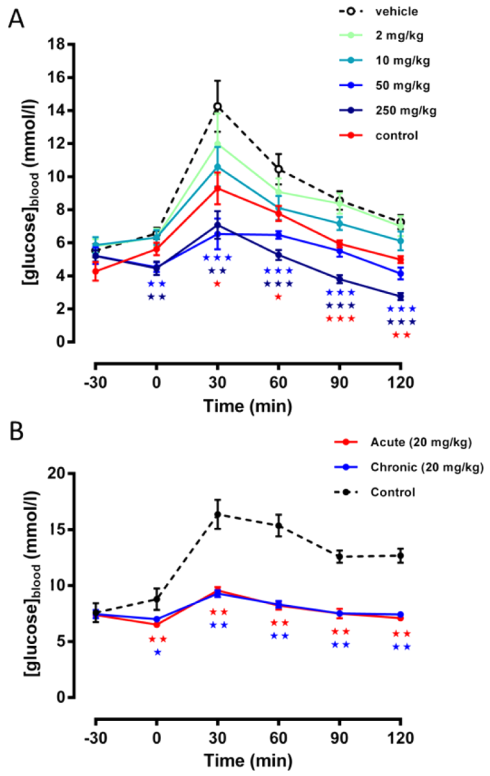

Figure 1. In vivo evaluation of **22** in mice on glucose tolerance. (A) Effect of **22** on acute IPGTT in normal mice. Mice were dosed ip with **22**, vehicle, or control (sitagliptin, 10 mg/kg). (B) Effect of **22** on OGTT in a chronic study in DIO mice: acute (4 weeks vehicle prior to treatment with **22**), chronic (4 weeks treatment with **22**), and control (vehicle). Means ± standard errors ($n = 6$) are shown (*, $p < 0.05$; **, $p < 0.01$; ***, $p < 0.001$).

a chronic oral glucose tolerance test (OGTT) study in DIO mice, which showed that **22** was more effective than **21** (see the Supporting Information) and that the effect of **22** was fully sustained after 29 days of daily oral treatment. Additional evaluation of **22** in rats confirmed a significant glucose lowering effect for the high doses already after 10 min and for all doses after 30 min (Figure 2). This was in agreement with an observed increase in plasma insulin concentration, with maximum concentration 15 min after glucose challenge. With an approximately 30-fold higher potency on human than on rodent receptors, it appears reasonable to expect that the effective dose would be correspondingly lower in humans.

In conclusion, optimization of the FFA1 alkyne agonists has resulted in the discovery of **22**, a highly potent FFA1 agonist with excellent physicochemical and pharmacokinetic properties.

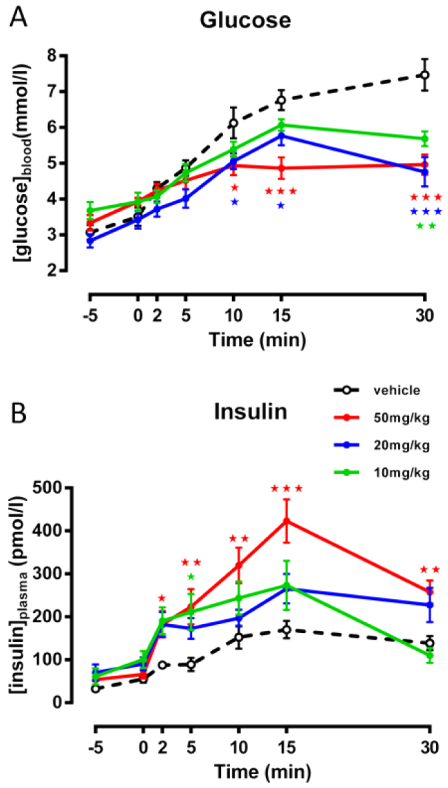

Figure 2. In vivo evaluation of **22** in Sprague–Dawley rats on glucose tolerance after oral dosing. (A) Effect on plasma glucose levels. (B) Effect on plasma insulin levels. Means ± standard errors ($n = 6$) are shown (*, $p < 0.05$; **, $p < 0.01$; ***, $p < 0.001$).

The compound demonstrated a potent effect on glucose tolerance in DIO mice, a situation that was sustained after 29 days of chronic dosing. The compound all together appears as a promising candidate for development of improved T2D therapeutics.

■ ASSOCIATED CONTENT

Supporting Information

Synthetic procedure, compound characterization, and biological assays. This material is available free of charge via the Internet at http://pubs.acs.org.

■ AUTHOR INFORMATION

Corresponding Author

*(T.U.) E-mail: ulven@sdu.dk.

Notes

The authors declare no competing financial interest.

■ ACKNOWLEDGMENTS

We thank Lone Overgaard Storm for excellent technical assistance and the Danish Council for Independent Research| Technology and Production (grant 09-070364), the Danish Council of Strategic Research (grant 11-116196), and the Canadian Institutes of Health Research (fellowship to B.D.H.) for financial support.

■ ABBREVIATIONS

BRET, bioluminescence resonance transfer; FFA1, free fatty acid receptor 1 (GPR40); IPGTT, intraperetoneal glucose

tolerance test; LE, ligand efficiency; LLE, ligand lipophilicity efficiency; OGTT, oral glucose tolerance test

REFERENCES

(1) Briscoe, C. P.; Tadayyon, M.; Andrews, J. L.; Benson, W. G.; Chambers, J. K.; Eilert, M. M.; Ellis, C.; Elshourbagy, N. A.; Goetz, A. S.; Minnick, D. T.; Murdock, P. R.; Sauls, H. R.; Shabon, U.; Spinage, L. D.; Strum, J. C.; Szekeres, P. G.; Tan, K. B.; Way, J. M.; Ignar, D. M.; Wilson, S.; Muir, A. I. The orphan G protein-coupled receptor GPR40 is activated by medium and long chain fatty acids. *J. Biol. Chem.* **2003**, *278*, 11303−11311.

(2) Itoh, Y.; Kawamata, Y.; Harada, M.; Kobayashi, M.; Fujii, R.; Fukusumi, S.; Ogi, K.; Hosoya, M.; Tanaka, Y.; Uejima, H.; Tanaka, H.; Maruyama, M.; Satoh, R.; Okubo, S.; Kizawa, H.; Komatsu, H.; Matsumura, F.; Noguchi, Y.; Shinobara, T.; Hinuma, S.; Fujisawa, Y.; Fujino, M. Free fatty acids regulate insulin secretion from pancreatic beta cells through GPR40. *Nature* **2003**, *422*, 173−176.

(3) Kotarsky, K.; Nilsson, N. E.; Flodgren, E.; Owman, C.; Olde, B. A human cell surface receptor activated by free fatty acids and thiazolidinedione drugs. *Biochem. Biophys. Res. Commun.* **2003**, *301*, 406−410.

(4) Medina, J. C.; Houze, J. B. GPR40 (FFAR1) modulators. *Annu. Rep. Med. Chem.* **2008**, *43*, 75−85.

(5) Holliday, N. D.; Watson, S. J.; Brown, A. J. Drug discovery opportunities and challenges at G protein coupled receptors for long chain free fatty acids. *Front. Endocrinol.* **2011**, *2*, 112.

(6) Blad, C. C.; Tang, C.; Offermanns, S. G protein-coupled receptors for energy metabolites as new therapeutic targets. *Nat. Rev. Drug Discovery* **2012**, *11*, 603−619.

(7) Burant, C. F.; Viswanathan, P.; Marcinak, J.; Cao, C.; Vakilynejad, M.; Xie, B.; Leifke, E. TAK-875 versus placebo or glimepiride in type 2 diabetes mellitus: a phase 2, randomised, double-blind, placebo-controlled trial. *Lancet* **2012**, *379*, 1403−1411.

(8) Christiansen, E.; Urban, C.; Merten, N.; Liebscher, K.; Karlsen, K. K.; Hamacher, A.; Spinrath, A.; Bond, A. D.; Drewke, C.; Ullrich, S.; Kassack, M. U.; Kostenis, E.; Ulven, T. Discovery of potent and selective agonists for the free fatty acid receptor 1 (FFA1/GPR40), a potential target for the treatment of type II diabetes. *J. Med. Chem.* **2008**, *51*, 7061−7064.

(9) Christiansen, E.; Urban, C.; Grundmann, M.; Due-Hansen, M. E.; Hagesaether, E.; Schmidt, J.; Pardo, L.; Ullrich, S.; Kostenis, E.; Kassack, M. U.; Ulven, T. Identification of a potent and selective free fatty acid receptor 1 (FFA1/GPR40) agonist with favorable physicochemical and in vitro ADME properties. *J. Med. Chem.* **2011**, *54*, 6691−6703.

(10) Christiansen, E.; Due-Hansen, M. E.; Urban, C.; Grundmann, M.; Schmidt, J.; Hansen, S. V. F.; Hudson, B. D.; Zaibi, M.; Markussen, S. B.; Hagesaether, E.; Milligan, G.; Cawthorne, M. A.; Kostenis, E.; Kassack, M. U.; Ulven, T. Discovery of a potent and selective free fatty acid receptor 1 agonist with low lipophilicity and high oral bioavailability. *J. Med. Chem.* **2013**, *56*, 982−992.

(11) Satoh, T.; Nanba, K.; Suzuki, S. Reduction of organic compounds with $NaBH_4$-transition metal salt systems 0.4. Selective hydrogenation of olefines in unsaturated esters. *Chem. Pharm. Bull.* **1971**, *19*, 817−820.

(12) Christiansen, E.; Due-Hansen, M. E.; Ulven, T. A rapid and efficient Sonogashira protocol and improved synthesis of free fatty acid 1 (FFA1) receptor agonists. *J. Org. Chem.* **2010**, *75*, 1301−1304.

(13) It was recently decided by IUPHAR to recommend the name FFA4 for the receptor previously known as GPR120 (http://www.iuphar.org).

(14) Shimpukade, B.; Hudson, B. D.; Hovgaard, C. K.; Milligan, G.; Ulven, T. Discovery of a potent and selective GPR120 agonist. *J. Med. Chem.* **2012**, *55*, 4511−4515.

(15) Sasaki, S.; Kitamura, S.; Negoro, N.; Suzuki, M.; Tsujihata, Y.; Suzuki, N.; Santou, T.; Kanzaki, N.; Harada, M.; Tanaka, Y.; Kobayashi, M.; Tada, N.; Funami, M.; Tanaka, T.; Yamamoto, Y.; Fukatsu, K.; Yasuma, T.; Momose, Y. Design, synthesis, and biological activity of potent and orally available G protein-coupled receptor 40 agonists. *J. Med. Chem.* **2011**, *54*, 1365−1378.

(16) Christiansen, E.; Due-Hansen, M. E.; Urban, C.; Grundmann, M.; Schroder, R.; Hudson, B. D.; Milligan, G.; Cawthorne, M. A.; Kostenis, E.; Kassack, M. U.; Ulven, T. Free fatty acid receptor 1 (FFA1/GPR40) agonists: mesylpropoxy appendage lowers lipophilicity and improves ADME properties. *J. Med. Chem.* **2012**, *55*, 6624−6628.

(17) Hopkins, A. L.; Groom, C. R.; Alex, A. Ligand efficiency: a useful metric for lead selection. *Drug Discovery Today* **2004**, *9*, 430−431.

(18) Leeson, P. D.; Springthorpe, B. The influence of drug-like concepts on decision-making in medicinal chemistry. *Nat. Rev. Drug Discovery* **2007**, *6*, 881−890.

(19) Christiansen, E.; Due-Hansen, M. E.; Urban, C.; Merten, N.; Pfleiderer, M.; Karlsen, K. K.; Rasmussen, S. S.; Steensgaard, M.; Hamacher, A.; Schmidt, J.; Drewke, C.; Petersen, R. K.; Kristiansen, K.; Ullrich, S.; Kostenis, E.; Kassack, M. U.; Ulven, T. Structure−activity study of dihydrocinnamic acids and discovery of the potent FFA1 (GPR40) agonist TUG-469. *ACS Med. Chem. Lett.* **2010**, *1*, 345−349.

(20) Negoro, N.; Sasaki, S.; Mikami, S.; Ito, M.; Suzuki, M.; Tsujihata, Y.; Ito, R.; Harada, A.; Takeuchi, K.; Suzuki, N.; Miyazaki, J.; Santou, T.; Odani, T.; Kanzaki, N.; Funami, M.; Tanaka, T.; Kogame, A.; Matsunaga, S.; Yasuma, T.; Momose, Y. Discovery of TAK-875: a potent, selective, and orally bioavailable GPR40 agonist. *ACS Med. Chem. Lett.* **2010**, *1*, 290−294.

Journal of Medicinal Chemistry

Brief Article

pubs.acs.org/jmc

Free Fatty Acid Receptor 1 (FFA1/GPR40) Agonists: Mesylpropoxy Appendage Lowers Lipophilicity and Improves ADME Properties

Elisabeth Christiansen,[†] Maria E. Due-Hansen,[†] Christian Urban,[‡] Manuel Grundmann,[§] Ralf Schröder,[§] Brian D. Hudson,[∥] Graeme Milligan,[∥] Michael A. Cawthorne,[⊥] Evi Kostenis,[§] Matthias U. Kassack,[‡] and Trond Ulven*[,†]

[†]Department of Physics, Chemistry and Pharmacy, University of Southern Denmark, Campusvej 55, DK-5230 Odense M, Denmark

[‡]Institute of Pharmaceutical and Medicinal Chemistry, University of Düsseldorf, Universitätsstrasse 1, D-40225 Düsseldorf, Germany

[§]Institute for Pharmaceutical Biology, University of Bonn, Nussallee 6, D-53115 Bonn, Germany

[∥]Molecular Pharmacology Group, Institute of Molecular, Cell and Systems Biology, College of Medical, Veterinary and Life Sciences, University of Glasgow, Glasgow G12 8QQ, Scotland, U.K.

[⊥]Clore Laboratory, University of Buckingham, Hunter Street, Buckingham MK18 1EG, U.K.

Supporting Information

ABSTRACT: FFA1 (GPR40) is a new target for treatment of type 2 diabetes. We recently identified the potent FFA1 agonist TUG-469 (**5**). Inspired by the structurally related TAK-875, we explored the effects of a mesylpropoxy appendage on **5**. The appendage significantly lowers lipophilicity and improves metabolic stability while preserving potency, resulting in discovery of the potent FFA1 agonist **13**.

INTRODUCTION

Current methods used for design, synthesis, screening, and optimization in drug discovery tend to produce compounds with higher than ideal lipophilicity, a property that recently has been repeatedly pointed at as a critical factor for the success of new potential drugs in the development stages because high lipophilicity is associated with poor absorption, metabolic instability, high promiscuity, toxic effects, and consequently a higher risk of attrition in clinical trials.[1−7] To counteract this, concepts such as ligand efficiency (LE, free energy binding divided by the number of non-hydrogen atoms),[8] ligand lipophilicity efficiency (LLE, logarithmic potency subtracted by log *P* or log *D*)[1] and ligand efficiency-dependent lipophilicity (LELP, log *P* divided by LE)[7] have been introduced and are increasingly being implemented in drug discovery programs and useful in directing optimization away from oversized and highly lipophilic compounds.

The free fatty acid receptor 1 (FFA1, also known as GPR40) is activated by medium- and long-chain free fatty acids (FFAs), is highly expressed on pancreatic *β*-cells, and enhances glucose-stimulated insulin secretion.[9−11] This observation has attracted considerable attention to the receptor as a new potential target for improved therapeutics for treatment of type 2 diabetes, and several potent and selective FFA1 agonists are now known (Chart 1).[12−26] Many of these ligands have relatively high lipophilicity, most likely resulting from fatty acids being used as initial leads and from the lipophilic nature of the FFA1 binding site. We recently addressed this issue in our alkyne series, where we were able to lower the lipophilicity of the compounds by replacing the terminal benzene ring by aromatic nitrogen containing heterocycles (cf. TUG-499 in Chart 1).[22]

In our program aimed at discovery of potent and selective FFA1 (GPR40) agonists, we identified 4-benzyloxydihydrocinnamic acid (TUG-20) in screening of a focused library of constrained FFA analogues.[19] Inspired by the subsequent publication of the related potent FFA1 agonist GW9508,[12] we explored the structure−activity relationships (SAR) around these compounds and found that whereas the central ether is favored for small compounds, a central amine is preferred when the structures are more extended such as for GW9508 and TUG-469.[19] The central amine has the additional advantage that it provides less lipophilic compounds. Takeda recently published their clinical candidate TAK-875, corresponding to a conformationally constrained analogue of TUG-469 with an

Chart 1. Representative FFA1 Agonists[a]

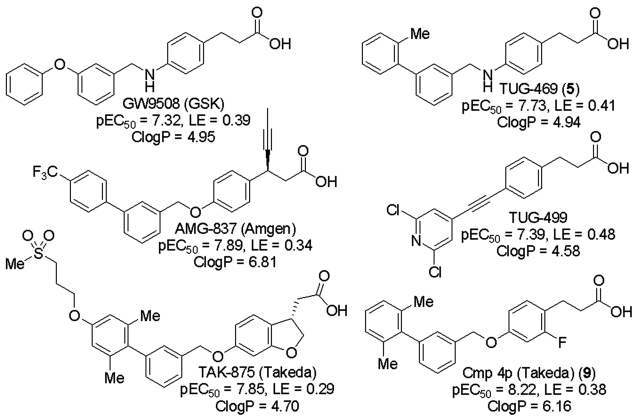

[a]ClogP is calculated by ChemBioDraw.

Received: February 14, 2012
Published: June 25, 2012

   dx.doi.org/10.1021/jm3002026 | *J. Med. Chem.* 2012, 55, 6624−6628

additional *ortho*-methyl and a *para*-mesylpropoxy chain on the biphenyl system and furthermore contains a central ether linker rather than the amine linker predicted by our SAR studies (Chart 1).[18] Calculations indicated that the mesylpropoxy appendage decrease lipophilicity by an order of magnitude. As the ClogP of **5** is in the uppermost part of the generally acceptable range, we were interested in exploring the effects of introducing a mesylpropoxy chain on this compound.

RESULTS AND DISCUSSION

Compounds **5**, **6**, and **9** were synthesized as described previously.[18−20] The mesylpropoxy-appended analogues **7** and **8** were synthesized as described for **5**[19] using the mesylpropoxy-substituted biphenyl building blocks **4b** and **4c**[18] (Scheme 1). The 2-fluoro substituted intermediate **3a** was prepared by a Heck coupling of **1** with ethyl acrylate followed by ester hydrolysis. Reductive amination of **2** with 2′-methylbiphenyl-3-carboxaldehyde followed by hydrogenation of the double bond over palladium provided **10** but in very poor yield (see Supporting Information (SI)). By swapping the first two steps and reducing **2** to **3a** followed by reductive coupling with **4d**, **4e**, and **4b**, compounds **11**−**13** were obtained, respectively, in moderate to good overall yields (Scheme 1).

Scheme 1[a]

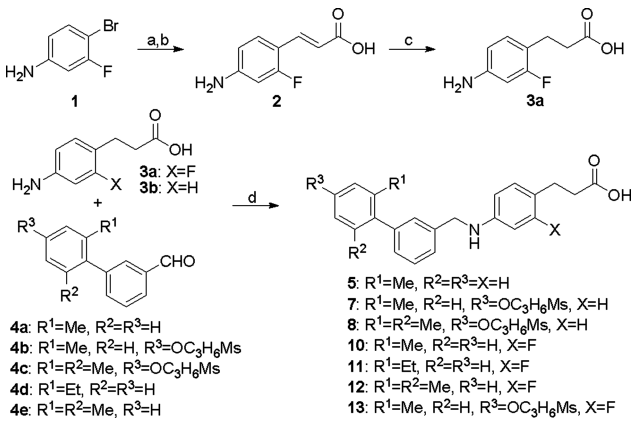

[a]Reagents, conditions and yields: (a) ethyl acrylate, $Pd(OAc)_2$, P(*o*-tolyl)$_3$, DIPEA, DMF, 80 °C, 4 h, 86%; (b) LiOH, THF, MeOH, H_2O, rt, 3 d, 99%; (c) Pd/C, MeOH, H_2, rt, 2 h, 73%; (d) $NaBH(OAc)_3$, CH_2Cl_2, AcOH (cat.), rt, 3−21 h, 38−67%.

In our assay, **5** is somewhat more potent than **6** (racemic TAK-875) but also more lipophilic, giving **6** a slightly higher LLE (Table 1). The potency of EC_{50} = 26 nM found for **6** is in excellent agreement with the activity reported by Takeda for TAK-875 (EC_{50} = 14 nM), given that this enantiomer is primarily responsible for the activity.[18] Takeda has also reported the racemic analogue of TAK-875 lacking the mesylpropoxy substituent to have pEC_{50} = 7.66, i.e., equipotent with TAK-875 when it is taken into account that one enantiomer is mainly responsible for the activity.[18] Thus, the mesylpropoxy tail appears to improve ADME properties by lowering lipophilicity rather than to increase potency.

We proceeded by attaching a corresponding mesylpropoxy tail to **5**. The resulting **7** indeed turned out equipotent with **5** but had lipophilicity reduced by one log unit and thereby obtained a significant advantage in terms of LLE. Introducing the second *ortho*-methyl group in the biphenyl system (**8**) resulted in a barely significant increase in potency and a drop in LLE due to increased lipophilicity.

The values for **6**−**8** in Table 1 are in the presence of 0.05% BSA. In the absence of BSA, the values were significantly lower (pEC_{50} 6.85 ± 0.04 for **6**, 7.46 ± 0.06 for **7**, and 7.52 ± 0.04 for **8**). BSA often reduces the observed potency by competitive binding of the ligand but can also increase potency by increasing solubility, presumably the explanation of the effects observed here.[27]

The precursor in the development of TAK-875 is the highly potent and lipophilic **9** (Cmp 4p in Chart 1), which differs from **5** in having a second *ortho*-methyl substituent on the biphenyl system, a central ether linker, and a 2-fluoro

Table 1. Effects of *para*-Mesylpropoxy Chain and Substituents on FFA1 Agonist Activity and Lipophilicity

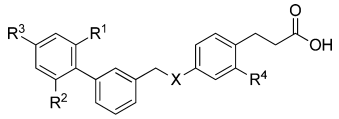

	R^1	R^2	R^3	R^4	X	FFA1 pEC_{50} (% efficacy)[a]	GPR120 pEC_{50} (% efficacy)	$LogD_{7.4}$ (ClogP)[b]	LE[c]	LLE[d]	HLM[e] (%)
5	Me	H	H	H	NH	7.73 ± 0.04 (114)	5.20 ± 0.02 (53)	2.49 ± 0.01 (4.9)	0.41	5.2 (2.8)	87
6[f]	Me	Me	MsC_3H_6O		O	7.59 ± 0.04 (91)[g]	n.t.[h]	2.24 ± 0.03 (4.7)	0.28	5.4 (2.9)	101
7	Me	H	MsC_3H_6O	H	NH	7.76 ± 0.03 (98)[g]	4.96 ± 0.07 (90)	1.43 ± 0.01 (3.9)	0.31	6.3 (3.8)	106
8	Me	Me	MsC_3H_6O	H	NH	7.83 ± 0.04 (92)[g]	n.t.[h]	1.77 ± 0.02 (4.4)	0.31	6.1 (3.7)	
9[i]	Me	Me	H	F	O	7.46 ± 0.04 (92)	5.08 ± 0.08 (82)	3.82 ± 0.13 (6.2)	0.37	3.6 (1.3)	42
10	Me	H	H	F	NH	8.03 ± 0.04 (102)	5.07 ± 0.04 (92)	2.86 ± 0.03 (5.4)	0.41	5.2 (2.7)	
11	Et	H	H	F	NH	7.63 ± 0.02 (101)	5.37 ± 0.08 (91)	2.88 ± 0.01 (5.9)	0.37	4.8 (1.7)	
12	Me	Me	H	F	NH	7.75 ± 0.02 (104)	4.03 ± 0.08 (78)	3.03 ± 0.04 (5.6)	0.38	4.7 (2.2)	
13	Me	H	MsC_3H_6O	F	NH	8.04 ± 0.02 (102)	4.36 ± 0.09 (66)	1.87 ± 0.01 (4.4)	0.32	6.2 (3.7)	100

[a]Efficacy is given as percentage of the full agonist TUG-20.[19] [b]$LogD_{7.4}$ values were determined by shake-flask procedure. ClogP values were calculated by the BioByte's algorithm as implemented in ChemBioDraw Ultra 12.0 (the "ClogP" option). [c]LE values were calculated by $-\Delta g = RT \ln K_D$, presuming $EC_{50} \approx K_D$.[8] [d]LLE values were calculated by the formula $pEC_{50} - LogD_{7.4}$ (values in parentheses were calculated by pEC_{50} − ClogP). [e]Stability toward human liver microsomes (HLM) was evaluated at Cerep Inc. (see the SI) [f]Racemic TAK-875 (structure in Chart 1). The pure (*S*)-enantiomer is previously reported by Takeda as with EC_{50} = 14 nM (pEC_{50} = 7.85) in a FLIPR assay with 0.1% BSA. [g]Tested with 0.05% BSA. [h]Not tested. [i]Previously reported by Takeda as an FFA1 agonist with EC_{50} = 5.7 nM (pEC_{50} = 8.22) in a FLIPR assay with 0.1% BSA.

dx.doi.org/10.1021/jm3002026 | *J. Med. Chem.* 2012, 55, 6624−6628

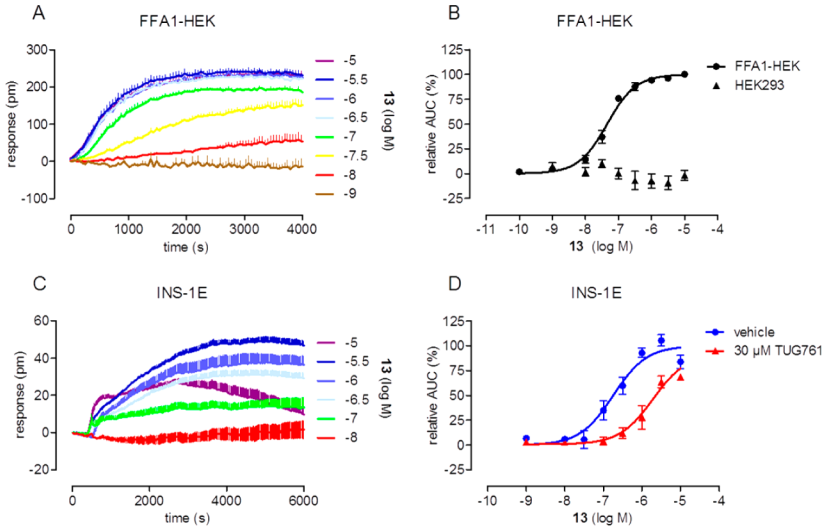

Figure 1. Activity of **13** on FFA1 transfected HEK293 cells and on the rat β-cell line INS-1E. (A) Representative traces (mean + SEM) from the dynamic mass redistribution (DMR) assay of HEK293 cells stably expressing the human FFA1 receptor (FFA1-HEK) and stimulated with the indicated concentrations of **13**. (B) Receptor activation in FFA1-HEK cells is concentration-dependent (pEC_{50}: 7.34 ± 0.06, n = 3); no activation is detectable in native HEK293 cells. (C) Representative traces from the DMR assay of INS-1E cells endogenously expressing FFA1. (D) Concentration-effect-curve of **13** on INS-1E cells (pEC_{50} = 6.74 ± 0.14, n = 6). Preincubation with the FFA1 antagonist TUG-761[22] (30 μM) resulted in a right-shifted curve (pEC_{50} = 5.71 ± 0.21, n = 3), confirming FFA1-dependent DMR responses.

substituent on the central benzene ring.[20] The compound surprisingly appeared significantly less potent in our assay than reported by Takeda. It is possible that the difference is related to Takeda using 0.1% BSA in the assay. We wished to explore the *ortho*-fluoro substituent, which was introduced by the Takeda group to resolve metabolic issues with preceding compounds but which also was found to slightly increase potency. Introducing the 2-fluoro substituent on **5** to give **10** indeed boosted potency to the single-digit nanomolar range but also increased lipophilicity correspondingly, leading to virtually unchanged or slightly decreased LE and LLE. Substituting the *ortho*-methyl for ethyl (**11**) gave a significant decrease in potency and a similar increase in lipophilicity. Surprisingly, a second *ortho*-methyl substituent (**12**) also resulted in decreased potency.

In an attempt to reach an optimal combination of high potency and moderate lipophilicity, the 2-fluoro substituent and the mesylpropoxy chain were introduced to **10** to give **13**. Again, whereas the two compounds exhibited identical potency, lipophilicity (ClogP and $logD_{7.4}$) was lowered by an order of magnitude. Despite the LE of **13** being significantly lower than **5** and **10** and that the compound exhibits an LLE value similar to **7** and **8**, we believe that **13** represents the optimal combination of high potency and acceptable lipophilicity in this series. In contrast to the other compounds with mesylpropoxy appendages, the potency of **13** was not affected by 0.05% BSA.

Lipophilicity is known to influence the metabolic stability by increasing interaction with enzymes. We found that **6** (racemic TAK-875), **7**, and **13** all were completely stable toward human liver microsomes, whereas the somewhat more lipophilic compound **5** had slightly reduced stability (Table 1). The significantly reduced stability of **9** (Chart 1) is in agreement with the higher lipophilicity of the compound.[24]

Compound **13** was examined further using a dynamic mass redistribution (DMR) assay, enabling real-time label-free detection of intracellular events.[28] Concentration dependent activation of hFFA1 transfected HEK293 cells was confirmed, with no detectable activity on native HEK293 cells (Figure 1). Likewise, **13** induced a concentration dependent response in insulin secreting rat β-cell line INS-1E endogenously expressing FFA1. Pretreatment with the FFA1 antagonist TUG-761[22] resulted in a right-shifted curve, and pretreatment with the selective FFA1 agonist TUG-499 (Chart 1 and ref 22) prevented activation by **13** (Figure S1, SI), demonstrating that the activity is mediated through FFA1. **13** was devoid of activity on the related receptors FFA2 and FFA3 (Figure S2, SI) and on nontransfected HEK293 cells in the DMR assays (Figure 1) and exhibited 4800-fold selectivity over GPR120, an order of magnitude higher than **5** (Table 1).

The pharmacokinetic properties of compounds **5** and **13** were investigated in mice. Both compounds were rapidly absorbed, and compound **13** exhibited twice as high exposure as **5** (Table 2). This effect can be rationalized by reduced first-pass metabolism due to the lower lipophilicity of **13**.

Table 2. Pharmacokinetic Parameters after Oral Dosing[a]

	C_{max} (ng/mL)	T_{max} (min)	AUC_{po} (ng·h/mL)
5	2360	15	2740
13	8748	15	5202

[a]Compounds were dosed p.o. at 10 mg/kg in mice (n = 3).

CONCLUSION

By combining features of the previously published compounds **5**, **6**, and **9**, we identified **13** as a compound with higher potency and lower lipophilicity than any previous FFA1 agonist. The 2-fluoro substituent increases both potency and lipophilicity by approximately the same degree and is therefore only an advantage as long as the compound is not already too lipophilic. The mesylpropoxy chain decreased lipophilicity by one log unit without affecting potency on FFA1. A consequence of the reduced lipophilicity was increased stability toward human liver microsomes. It seems possible that attachment of mesylalkoxy or similar groups can represent a general strategy for lowering the lipophilicity and thereby

dx.doi.org/10.1021/jm3002026 | J. Med. Chem. 2012, 55, 6624−6628

"rescuing" otherwise problematic compound series. The viability of this strategy is currently being explored on other compound series.

EXPERIMENTAL SECTION

All commercial starting materials and solvents were used without further purification unless otherwise stated. THF was freshly distilled from sodium/benzophenone. DIPEA was dried over 4 Å sieves, and anhydrous DMF was purchased from Sigma-Aldrich. Purification by flash chromatography was carried out using silica gel 60 (0.040−0.063 mm, Merck). ^{1}H and ^{13}C NMR spectra were recorded at 400 MHz and 101 MHz, respectively, and calibrated relative to TMS internal standard or residual solvent peak. High-resolution mass spectra (HRMS) were obtained on a Bruker micrOTOF-Q II (ESI). HPLC analysis was performed using a Dionex 120 C18 column (5 μ, 4.6 × 150 mm^2); flow, 1 mL/min; 10% acetonitrile in water (0−1 min), 10−100% acetonitrile in water (1−10 min), 100% acetonitrile (11−15 min), with both solvents containing 0.05% TFA as modifier; UV detection at 254 nm. Purity was determined by HPLC analysis and confirmed by inspection of NMR spectra. All target compounds have >95% purity.

(*E*)-3-(4-Amino-2-fluorophenyl)acrylic Acid (2). Step 1: A dry Schlenk flask was charged with 4-bromo-3-fluoroaniline (1140 mg, 6.01 mmol), $Pd(OAc)_2$ (67 mg, 0.30 mmol), tris(2-methylphenyl)-phosphine (182 mg, 0.60 mmol), DMF (4.2 mL), and DIPEA (4.2 mL) under N_2-flow. The flask was evacuated and backfilled with argon before addition of ethyl acrylate (0.8 mL, 7.36 mmol) and heated to 80 °C for 4 h. The reaction was cooled to room temperature, added water, and extracted with EtOAc. The organic phase was washed with water and brine, dried ($MgSO_4$), and concentrated. The residue was purified by flash chromatography (SiO_2, EtOAc:petroleum ether, 1:2) to give ethyl 4-amino-2-fluorocinnamate (1079 mg, 86%) as a yellow solid; R_f = 0.19 (EtOAc:petroleum ether, 1:2). ^{1}H NMR ($CDCl_3$) δ 7.71 (d, J = 16.1 Hz, 1H), 7.31 (t, J = 8.3 Hz, 1H), 6.42 (dd, J = 8.4 Hz, 2.3 Hz, 1H), 6.35 (dd, J = 12.6 Hz, 2.1 Hz, 1H), 6.32 (d, J = 16.1 Hz, 1H), 4.24 (q, J = 7.1 Hz, 2H), 4.08 (s, 2H), 1.32 (t, J = 7.1 Hz, 3H). ^{13}C NMR ($CDCl_3$) δ 167.6, 162.8 (d, J = 253.5 Hz), 150.2 (d, J = 12.1 Hz), 137.7 (d, J = 2.4 Hz), 130.4 (d, J = 5.1 Hz), 116.0 (d, J = 7.1 Hz), 112.5 (d, J = 13.1 Hz), 110.9 (d, J = 2.0 Hz), 101.6 (d, J = 26.3 Hz), 60.3, 14.3. Step 2: A solution of ethyl 4-amino-2-fluorocinnamate (1002 mg, 4.79 mmol) in THF (32 mL) was added to a solution of $LiOH·H_2O$ (567 mg, 20.0 mmol) in H_2O (16 mL), and MeOH (5 mL) was added to give a homogeneous solution. The reaction was stirred at room temperature until complete hydrolysis, then added aqueous HCl (1 M) until pH <2 and extracted with EtOAc (×3). The combined organic phases were washed with brine, dried ($MgSO_4$), and concentrated to give 858 mg (99%) of **2** as an orange solid; t_R = 8.03 min (HPLC). ^{1}H NMR (MeOH-d_4) δ 7.70 (d, J = 16.0 Hz, 1H), 7.36 (t, J = 8.5 Hz, 1H), 6.48 (dd, J = 8.5 Hz, 2.2 Hz, 1H), 6.38 (dd, J = 13.5 Hz, 2.2 Hz, 1H), 6.26 (d, J = 16.0 Hz, 1H), 4.91 (s, 2H). ^{13}C NMR (MeOH-d_4) δ 171.4, 164.5 (d, J = 250.5 Hz), 154.5 (d, J = 13.3 Hz), 139.9 (d, J = 3.0 Hz), 131.3 (d, J = 5.1 Hz), 115.1 (d, J = 7.1 Hz), 111.8 (d, J = 1.8 Hz), 111.5 (d, J = 12.1 Hz), 101.3 (d, J = 26.3 Hz).

3-(4-Amino-2-fluorophenyl)propanoic Acid (3a). To a solution of **2** (388 mg, 2.14 mmol) in MeOH (15 mL) was added 10% Pd/C (35 mg). The reaction mixture was placed under argon, the argon was replaced with H_2, and the reaction mixture was stirred under ambient pressure. After 2 h, the reaction mixture was filtered through Celite, concentrated, and purified by flash chromatography (SiO_2, EtOAc) to give **3a** (285 mg, 73%) as a pale-brown solid; t_R = 4.88 min (HPLC). ^{1}H NMR (DMSO-d_6) δ 12.09 (s, 1H), 6.89 (t, J = 8.7 Hz, 1H), 6.39−6.23 (m, 2H), 5.19 (s, 2H), 2.65 (t, J = 7.6 Hz, 2H), 2.40 (t, J = 7.7 Hz, 2H). ^{13}C NMR (DMSO-d_6) δ 173.7, 161.2 (d, J = 240.7 Hz), 149.0 (d, J = 11.5 Hz), 130.5 (d, J = 7.1 Hz), 113.3 (d, J = 16.5 Hz), 109.8 (d, J = 2.1 Hz), 100.2 (d, J = 25.0 Hz), 34.5, 23.2 (d, J = 2.1 Hz).

3-(2-Fluoro-4-(((2′-methyl-4′-(3-(methylsulfonyl)propoxy)-[1,1′-biphenyl]-3-yl)methyl)amino)-phenyl)propanoic Acid (13). A dry flask charged with 2′-methyl-4′-(3-(methylsulfonyl)-propoxy)-[1,1′-biphenyl]-3-carbaldehyde (**4b**, 35 mg, 0.11 mmol), 3-(4-amino-2-fluorophenyl)propanoic acid (**3a**, 19 mg, 0.11 mmol), CH_2Cl_2 (1 mL) and AcOH (1 drop) under argon was added $NaBH(OAc)_3$ (34 mg, 0.16 mmol) and stirred at room temperature until consumption of the starting material. The reaction mixture was quenched with water and aqueous HCl (1 M), and extracted with CH_2Cl_2. The combined organic phases were washed with brine, dried over ($MgSO_4$), and concentrated. The residue was purified by flash chromatography (SiO_2, EtOAc:petroleum ether, 1:2) to give 30 mg (58%) of **13** as a light-brown foam; R_f = 0.54 (EtOAc) (purity 98.1% by HPLC). ^{1}H NMR (acetone-d_6) δ 7.40−7.29 (m, 3H), 7.22−7.07 (m, 2H), 7.05−6.94 (m, 1H), 6.90−6.78 (m, 2H), 6.48−6.32 (m, 2H), 4.40 (s, 2H), 4.18 (t, J = 6.1 Hz, 2H), 3.35−3.26 (m, 2H), 2.99 (s, 3H), 2.77 (t, J = 7.7 Hz, 2H), 2.49 (t, J = 7.7 Hz, 2H), 2.34−2.19 (m, 2H), 2.18 (s, 3H). ^{13}C NMR (acetone-d_6) δ 174.3, 163.8 (d, J = 241.4 Hz), 158.9, 150.1 (d, J = 11.1 Hz), 142.6, 140.7, 137.4, 135.5, 131.7 (d, J = 8.1 Hz), 131.5, 129.1, 128.6, 126.4, 117.3, 115.5 (d, J = 16.2 Hz), 112.7, 109.7 (d, J = 2.0 Hz), 100.0 (d, J = 26.3 Hz), 66.6, 52.0, 48.0, 40.8, 30.1, 24.5 (d, J = 2.0 Hz), 24.5, 23.5, 20.8. ESI-MS calcd for $C_{27}H_{30}FNO_5SNa$ (M + Na^+), 500.1901; found, 500.1916.

ASSOCIATED CONTENT

Supporting Information

Synthetic procedures and compound characterization, procedures for $logD_{7.4}$ determination and biological assays. This material is available free of charge via the Internet at http://pubs.acs.org.

AUTHOR INFORMATION

Corresponding Author

*Phone: +45 6550 2568. Fax: +45 6615 8780. E-mail: ulven@sdu.dk.

Notes

The authors declare no competing financial interest.

ACKNOWLEDGMENTS

We thank Lone Overgaard Storm for excellent technical support, Corning and Perkin-Elmer for instrument support, and the Danish Council for Independent Research|Technology and Production (grant 09-070364) and the Danish Council for Strategic Research (grant 11-116196) for financial support.

ABBREVIATIONS USED

ADME, absorption distribution metabolism excretion; AUC, area under the curve; BSA, bovine serum albumin; DIPEA, diisopropylethylamine; DMR, dynamic mass redistribution; FFA, free fatty acid; FFA1, free fatty acid receptor 1 (GPR40); HEK, human embryonic kidney; SAR, structure−activity relationships

REFERENCES

(1) Leeson, P. D.; Springthorpe, B. The influence of drug-like concepts on decision-making in medicinal chemistry. *Nature Rev. Drug Discovery* **2007**, *6*, 881−890.

(2) Hann, M. M. Molecular obesity, potency and other addictions in drug discovery. *MedChemCommun* **2011**, *2*, 349−355.

(3) Waring, M. J. Lipophilicity in drug discovery. *Expert Opin. Drug Discovery* **2010**, *5*, 235−248.

(4) Gleeson, M. P. Generation of a set of simple, interpretable ADMET rules of thumb. *J. Med. Chem.* **2008**, *51*, 817−834.

(5) Walters, W. P.; Green, J.; Weiss, J. R.; Murcko, M. A. What Do Medicinal Chemists Actually Make? A 50-Year Retrospective. *J. Med. Chem.* **2011**, *54*, 6405−6416.

(6) Tarcsay, A.; Nyiri, K.; Keseru, G. M. The Impact of Lipophilic Efficiency on Compound Quality. *J. Med. Chem.* **2012**, *55*, 1252−1260.
(7) Keseru, G. M.; Makara, G. M. The influence of lead discovery strategies on the properties of drug candidates. *Nature Rev. Drug Discovery* **2009**, *8*, 203−212.
(8) Hopkins, A. L.; Groom, C. R.; Alex, A. Ligand efficiency: a useful metric for lead selection. *Drug Discovery Today* **2004**, *9*, 430−431.
(9) Itoh, Y.; Kawamata, Y.; Harada, M.; Kobayashi, M.; Fujii, R.; Fukusumi, S.; Ogi, K.; Hosoya, M.; Tanaka, Y.; Uejima, H.; Tanaka, H.; Maruyama, M.; Satoh, R.; Okubo, S.; Kizawa, H.; Komatsu, H.; Matsumura, F.; Noguchi, Y.; Shinobara, T.; Hinuma, S.; Fujisawa, Y.; Fujino, M. Free fatty acids regulate insulin secretion from pancreatic beta cells through GPR40. *Nature* **2003**, *422*, 173−176.
(10) Briscoe, C. P.; Tadayyon, M.; Andrews, J. L.; Benson, W. G.; Chambers, J. K.; Eilert, M. M.; Ellis, C.; Elshourbagy, N. A.; Goetz, A. S.; Minnick, D. T.; Murdock, P. R.; Sauls, H. R.; Shabon, U.; Spinage, L. D.; Strum, J. C.; Szekeres, P. G.; Tan, K. B.; Way, J. M.; Ignar, D. M.; Wilson, S.; Muir, A. I. The orphan G protein-coupled receptor GPR40 is activated by medium and long chain fatty acids. *J. Biol. Chem.* **2003**, *278*, 11303−11311.
(11) Kotarsky, K.; Nilsson, N. E.; Flodgren, E.; Owman, C.; Olde, B. A human cell surface receptor activated by free fatty acids and thiazolidinedione drugs. *Biochem. Biophys. Res. Commun.* **2003**, *301*, 406−410.
(12) Briscoe, C. P.; Peat, A. J.; McKeown, S. C.; Corbett, D. F.; Goetz, A. S.; Littleton, T. R.; McCoy, D. C.; Kenakin, T. P.; Andrews, J. L.; Ammala, C.; Fornwald, J. A.; Ignar, D. M.; Jenkinson, S. Pharmacological regulation of insulin secretion in MIN6 cells through the fatty acid receptor GPR40: identification of agonist and antagonist small molecules. *Br. J. Pharmacol.* **2006**, *148*, 619−628.
(13) Garrido, D. M.; Corbett, D. F.; Dwornik, K. A.; Goetz, A. S.; Littleton, T. R.; McKeown, S. C.; Mills, W. Y.; Smalley, T. L.; Briscoe, C. P.; Peat, A. J. Synthesis and activity of small molecule GPR40 agonists. *Bioorg. Med. Chem. Lett.* **2006**, *16*, 1840−1845.
(14) McKeown, S. C.; Corbett, D. F.; Goetz, A. S.; Littleton, T. R.; Bigham, E.; Briscoe, C. P.; Peat, A. J.; Watson, S. P.; Hickey, D. M. B. Solid phase synthesis and SAR of small molecule agonists for the GPR40 receptor. *Bioorg. Med. Chem. Lett.* **2007**, *17*, 1584−1589.
(15) Christiansen, E.; Urban, C.; Merten, N.; Liebscher, K.; Karlsen, K. K.; Hamacher, A.; Spinrath, A.; Bond, A. D.; Drewke, C.; Ullrich, S.; Kassack, M. U.; Kostenis, E.; Ulven, T. Discovery of potent and selective agonists for the free fatty acid receptor 1 (FFA1/GPR40), a potential target for the treatment of type II diabetes. *J. Med. Chem.* **2008**, *51*, 7061−7064.
(16) Tan, C. P.; Feng, Y.; Zhou, Y. P.; Eiermann, G. J.; Petrov, A.; Zhou, C. Y.; Lin, S. N.; Salituro, G.; Meinke, P.; Mosley, R.; Akiyama, T. E.; Einstein, M.; Kumar, S.; Berger, J. P.; Mills, S. G.; Thornberry, N. A.; Yang, L. H.; Howard, A. D. Selective small-molecule agonists of G protein-coupled receptor 40 promote glucose-dependent insulin secretion and reduce blood glucose in mice. *Diabetes* **2008**, *57*, 2211−2219.
(17) Zhou, C. Y.; Tang, C.; Chang, E.; Ge, M.; Lin, S. N.; Cline, E.; Tan, C. P.; Feng, Y.; Zhou, Y. P.; Eiermann, G. J.; Petrov, A.; Salituro, G.; Meinke, P.; Mosley, R.; Akiyama, T. E.; Einstein, M.; Kumar, S.; Berger, J.; Howard, A. D.; Thornberry, N.; Mills, S. G.; Yang, L. H. Discovery of 5-aryloxy-2,4-thiazolidinediones as potent GPR40 agonists. *Bioorg. Med. Chem. Lett.* **2010**, *20*, 1298−1301.
(18) Negoro, N.; Sasaki, S.; Mikami, S.; Ito, M.; Suzuki, M.; Tsujihata, Y.; Ito, R.; Harada, A.; Takeuchi, K.; Suzuki, N.; Miyazaki, J.; Santou, T.; Odani, T.; Kanzaki, N.; Funami, M.; Tanaka, T.; Kogame, A.; Matsunaga, S.; Yasuma, T.; Momose, Y. Discovery of TAK-875: A Potent, Selective, and Orally Bioavailable GPR40 Agonist. *ACS Med. Chem. Lett.* **2010**, *1*, 290−294.
(19) Christiansen, E.; Due-Hansen, M. E.; Urban, C.; Merten, N.; Pfleiderer, M.; Karlsen, K. K.; Rasmussen, S. S.; Steensgaard, M.; Hamacher, A.; Schmidt, J.; Drewke, C.; Petersen, R. K.; Kristiansen, K.; Ullrich, S.; Kostenis, E.; Kassack, M. U.; Ulven, T. Structure−activity study of dihydrocinnamic acids and discovery of the potent FFA1 (GPR40) agonist TUG-469. *ACS Med. Chem. Lett.* **2010**, *1*, 345−349.
(20) Sasaki, S.; Kitamura, S.; Negoro, N.; Suzuki, M.; Tsujihata, Y.; Suzuki, N.; Santou, T.; Kanzaki, N.; Harada, M.; Tanaka, Y.; Kobayashi, M.; Tada, N.; Funami, M.; Tanaka, T.; Yamamoto, Y.; Fukatsu, K.; Yasuma, T.; Momose, Y. Design, Synthesis, and Biological Activity of Potent and Orally Available G Protein-Coupled Receptor 40 Agonists. *J. Med. Chem.* **2011**, *54*, 1365−1378.
(21) Walsh, S. P.; Severino, A.; Zhou, C. Y.; He, J. F.; Liang, G. B.; Tan, C. P.; Cao, J.; Eiermann, G. J.; Xu, L.; Salituro, G.; Howard, A. D.; Mills, S. G.; Yang, L. H. 3-Substituted 3-(4-aryloxyaryl)-propanoic acids as GPR40 agonists. *Bioorg. Med. Chem. Lett.* **2011**, *21*, 3390−3394.
(22) Christiansen, E.; Urban, C.; Grundmann, M.; Due-Hansen, M. E.; Hagesaether, E.; Schmidt, J.; Pardo, L.; Ullrich, S.; Kostenis, E.; Kassack, M. U.; Ulven, T. Identification of a potent and selective free fatty acid receptor 1 (FFA1/GPR40) agonist with favorable physicochemical and in vitro ADME properties. *J. Med. Chem.* **2011**, *54*, 6691−6703.
(23) Houze, J. B.; Zhu, L.; Sun, Y.; Akerman, M.; Qiu, W.; Zhang, A. J.; Sharma, R.; Schmitt, M.; Wang, Y.; Liu, J.; Liu, J.; Medina, J. C.; Reagan, J. D.; Luo, J.; Tonn, G.; Zhang, J.; Lu, J. Y.-L.; Chen, M.; Lopez, E.; Nguyen, K.; Yang, L.; Tang, L.; Tian, H.; Shuttleworth, S. J.; Lin, D. C. H. AMG 837: A Potent, Orally Bioavailable GPR40 Agonist. *Bioorg. Med. Chem. Lett.* **2012**, *22*, 1267−1270.
(24) Negoro, N.; Sasaki, S.; Ito, M.; Kitamura, S.; Tsujihata, Y.; Ito, R.; Suzuki, M.; Takeuchi, K.; Suzuki, N.; Miyazaki, J.; Santou, T.; Odani, T.; Kanzaki, N.; Funami, M.; Tanaka, T.; Yasuma, T.; Momose, Y. Identification of Fused-Ring Alkanoic Acids with Improved Pharmacokinetic Profiles that Act as G Protein-Coupled Receptor 40/Free Fatty Acid Recptor 1 Agonists. *J. Med. Chem.* **2012**, *55*, 1538−1552.
(25) Mikami, S.; Kitamura, S.; Negoro, N.; Sasaki, S.; Suzuki, M.; Tsujihata, Y.; Miyazaki, T.; Ito, R.; Suzuki, N.; Miyazaki, J.; Santou, T.; Kanzaki, N.; Funami, M.; Tanaka, T.; Yasuma, T.; Momose, Y. Discovery of Phenylpropanoic Acid Derivatives Containing Polar Functionalities as Potent and Orally Bioavailable G Protein-Coupled Receptor 40 Agonists for the Treatment of Type 2 Diabetes. *J. Med. Chem.* **2012**, *55*, 3756−3776.
(26) Negoro, N.; Sasaki, S.; Mikami, S.; Ito, M.; Tsujihata, Y.; Ito, R.; Suzuki, M.; Takeuchi, K.; Suzuki, N.; Miyazaki, J.; Santou, T.; Odani, T.; Kanzaki, N.; Funami, M.; Morohashi, A.; Nonaka, M.; Matsunaga, S.; Yasuma, T.; Momose, Y. Optimization of (2,3-Dihydro-1-benzofuran-3-yl)acetic Acids: Discovery of a Non-Free Fatty Acid-Like, Highly Bioavailable G Protein-Coupled Receptor 40/Free Fatty Acid Receptor 1 Agonist as a Glucose-Dependent Insulinotropic Agent. *J. Med. Chem.* **2012**, *55*, 3960−3974.
(27) Ashton, W. T.; Sisco, R. M.; Yang, Y. T.; Lo, J. L.; Yudkovitz, J. B.; Cheng, K.; Goulet, M. T. Substituted indole-5-carboxamides and -acetamides as potent nonpeptide GnRH receptor antagonists. *Bioorg. Med. Chem. Lett.* **2001**, *11*, 1723−1726.
(28) Schroder, R.; Janssen, N.; Schmidt, J.; Kebig, A.; Merten, N.; Hennen, S.; Muller, A.; Blattermann, S.; Mohr-Andra, M.; Zahn, S.; Wenzel, J.; Smith, N. J.; Gomeza, J.; Drewke, C.; Milligan, G.; Mohr, K.; Kostenis, E. Deconvolution of complex G protein-coupled receptor signaling in live cells using dynamic mass redistribution measurements. *Nature Biotechnol.* **2010**, *28*, 943−950.

Epilogue

The discovery of selective and potent FFA1 agonists provides a valuable means not only as tool compounds to study receptor biology in a controlled *in vitro* environment but also as potential structures for the development of drug like molecules with the aim to be employed *in vivo*, even in the treatment of type 2 diabetes in the long run. Because of this perspective the compounds were not only tested with traditional endpoint assays such as the detection of intracellular calcium flux and inositolmonophosphate (IP) production but also with a label-free technology that is capable to display compound behavior as an integrated cell response, thereby allowing for the disclosure of receptor-independent ("off-target") effects. This additional information is helpful to evaluate the compounds more accurately, particularly with regard to a possible use of the FFA1-targeted ligands as drug compounds. By the same token, we also reported on *in vivo* relevant parameters, such as ADME (administration, distribution, metabolism and elimination) properties, compound toxicity and the ability to modulate insulin-secretion.

In this chapter, we demonstrated a way to stepwise evolve small molecule compounds to more favorable FFA1-targeted ligands. Structure-activity relationship investigations lead to insights into the incremental construction of FFA1 ligands.

Starting point for this optimization process was the compound TUG-424, an already potent but lipophilic FFA1 selective agonist[1]. By introducing polar substituents in the terminal benzene ring, a series of derivatives were synthesized and analyzed for their potency and physicochemical properties. In TUG-488 (compound 40) the methyl group at the terminal benzene ring of TUG-424 was replaced by a cyanomethyl substituent, which significantly lowered the lipophilicity and enhanced potency as described in the first publication. In the second paper of this chapter, we presented TUG-770 as an optimized TUG-488 derivative. By introducing a fluorine substituent in the middle benzene ring the potency could be further enhanced at the expense of a slightly increased lipophilicity. However, the fluoro-substituted structure significantly improved the compound's metabolic stability. In the third paper, a previously published compound TUG-469[2] was finally evolved inspired by the clinically exploited drug TAK-875/fasiglifam[3]. A mesylpropoxy appendage on the precursor compound resulted in a higher potent but less lipophilic FFA1 prevalent agonist TUG-905 (compound 13).

The discovery and optimization of selective receptor ligands is an important task since the prevailing concepts of pharmacological treatments are built on selective and potent compounds. Further in-depth biological studies are highly reliant to good quality and potent FFA1 agonists. The high potency of these ligands allows for a detailed exploration and gives greater headroom for pharmacological

characterization in a variety of experimental settings and cellular backgrounds. As shown in the aforementioned chapter (see chapter 4), selective small molecule FFA1 ligands (activators and inhibitors) prove very useful to elucidate the biology of the FFA1 receptor.

References

1. Christiansen, E. *et al.* Discovery of potent and selective agonists for the free fatty acid receptor 1 (FFA(1)/GPR40), a potential target for the treatment of type II diabetes, *J. Med. Chem.* **51,** 7061–7064 (2008).
2. Christiansen, E. *et al.* Structure-Activity Study of Dihydrocinnamic Acids and Discovery of the Potent FFA1 (GPR40) Agonist TUG-469, *ACS Med Chem Lett* **1,** 345–349 (2010).
3. Tsujihata, Y. Discovery and development of a selective GPR40/FFAR1 agonist, fasiglifam, for treatment of type 2 diabetes mellitus, *Folia Pharmacol. Jpn.* **144,** 59–63 (2014).

Section IV

Chapter 6: Non-canonical cNMPs

Prologue

As in most biomedical research areas, technological advances are a driving force in the discovery process and are in the center of new scientific findings. The history of research on cyclic nucleotide monophosphates (cNMPs) has not been straightforward from the first hints in the discovery of the non-canonical cyclic nucleotides cCMP and cUMP to their biological function as *second messengers*[1]. The acknowledgement of non-canonical cNMPs as true *second messenger* has been compromised by erroneous findings and methodological issues. Claims of a selective cCMP generating enzyme could not be backed by further investigations[2,3]. In analogy to chapter 4, immunostaining data likewise in the field of cNMP research are questionable due to antibody cross-reactivity[4]. Furthermore, due to technical limitations initial attempts to quantify cNMP levels were doomed to failure[5,6], whereas standard methods such as high performance liquid chromatography (HPLC) suffer from low sensitivity[7] and radiometric analyses are only applicable to cell-free systems[8]. Hence, methodological issues emerge as a crux of preceding cNMP research. Beyond the cNMP research field, a critical examination of the strengths and weaknesses of the techniques employed in a particular research question should generally be addressed as already discussed in chapter 1 and 4. The above mentioned methodological setbacks led to a negative perception of cCMP and cUMP research in the scientific community and might explain why non-canonical cNMPs were long ignored or overlooked as *second messenger* molecules.

A molecule to be considered as *second messenger* must fulfill several criteria[9–11]. In essence, this is the quest for (i) a generating system upon stimulation with a *first messenger*, (ii) a cellular effector system that controls (iii) a biological function in cells, organs or tissues. To control the effect a (iv) signal terminating system must be present.
Finally, a recent revival of research activities in the field of non-canonical cNMPs using state-of-the-art experimental techniques (HPLC-MS/MS, HPLC-MS/TOF and DMR) and key experimental tools (cNMP-AMs and bacterial toxins such as ExoY) gave the field of non-canonical cNMP research a strong boost, thereby providing evidence for a true *second messenger* role of cCMP and cUMP[1].

As a method that displays compound behavior as an integrated cell response, the DMR technology in particular (also see Chapter 1) provides priceless insights into uncharted biological effects. The label-

free measurement principle allows the recording of cellular activity in a pathway-unbiased yet pathway-specific fashion[12].

On the part of molecular tools recently introduced, acetoxymethyl ester of cNMPs (cNMP-AM) allow detailed insight into the biological effects of cNMPs[13]. They represent a novel class of chemically modified substances that can cross the cell membrane and release the actual active cNMP part of the molecule in the cytosol. This *in situ* triggering of signaling transduction is an elegant way to overcome previous issues with modulators of the intracellular cNMP level that were either natural (toxins) or synthetic (cNMP-derivatives) in nature. Nevertheless, we also took advantage of bacterial toxins such as ExoY and CyaA. The first toxin derives from the bacterium *Pseudomonas aeruginosa* and increases intracellular levels of cGMP and cUMP causing τ-phosphorylation and microtubule breakdown[14,15]. In turn, endothelial cells produce gaps that cannot be repaired by the host for a prolonged time. Thus, ExoY represents a bacterial edema factor, assumedly playing a role in the pathological process of *P. aeruginosa*-induced lung injury[15]. CyaA on the other side is an endotoxin of the bacterium *Bordetella pertussis*, which is mainly responsible for the whooping cough disease. This protein induces massive generation of cAMP and also cCMP contributing to the clinical pathology of pertussis (whooping cough)[7,16,17]. CyaA paralyzes immune cell function and facilitates bacterial survival. Although the *in vivo* relevance of the specific cNMP elevation remains unclear, the two bacterial toxins together with the chemically modified cNMP analogues proved exquisitely useful to dissect the biological function of cCMP and cUMP.

In this chapter, as well as in Chapter 1, 2 and 3, the advent of novel technologies or experimental methods paved the way for a fruitful scientific journey. In the following paper we further elucidate the biological functions of cCMP and cUMP taking advantage of novel yet validated experimental techniques and tool compounds, thereby contributing to the conclusion that cCMP and cUMP can unequivocally be considered as true *second messenger* molecules[1].

References

1. Seifert, R. cCMP and cUMP: emerging second messengers, *Trends Biochem. Sci.* **40,** 8–15 (2015).
2. Cech, S. Y. & Ignarro, L. J. Cytidine 3',5'-monophosphate (cyclic CMP) formation in mammalian tissues, *Science* **198,** 1063–1065 (1977).
3. Gaion, R. M. & Krishna, G. Cytidylate cyclase. The product isolated by the method of Cech and Ignarro is not cytidine 3’,5’-monophosphate, *Biochemical and Biophysical Research Communications* **86,** 105–111 (1979).
4. Anderson, T. R. Cyclic cytidine 3',5'-monophosphate (cCMP) in cell regulation, *Molecular and Cellular Endocrinology* **28,** 373–385 (1982).
5. Newton, R. P. Salih, S. G. Salvage, B. J. & Kingston, E. E. Extraction, purification and identification of cytidine 3',5'-cyclic monophosphate from rat tissues, *Biochem. J.* **221,** 665–673 (1984).
6. Newton, R. P. *et al.* Extraction, purification, identification and metabolism of 3',5'-cyclic UMP, 3',5'-cyclic IMP and 3',5'-cyclic dTMP from rat tissues, *Biochem. J.* **236,** 431–439 (1986).
7. Göttle, M. *et al.* Cytidylyl and uridylyl cyclase activity of bacillus anthracis edema factor and Bordetella pertussis CyaA, *Biochemistry* **49,** 5494–5503 (2010).
8. Seifert, R. & Dove, S. Inhibitors of Bacillus anthracis edema factor, *Pharmacol. Ther.* **140,** 200–212 (2013).
9. Hardman, J. G. Robison, G. A. & Sutherland, E. W. Cyclic nucleotides, *Annu. Rev. Physiol.* **33,** 311–336 (1971).
10. Schultz, G. & Rosenthal, W. Prinzipien der transmembranären Signalumsetzung bei der Wirkung von Hormonen und Neurotransmittern, *Arzneimittelforschung* **35,** 1879–1885 (1985).
11. Gao, Y. & Vanhoutte, P. M. Tissues cIMPly do not lie, *Naunyn Schmiedebergs Arch. Pharmacol.* **387,** 901–903 (2014).
12. Schröder, R. *et al.* Deconvolution of complex G protein-coupled receptor signaling in live cells using dynamic mass redistribution measurements, *Nat. Biotechnol.* **28,** 943–949 (2010).
13. Schultz, C. *et al.* Membrane-permeant derivatives of cyclic AMP optimized for high potency, prolonged activity, or rapid reversibility, *Mol Pharmacol* **46,** 702–708 (1994).
14. Ochoa, C. D. Alexeyev, M. Pastukh, V. Balczon, R. & Stevens, T. Pseudomonas aeruginosa exotoxin Y is a promiscuous cyclase that increases endothelial tau phosphorylation and permeability, *J. Biol. Chem.* **287,** 25407–25418 (2012).
15. Stevens, T. C. *et al.* The Pseudomonas aeruginosa exoenzyme Y impairs endothelial cell proliferation and vascular repair following lung injury, *Am. J. Physiol. Lung Cell Mol. Physiol.* **306,** L915-24 (2014).
16. Göttle, M. *et al.* Molecular analysis of the interaction of Bordetella pertussis adenylyl cyclase with fluorescent nucleotides, *Mol. Pharmacol.* **72,** 526–535 (2007).
17. Hewlett, E. L. *et al.* Pertussis pathogenesis--what we know and what we don't know, *J. Infect. Dis.* **209,** 982–985 (2014).

Biochemical and Biophysical Research Communications 451 (2014) 497–502

Contents lists available at ScienceDirect

Biochemical and Biophysical Research Communications

journal homepage: www.elsevier.com/locate/ybbrc

cNMP-AMs mimic and dissect bacterial nucleotidyl cyclase toxin effects

Ulrike Beckert [a,1], Manuel Grundmann [b,1], Sabine Wolter [a,1], Frank Schwede [c,1], Holger Rehmann [d], Volkhard Kaever [e], Evi Kostenis [b], Roland Seifert [a,*]

[a] Institute of Pharmacology, Hannover Medical School, Carl-Neuberg-Str. 1, D-30625 Hannover, Germany
[b] Institute of Pharmaceutical Biology, Nussallee 6, D-53115 Bonn, Germany
[c] Biolog Life Science Institute, Flughafendamm 9a, D-28199 Bremen, Germany
[d] Molecular Cancer Research, University Medical Center Utrecht, Universiteitsweg 100, NL-3584 Utrecht, The Netherlands
[e] Core Unit Metabolomics, Hannover Medical School, Carl-Neuberg-Str. 1, D-30625 Hannover, Germany

ARTICLE INFO

Article history:
Received 18 July 2014
Available online 7 August 2014

Keywords:
cNMP-AM
Prodrug
cUMP
cCMP
Dynamic mass distribution
Gene expression

ABSTRACT

In addition to the well-known second messengers cAMP and cGMP, mammalian cells contain the cyclic pyrimidine nucleotides cCMP and cUMP. The *Pseudomonas aeruginosa* toxin ExoY massively increases cGMP and cUMP in cells, whereas the *Bordetella pertussis* toxin CyaA increases cAMP and, to a lesser extent, cCMP. To mimic and dissect toxin effects, we synthesized cNMP-acetoxymethylesters as prodrugs. cNMP-AMs rapidly and effectively released the corresponding cNMP in cells. The combination of cGMP-AM plus cUMP-AM mimicked cytotoxicity of ExoY. cUMP-AM and cGMP-AM differentially activated gene expression. Certain cCMP and cUMP effects were independent of the known cNMP effectors protein kinases A and G and guanine nucleotide exchange factor Epac. In conclusion, cNMP-AMs are useful tools to mimic and dissect bacterial nucleotidyl cyclase toxin effects.

1. Introduction

cAMP and cGMP are well-established second messengers [1,2]. In addition to these cyclic purine nucleotides, mammalian cells contain the cyclic pyrimidine nucleotides cCMP and cUMP [3,4]. Soluble adenylyl cyclase plays a key role in maintaining basal cNMP concentrations in mammalian cells [4]. The *Pseudomonas aeruginosa* nucleotidyl cyclase toxin ExoY induces massive increases in cGMP and cUMP in mammalian cells and smaller increases in cAMP and cCMP [5]. In contrast, the *Bordetella pertussis* nucleotidyl cyclase toxin CyaA massively increases cAMP and, to a lesser extent, cCMP [5]. ExoY induces lung damage and necrosis of cells [5,6]. However, given the fact that ExoY increases the levels of all four cNMPs, it is impossible to answer the question what the contribution of any given cNMP to the biological toxin effect is. In order to address this problem, we studied the set of four cNMP-AMs shown in Fig. 1. In cNMP-AMs, the hydrophilic phosphate group is protected by an acetoxymethylester so that the compounds can penetrate the plasma membrane [7]. Within the cells, the cNMP moiety is released and induces biological effects. As control compound, we used PO_4-AM_3. Here, we show that cNMP-AMs are useful experimental tools to mimic and dissect bacterial nucleotidyl cyclase toxin effects.

2. Materials and methods

2.1. Materials

Rp-cAMPS, Rp-8-Br-cAMPS, Rp-8-Br-PET-cGMPS, Rp-8-pCPT-cGMPS, 8-pCPT-2′-O-Me-cAMP, cNMPs and PO_4-AM_3 were obtained from Biolog LSI (Bremen, Germany).

Abbreviations: AM, acetoxymethylester; cAMP, adenosine 3′,5′-cyclic monophosphate; cGMP, guanosine 3′,5′-cyclic monophosphate; cCMP, cytidine 3′,5′-cyclic monophosphate; cNMP, 3′,5′-cyclic nucleoside monophosphate; cUMP, uridine 3′,5′-cyclic monophosphate; DMR, dynamic mass redistribution; PKA, cAMP-dependent protein kinase; PKG, cGMP-dependent protein kinase; Epac, exchange protein directly activated by cAMP; PO_4-AM_3, phosphate tris(acetoxymethyl)ester; Rp-8-Br-cAMPS, (Rp)-8-bromoadenosine-3′,5′-cyclic monophosphorothioate; Rp-cAMPS, (Rp)-adenosine-3′,5′-cyclic monophosphorothioate; Rp-8-Br-PET-cGMPS, (Rp)-β-phenyl-1, N^2-etheno-8-bromoguanosine-3′,5′-cyclic monophosphorothioate; Rp-8-pCPT-cGMPS, (Rp)-8-(*para*-chlorophenylthio)guanosine-3′,5′-cyclic monophosphorothioate; 8-pCPT-2′-O-Me-cAMP, 8-(4-chlorophenylthio)-2′-O-methyladenosine-3′,5′-cyclic monophosphate; RT-PCR, real-time PCR; EBAO, ethidium bromide acridine orange.

* Corresponding author. Address: Institute of Pharmacology, Hannover Medical School, Carl-Neuberg-Str. 1, D-30625 Hannover, Germany. Fax: +49 511 532 4081.
E-mail addresses: beckert-ulrike81@email.de (U. Beckert), grundmann@uni-bonn.de (M. Grundmann), wolter.sabine@mh-hannover.de (S. Wolter), fs@biolog.de (F. Schwede), h.rehmann@UMCutrecht.nl (H. Rehmann), kaever.volkhard@mh-hannover.de (V. Kaever), kostenis@uni-bonn.de (E. Kostenis), seifert.roland@mh-hannover.de (R. Seifert).
[1] These authors contributed equally to this work.

http://dx.doi.org/10.1016/j.bbrc.2014.07.134
0006-291X/

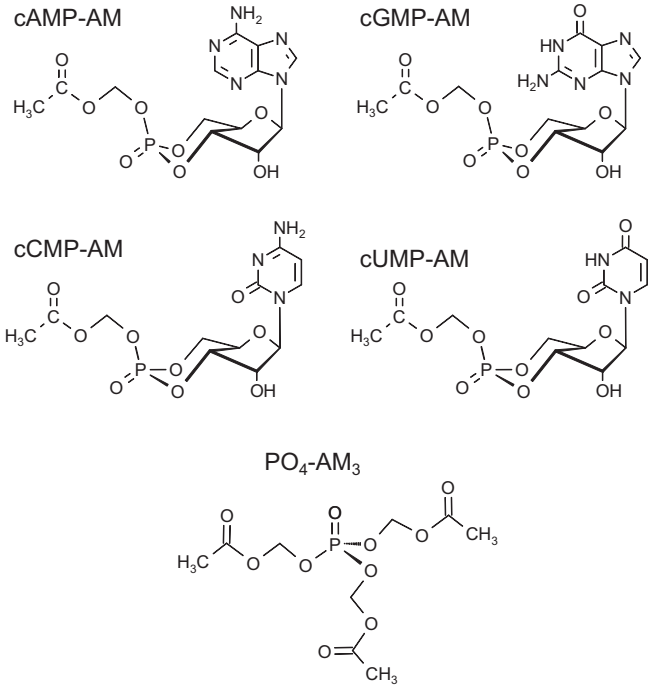

Fig. 1. Structures of cNMP-AMs and PO_4-AM_3. The AM group neutralizes the negative charge of the cNMP phosphate group. Accordingly, AM compounds can penetrate the plasma membrane. In the cytosol, esterases cleave the AM compounds, releasing the free cNMP and phosphate, respectively. Please note that PO_4-AM_3 contains three AM groups. Accordingly, in experiments, PO_4-AM_3 is used at threefold lower concentrations than cNMP-AMs. In order to avoid cleavage of AM compounds by extracellular esterases, experiments should be performed in the absence of serum supplementation.

2.2. Synthesis of cCMP-AM and cUMP-AM

All chromatographic experiments were performed at ambient temperature. The analytical HPLC-system consisted of a L 6200 pump, a L 4250 variable wavelength UV/Vis-detector, and a D 7500 chromato-integrator (all Merck-Hitachi, Darmstadt, Germany). The stationary phases were YMC ODS-A 12 nm, S-11 μm (YMC, Dinslaken, Germany) or Kromasil 100-10, RP-8 (Eka Nobel, Bohus, Sweden) in 250 × 4.6 mm stainless steel columns with Gemini C18, 4 × 3 mm Security guard columns (Phenomenex, Aschaffenburg, Germany). Semipreparative HPLC was performed with a LC-8A preparative liquid chromatograph (Shimadzu, Duisburg, Germany), a preparative K 2001 UV-detector (Knauer, Berlin, Germany), a L200E analog recorder (Linseis, Selb, Germany), and either YMC ODS-A 12 nm, S-11 μm (YMC) as stationary phase in a 250 × 20 mm stainless steel column (CS-Chromatography Service, Düren, Germany). Mass spectra were recorded with an Esquire LC 6000 spectrometer (Bruker Daltonics, Bremen, Germany) in the ESI-MS mode with 50/49.9/0.1 (v/v/v) propanol-2/water/formic acid as matrix. UV-spectra for preparation of aliquots were recorded with a Helios β-spectrometer (Spectronic Unicam, Leeds, UK) in aqueous phosphate buffer, pH 7. All reagents were of analytical grade or the best grade available from commercial suppliers.

2.2.1. cCMP-AM

220 μmol cCMP (diisopropylethylammonium salt) were carefully dried and suspended in 10 mL acetonitrile. After addition of 1100 μmol (110 μL; 5 equivalents) acetoxymethyl bromide and 1320 μmol (305 mg; 6 equivalents) Ag_2O, the reaction mixture was stirred vigorously at ambient temperature for 35 min. Progress of AM-ester formation was monitored by analytical HPLC with 16% (v/v) acetonitrile, 20 mM triethylammonium formate (pH 6.80) as eluent. After reaction was completed, solid Ag_2O was removed by filtration through a 0.2 μm PTFE membrane, and 2 mL aliquots of the raw mixture were evaporated under reduced pressure with oil pump vacuum. The residue was redissolved in DMF (~2–3 mL) and purified by semipreparative HPLC using 15% (v/v) acetonitrile as eluent. Product fractions were evaporated under reduced pressure to produce 84.5 μmol cCMP-AM as mixture of axial and equatorial isomers with a purity of >99.5% (yield: 38.4%). Formula: $C_{12}H_{16}N_3O_9P$ (MW: 377.2); ESI-MS pos. mode: *m/z* 378 $(M + H)^+$, *m/z* 479 $(M + H + TEA)^+$; neg. mode: *m/z* 376 $(M - H)^-$, *m/z* 304 $(M - AM - H)-$; UV–VIS (pH 7.0) λ_{max} 270 nm (ε = 9000).

2.2.2. cUMP-AM

Synthesis and work-up of cUMP-AM was performed in parallel reactions with 3 × 500 μmol cUMP (silver salt) and 2500 μmol (250 μL; 5 eq.) acetoxymethyl bromide in 30 mL acetonitrile as described for cCMP-AM. The reaction was monitored by analytical HPLC (Kromasil) with 15% (v/v) acetonitrile, pH 5 (0.25 μL acetic acid per 1 L), and the raw product was purified by semipreparative HPLC (Kromasil) with 5–10% (v/v) acetonitrile. Product-containing fractions were evaporated *in vacuo* and 110.7 μmol cUMP-AM were obtained as a mixture of isomers with a purity of 98.78% (yield: 7.4%). Formula: $C_{12}H_{15}N_2O_{10}P$ (MW: 378.2); ESI-MS pos. mode: *m/z* 401 $(M + H + Na)^+$, *m/z* 379 $(M + H)^+$; neg. mode: *m/z* 305 $(M - AM - H)^-$, *m/z* 377 $(M - H)^-$; UV–VIS (pH 7.0) λ_{max} 260 nm (ε = 10000).

2.3. DMR measurements

For DMR measurements a beta version of the Corning Epic biosensor (Corning, Corning, NY, USA) or the Enspire multimode reader (Perkin Elmer, Hamburg, Germany) that contains an integrated DMR module was used. Each well of the DMR biosensor microplate contains a grating biosensor that guides polarized broadband light through the bottom of the plate generating an electromagnetic field that extends 150 nm into the cell layer. As a result of cellular response, relocation of intracellular constituents leads to a local change of refraction index that is translated into a wavelength shift (in pm) of the reflected light. The magnitude of this wavelength shift is proportional to the amount of DMR. Increase of mass contributes positively and decreases negatively to the overall response. The resulting optical signatures reflect cellular processes such as shape change, cytoskeletal reorganization or cellular adhesion as a consequence of engagement of intracellular signaling cascades.

DMR measurements were performed as described [8]. In brief, HEK293 and B103 cells were seeded into 384-well fibronectin coated DMR biosensor microplates with a density of 15,000 cells per well and grown overnight (at 37 °C and 5% (v/v) CO_2) to confluent monolayers. Esterases present in the serum supplements of the cell culture medium can degrade the test compounds by hydrolysis of esters and, therefore, strongly reduce cell-loading efficiency. Hence, after removal of medium cells were washed at least twice with HBSS containing 20 mM HEPES (DMR buffer) to ensure absence of serum supplements, and a residual volume of 30 μL of DMR buffer was left in each well. Immediately before DMR registration test compounds were prepared at 4× final concentration in pre-warmed DMR buffer and placed into the compound source plate. Then, the sensor plate was scanned and a baseline optical reading was recorded. Finally, 10 μL of compound solutions were

transferred into the sensor plate and DMR was monitored for at least 9000 s.

2.4. Other methods

cNMP quantitation in cells was performed via HPLC–MS/MS as described using a QTrap5500 triple quadrupole mass spectrometer (ABSCIEX, Foster City, CA, USA) [9,10]. Cell culture and B103 cell transfection with ExoY plasmid was performed as described [3–5]. Cell viability was assessed using light microscopy and EABO staining [11]. FACS analysis of cell viability was performed as described [5]. Guanine nucleotide exchange factor activity of Epac1 on Rap1B was determined with the fluorescent GDP analog 2′,3′-O-(N-methylanthraniloyl)-GDP as described [12]. Gene expression in B103 cells was performed using the "Whole Rat Genome Oligo Microarray 4 × 44 Kv2″ (Agilent, Böblingen, Germany) containing 45,220 oligonucleotide probes. For RT-PCR studies, HEK293 cells were incubated with different compounds for 1 h, followed by TaqMan probe analysis for c-fos using the ΔΔCt method [11].

2.5. Statistics

Data are presented as means ± SD, and are based on 4–8 independent experiments.

3. Results

In B103 neuroblastoma cells, ExoY induces massive increases in cGMP and cUMP and necrosis [5]. cGMP-AM (200 μM for 4 h) increased cGMP levels in B103 cells to a similar extent as did a 4-h treatment of cells with *P. aeruginosa* expressing ExoY (Fig. 2) [5]. By analogy, cUMP-AM (200 μM for 4 h) was similarly effective at increasing cUMP as a 4-h treatment of cells with *P. aeruginosa* expressing ExoY (Fig. 2) [5]. The combination of cGMP-AM and cUMP-AM yielded similar levels of the cognate cNMPs as treatment with the single cNMP-AM. cGMP-AM and cUMP-AM exhibited no effect on cAMP and cCMP levels. cUMP-AM induced a small cGMP increase which may be due to blockade of a cGMP-degrading phoshopdiesterase by cUMP. The control compound PO_4-AM_3 had no effect on cNMP levels. The uptake of cNMP-AMs into cells was very rapid, i.e. already after 5 min significant levels of the free cognate cNMP were reached, and levels remained elevated at least for 6 h (later time points were not studied) (Fig. S1). In contrast, non-cognate cNMP levels remained low.

Under control conditions B103 cells grew as monolayer with neurite extensions (Fig. 3A–C) [11]. Green color in the EBAO staining is indicative for cell viability. cGMP-AM had little effect on cell morphology and viability (Fig. 3D–F). In contrast, cUMP-AM induced marked cell clustering but no marked decrease in cell viability (Fig. 3G–I). The combination of cGMP-AM and cUMP-AM resulted in detachment of the cells from the surface and a massive decrease in viability as evident by change in cell staining from green to red (Fig. 3J–L). Analysis of cell viability by FACS [5] revealed an increase in the percentage of necrosis from ~2–3% in control cells or cells treated with either cGMP-AM or cUMP-AM alone to 54% in cells treated with the combination of cGMP-AM plus cUMP-AM (data not shown). Transfection of B103 cells with ExoY induced similar morphological changes as treatment with cGMP-AM plus cUMP-AM. Specifically, we observed cell rounding and cell clustering and an increase in increase in the percentage of necrotic and apoptotic cells (Fig. S2D–F). These data fit to the recently reported FACS analysis data [5]. In contrast, transfection of B103 cells with the catalytically inactive ExoY mutant K81M did not result in cell rounding, cell clustering, apoptosis and necrosis (Fig. S2A–C).

Morphological and viability changes in B103 cells following exposure to cGMP-AM and cUMP-AM were accompanied by changes in gene expression after a 2 h incubation (Fig. S3). We conducted a microarray analysis encompassing ⩾45,000 genes. Somewhat unexpectedly, we found that expression of only few genes changed significantly. Specifically, cGMP-AM significantly increased expression of the cyclic-dependent kinase inhibitor 1 (cdkn1a, regulator of cell cycle progression), early response gene 1 (egr1, promoting neuronal differentiation and neurite growth), egr2 and inducible heme oxigenase 1 (hmox1, a redox gene usually elevated by heavy metals, endotoxin and oxidizing compounds). cUMP-AM increased expression of cdkn1a, egr1, egr2, growth differentiation factor 15 (gdf15, a neuroprotective and neurotrophic factor) and small GTPase inhibitor of RhoA (rnd1, promoting neuronal differentiation and neurite growth). cUMP-AM was more effective at inducing expression of cdkn1a, egr1 and rnd1 than cGMP-AM, whereas the opposite was true for hmox1. Collectively, these data show that cGMP-AM and cUMP-AM alter expression of few genes associated with cell cycle, cell differentiation and cell stress. The selective effects of cGMP-AM and cUMP-AM on the expression of only few genes argues against non-specific effects of the cNMPs.

We also addressed the question whether cNMP-AMs are feasible for dissecting the mechanisms underlying the biological effects

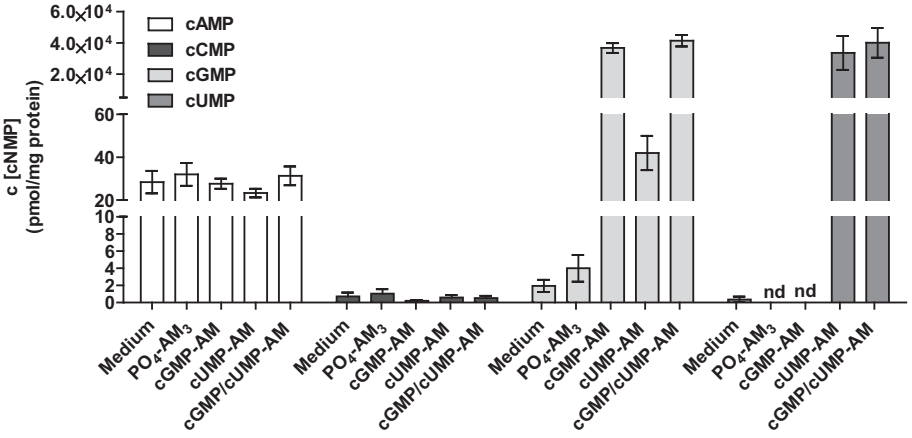

Fig. 2. cGMP- and cUMP-uptake of B103 cells after cGMP-AM and cUMP-AM incubation. 4 × 10^5 B103 cells were incubated for 24 h in low-serum medium and then treated with 200 μM cGMP-AM and cUMP-AM alone or with a 1:1 mixture of both (each 200 μM final) at 37 °C for 4 h. PO_4-AM_3 66 μM and 132 μM served as analog control. Subsequently, cells were processed for HPLC–MS/MS quantitation of cNMPs. nd: not detected.

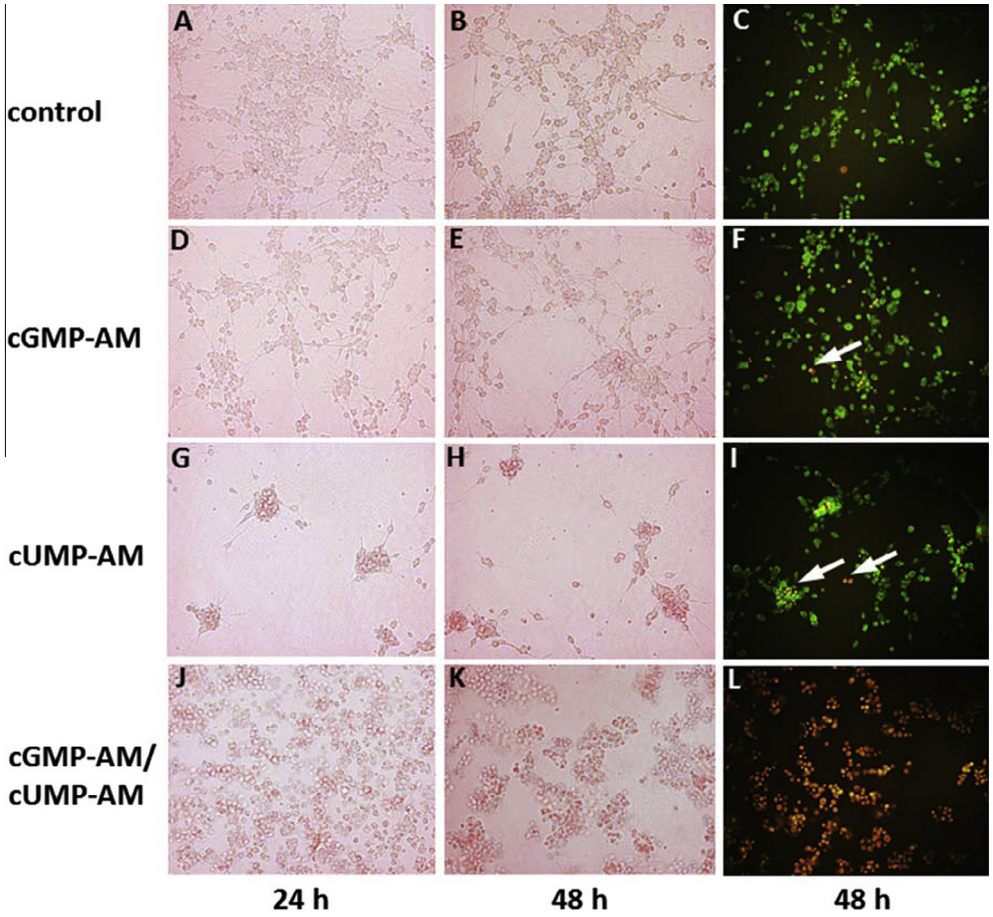

Fig. 3. ExoY mimicry by cGMP-AM and cUMP-AM in B103 cells. B103 cells were incubated with 200 μM of cGMP-AM, cUMP-AM and a 1:1 mixture of cGMP-AM/cUMP-AM, respectively. PO_4-AM_3 in a concentration of 132 μM served as control. C, F, I and L represent EBAO stained cells. All other panels represent unstained cells. White arrows indicate representative apoptotic/necrotic cells. The experiment was conducted at least three times. Green = viable cells, red = apoptotic/necrotic cells. Magnification, 200-fold. (For interpretation of the references to color in this figure legend, the reader is referred to the web version of this article.)

of individual cNMPs. For these studies we used the holistic DMR assay that has already been very successfully applied with regard to the dissection of signaling pathways activated by G protein-coupled receptors [8]. The DMR assay is very sensitive in terms of picking up cell signals, and therefore, we hoped that we could use cNMP-AMs at lower concentrations than for mimicry of ExoY effects (Figs. 2, 3, S2 and S3) [5]. Such a procedure would facilitate studies with inhibitors of known cNMP targets, i.e. PKA and PKG because such inhibitors compete with intracellular cNMPs for binding to kinases [13]. cAMP-AM up to 100 μM had no effect on DMR in HEK cells (Fig. 4A). cGMP-AM exhibited only a small and delayed signal (Fig. 4B). In marked contrast, cCMP-AM induced large and sluggish DMR signals, reaching saturation between 50 and 100 μM (Fig. 4C). cUMP-AM (100 μM) induced substantial larger DMR signals than cCMP-AM (Fig. 4D). In contrast to cCMP-AM, cUMP-AM also exhibited a pronounced rapid DMR response phase. In addition, the cUMP-AM response was not yet saturated at 100 μM. Control experiments revealed that PO_4-AM_3, the non-esterified cNMPs themselves and the membrane-permeable Epac activator 8-pCPT-2′-O-Me-cAMP (up to 300 μM) had no effect on DMR responses (data not shown). A combination of PKG inhibitors suppressed the responses of cUMP-AM more effectively than a combination of PKA inhibitors (Fig. 4E). The addition of PKA inhibitors on top of PKG inhibitors exhibited no additional inhibitory effect. Whereas PKA inhibitors strongly inhibited the DMR response of cCMP-AM, PKG inhibitors potentiated the cCMP response and unmasked a rapid signature (Fig. 4F). Addition of PKA inhibitors on top of PKG inhibitors had no additional effect.

Similar to the observations made for HEK293 cells, cCMP-AM induced a delayed DMR response in B103 cells (Fig. S4). Again, PKA inhibitors strongly reduced the cCMP-AM signal, whereas PKG inhibitors unmasked a rapid cCMP-AM response. PKA inhibitors had no effect in the presence of PKG inhibitors. In HEK293 cells, cCMP-AM slightly increased c-Fos expression (Fig. S5). The effect of cCMP-AM on c-Fos expression was strongly potentiated by a PKA or PKG inhibitor and a combination of both inhibitors. Finally, we assessed the effects of cCMP and cUMP on the activity of purified Epac. cCMP up to 100 μM, in contrast to cAMP, had virtually no stimulatory effect on Epac, and even an increase of cCMP of up to 1 mM resulted only in a minimal response (Fig. S6). cUMP was ineffective at activating Epac.

4. Discussion

cNMP-AMs enter cells and release the cNMP into the cytosol following cleavage of the ester. Sustained and high cNMP levels result, with no marked evidence for cross-regulation of other cNMPs by a given cNMP-AM. The control compound PO_4-AM_3 is also inert with respect to cNMP increases. The combination of cGMP-AM and cUMP-AM mimics the effects of the *P. aeruginosa* nucleotidyl cyclase toxin ExoY with respect to intracellular cGMP and cUMP levels and cytotoxicity [5]. The combination of both

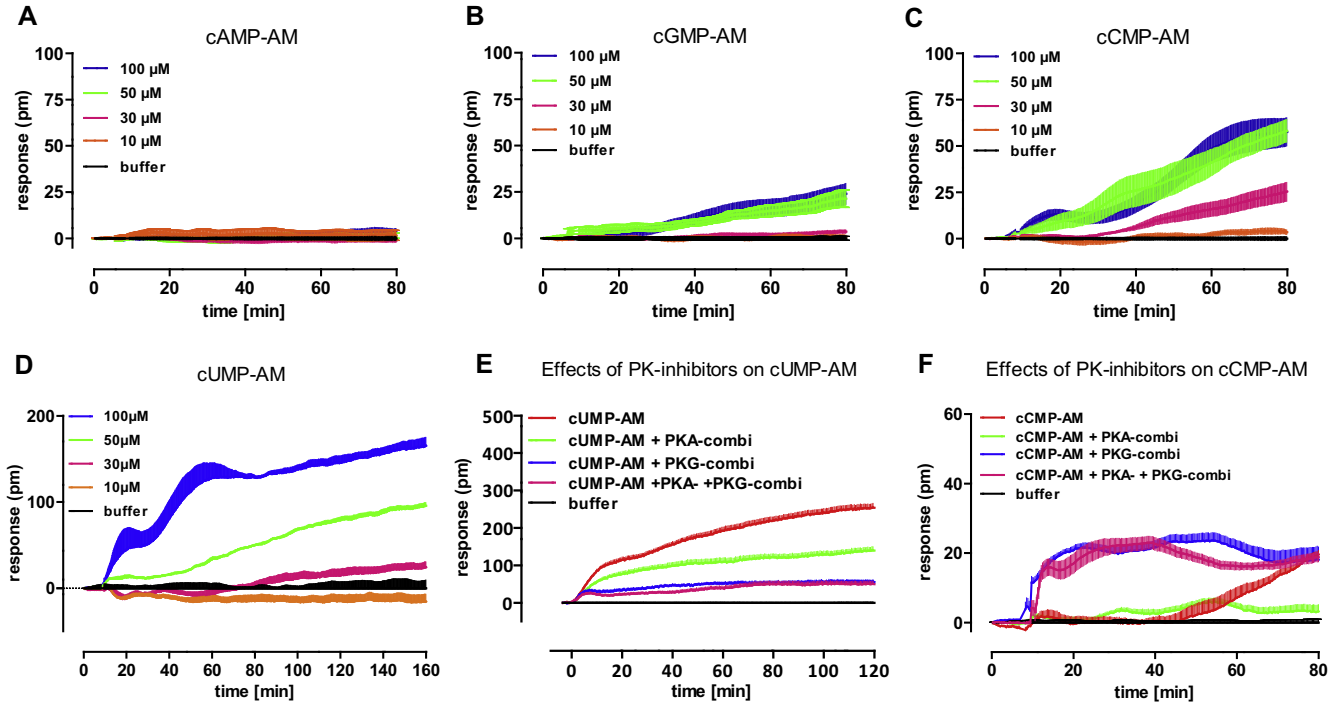

Fig. 4. DMR responses in HEK293 cells treated with cNMP-AMs. DMR tracings of HEK293 cells treated with cAMP-AM (A), cGMP-AM (B), cCMP-AM (C), and cUMP-AM (AM) (D) for 80 min. (E) HEK293 cells treated with 50 µM cUMP-AM in the presence or absence of PKA inhibitors (500 µM Rp-8-Br-cAMPS and 500 µM Rp-cAMPS) and/or PKG inhibitors (300 µM Rp-8-Br-PET-cGMPS and 500 µM Rp-8-pCPT-cGMPS). (F) HEK293 cells treated with 10 µM cCMP-AM in the presence or absence of PKA inhibitors (500 µM Rp-8-Br-cAMPS and 500 µM Rp-cAMPS) and/or PKG inhibitors (300 µM Rp-8-Br-PET-cGMPS and 500 µM Rp-8-pCPT-cGMPS). Traces are corrected for the effects of the inhibitors alone in the absence of cNMP-AMs.

cNMP-AMs was required for toxin mimicry. cGMP and cUMP are functionally not equivalent because only cUMP-AM induced morphological changes alone and moreover, cGMP-AM and cUMP-AM exhibited differential effects on gene expression.

cCMP-AM and cUMP-AM induce pronounced DMR responses. The responses were observed at low compound concentrations (10–100 µM) and were not mimicked by cAMP-AM, cGMP-AM, PO_4-AM_3 or non-esterified cNMPs. All these data indicate the DMR responses by cCMP-AM and cUMP-AM are specific for the intracellularly released cNMP. Dissection between effects of cCMP and cUMP *versus* cAMP and cGMP is critical for postulating a second messenger role of the former cNMPs. Both, the effects of cCMP and cUMP are partially mediated by PKA as revealed by the partial inhibitory effects of PKA inhibitors. The EC_{50} values of cCMP and cUMP for PKA and PKG activation [14] fit well to the concentrations required for induction of DMR responses by cNMP-AMs. cCMP and cUMP are also partial activators of purified PKG [14], and modulation of DMR responses of cCMP-AM and cUMP-AM by PKG inhibitors is consistent with a role of PKG in cell responses. However, while in the case of cUMP, PKG plays a stimulatory role, in case of cCMP, PKG exerts a tonic inhibition that is released by PKG inhibition and dominates the PKA regulation. These data also indicate that cCMP and cUMP act *via* different mechanisms. This interpretation is supported by the different cCMP and cUMP kinetics. An implication of these data is that ExoY from *P. aeruginosa* (predominantly increasing cUMP) and CyaA from *B. pertussis* (predominantly increasing cCMP) [5] manipulate mammalian signal transduction pathways in different manners and address distinct intracellular targets. Furthermore, there is no evidence for a role of Epac in DMR responses. Most importantly, the persistence of cCMP-AM DMR and gene expression responses in the presence of PKA and PKG inhibitors and the inefficiency of cCMP and cUMP at activating Epac indicate that additional effector proteins for these cNMPs exist.

In conclusion, the present study has made an important contribution towards elucidation of the pathophysiological effects of ExoY and different second messenger functions of cCMP and cUMP. cGMP and cUMP, can be clearly dissociated from each other, and cCMP and cUMP induce distinct cellular responses that cannot be explained by the known cNMP effector proteins PKA, PKG and Epac. The next two steps in the elucidation of the second messenger functions of cCMP and cUMP are straightforward. First, we need to identify the specific binding proteins of cCMP and cUMP. The appropriate methodologies are already in place [15]. Second, the research community is invited to follow the paradigm outlined in this study and examine the biological effects of cNMP-AMs alone and in combination in multiple systems to understand the (patho)physiological roles of cUMP and cCMP. A recent study revealed that cCMP and cUMP are present in numerous mammalian cell culture lines and primary mammalian cells and that any given cell type possesses a unique cNMP pattern [16]. Based on these data it can be assumed that cCMP and cUMP play important biological roles in many systems. These cNMP roles can be unmasked with cNMP-AMs. Lastly, it should be kept in mind that it is not only important to add a single cNMP-AM to cells. Rather, cNMP-AM combinations are critical, mimicking intracellular cNMP patterns.

Acknowledgments

We thank Mrs. Annette Garbe and Mrs. Juliane von der Ohe for expert technical assistance.

Appendix A. Supplementary data

Supplementary data associated with this article can be found, in the online version, at http://dx.doi.org/10.1016/j.bbrc.2014.07.134.

References

[1] J.M. Gancedo, Biological roles of cAMP: variations on a theme in the different kingdoms of life, Biol. Rev. Camb. Philos. Soc. 88 (2013) 645–668.

[2] J. Schlossmann, E. Schinner, CGMP becomes a drug target, Naunyn-Schmiedebergs Arch. Pharmacol. 385 (2012) 243–252.

[3] K.Y. Beste, C.M. Spangler, H. Burhenne, et al., Nucleotidyl cyclase activity of particulate guanylyl cyclase A: comparison with particulate guanylyl cyclases E and F, soluble guanylyl cyclase and bacterial adenylyl cyclases CyaA and edema factor, PLoS One 8 (2013) e70223.

[4] A. Hasan, K.Y. Danker, S. Wolter, et al., Soluble adenylyl cyclase accounts for high basal cCMP and cUMP concentrations in HEK293 and B103 cells, Biochem. Biophys. Res. Commun. 448 (2014) 236–240.

[5] U. Beckert, S. Wolter, C. Hartwig, et al., ExoY from *Pseudomonas aeruginosa* is a nucleotidyl cyclase with preference for cGMP and cUMP formation, Biochem. Biophys. Res. Commun. 450 (2014) 870–874.

[6] T.C. Stevens, C.D. Ochoa, K.A. Morrow, et al., The *Pseudomonas aeruginosa* exoenzyme Y impairs endothelial cell proliferation and vascular repair following lung injury, Am. J. Physiol. Lung Cell. Mol. Physiol. 306 (2014) L915–L924.

[7] C. Schultz, M. Vajanaphanich, H.G. Genieser, et al., Membrane-permeant derivatives of cyclic AMP optimized for high potency, prolonged activity, or rapid reversibility, Mol. Pharmacol. 46 (1994) 702–708.

[8] R. Schröder, N. Janssen, J. Schmidt, et al., Deconvolution of complex G protein-coupled receptor signaling in live cells using dynamic mass distribution, Nat. Biotechnol. 28 (2010) 943–949.

[9] H. Bähre, K.Y. Danker, J.P. Stasch, et al., Nucleotidyl cyclase activity of soluble guanylyl cyclase in intact cells, Biochem. Biophys. Res. Commun. 443 (2014) 1195–1199.

[10] K.Y. Beste, H. Burhenne, V. Kaever, et al., Nucleotidyl cyclase activity of soluble guanylyl cyclase $\alpha_1\beta_1$, Biochemistry 51 (2012) 194–204.

[11] L. Kinast, J. von der Ohe, H. Burhenne, et al., Impairment of adenylyl cyclase 2 function and expression in hypoxanthine phosphoribosyltransferase-deficient rat B103 neuroblastoma cells as model for Lesch-Nyhan disease: BODIPY-forskolin as pharmacological tool, Naunyn-Schmiedebergs Arch. Pharmacol. 385 (2012) 671–683.

[12] H. Rehmann, Characterization of the Rap-specific exchange factor Epac by cyclic nucleotides, Methods Enzymol. 407 (2006) 159–173.

[13] F. Schwede, E. Maronde, H. Genieser, et al., Cyclic nucleotide analogs as biochemical tools and prospective drugs, Pharmacol. Ther. 87 (2000) 199–226.

[14] S. Wolter, M. Golombek, R. Seifert, Differential activation of cAMP- and cGMP-dependent protein kinases by cyclic purine and pyrimidine nucleotides, Biochem. Biophys. Res. Commun. 415 (2011) 563–566.

[15] A. Hammerschmidt, B. Chatterji, J. Zeiser, et al., Binding of regulatory subunits of cyclic AMP-dependent protein kinase to cyclic CMP agarose, PLoS One 7 (2012) e39848.

[16] C. Hartwig, H. Bähre, S. Wolter, et al., CAMP, cGMP, cCMP and cUMP concentrations across the tree of life: High cCMP and cUMP levels in astrocytes, Neurosci. Lett. 579 (2014) 183–187.

Epilogue

In comparison to other domains of life, cUMP and cCMP are mainly present in mammalian cells suggesting that, from an evolutionary perspective, cUMP and cCMP represent a relatively young group of substances[1]. This might indicate that these molecules undertake a more specialized task in the signaling network of mammalian cells. Due to the organization of signaling networks by so-called signaling hubs, it is not surprising that canonical and non-canonical cNMPs show overlapping target specificity. In this chapter, we have shown that both cCMP and cUMP signal via interaction with protein kinase A (PKA) and protein kinase G (PKG), targets that are frequently associated to the signaling axis of cAMP and cGMP. These protein kinases are key regulators in the wide spectrum of biological functions of canonical cyclic nucleotide *second messenger*. However, we found that non-canonical cNMPs do not target exchange proteins directly activated by cAMP (epac), which act as guanine nucleotide exchange factors (GEF) for small GTPases such as Rap[2]. Furthermore, the holistic DMR readout could clearly distinguish between the signal composition of cAMP/cGMP and cCMP/cUMP. The unbiased real-time methodological approach even allowed distinguishing between cCMP and cUMP mediated cell response, since the non-canonical cNMPs are differently modulated by PKG. While PKG plays a stimulatory role for cUMP-signaling, it acts as an inhibitory regulator of cCMP-signaling. Moreover, the non-canonical cNMPs, in contrast to cAMP and cGMP, show overall different kinetics in the process of cell activation, another indicator of different biological function. This notion is substantiated by distinct pathophysiological consequences of infection with either bacterial toxin ExoY or CyaA, which can clearly distinguish in the activation of cUMP and cCMP production, and the infection with edema factor (EF) derived from *Bacillus anthracis* that primarily increases cAMP levels. In synopsis with data from other publications regarding the generation and termination of cCMP and cUMP, these molecules can now be classified as true second messengers[3].

This study demonstrated the importance of powerful and well-characterized tool compounds that interrogate the label-free readout to decode signal transduction. As described in chapter 1 and 2 and several other publications[4–6], the explanatory power of label-free readouts inevitably relies on the availability of and the combination with tool compounds.

As already mentioned in the introductory section, signal transduction pathways are better be conceived as signaling networks rather than linear pathways because they are inevitably associated with high structural texture and complexity that will continue to challenge researchers to thoroughly investigate signal transduction processes[7]. Tending to oversimplification or reductionism in the overall approach in drug research is sometimes indispensable with regard to the challenge of studying complex biological processes. Indeed, this approach results in considerable short-term success, although long-term achievements are with regard to high attrition rates of drug candidates

in all stages of the development process questionable[8–10]. Label-free techniques, such as dynamic mass redistribution assays, provide an important means to display biological processes authentically and thus broaden the view to a more translational biology-orientated approach. The perception of these innovative methods indicates a general reorientation to holistic readouts, such as whole organ experiments, which were at the forefront of drug discovery in former times[11,12]. Intriguingly, in these same times, many medically highly valuable drugs were discovered. With regard to the shift in mindset, the return of holistic label-free methods is sometimes described as a "back to the future-approach"[13].

Label-free assays were used in every previous chapter of this thesis. However, unlike in the aforementioned chapters, where we focused on the investigation of signaling mediated by surface receptors, we here used the DMR technique to study signal transduction at a *post-receptor* level, which is – to our knowledge – the first report on the attempt to decipher cell signaling beyond membrane receptor generated cell responses using this methodological approach.

References

1. Hartwig, C. *et al.* cAMP, cGMP, cCMP and cUMP concentrations across the tree of life: High cCMP and cUMP levels in astrocytes, *Neurosci. Lett.* **579,** 183–187 (2014).
2. Schmidt, M. Dekker, F. J. & Maarsingh, H. Exchange protein directly activated by cAMP (epac): a multidomain cAMP mediator in the regulation of diverse biological functions, *Pharmacol. Rev.* **65,** 670–709 (2013).
3. Seifert, R. cCMP and cUMP: emerging second messengers, *Trends Biochem. Sci.* **40,** 8–15 (2015).
4. Grundmann, M. & Kostenis, E. Label-free biosensor assays in GPCR screening, *Methods Mol. Biol.* **1272,** 199–213 (2015).
5. Schröder, R. *et al.* Deconvolution of complex G protein-coupled receptor signaling in live cells using dynamic mass redistribution measurements, *Nat. Biotechnol.* **28,** 943–949 (2010).
6. Hennen, S. *et al.* Decoding signaling and function of the orphan G protein-coupled receptor GPR17 with a small-molecule agonist, *Sci Signal* **6,** ra93 (2013).
7. Gomperts, B. D. Kramer, I. M. & Tatham, P. E. R. *Signal transduction.* 2nd ed. (Elsevier Acad. Press, Amsterdam, 2009).
8. Hutchinson, L. & Kirk, R. High drug attrition rates--where are we going wrong?, *Nat Rev Clin Oncol* **8,** 189–190 (2011).
9. Martin, J. Addressing attrition in early drug discovery by label-free methodologies: receptor pharmacology in native cells. *Int Drug Discov,* 38–45 (2010).
10. Moreno, L. & Pearson, A. D. J. How can attrition rates be reduced in cancer drug discovery?, *Expert Opin Drug Discov* **8,** 363–368 (2013).

11. Dick, E. Rajamohan, D. Ronksley, J. & Denning, C. Evaluating the utility of cardiomyocytes from human pluripotent stem cells for drug screening, *Biochem. Soc. Trans.* **38,** 1037–1045 (2010).

12. McKim, J. M. Building a tiered approach to in vitro predictive toxicity screening: a focus on assays with in vivo relevance, *Comb. Chem. High Throughput Screen.* **13,** 188–206 (2010).

13. Rocheville, M. Martin, J. Jerman, J. & Kostenis, E. Mining the potential of label-free biosensors for seven-transmembrane receptor drug discovery, *Prog Mol Biol Transl Sci* **115,** 123–142 (2013).

Chapter 7: G protein inhibitor BIM

Prologue

Studying signal transduction at both the receptor and the *post*-receptor level indispensably demands for well-suited methods to selectively inhibit distinct components in signaling networks. For instance, this can be achieved genetically by *knock-down* or *knock-out*, or pharmacologically using molecular inhibitors as tools. Since defects or dysfunction of signal transduction is the crux of the matter in almost all diseases, discovering inhibitors of certain signaling events represents an attractive goal for future treatment options[1]. The understanding of their mode-of-action is essential to gain mechanistic insights into signaling networks. Compounds that activate (agonists) or inhibit (antagonists) signaling at the receptor level have been widely used with great success to decipher signal transduction. If selective perturbation of distinct receptors is amenable, inhibitors attract much attention. However, although equally relevant, pharmacological inhibition at the *post-receptor* level is largely underexploited[2] and thus mechanistic studies on the inhibition of signaling partners at this level are often lacking.

As already detailed in the introduction, G protein-coupled receptors (GPCRs) represent cellular signaling hubs that regulate the signal generation from outside the cell into the intracellular compartments. These receptors are extremely variable and can produce a plethora of different cellular signaling events[3–5]. Therefore, they are ideal targets to study the regulation of signaling networks. G proteins belong to the group of GTPases and are molecular switches that play a crucial role in the transmission of cell signaling[6,7]. These proteins can occur in an inactive, GDP-bound, and an active, GTP-bound, state that are regulated by interaction with other proteins such as guanine-nucleotide exchange factors (GEFs) or GTPase-activating proteins (GAPs). Heterotrimeric G proteins consist of three subunits (α, β and γ), of which the α subunit is a target for specific G protein inhibition. The bacterial product pertussis toxin (PTX) from *Bordetella pertussis* selectively inhibits $G\alpha_i$ subunits by ADP-ribosylation and thereby prevents $G\alpha_i$ signaling through uncoupling of the G protein from the receptor. The natural product YM-254890 from *Chromobacterium sp.* was characterized as selective $G\alpha_q$ inhibitor[8,9]. YM-254890 restricts GDP exit from the guanine nucleotide-binding pocket within the α_q subunits by impairing the linker flexibility between the GTPase and the helical domain and is therefore dubbed guanine nucleotide dissociation inhibitor (GDI). However, no cell membrane-permeable compound to date can inhibit $G\alpha_s$ or $G\alpha_{12/13}$.

BIM-46174 (= BIM) and its dimer BIM-46187 were initially published as pan-G protein inhibitor and thus could represent attractive compounds to distinguish between G protein-dependent and G protein-independent GPCR-mediated signaling[10,11]. In this chapter, BIM is characterized in detail and

is redefined as a G protein inhibitor that does not act as a pan G protein inhibitor in all cells, but as a selective $G\alpha_q$-inhibitor in a cell-type dependent manner. As the aforementioned chapter clearly stated, tool compounds that selectively modulate distinct signaling events proof valuable as "signaling decoders". G protein inhibitors that function as such "signaling decoders" will help understanding signaling networks in both physiological and pathological contexts.

References

1. Lin, A. & Liu, Z.-g. Cell signaling review series, *Cell Res* **18,** 327 (2008).
2. Overington, J. P. Al-Lazikani, B. & Hopkins, A. L. How many drug targets are there?, *Nat Rev Drug Discov* **5,** 993–996 (2006).
3. Kenakin, T. & Miller, L. J. Seven transmembrane receptors as shapeshifting proteins: the impact of allosteric modulation and functional selectivity on new drug discovery, *Pharmacol. Rev.* **62,** 265–304 (2010).
4. Kenakin, T. P. Biased signalling and allosteric machines: new vistas and challenges for drug discovery, *Br. J. Pharmacol.* **165,** 1659–1669 (2012).
5. Kenakin, T. & Christopoulos, A. Signalling bias in new drug discovery: detection, quantification and therapeutic impact, *Nat Rev Drug Discov* **12,** 205–216 (2013).
6. Milligan, G. & Kostenis, E. Heterotrimeric G-proteins: a short history, *Br. J. Pharmacol.* **147 Suppl 1,** S46-55 (2006).
7. Oldham, W. M. & Hamm, H. E. Heterotrimeric G protein activation by G-protein-coupled receptors, *Nat. Rev. Mol. Cell Biol.* **9,** 60–71 (2008).
8. Nishimura, A. *et al.* Structural basis for the specific inhibition of heterotrimeric Gq protein by a small molecule, *Proc. Natl. Acad. Sci. U.S.A.* **107,** 13666–13671 (2010).
9. Takasaki, J. *et al.* A novel Galphaq/11-selective inhibitor, *J. Biol. Chem.* **279,** 47438–47445 (2004).
10. Prévost, G. P. *et al.* Anticancer activity of BIM-46174, a new inhibitor of the heterotrimeric Galpha/Gbetagamma protein complex, *Cancer Res.* **66,** 9227–9234 (2006).
11. Ayoub, M. A. *et al.* Inhibition of heterotrimeric G protein signaling by a small molecule acting on Galpha subunit, *J. Biol. Chem.* **284,** 29136–29145 (2009).

CellPress

Chemistry & Biology
Article

A Cell-Permeable Inhibitor to Trap $G\alpha_q$ Proteins in the Empty Pocket Conformation

Anna-Lena Schmitz,[1] Ramona Schrage,[2] Evelyn Gaffal,[3] Thomas H. Charpentier,[4] Johannes Wiest,[5] Georg Hiltensperger,[5] Julia Morschel,[1] Stephanie Hennen,[1] Daniela Häußler,[6] Velten Horn,[7] Daniela Wenzel,[8] Manuel Grundmann,[1] Katrin M. Büllesbach,[1] Ralf Schröder,[1] H. Henning Brewitz,[9] Johannes Schmidt,[1] Jesús Gomeza,[1] Céline Galés,[10] Bernd K. Fleischmann,[8] Thomas Tüting,[3] Diana Imhof,[9] Daniel Tietze,[7] Michael Gütschow,[6] Ulrike Holzgrabe,[5] John Sondek,[11] T. Kendall Harden,[4] Klaus Mohr,[2] and Evi Kostenis[1,*]

[1]Molecular, Cellular, and Pharmacobiology Section, Institute of Pharmaceutical Biology, University of Bonn, Nussallee 6, 53115 Bonn, Germany

[2]Pharmacology and Toxicology Section, Institute of Pharmacy, University of Bonn, Gerhard-Domagk-Straße 3, 53121 Bonn, Germany

[3]Department of Dermatology and Allergy, Laboratory of Experimental Dermatology, University of Bonn, Sigmund-Freud-Straße 25, 53105 Bonn, Germany

[4]Department of Pharmacology, School of Medicine, University of North Carolina, Chapel Hill, NC 27599-7365, USA

[5]Pharmaceutical and Medicinal Chemistry, Institute of Pharmacy and Food Chemistry, University of Würzburg, Am Hubland, 97074 Würzburg, Germany

[6]Pharmaceutical Chemistry I, Institute of Pharmacy, University of Bonn, An der Immenburg 4, 53121 Bonn, Germany

[7]Eduard-Zintl-Institute of Inorganic and Physical Chemistry, Technische Universität Darmstadt, Alarich-Weiss-Straße 8, 64287 Darmstadt, Germany

[8]Institute of Physiology I, Life and Brain Center, University of Bonn, Sigmund-Freud-Straße 25, 53105 Bonn, Germany

[9]Pharmaceutical Chemistry I, Institute of Pharmacy, University of Bonn, Brühler Straße 7, 53119 Bonn, Germany

[10]Institut des Maladies Métaboliques et Cardiovasculaires, Institut Nataional de la Santé et de la Recherche Médicale, Université Toulouse III Paul Sabatier, 31432 Toulouse, France

[11]Department of Pharmacology and Department of Biochemistry and Biophysics and Lineberger Comprehensive Cancer Center, University of North Carolina School of Medicine, Chapel Hill, NC 27599-7365, United States

*Correspondence: kostenis@uni-bonn.de

http://dx.doi.org/10.1016/j.chembiol.2014.06.003

SUMMARY

In spite of the crucial role of heterotrimeric G proteins as molecular switches transmitting signals from G protein-coupled receptors, their selective manipulation with small molecule, cell-permeable inhibitors still remains an unmet challenge. Here, we report that the small molecule BIM-46187, previously classified as pan-G protein inhibitor, preferentially silences $G\alpha_q$ signaling in a cellular context-dependent manner. Investigations into its mode of action reveal that BIM traps $G\alpha_q$ in the empty pocket conformation by permitting GDP exit but interdicting GTP entry, a molecular mechanism not yet assigned to any other small molecule Gα inhibitor to date. Our data show that Gα proteins may be "frozen" pharmacologically in an intermediate conformation along their activation pathway and propose a pharmacological strategy to specifically silence Gα subclasses with cell-permeable inhibitors.

INTRODUCTION

Heterotrimeric αβγ guanine-nucleotide-binding proteins (G proteins) are molecular switches that relay signals from activated G protein-coupled receptors (GPCRs) to (intra)-cellular effector systems such as ion channels or enzymes that, in turn, control production, release, or degradation of second messengers (Wall et al., 1998; Neves et al., 2002; Milligan and Kostenis, 2006; Johnston and Siderovski, 2007; Oldham and Hamm, 2008). These G proteins function by adopting two principal conformational states: an "off state" in which guanosine diphosphate (GDP)-bound Gα is in complex with the Gβγ heterodimer, and an "on state" in which guanosine triphosphate (GTP)-bound Gα is liberated from its Gβγ binding partner. Ligand-activated GPCRs act as guanine nucleotide exchange factors (GEFs) for G proteins that stimulate exchange of GDP for GTP on the Gα subunit (Wall et al., 1998; Johnston and Siderovski, 2007; Oldham and Hamm, 2008; Kimple et al., 2011). Crystal structures have been resolved for both GDP-bound inactive and GTP-bound active conformations and have shed light on the discrete differences of these nucleotide-dependent conformational states (Oldham and Hamm, 2008). Consequently, efforts have been undertaken to develop nucleotide-state-selective inhibitors for both inactive GDP-bound heterotrimers and active GTP-bound Gα or Gβγ dimers (Johnston et al., 2008; Bonacci et al., 2006). Despite enormous advances in understanding structure and function of Gα proteins at a mechanistic level since their discovery, very few small molecule Gα subunit inhibitors with activity in whole cells have been reported to date (Smrcka, 2013). In fact, of the four families of Gα proteins ($G\alpha_{i/o}$, $G\alpha_s$, $G\alpha_{q/11}$, and $G\alpha_{12/13}$) only $G\alpha_{i/o}$ proteins can be specifically inhibited with pertussis toxin (PTX), which has served as an invaluable probe to analyze GPCR signaling mechanisms and $G\alpha_i$-mediated cell responses (Mangmool and Kurose, 2011; Saulière et al., 2012; Ashkenazi et al., 1989; Wong et al., 1991; Itoh et al., 2003). PTX, however, cannot be considered a small molecule but represents

a typical A-B toxin using its A protomer to ADP-ribosylate $G\alpha_{i/o}$ protein family members and thereby uncouple receptors from their cognate G proteins (Mangmool and Kurose, 2011; West et al., 1985). YM-254890, a cyclic depsipeptide isolated from the fermentation broth of *Chromobacterium* sp. QS3666, has recently been shown to specifically silence function of $G\alpha_{q/11}$ proteins, including $G\alpha_{14}$ (Takasaki et al., 2004; Nishimura et al., 2010).

YM-254890 is the only inhibitor for which high-resolution structural information is available to provide the framework for understanding its mechanism of action at the molecular level. A major shortcoming of YM-254890 is that it is not commercially available and, therefore, is only accessible for very few research laboratories worldwide.

In spite of their diverse structures, all inhibitors of $G\alpha$ function apparently share a common mechanism of action, i.e., bind to $G\alpha$ subunits to prevent receptor-mediated or intrinsic nucleotide exchange (Smrcka, 2013). This mechanism of action also was proposed for two small molecules, BIM-46174 and BIM-46187, suggested as experimental anticancer drugs (Prévost et al., 2006; Ayoub et al., 2009). BIM-46174 was identified in a differential screening approach as a molecule that inhibits cyclic AMP (cAMP) production in MCF7 cancer cells that were pretreated with the irreversible $G\alpha_s$ activator choleratoxin but not in those pretreated with the direct adenylyl cyclase activator forskolin (Prévost et al., 2006). Such a screening strategy allows identification of compounds that target $G\alpha_s$ proteins but not $G\alpha_s$-sensitive receptors or adenylyl cyclases. Additional mechanistic investigations revealed that both BIM molecules display an intriguing pharmacological phenotype in that they do not only target heterotrimeric G proteins of the $G\alpha_s$ family but also target $G\alpha_{q/11}$, $G\alpha_{i/o}$, and $G\alpha_{12/13}$ proteins, a feature referred to as pan-G protein inhibition (Prévost et al., 2006; Ayoub et al., 2009).

An initial goal of the present study was to take advantage of the pan-G protein inhibitory nature of BIM-46187 to specifically investigate G protein-independent signaling. However, we found that BIM-46187 does not abolish signaling of all $G\alpha$ subfamilies equally but instead acts in a cellular context-dependent manner, ranging from pan-G protein inhibition to selective $G\alpha_q$ silencing. We identified mammalian human embryonic kidney 293 (HEK293) and Chinese hamster ovary (CHO) cells, two cell lines frequently used to examine signaling of recombinant or endogenous GPCRs, as hosts in which BIM-46187 specifically silences $G\alpha_q$ over $G\alpha_s$, $G\alpha_i$, and $G\alpha_{13}$ proteins. Based on the $G\alpha_q$-specific inhibition, we investigated the molecular mechanism underlying BIM-46187 action. Our results are consistent with the idea that BIM-46187 targets $G\alpha$ proteins and show that it interferes with agonist function, but not agonist binding to $G\alpha_q$-sensitive GPCRs, by exhibiting a mechanism not yet assigned to any other small molecule $G\alpha$ inhibitor to date.

RESULTS

BIM-46174 and the more stable derivative BIM-46187 (Figure 1A, also referred to as BIM-monomer and BIM-dimer, respectively) are two small molecules that interdict signaling of GPCRs by direct binding to and inhibition of α subunits of heterotrimeric G proteins (Prévost et al., 2006; Ayoub et al., 2009). Both molecules are thought to inhibit all $G\alpha$ subfamilies equally and therefore serve to silence receptor signaling in complex pathologies that involve multiple GPCRs (Smrcka, 2013; Prévost et al., 2006). We wanted to take advantage of the pan-G protein inhibitors to specifically dissect G-protein-dependent versus G-protein-independent signaling events mediated by cell surface GPCRs. We hypothesized that the free thiol group-containing monomeric BIM should be intrinsically sensitive to oxidation; therefore, we initially investigated stability in aqueous solution (D_2O) over time by nuclear magnetic resonance (NMR) spectroscopy (Figure 1B). NMR spectra are clearly indicative of BIM-monomer oxidation in a time-dependent manner: After 48 hr, BIM-monomer is virtually undetectable (Figure 1C). Since the integration area of the signals correlates with the concentration of BIM-monomer, we were able to deduce a half-life of 11.4 hr for this first-order reaction (Figure 1D and Table S1 available online). We reasoned that oxidation of BIM-monomer should depend on the presence of reducing agents and therefore examined stability by NMR in D_2O containing reactive thiols (L-cysteine, glutathione [GSH]), and mercaptoethanol. Indeed, under these conditions, quantitative formation of covalent complexes with selected thiols was observed: BIM-cysteine, BIM-mercaptoethanol, and BIM-dimer (Figure S1). Additionally, we investigated the stability of both BIM-monomer and -dimer during cellular assays by analyzing the cell culture supernatant with liquid chromatography-mass spectrometry. We identified BIM-cysteine, BIM-mercaptoethanol, BIM-dimer, or BIM-monomer, respectively, after 24 hr at 37°C (Figure S2). These data suggest that (1) assessment of biological activity of BIM-monomer should take into account that extracellular BIM-monomer might be entirely converted to BIM-dimer during the assay period, and (2) that both BIM molecules are prone to formation of redox-reversible adducts when thiol-containing components are present. This notion might be particularly relevant when antiproliferative activity of BIM is assessed, because such assays typically range from many hours to days.

Despite the short duration of assays that assess GPCR activity by quantifying intracellular second messengers and the absence of reducing agents in these assays, we chose the chemically more stable BIM-dimer for further studies. In agreement with the inability of BIM to affect cAMP production in the breast cancer MCF7 and COS7 cell background upon stimulation with the direct adenylyl cyclase mimetic forskolin (Prévost et al., 2006; Ayoub et al., 2009), it did not blunt cAMP synthesis in forskolin-stimulated HEK293 cells (Figure 2A). It is surprising, however, that BIM also was largely ineffective when cAMP production was triggered with prostaglandin E_1 (PGE_1), a bona fide stimulus of the $G\alpha_s$-linked E prostanoid EP2 and EP4 receptors that are endogenously expressed in this cell system (Figure 2B). Proper functionality of our cAMP assay was ascertained by preincubation of cells in the presence of an EP2/EP4 antagonist, which completely blunted PGE_1-mediated cAMP synthesis (Figure S3). Lack of BIM inhibition of $G\alpha_s$-coupled receptor signaling is not due to BIM decomposition during the assay period, because BIM significantly dampened EP2/EP4 receptor signaling in a COS7 cell background (Figure 2C). We therefore reasoned that BIM interferes with G protein signaling in a cell-type-specific manner. Such a pharmacological phenotype would be of relevance for an anticancer agent, particularly if it is applied under the assumption that the entire set of G protein pathways is silenced simultaneously in any cell type.

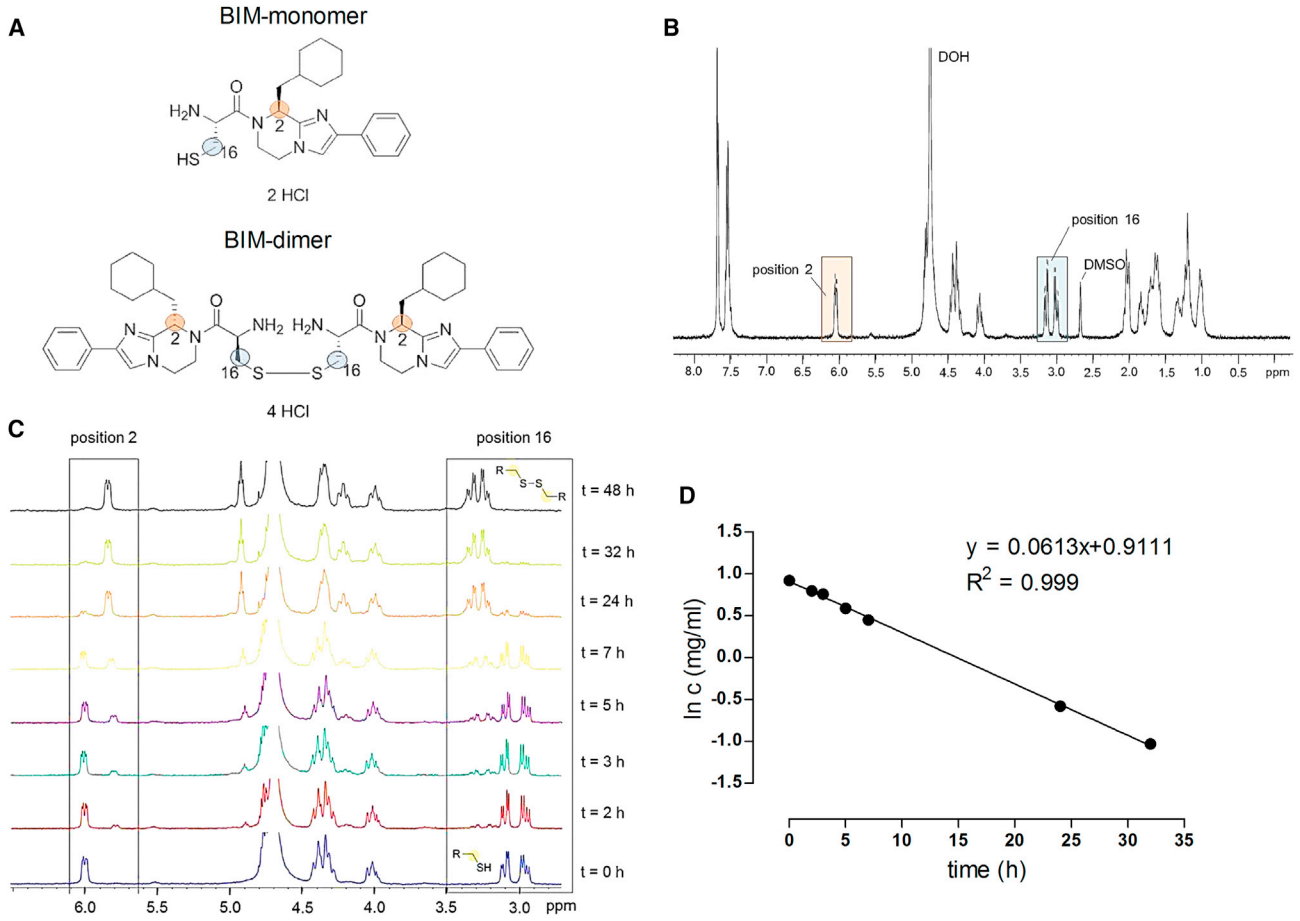

Figure 1. Structures of BIM-Monomer and BIM-Dimer and Stability in Aqueous Solution, D_2O, as Determined by NMR Spectroscopy

(A) Chemical structures of the BIM-monomer and the BIM-dimer.

(B) ^1H NMR of the BIM-monomer at t = 0 hr. The signals at δ = 7.4–7.8 ppm belong to the protons of the aromatic moiety and the imidazole ring. The signal at δ = 6.0 ppm corresponds to the proton in position 2 and the area from δ = 4.0 to 5.0 ppm comprises the protons of position 12, 13 and 15 partially overlayed by the residual solvent (DOH) signal. At about δ = 3 ppm, the diastereotopic methylene protons next to the thiol group resonate (position 16), followed by the DMSO signal and the high-field shifted protons of the cyclohexylmethyl group.

(C) Oxidation of the BIM-monomer over time. The oxidation process can be observed using the protons in position 2 and 16. At t = 0 hr, only the proton signals of the monomer were observed. Within 48 hr, the integration areas of the signals of the monomer protons decrease, while the dimer signals increase until 100% dimer was observed at t = 48 hr. h, hours. R-SH denotes BIM-monomer, and R-S-S-R denotes BIM-dimer.

(D) A diagram of the natural logarithm of the concentration (ln c) of BIM-monomer versus time. Since the integration area of the signals in (C) correlates with the concentration of the BIM-monomer, a half-life of 11.4 hr is calculated for this first-order reaction.

See also Figures S1 and S2 and Table S1.

To explore the consequences of BIM exposure for functionality of the remaining G protein pathways, HEK293 cells were treated with a set of different stimuli for $G\alpha_i$-, $G\alpha_q$-, and $G\alpha_{13}$-linked receptors that are natively or were exogenously expressed in this cell system. It is interesting that preincubation of cells with BIM completely abolished signaling of $G\alpha_q$-sensitive receptors (Figures 3A–3C) but hardly affected signaling of those that are functionally coupled to $G\alpha_i$ proteins (Figures 3D–3F). Even when cells were preincubated with 100 μM of BIM—the highest applicable concentration—robust $G\alpha_i$ activation was still detected. A similar lack of BIM inhibition was observed when GPCR engagement of $G\alpha_{13}$ signaling was recorded using lysophosphatidylinositol and its target receptor GPR55 in bioluminescence resonance energy transfer (BRET) assays. We recorded a substantial agonist-promoted decrease in BRET in cells coexpressing GPR55 along with the energy donor $G\alpha_{13}$-106*R*Luc8, the energy acceptor $G\gamma_2$-GFP[10], and unlabeled $G\beta_1$. This BRET decrease reflects the separation of the Gα-helical domain from the N terminus of Gγ thereby creating the route for GDP exit and GTP entry (Galés et al., 2006; Saulière et al., 2012). Pretreatment of transfected cells with BIM did not alter GPR55-$G\alpha_{13}$ activation (Figure 3G) but significantly blunted activation-dependent rearrangement of the $G\alpha_q$-$\beta_1\gamma_2$ heterotrimer triggered with carbachol via muscarinic M3 receptors (Figure 3H). These results suggest that the BRET partners used are suitable for examining inhibition of G protein signaling by BIM and that BIM is competent to interdict $G\alpha_q$ but not $G\alpha_{13}$ signaling.

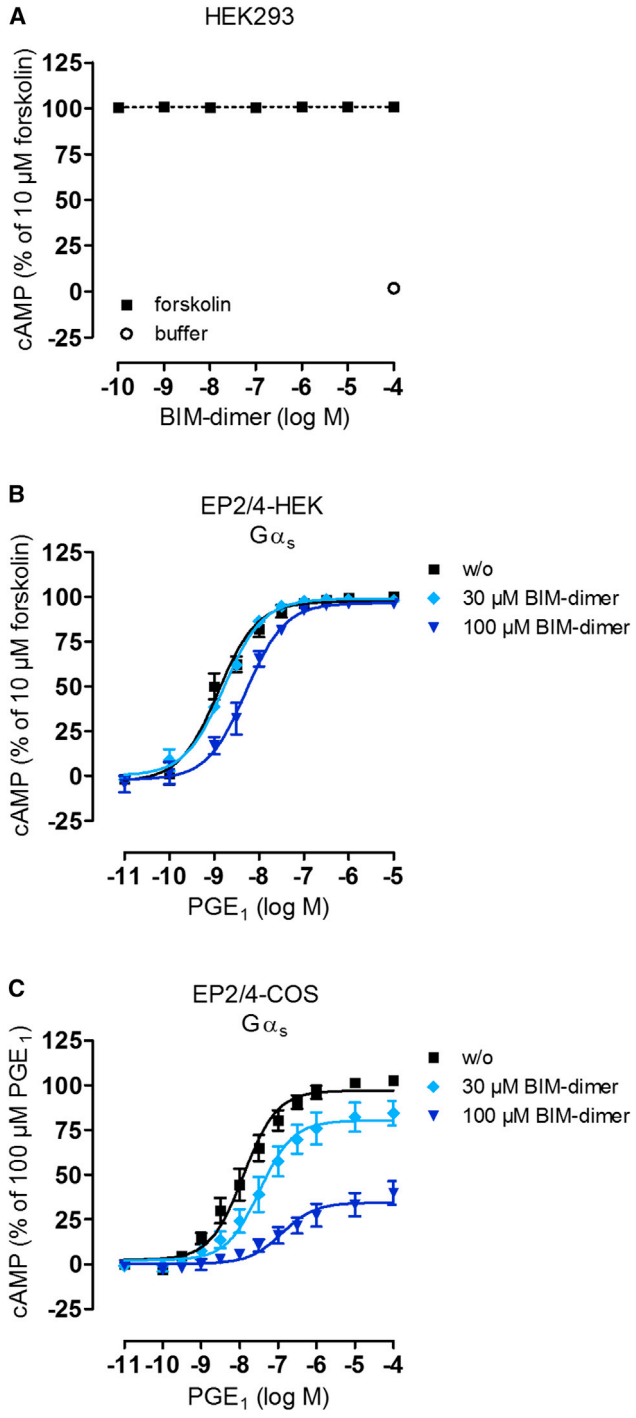

Figure 2. Effects of BIM on Cellular cAMP Levels in an HEK293 and COS7 Cell Background

(A) Increasing concentrations of BIM do not lower forskolin-mediated cAMP production in HEK293 cells.

(B) BIM slightly diminishes cAMP signaling of the $G\alpha_s$-sensitive EP2/EP4 receptors in HEK293 cells. Negative logarithm of EC_{50} (pEC_{50}) for PGE_1 (without [w/o] BIM) = 8.91 ± 0.07; pEC_{50} for PGE_1 (100 µM BIM) = 8.29 ± 0.06.

(C) BIM largely suppresses prostaglandin E_1-mediated cAMP production in COS7 cells. Data shown in (A) through (C) are mean values ± SEM of three to ten independent experiments, each performed in triplicate.

See also Figure S3.

So far, BIM has been applied to a number of different cancer cell lines, such as breast cancer MCF7 and human colorectal cancer HCT8/S11 and HT29, among many others (Ayoub et al., 2009; Prévost et al., 2006). Nonetheless, its utility to silence all G protein signaling pathways in immortalized cell lines that are frequently used for recombinant expression such as HEK293 or CHO is undefined. So far, only COS7 cells have been used as an immortalized host in elegant studies to examine the mechanism of BIM action in great detail (Ayoub et al., 2009). We therefore investigated the influence of BIM on second messenger pathways using CHO cells as an expression system. Again, BIM did not exert pan-G protein inhibitory activity but rather targeted $G\alpha_q$ proteins as evidenced by the clear preference to interdict signaling of the $G\alpha_q$-sensitive muscarinic M1 receptor over $G\alpha_s$-linked prostanoid and $G\alpha_i$-linked serotonin receptors (Figures 4A–4C). A similar preference for inhibition of $G\alpha_q$-signaling was observed when monomeric BIM was applied in analogous second messenger assays, both in CHO (Figures 4D–4F) and HEK cell backgrounds (Figures 4G–4I). From these data, we infer that (1) cellular context-dependent inhibition of $G\alpha_q$ signaling is not related to the inability of the cells to convert dimeric BIM into its reduced counterpart, and hence to different reductive capacities of cells; and (2) dimeric BIM is superior to monomeric BIM for silencing of $G\alpha_q$ signaling, at least in the CHO and HEK cell backgrounds.

We next addressed whether the absence of pan-G protein inhibition may be related to the export of BIM via multidrug transporters. If BIM was a substrate for active outward transport, inhibition of BIM efflux by coadministration of a transport inhibitor should improve its capacity to interdict $G\alpha_q$ signaling. To test this assumption, we pretreated HEK cells, which endogenously express multidrug transporters, with MK571 or elacridar to block efflux protein activity. MK571 inhibits MRP1 and MRP2, two transporters that export hydrophilic molecules and GSH conjugates (Wortelboer et al., 2003; Leyers et al., 2008). Elacridar inhibits P-glycoprotein (P-gp) and breast cancer resistance protein (BCRP), the former preferring hydrophobic and the latter transporting rather diverse and nonconjugated compounds (Ahmed-Belkacem et al., 2005). None of the applied inhibitors rendered $G\alpha_q$ signaling more sensitive toward BIM inhibition (Figure S4). Thus, we conclude that export of BIM via multidrug transporters does not account for cell-type-specific differences in G protein inhibition profiles.

It is interesting to note that BIM displays antiproliferative effects in HEK cells (Prévost et al., 2006) yet only silences $G\alpha_q$ signaling in this cellular background. Furthermore, the effective concentration of BIM to inhibit cellular proliferation is much lower as compared with the concentration required to achieve full silencing of $G\alpha_q$ signaling (compare Prévost et al., 2006 with Figure 3). Such data imply that inhibition of $G\alpha_q$ signaling may be sufficient for blockade of cellular proliferation or that the antiproliferative effects of BIM are unrelated to pan-G protein inhibition. To explore a mechanistic link between G protein inhibition and abrogation of cell growth, we chose to directly compare these parameters in the patient-derived human skin cancer cell line MZ7. BIM exhibited concentration-dependent inhibition of cell growth in MZ7 cells as evidenced by crystal violet staining and determination of cell viability in parallel treatment groups (Figure 5A). A similar reduction of cell growth was obtained on

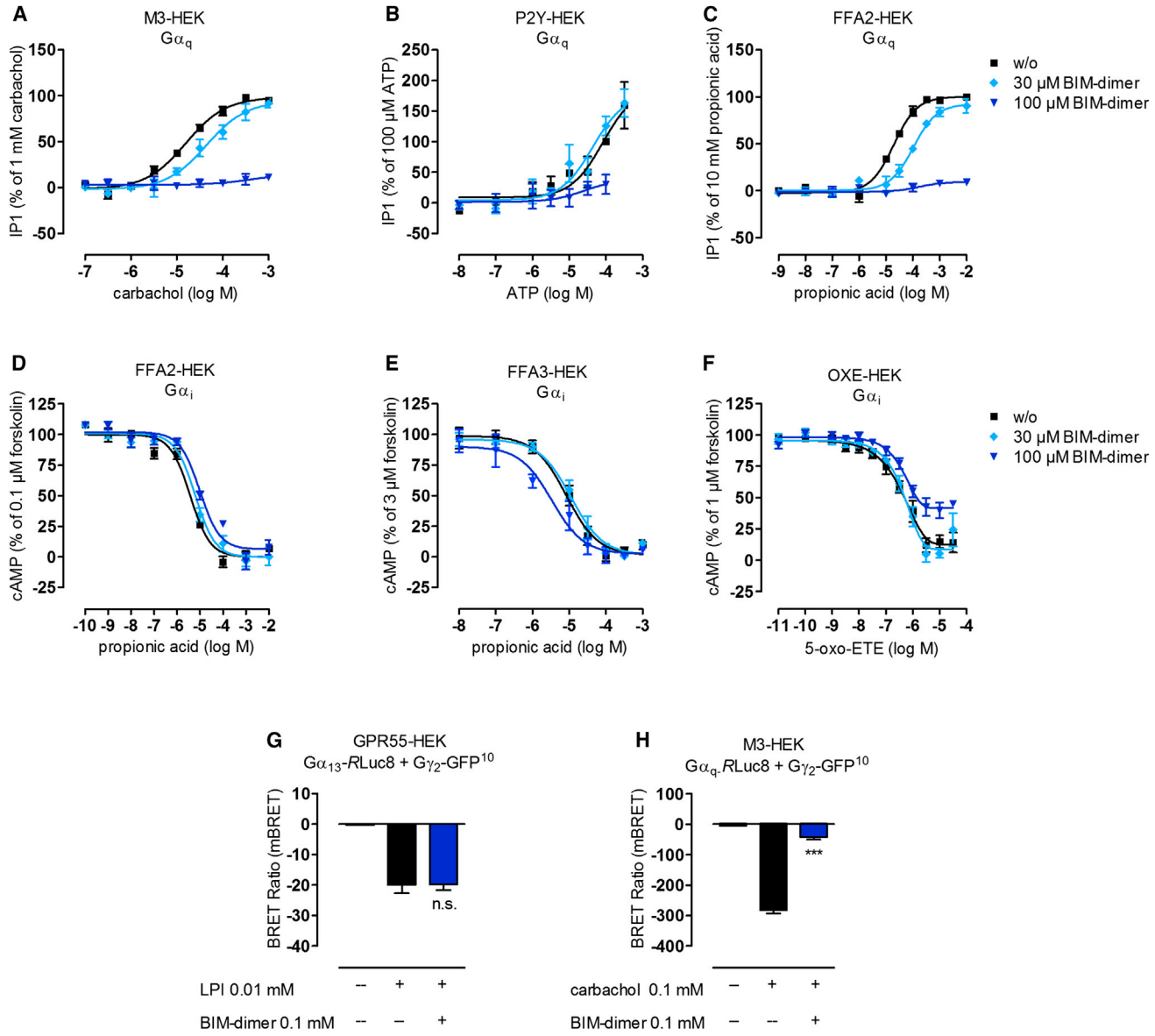

Figure 3. BIM Interdicts Gαq Signaling but Not Gαi or Gα13 Signaling in HEK293 Cells

(A–C) BIM (100 µM) silences Gαq activation induced by stimulation of three Gαq-sensitive receptors (muscarinic M3, P2Y, and FFA2) with their cognate agonists carbachol, ATP, and propionic acid, respectively. w/o, without.

(D–F) BIM (100 µM) hardly affects productive Gαi interaction of FFA2 and FFA3, as well as OXE-R.

(G and H) BIM does not block molecular rearrangement of activated Gα13 (G) but efficiently dampens activation of the Gαq-BRET biosensor (H). Opening of the nucleotide binding pocket is detected as BRET decrease after receptor activation in HEK293 cells transfected to express Gα13-106*R*Luc8 + Gγ2-GFP[10] + unlabeled Gβ1 (G) or Gαq-97*R*Luc8 + Gγ2-GFP[10] + unlabeled Gβ1 (H). ***p < 0.001; n.s., not significant.

The means ± SEM in (A) through (F) or + SEM in (G) and (H) of three to six independent experiments, each conducted in triplicate, are shown.

treatment with the DNA-replication inhibitor aphidicolin, which inhibits cell cycle progression at the G1/S phase (Figure 5A). However, aphidicolin-arrested cells resumed cell growth on inhibitor removal as opposed to BIM-treated cells, indicating that BIM likely induces cell death. It is interesting that inhibition of cell growth by BIM was maximal at 10 µM, yet an even greater 10-fold increase of BIM concentration was required to dampen cellular signaling via Gαi, Gαs, and Gαq pathways (Figures 5B–5D). BIM inhibition of second messenger pathways appears to occur specifically at the level of the G proteins, even at these high concentrations, because prior addition of 100 µM BIM completely blocked endothelin-1, but not thapsigargin-induced Ca^{2+} mobilization (Figure 5B), and because BIM did not lower cAMP production triggered with forskolin (Figure S5) but completely prevented cAMP formation in response to adrenocorticotropic hormone (ACTH), a stimulus for the Gαs-sensitive melanocortin 1 (MC1) receptor (Figure 5C). Together, these data indicate that BIM does indeed silence all three second

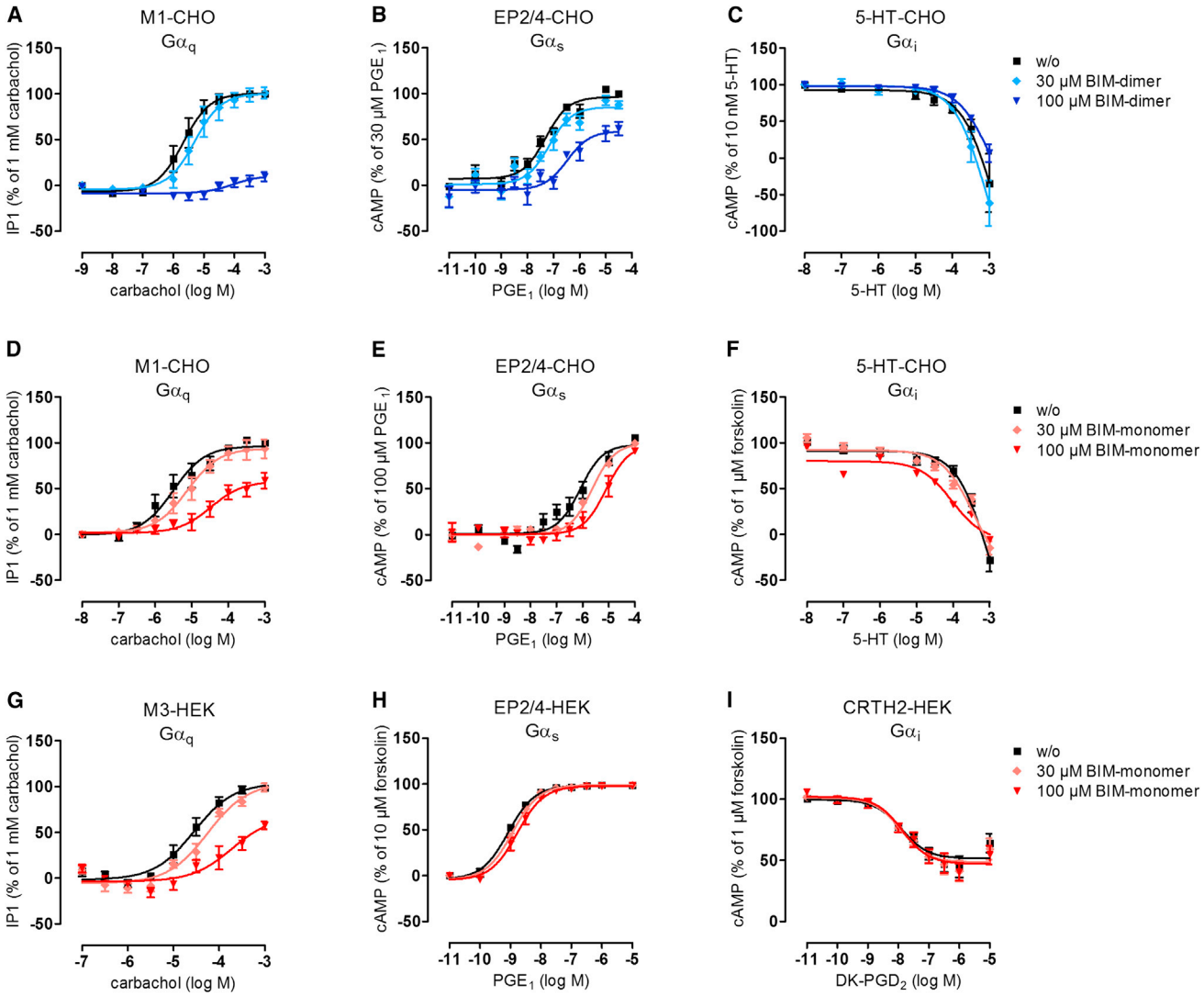

Figure 4. Monomeric and Dimeric BIM Preferentially Silence $G\alpha_q$ Signaling in a CHO and HEK293 Cell Background

(A–C) Dimeric BIM almost completely blunts $G\alpha_q$ signaling over $G\alpha_s$ and $G\alpha_i$ signaling in CHO cells transfected to express the muscarinic M1 receptor (A) or endogenously expressing $G\alpha_s$-linked EP2/EP4 receptors (B) and the $G\alpha_i$-sensitive serotonin 5-HT receptors (C).

(D–F) Monomeric BIM resembles dimeric BIM in its ability to preferentially silence $G\alpha_q$ signaling of the muscarinic M1 receptor (D) over $G\alpha_s$ signaling of EP2/EP4 receptors (E) or $G\alpha_i$ signaling of serotonin 5-HT receptors (F) in a CHO cell background yet displays reduced potency and efficacy.

(G–I) Monomeric BIM partially diminishes $G\alpha_q$ activation of the muscarinic M3 receptor in HEK293 cells (G) but does not dampen signaling mediated via $G\alpha_s$-sensitive EP2/EP4 receptors (H) or $G\alpha_i$-sensitive CRTH2 receptors (I). Means ± SEM of at least three experiments, each conducted in triplicate, are shown.

messenger pathways in the cancer MZ7 cell background but at concentrations clearly exceeding those required to inhibit cell growth. This discrepancy may be explained by (1) short (second messenger assays) versus long (cell growth assays) BIM preincubation times; (2) cumulative/cooperative effects of BIM in cell growth assays, where multiple signaling pathways are silenced simultaneously; and/or (3) abrogation of ligand-stimulated signaling (second messenger assays) versus endogenous receptor signaling (cell growth assays).

Context-dependent pharmacology of GPCR ligands is a well-known phenomenon that is widely appreciated. Often, cell-type-specific differences in the relative amount or stoichiometry of signaling components may account for functionally different effects of ligands across cell lines (Kenakin and Christopoulos, 2013). We therefore investigated whether the extent of BIM inhibition may be related to the level of expression of its protein target. To this end, HEK293 cells were enriched with increasing amounts of $G\alpha_q$ proteins using a gene dosing approach (Figures 6A and 6B), and sensitivity of $G\alpha_q$ proteins toward BIM inhibition was examined in assays monitoring inositol monophosphate (IP1) production upon stimulation of endogenous muscarinic M3 receptors with carbachol. Indeed, a clear correlation between BIM inhibition and $G\alpha_q$ expression could be detected: BIM inhibition gradually declined when cellular abundance of $G\alpha_q$ proteins was raised (Figure 6C). These data imply a link between the expression level of BIM target proteins and the extent

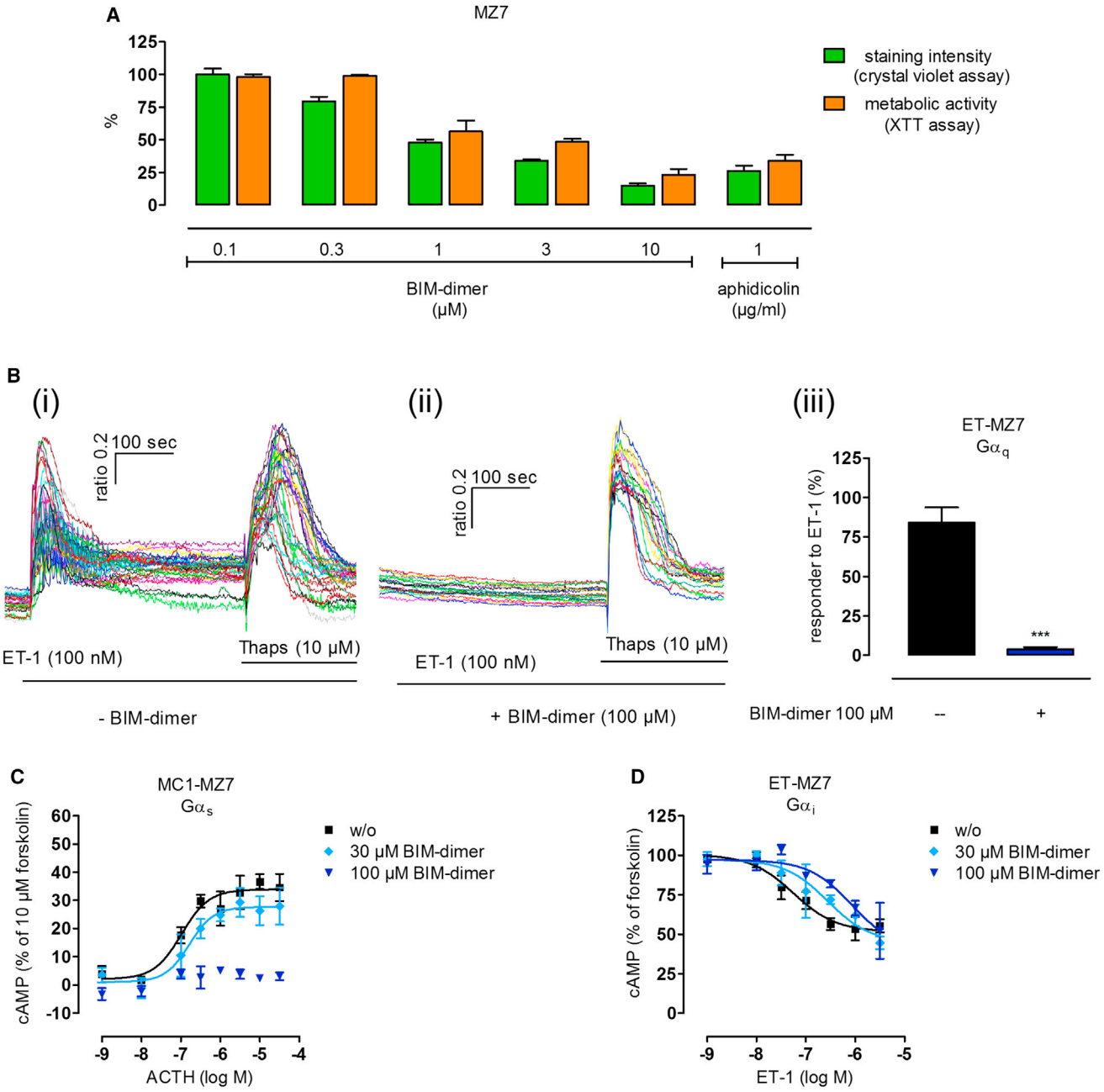

Figure 5. BIM Inhibits Cell Growth and Second Messenger Production in the Patient-Derived MZ7 Cancer Cell Background

(A) MZ7 cancer cells were exposed to the indicated concentrations of BIM or the cell cycle inhibitor aphidicolin for 72 hr and cell proliferation was assessed by crystal violet staining (green bars). In parallel treatment groups cell viability was measured using the XTT-based cell viability kit (orange bars), means + SEM, n = 3.

(B) In (i), untreated MZ7 cells respond to both the $G\alpha_q$–stimulus endothelin-1 (ET-1) and thapsigargin (Thaps). (ii) BIM completely blunts Ca^{2+} mobilization triggered with ET-1 but does not impair thapsigargin-induced release of Ca^{2+} from the endoplasmic reticulum. (iii) Quantification of Ca^{2+} traces in the absence and presence of BIM in single cells. Data in (i) and (ii) show representative traces; data in (iii) are means + SEM of n = 159 cells. sec, seconds. ***$p < 0.001$.

(C) At a concentration of 100 μM, BIM silences $G\alpha_s$-mediated cAMP production induced via ACTH and its cognate $G\alpha_s$-linked MC1 receptor.

(D) BIM diminishes $G\alpha_i$ coupling of endogenous ET-1 receptors. Data shown in (C) and (D) are means ± SEM of three to ten independent experiments, each conducted in triplicate.

See also Figure S5.

of BIM inhibition. We reasoned that the disparate G protein inhibition profiles observed in MZ7 versus HEK293 cells might also be related to cellular Gα abundance and quantified expression of $G\alpha_q$, $G\alpha_s$, and $G\alpha_i$ proteins by immunoblotting in both cell lines. Figures 6D–6F reveal equal expression of $G\alpha_q$ but significantly lower abundance of $G\alpha_s$ in the MZ7 background. These data lend further support to the notion that Gα subunit expression and BIM inhibition might be mechanistically linked.

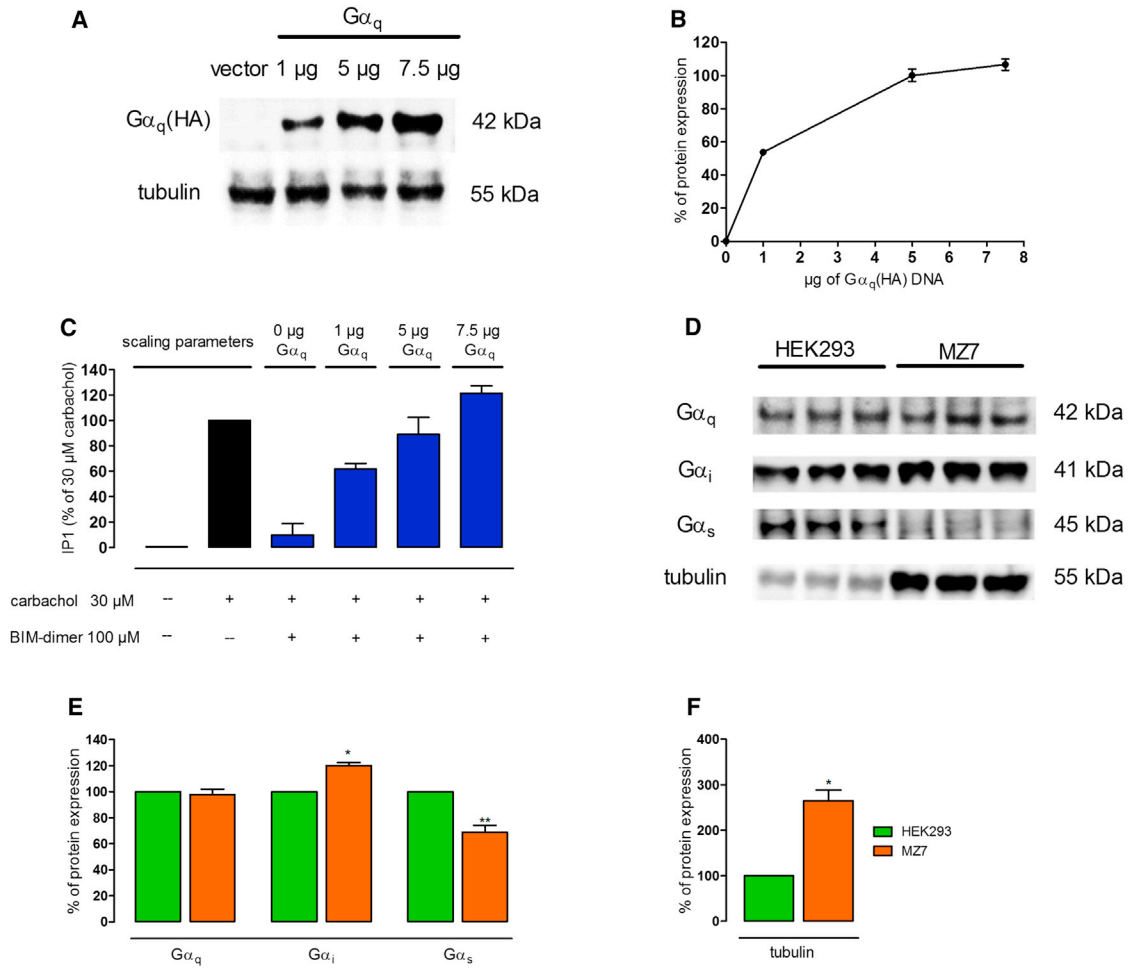

Figure 6. Mechanistic Link between Sensitivity toward BIM Inhibition and Cellular Abundance of BIM Target Proteins

(A) Immunoblot detection of HEK293 lysates prepared after transfection with the indicated amounts of $G\alpha_q$ plasmid complementary DNA harboring an internal HA-epitope tag. Membranes were reprobed for tubulin to ensure equal sample loading and transfer. Shown is one representative of four independent experiments.

(B) Densitometric analysis of the immunoblot experiments depicted in (A). Means ± SEM of four individual experiments are shown.

(C) Enrichment of HEK293 cells with the indicated amounts of $G\alpha_q$ proteins is inversely related to BIM inhibition of $G\alpha_q$ signaling (means ± SEM, n = 4).

(D) Immunoblot detection of lysates prepared from native HEK293 and MZ7 cells. Membranes were initially probed for $G\alpha_q$, $G\alpha_i$, and $G\alpha_s$ proteins and then reprobed for tubulin to ensure equal sample loading and transfer. Shown is one representative of three independent experiments.

(E and F) Densitometric analysis of the immunoblot experiments depicted in (D); means + SEM, n = 3.

However, enhanced abundance of $G\alpha_i$ proteins in MZ7 cells is incongruent with our hypothesis. Together, these data may help explain the absence of pan-G protein inhibition across diverse cell lines yet also indicate that variation in $G\alpha$ expression does not exclusively account for cell-type-dependent pharmacology of BIM. Clearly, the mechanistic basis underlying cellular context-dependent inhibition must be ascribed to additional reasons why this apparent paradox exists between $G\alpha_q$ selective inhibition in some cells and pan-G protein inhibition in others.

We were intrigued by the finding that BIM might serve to specifically abrogate $G\alpha_q$ signaling in defined cellular environments and wanted to ascertain that perturbation of $G\alpha_q$-sensitive receptor function is not due to disruption of agonist binding. We chose the carbachol-ligated muscarinic M1 receptor as a model system using radioligand competition assays. Our binding assays in whole CHO-M1 cells clearly revealed that BIM did not impair but rather enhanced carbachol displacement of the radio-antagonist [^{3}H]N-methylscopolamine ([^{3}H]NMS) from M1 receptors (Figure 7A). Hence, inhibition of $G\alpha_q$ signaling by BIM in CHO-M1 cells is due to BIM interference with agonist function but not agonist binding.

BIM has been reported to completely prevent G protein activation in [^{35}S]GTPγS binding assays, regardless of whether activation is achieved with a ligand-occupied GPCR, the direct G protein activators mastoparan or AlF_4^-, or the $G\alpha_i$ mimetic FUB132 (Prévost et al., 2006; Ayoub et al., 2009). While all of these studies support a direct action of BIM on the $G\alpha$ protein itself, it has not yet been clarified whether BIM impairs GDP exit or GTP entry. To discriminate between these possibilities, we performed radioligand binding assays on membranes isolated from CHO-M1 cells using the radio-antagonist [^{3}H]NMS. Initial homologous competition experiments indicated that BIM

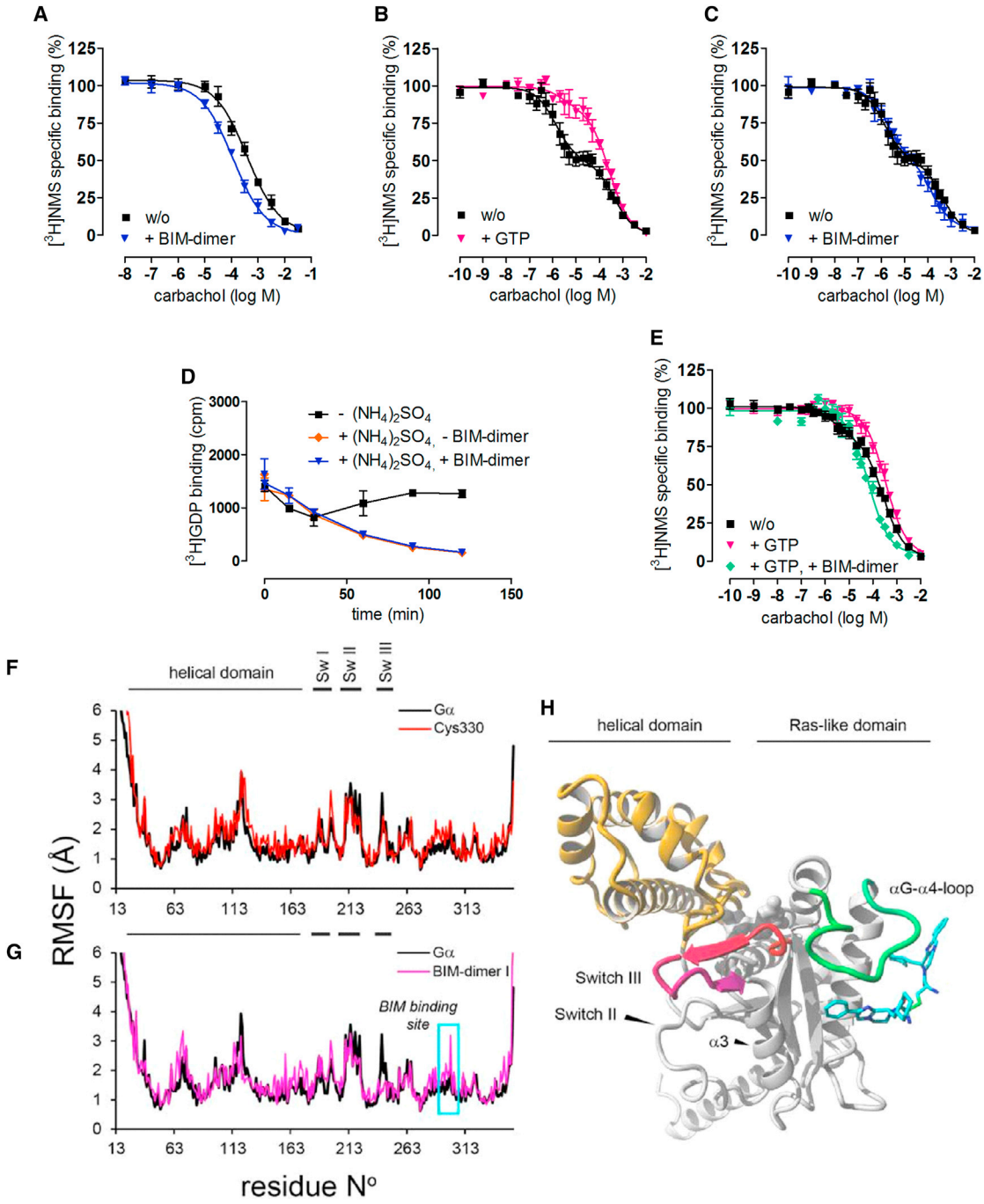

Figure 7. Effect of BIM on Carbachol Recognition of the M1 Muscarinic Receptor in Radioligand Competition Binding Assays and on [^{3}H]GDP Dissociation from Purified Gα_q

(A) BIM (100 μM) enhances carbachol affinity to muscarinic M1 receptors labeled with the radio-antagonist [^{3}H]NMS in whole CHO-M1 cells: $pKI_{(control)}$ = 3.61 ± 0.08, (n = 6); $pKI_{(BIM)}$ = 4.09 ± 0.09, n = 3, $p < 0.05$. w/o, without.

(B) In membrane preparations from CHO-M1 cells, carbachol competes for [^{3}H]NMS sites with high and low affinity. In the presence of 1 mM GTP, 51% of the high-affinity sites were converted to low-affinity sites.

(C) BIM (100 μM) does not impair formation of high-affinity agonist complexes in CHO-M1 membranes.

(D) BIM (100 μM) does not impair [^{3}H]GDP dissociation from purified recombinant Gα_q. [^{3}H]GDP was preloaded on Gα_q for 18 hr before dissociation was visualized in the presence of 750 mM $(NH_4)_2SO_4$.

(E) BIM counteracts the effect of GTP on high-affinity agonist binding in membrane preparations from CHO-M1 cells. In the absence of GTP, 20% of receptors resumed the high-affinity state that was reversed entirely in the presence of GTP, the effect of which was counteracted by BIM. Data in (A) through (E) are means ± SEM of three to four independent experiments, each conducted at least in duplicate.

(legend continued on next page)

did not compromise antagonist recognition of the M1 receptor (Figure S6). If BIM acted as guanine-nucleotide dissociation inhibitor (GDI), i.e., precluded GDP exit from the nucleotide binding pocket, it would be evident as inhibition of high-affinity agonist binding, a conformational receptor state that is stabilized by the nucleotide-free, empty-pocket G protein (De Lean et al., 1980; Oldham and Hamm, 2008; Rodbell et al., 1971). Note that high-affinity ternary complexes can only be visualized when guanine nucleotides are absent but are short-lived intermediates in intact cells where guanine nucleotides are abundant (Rodbell et al., 1971; Oldham and Hamm, 2008; Seifert et al., 1999; De Lean et al., 1980). We also detected high affinity-binding of carbachol to G-protein-coupled and low-affinity binding to G-protein-uncoupled M1 receptors in [^{3}H]NMS competition binding assays (Figure 7B and Table S2). GTP (1 mM) almost completely converted the high-affinity sites to a low-affinity population because, under these conditions, GDP is rapidly exchanged for GTP and the short-lived empty pocket conformation is no longer detectable (Figure 7B and Table S2). In contrast, high-affinity agonist binding was indistinguishable in the absence and presence of BIM, suggesting that it does not uncouple receptors from their cognate G proteins (Figure 7C and Table S2). Thus, despite the presence of BIM, stable active-state complexes do form, indicating that BIM uncouples high-affinity agonist binding from agonist function. This mode of action can only be rationalized if BIM permitted GDP exit but precluded GTP entry. To further substantiate the proposed mechanism of action, we measured [^{3}H]GDP dissociation from purified recombinant $G\alpha_q$. Since $G\alpha_q$-bound GDP dissociates very slowly (Chidiac et al., 1999), we took advantage of $(NH_4)_2SO_4$ to accelerate and, therefore, visualize its dissociation. GDP dissociation in the presence of 750 mM $(NH_4)_2SO_4$ was complete within 120 min but, notably, unaffected by the presence of BIM (Figure 7D). These data strongly suggest that BIM does not act as a GDI but permits egress of GDP from the nucleotide binding pocket. BIM, however, does counteract the effect of GTP on high-affinity agonist binding (Figure 7E). Therefore, our results are entirely consistent with the view that BIM inhibits $G\alpha_q$ function by permitting GDP exit but precluding GTP entry, i.e., "freezes" $G\alpha_q$ in the empty pocket conformational intermediate along the activation pathway.

To rationalize this mode of inhibitor action, we conducted docking experiments and all-atom molecular dynamics (MD) simulations to assess the effect of BIM on motions required for nucleotide exchange. Given the absence of mutagenic mapping or structural data, two scenarios were taken into consideration. The first scenario was covalent attachment to cysteine residues that are conserved among all $G\alpha$ proteins but are not part of the $G\alpha/G\beta\gamma$ interface (C144 and C330 within $G\alpha_q$). This assumption is based on the notion that BIM, in principle, inhibits all $G\alpha$ subfamilies but does not impair formation of $G\alpha$-$G\beta\gamma$ heterotrimers in vitro (Ayoub et al., 2009). The second scenario was noncovalent binding to an epitope within $G\alpha$, as determined through independent molecular docking experiments. Docking results reveal high binding energies and a large overlap in the binding sites for BIM-monomer and -dimer, respectively, at least for the best scoring cluster conformations (Figure S7 and Table S3).

We then subjected the individual $G\alpha$-BIM complexes to all-atom MD simulations. We calculated average protein structures and used fluctuations of $C\alpha$ residues relative to the average structure as a measure of dynamic motion, which is often linked to intrinsic domain motion (Jones et al., 2012). As shown in Figure 7F, fluctuations in GDP-$G\alpha_q$ (indicated by black trace) are greatest in the three switch regions of the Ras-like domain and in the αB-αC loop of the helical domain (please note that the energy donor *R*Luc of our $G\alpha_q$ BRET sensor is inserted into the αB-αC loop). When BIM is covalently bound to Cys330 within $G\alpha_q$ (Figure 7F, red trace), the magnitude of local fluctuations in switch regions II and III and in the αB-αC loop is clearly diminished. This reduction in local mobility aligns well with the impaired helical domain motion that is detected in our BRET experiments (compare with Figure 3H). In contrast, when BIM is linked to Cys144, only switch region II and the αB-αC loop display reduced mobility (Figure S8, blue trace). It is intriguing that we observed even higher reduction in local fluctuations, particularly in switch region III for the best scoring complex conformation of BIM-dimer (Figure 7G, magenta trace, and Figure 7H). No changes in the local fluctuations were recorded for the other complex conformations analyzed with all-atom MD simulations (Figures S8B–S8D). Together, we propose three potential binding sites for BIM. All of these sites are compatible with the notion that BIM impairs intradomain motion within $G\alpha$ by compromising local mobility, most likely the conformational changes required for GTP binding in the switch regions, and additionally, the large motion of the helical domain away from the Ras-like domain, a prerequisite for GDP/GTP exchange.

DISCUSSION

Great therapeutic interest exists for modulation of GPCR-promoted signal transduction. Although most current therapies utilize receptor agonists or antagonists (Rask-Andersen et al., 2011), manipulation of GPCR signaling at steps distal to receptors, such as on the level of heterotrimeric G proteins, is an attractive alternative, particularly for diseases with complex pathologies, involving multiple receptors and signaling pathways (Smrcka, 2013). One example for small molecules interfering with GPCR signaling at the postreceptor level are the imidazopyrazine derivatives BIM-46174 and its more stable derivative BIM-46187 (Figure 1A), each reported to dampen cellular signaling of all four families of heterotrimeric G proteins equally, a property coined pan-G protein inhibition (Prévost et al., 2006; Ayoub et al., 2009). The pan-G protein inhibition may represent an innovative molecular intervention to target oncogenic signaling pathways.

We wanted to take advantage of the pan-G protein inhibitory nature of BIM to study G-protein-independent signaling but

(F and G) Root-mean-square-fluctuations (RMSF) as a function of their residue number for the indicated simulation. (F) Simulation of GDP-$G\alpha_q$ (black trace), BIM covalently bound to GDP-$G\alpha_q$ (red trace). (G) Simulation of GDP-$G\alpha_q$ (black trace), BIM-dimer complex conformation I (BIM-GDP-$G\alpha_q$, magenta trace). The BIM-dimer binding site encompassing residues 292–311 (αG-α4 loop and α4 helix) is boxed in light blue.
(H) BIM-dimer complex conformation I after 10 ns of MD simulation.
See also Figures S6–S8 and Table S2.

made three significant observations: (1) BIM does not silence all G protein subfamilies equally but rather interferes with G protein signaling in a cellular context-dependent manner; (2) BIM may even serve to specifically silence $G\alpha_q$ signaling in defined cellular backgrounds; and (3) BIM inhibits $G\alpha\beta\gamma$ heterotrimer function via interference with nucleotide cycling, using a unique molecular mechanism: precluding GTP entry into rather than GDP exit from the nucleotide binding pocket.

Inhibition of heterotrimeric G proteins may be achieved on the level of the $\alpha\beta\gamma$ heterotrimer or on the level of the dissociated subunits. Of the few existing inhibitors for G protein signaling, mechanistic details at the structural level are only available for the $G\alpha_q$-selective YM-254890 (Nishimura et al., 2010). Its binding mode, as elucidated by means of mutagenesis and structural data, provides a plausible mechanism for inhibition of GDP release. A similar mechanism of action has been proposed for suramin, a polysulphonated molecule with a preference for inhibiting $G\alpha_s$ proteins, but this molecule is of limited utility in cell-based assays because it does not cross cell membranes due to its strong negative charge (Smrcka, 2013; Hohenegger et al., 1998). BIM has also been proposed to interfere with the GDP/GTP exchange reaction, but it has not been clarified whether BIM resembles suramin and YM in that it prevents receptor-stimulated GDP release. To address this question, we performed radioligand binding studies under conditions that allow assessment of nucleotide-sensitive binding states of GPCRs. Agonist docking to GPCRs promotes an active receptor state that engages heterotrimeric G proteins and initially triggers GDP release from the $G\alpha$ subunit (Oldham and Hamm, 2008). Nucleotide-free G proteins, in turn, stabilize the agonist-bound active state of GPCRs. These active-state ternary complexes can only be observed when guanine nucleotides are absent but are transient conformational intermediates in intact cells where GTP and GDP are abundant (Rodbell et al., 1971; De Lean et al., 1980; Seifert et al., 1999). Herein, we took advantage of the formation of such active-state ternary complexes as indicators for the mechanism of interference of BIM with the nucleotide-bound state of $G\alpha$. It is well accepted that high-affinity agonist binding can be disrupted with high concentrations of guanine nucleotides such as GTP because, under these conditions, GDP is rapidly exchanged for GTP and the short-lived empty pocket conformation is no longer detectable. Therefore, agents that act like GTP, i.e., promote the uncoupling of the activated G protein from the receptor, can be identified in radioligand binding assays. Similarly, such assays are ideal for identifying molecules that stabilize GDP-bound $G\alpha$, i.e., act as guanine nucleotide dissociation inhibitors (GDIs). Both GDIs and G-protein-uncoupling agents share the capacity to convert high-affinity agonist sites into low-affinity agonist sites. BIM has been reported to interdict function of $G\alpha\beta\gamma$ heterotrimers (Prévost et al., 2006; Ayoub et al., 2009). Inhibition of heterotrimer signaling can only be achieved with molecules that preclude nucleotide exchange. Because BIM does not compromise high-affinity agonist binding, it must, consequently, permit GDP exit and occurrence of the nucleotide-free, empty pocket transition state of the G protein. Therefore, lack of perturbance of high-affinity agonist binding by BIM can only be rationalized if BIM interfered with GTP entry. Such a mechanism would be entirely consistent with the ability of BIM to permit [^{3}H]GDP dissociation from purified $G\alpha_q$ proteins (Figure 7D). It also explains why BIM enhances carbachol binding to muscarinic M1 receptors in intact cells (Figure 7A), because a GTP entry inhibitor likely prolongs the lifetime of active-state complexes. This mechanism also rationalizes why BIM is incompetent to completely prevent opening of the nucleotide binding pocket of activated $G\alpha_q$-$\beta\gamma$ proteins (Figure 3H) in our BRET assay. In this experimental setup, $G\alpha_q$-*R*Luc is coexpressed with $G\gamma_2$-GFP[10] and responds with negative BRET on agonist stimulation of a $G\alpha_q$-sensitive GPCR. This BRET decrease is indicative of the separation of the $G\alpha$-helical domain from the N terminus of $G\gamma$ and reliably reflects opening of the nucleotide binding pocket, thereby creating the route for GDP exit and GTP entry (Galés et al., 2006; Saulière et al., 2012). In the presence of receptor antagonists, agonist-mediated BRET decrease can be entirely prevented (Galés et al., 2006; Saulière et al., 2012). Inhibitors of G protein function that act as GDIs, such as pertussis toxin, also completely abolish agonist-mediated BRET in this experimental setting (Galés et al., 2006). BIM, in contrast, significantly diminishes negative BRET in response to agonist stimulation but does not completely abolish opening of the nucleotide binding pocket of $G\alpha_q$. We infer from these BRET data (Figure 3H)—in conjunction with our radioligand binding, docking, and MD simulations, as well as in vitro GDP dissociation studies (Figure 7)—that BIM interdicts $G\alpha\beta\gamma$ heterotrimer function by permitting GDP escape but preventing GTP entry. Thus, BIM can be classified as a $G\alpha_q$-specific GTP entry inhibitor that traps $G\alpha_q$ in the empty pocket conformation, thereby blocking receptor-catalyzed activation of the $G\alpha\beta\gamma$ heterotrimer, a mechanism of action not yet assigned to any other small molecule $G\alpha$ inhibitor to date.

SIGNIFICANCE

Exchange of GDP for GTP on the $G\alpha$ subunit is the key step toward G protein activation and initiation of downstream signaling. Structural, biochemical, and biophysical studies on active and inactive conformations of heterotrimeric G proteins have led to the recognition that $G\alpha$ subunits are endowed with numerous clefts amenable for small molecule targeting. However, few $G\alpha$ inhibitors with activities in cellular systems are available to date. Our study is significant for two reasons: first, we show that two small molecules, BIM-46174 and BIM-46187, previously classified as pan-G protein inhibitors, preferably silence $G\alpha_q$ signaling depending on the cellular background. Although the mechanistic basis underlying these disparate, cell-type-dependent G protein inhibition profiles are not clear, BIM molecules may be exploited as lead structures for generation of $G\alpha$ protein subfamily selective probes, which would be highly desired to understand the contribution of G protein signaling in physiology and disease. Our study also provides a rationale for the development of small molecule probes interrogating $G\alpha_q$'s molecular and physiological functions and its potential as a therapeutic target.

Second, and more significantly, this study proves that cell-permeable inhibitors for $G\alpha$ proteins may be developed that "freeze" $G\alpha$ in its empty pocket conformation, an intermediate conformation along the activation pathway. Such inhibitors enrich the mechanistic portfolio of $G\alpha$ modulators and

may constitute important molecules for cocrystallization with Gα to provide deeper insight into the nucleotide-free conformation of Gα proteins. This knowledge will help to refine our picture on the complex series of conformational transitions from agonist binding to G protein activation—events that underlie a host of cellular responses in hormone and neurotransmitter signaling and, therefore, rank among the most fundamental issues in signal transduction.

EXPERIMENTAL PROCEDURES

Cell Culture

HEK293 and COS7 cells were maintained in high glucose Dulbecco's modified Eagle's medium (DMEM) supplemented with 10% (v/v) fetal bovine serum and 1% penicillin/streptomycin mixture at 37°C and 5% CO_2 in a humidified atmosphere. For culture of human CRTH2-HEK cells, 0.4 mg/ml G418 (InvivoGen) was added to the medium. Stable human free fatty acid receptor 3 (FFA3) Flp-In T-REx and human free fatty acid receptor 2 (FFA2) Flp-In T-REx cells were cultured in DMEM supplemented with 10% fetal calf serum (FCS), 1% penicillin/streptomycin mixture, 15 μg/ml blasticidin, and 100 μg/ml hygromycin B. Expression from the Flp-In locus was induced by treatment with 1 μg/ml doxycycline for 16–18 hr. HEK293 cells stably coexpressing the human 5-oxo-eicosatetraenoic acid receptor (OXE-R) and the promiscuous $G\alpha_{16}$ protein (HEK-OXER-$G\alpha_{16}$ cells) were maintained in DMEM supplemented with 10% FCS, 1% penicillin/streptomycin mixture, 0.25 mg/ml hygromycin B, and 0.4 mg/ml G418.

CHO-K1 cells were cultured in Ham's nutrient mixture F-12 GlutaMAX supplemented with 10% (v/v) FCS and 1% penicillin/streptomycin mixture. CHO-M1 cells were maintained in the same medium additionally supplemented with 0.2 mg/ml G418.

The autologous human melanoma cell line MZ7-MEL was established from a splenic melanoma metastasis in 1988. Cells were cultured in complete RPMI 1640 medium supplemented with 10% FCS (Biochrome), 2 mM L-glutamine (GIBCO), 10 mM nonessential amino acids (GIBCO), 1 mM HEPES (GIBCO), 20 μM 2-mercaptoethanol, 100 IU/ml penicillin, and 100 μg/ml streptomycin (Invitrogen).

Transfection

For gene dosing experiments, the calcium phosphate DNA precipitation method was used as described elsewhere (Kostenis et al., 2005). Assays were performed 48 hr after transfection.

Second Messenger cAMP and IP1 Accumulation Assays

Changes of the intracellular second messengers cAMP and IP1 were quantified with the HTRF-cAMP dynamic kit and the HTRF-IP1 kit, respectively (CisBio International), on a Mithras LB 940 reader (Berthold Technologies) according to the manufacturer's instructions and as described elsewhere in detail (Schröder et al., 2009; Schmidt et al., 2011). If BIM or its solvent were present during the assay, it was preincubated for 2 hr at 37°C.

Crystal Violet Staining

Human melanoma cell line MZ7-MEL was seeded into 96-well plates (2×10^4 per well) in complete RPMI medium. BIM was added to the cells in various concentrations (0.1, 0.3, 1, 3. and 10 μM) along with its vehicle. After 72 hr, cells were washed with PBS and fixed with 4% paraformaldehyde for 5 min. Afterward, cells were stained with 0.05% crystal violet dye for 30 min, rinsed twice with tap water, and thoroughly dried. Staining intensity was measured using the Li-Cor Odysee SA imaging system. Values are expressed as percentage staining intensity ± SEM relative to control.

Colorimetric XTT Assay

Human melanoma cell line MZ7-MEL was seeded into 96-well plates (2×10^4 per well). Solvent control, BIM (0.1, 1, 10 and 100 μM), or the cell cycle inhibitor aphidicolin (1 μg/ml) were added in various concentrations to the cells. After 72 hr, cell viability was measured using the XTT-based Cell Proliferation Kit II (Roche) according to the manufacturer's protocols. Absorption was measured at 405 nm using an ELISA-Reader. Results are expressed as percentage metabolic activity ± SEM relative to control.

Western Blot

Protein lysates were prepared from native HEK293 and MZ7-MEL cells as well as HEK293 cells transfected with different amounts of hemagglutinin (HA)-tagged $G\alpha_q$ protein. Samples (10 or 20 μg of protein) were dissolved in SDS-PAGE sample buffer, heated at 70°C for 10 min, fractionated on 10% acrylamide gels, and electrically transferred to nitrocellulose membranes. Membranes were blocked with Roti Block (Carl Roth) and then incubated in primary antibody solution: anti-HA (#11583816001, Roche); anti-β-tubulin (#3708-100, BioVision); anti-$G\alpha_{q/11}$ (sc-392), anti-$G\alpha_s$ (sc-823), and anti-$G\alpha_{i3}$ (sc-262, all from Santa Cruz Biotechnology). Bound antibodies were detected with an anti-rabbit horseradish-peroxidase-conjugated secondary antibody (ABIN 102010, antibodies-online), visualized by ECL Prime Western blotting reagent (RPN2232, Amersham), and quantified by densitometry (GelScan V6.0 Software).

Single Cell $[Ca^{2+}]_i$ Imaging

MZ7-MEL tumor cells were incubated for 2 hr with BIM (100 μM) or its solvent DMSO (1:500) in RPMI medium (20% FCS) at 37°C, and mobilization of $[Ca^{2+}]_i$ was monitored as outlined in detail in Supplemental Experimental Procedures.

BRET

G protein activation was quantified in HEK293 cells transiently transfected to express GPR55, $G\alpha_{13}$-106*R*Luc8 (human muscarinic receptor M3 and $G\alpha_q$-97*R*Luc8 for $G\alpha_q$ pathway), $G\gamma_2$-GFP[10], and unlabeled $G\beta_1$. Assays were performed 48 hr after transfection. Cells were detached and resuspended in Hank's balanced salt solution with 20 mM HEPES at a density of 1.06×10^6 cells per ml. A volume of 170 μl cell suspension was seeded in 96-well microplates and incubated with BIM or buffer for 2 hr. After agonist addition, cells were incubated for 2 min (1 min for carbachol). G protein activation was measured after the addition of *R*Luc substrate DeepBlueC coelenterazine (Gold Biotechnology). To detect BRET, light emission at 400 and 515 nm was measured sequentially using a Mithras LB 940 instrument. The BRET signal (milliBRET ratio) was determined by calculating the ratio of the light emitted by the fluorescence acceptor GFP[10] (515 nm) and the light emitted by *R*luc (400 nm).

Other Methods

For synthesis of BIM-monomer and -dimer, remaining experimental procedures, and a more detailed description of the aforementioned procedures, see the Supplemental Information.

Data Analysis

Results are expressed as mean values ± SEM and were analyzed using GraphPad Prism 5.04 (Graph Pad). Half maximal effective concentration (EC_{50}) values were determined by nonlinear regression, and comparison between two experimental groups was based on a two-tailed Student t test. The p values were considered as significant (*$p < 0.05$), very significant (**$p < 0.01$), and extremely significant (***$p < 0.001$).

SUPPLEMENTAL INFORMATION

Supplemental Information includes Supplemental Experimental Procedures, eight figures, and three tables and can be found with this article online at http://dx.doi.org/10.1016/j.chembiol.2014.06.003.

ACKNOWLEDGMENTS

We are grateful to Nina Heycke for expert technical assistance. This work was supported by the Danish Council for Independent Research, Technology and Production (grant 09-070364 to E.K.), by Deutsche Forschungsgemeinschaft (DFG) Research Unit 926 (Project SP8 to D.W. and B.K.F.), and by a junior research group of the State of North Rhine Westphalia (D.W.). K.B. is a member of the DFG-funded Research Training Group RTG 1873.

Received: March 4, 2014
Revised: June 4, 2014
Accepted: June 9, 2014
Published: July 17, 2014

REFERENCES

Ahmed-Belkacem, A., Pozza, A., Muñoz-Martínez, F., Bates, S.E., Castanys, S., Gamarro, F., Di Pietro, A., and Pérez-Victoria, J.M. (2005). Flavonoid structure-activity studies identify 6-prenylchrysin and tectochrysin as potent and specific inhibitors of breast cancer resistance protein ABCG2. Cancer Res. *65*, 4852–4860.

Ashkenazi, A., Ramachandran, J., and Capon, D.J. (1989). Acetylcholine analogue stimulates DNA synthesis in brain-derived cells via specific muscarinic receptor subtypes. Nature *340*, 146–150.

Ayoub, M.A., Damian, M., Gespach, C., Ferrandis, E., Lavergne, O., De Wever, O., Banères, J.-L., Pin, J.-P., and Prévost, G.P. (2009). Inhibition of heterotrimeric G protein signaling by a small molecule acting on Galpha subunit. J. Biol. Chem. *284*, 29136–29145.

Bonacci, T.M., Mathews, J.L., Yuan, C., Lehmann, D.M., Malik, S., Wu, D., Font, J.L., Bidlack, J.M., and Smrcka, A.V. (2006). Differential targeting of Gbetagamma-subunit signaling with small molecules. Science *312*, 443–446.

Chidiac, P., Markin, V.S., and Ross, E.M. (1999). Kinetic control of guanine nucleotide binding to soluble Galpha(q). Biochem. Pharmacol. *58*, 39–48.

De Lean, A., Stadel, J.M., and Lefkowitz, R.J. (1980). A ternary complex model explains the agonist-specific binding properties of the adenylate cyclase-coupled beta-adrenergic receptor. J. Biol. Chem. *255*, 7108–7117.

Galés, C., Van Durm, J.J.J., Schaak, S., Pontier, S., Percherancier, Y., Audet, M., Paris, H., and Bouvier, M. (2006). Probing the activation-promoted structural rearrangements in preassembled receptor-G protein complexes. Nat. Struct. Mol. Biol. *13*, 778–786.

Hohenegger, M., Waldhoer, M., Beindl, W., Böing, B., Kreimeyer, A., Nickel, P., Nanoff, C., and Freissmuth, M. (1998). Gsalpha-selective G protein antagonists. Proc. Natl. Acad. Sci. USA *95*, 346–351.

Itoh, Y., Kawamata, Y., Harada, M., Kobayashi, M., Fujii, R., Fukusumi, S., Ogi, K., Hosoya, M., Tanaka, Y., Uejima, H., et al. (2003). Free fatty acids regulate insulin secretion from pancreatic beta cells through GPR40. Nature *422*, 173–176.

Johnston, C.A., and Siderovski, D.P. (2007). Receptor-mediated activation of heterotrimeric G-proteins: current structural insights. Mol. Pharmacol. *72*, 219–230.

Johnston, C.A., Willard, F.S., Ramer, J.K., Blaesius, R., Roques, C.N., and Siderovski, D.P. (2008). State-selective binding peptides for heterotrimeric G-protein subunits: novel tools for investigating G-protein signaling dynamics. Comb. Chem. High Throughput Screen. *11*, 370–381.

Jones, J.C., Jones, A.M., Temple, B.R.S., and Dohlman, H.G. (2012). Differences in intradomain and interdomain motion confer distinct activation properties to structurally similar Gα proteins. Proc. Natl. Acad. Sci. USA *109*, 7275–7279.

Kenakin, T., and Christopoulos, A. (2013). Signalling bias in new drug discovery: detection, quantification and therapeutic impact. Nat. Rev. Drug Discov. *12*, 205–216.

Kimple, A.J., Bosch, D.E., Giguère, P.M., and Siderovski, D.P. (2011). Regulators of G-protein signaling and their Gα substrates: promises and challenges in their use as drug discovery targets. Pharmacol. Rev. *63*, 728–749.

Kostenis, E., Martini, L., Ellis, J., Waldhoer, M., Heydorn, A., Rosenkilde, M.M., Norregaard, P.K., Jorgensen, R., Whistler, J.L., and Milligan, G. (2005). A highly conserved glycine within linker I and the extreme C terminus of G protein alpha subunits interact cooperatively in switching G protein-coupled receptor-to-effector specificity. J. Pharmacol. Exp. Ther. *313*, 78–87.

Leyers, S., Häcker, H.-G., Wiendlocha, J., Gütschow, M., and Wiese, M. (2008). A 4-aminobenzoic acid derivative as novel lead for selective inhibitors of multidrug resistance-associated proteins. Bioorg. Med. Chem. Lett. *18*, 4761–4763.

Mangmool, S., and Kurose, H. (2011). G(i/o) protein-dependent and -independent actions of Pertussis Toxin (PTX). Toxins (Basel) *3*, 884–899.

Milligan, G., and Kostenis, E. (2006). Heterotrimeric G-proteins: a short history. Br. J. Pharmacol. *147* (*Suppl. 1*), S46–S55.

Neves, S.R., Ram, P.T., and Iyengar, R. (2002). G protein pathways. Science *296*, 1636–1639.

Nishimura, A., Kitano, K., Takasaki, J., Taniguchi, M., Mizuno, N., Tago, K., Hakoshima, T., and Itoh, H. (2010). Structural basis for the specific inhibition of heterotrimeric Gq protein by a small molecule. Proc. Natl. Acad. Sci. USA *107*, 13666–13671.

Oldham, W.M., and Hamm, H.E. (2008). Heterotrimeric G protein activation by G-protein-coupled receptors. Nat. Rev. Mol. Cell Biol. *9*, 60–71.

Prévost, G.P., Lonchampt, M.O., Holbeck, S., Attoub, S., Zaharevitz, D., Alley, M., Wright, J., Brezak, M.C., Coulomb, H., Savola, A., et al. (2006). Anticancer activity of BIM-46174, a new inhibitor of the heterotrimeric Galpha/Gbetagamma protein complex. Cancer Res. *66*, 9227–9234.

Rask-Andersen, M., Almén, M.S., and Schiöth, H.B. (2011). Trends in the exploitation of novel drug targets. Nat. Rev. Drug Discov. *10*, 579–590.

Rodbell, M., Krans, H.M., Pohl, S.L., and Birnbaumer, L. (1971). The glucagon-sensitive adenyl cyclase system in plasma membranes of rat liver. IV. Effects of guanylnucleotides on binding of 125I-glucagon. J. Biol. Chem. *246*, 1872–1876.

Saulière, A., Bellot, M., Paris, H., Denis, C., Finana, F., Hansen, J.T., Altié, M.-F., Seguelas, M.-H., Pathak, A., Hansen, J.L., et al. (2012). Deciphering biased-agonism complexity reveals a new active AT1 receptor entity. Nat. Chem. Biol. *8*, 622–630.

Schmidt, J., Smith, N.J., Christiansen, E., Tikhonova, I.G., Grundmann, M., Hudson, B.D., Ward, R.J., Drewke, C., Milligan, G., Kostenis, E., and Ulven, T. (2011). Selective orthosteric free fatty acid receptor 2 (FFA2) agonists: identification of the structural and chemical requirements for selective activation of FFA2 versus FFA3. J. Biol. Chem. *286*, 10628–10640.

Schröder, R., Merten, N., Mathiesen, J.M., Martini, L., Kruljac-Letunic, A., Krop, F., Blaukat, A., Fang, Y., Tran, E., Ulven, T., et al. (2009). The C-terminal tail of CRTH2 is a key molecular determinant that constrains Galphai and downstream signaling cascade activation. J. Biol. Chem. *284*, 1324–1336.

Seifert, R., Gether, U., Wenzel-Seifert, K., and Kobilka, B.K. (1999). Effects of guanine, inosine, and xanthine nucleotides on beta(2)-adrenergic receptor/G(s) interactions: evidence for multiple receptor conformations. Mol. Pharmacol. *56*, 348–358.

Smrcka, A.V. (2013). Molecular targeting of Gα and Gβγ subunits: a potential approach for cancer therapeutics. Trends Pharmacol. Sci. *34*, 290–298.

Takasaki, J., Saito, T., Taniguchi, M., Kawasaki, T., Moritani, Y., Hayashi, K., and Kobori, M. (2004). A novel Galphaq/11-selective inhibitor. J. Biol. Chem. *279*, 47438–47445.

Wall, M.A., Posner, B.A., and Sprang, S.R. (1998). Structural basis of activity and subunit recognition in G protein heterotrimers. Structure *6*, 1169–1183.

West, R.E., Jr., Moss, J., Vaughan, M., Liu, T., and Liu, T.Y. (1985). Pertussis toxin-catalyzed ADP-ribosylation of transducin. Cysteine 347 is the ADP-ribose acceptor site. J. Biol. Chem. *260*, 14428–14430.

Wong, Y.H., Federman, A., Pace, A.M., Zachary, I., Evans, T., Pouysségur, J., and Bourne, H.R. (1991). Mutant alpha subunits of Gi2 inhibit cyclic AMP accumulation. Nature *351*, 63–65.

Wortelboer, H.M., Usta, M., van der Velde, A.E., Boersma, M.G., Spenkelink, B., van Zanden, J.J., Rietjens, I.M.C.M., van Bladeren, P.J., and Cnubben, N.H.P. (2003). Interplay between MRP inhibition and metabolism of MRP inhibitors: the case of curcumin. Chem. Res. Toxicol. *16*, 1642–1651.

Epilogue

In this publication, BIM was characterized and suggested to reconsider the mode-of-action from a pan G protein inhibitor to a cell background-dependent $G\alpha_q$-selective inhibitor. We could further reveal a to-date unprecedented mechanism of G protein inhibition. Thus, BIM-46174 is the first member of the new class of GTP entry inhibitors. It stabilizes the empty pocket conformation of the G protein that occurs when GDP exits its binding site and the G protein changes shape into an intermediary state before GTP enters the protein[1]. In contrast to the selective $G\alpha_q$-inhibitor YM-254890 or the selective $G\alpha_s$-inhibitor suramin, which function as guanine nucleotide dissociation inhibitors (GDI)[2–4], BIM-46174 does not exclude GDP exit, nor does it preclude coupling between the G protein and its GPCR as PTX does[5,6]. BIM-46174 freezes the state between GDP exit and GTP entry, thus allowing for the occurrence of high affinity states between the GPCR and its cognate G protein. The exact mechanism how BIM-46174 interacts with the G protein remains concealed, although two cysteine residues within the Gα subunit for a covalent modification by the inhibitor were identified but the possibility for a noncovalent interaction could not be ruled out.

As GPCRs play a role in virtually every process in humans it is not an unexpected finding that GPCRs are also involved in many cancer types[7,8]. Likewise G proteins are involved in many cancers, especially mutated forms of Gα subunits are reported to be associated with certain forms of cancer[9,10]. Importantly, some mutations lead to constitutive G protein activity by preventing GTP hydrolysis whereas others show high basal levels of GDP/GTP exchange[11,12]. Cancer cells overexpressing those latter types of mutated G proteins would be sensitive to treatment with GDP exit inhibitors or GTP entry inhibitors, such as BIM-46174. GTPase deficient mutants of G proteins, however, would be resistant to pharmacological intervention with either type of G protein inhibitor once the G protein is in the active state (i.e. the GTP-bound state).

There are also concerns about a pharmacological anti-cancer strategy that targets ubiquitously expressed proteins, which are moreover involved in a huge amount of biological processes. Considerable fear exists about severe side effects of such treatments but those might be outweighed by the beneficial anti-cancer effects and would not be a backward step in synopsis with the majority of currently used anti-cancer medicines that share these disadvantages[3]. Another effort to circumvent systemic side effects would be a locally limited use, which is *a priori* restricted to stationary types of cancer. While there has already been promising results from personalized treatments of cancer types, which are characterized by specific mutations in certain key signaling regulators, there is indubitably hope to be able to inhibit disease-relevant mutant forms of G proteins. In turn, this implies a feasible way to selectively target those proteins while simultaneously ignoring proper G protein function. Beside the here discussed Gα subunit inhibition, selective βγ

subunit inhibition could be a suitable practice, since signaling of the Gα subunit, which is independent of the βγ subunit, would be preserved[3].

In this publication, a new mechanism of G protein inhibition was presented. BIM-46174 expands the repertoire of signal transduction modulating tool compounds. In the future this toolbox could help to further investigate G protein inhibition for $G\alpha_s$ and $G\alpha_{12/13}$ mediated pathways, which to date cannot be inhibited in a biologically relevant way. Together with true pan G protein inhibitors these tools would provide an important means to study G protein-independent signaling, which is frequently discussed and associated with β-arrestin signaling, although it has never been corroborated because to date no pan G protein inhibitor exists. Workarounds such as overstimulation of all G proteins with aluminiumfluoride or mastoparan are not suited to authentically reflect inhibited G protein signaling. In conclusion, the discovery of true G protein inhibitors with potentially new mechanisms is highly desirable.

References

1. Abdulaev, N. G. *et al.* The receptor-bound "empty pocket" state of the heterotrimeric G-protein alpha-subunit is conformationally dynamic, *Biochemistry* **45,** 12986–12997 (2006).
2. Hohenegger, M. *et al.* Gsalpha-selective G protein antagonists, *Proc. Natl. Acad. Sci. U.S.A.* **95,** 346–351 (1998).
3. Smrcka, A. V. Molecular targeting of Gα and Gβγ subunits: a potential approach for cancer therapeutics, *Trends Pharmacol. Sci.* **34,** 290–298 (2013).
4. Nishimura, A. *et al.* Structural basis for the specific inhibition of heterotrimeric Gq protein by a small molecule, *Proc. Natl. Acad. Sci. U.S.A.* **107,** 13666–13671 (2010).
5. Galés, C. *et al.* Probing the activation-promoted structural rearrangements in preassembled receptor-G protein complexes, *Nat. Struct. Mol. Biol.* **13,** 778–786 (2006).
6. West, R. E. Moss, J. Vaughan, M. Liu, T. & Liu, T. Y. Pertussis toxin-catalyzed ADP-ribosylation of transducin. Cysteine 347 is the ADP-ribose acceptor site, *J. Biol. Chem.* **260,** 14428–14430 (1985).
7. Lappano, R. & Maggiolini, M. G protein-coupled receptors: novel targets for drug discovery in cancer, *Nat Rev Drug Discov* **10,** 47–60 (2011).
8. Dorsam, R. T. & Gutkind, J. S. G-protein-coupled receptors and cancer, *Nat. Rev. Cancer* **7,** 79–94 (2007).
9. Cárdenas-Navia, L. I. *et al.* Novel somatic mutations in heterotrimeric G proteins in melanoma, *Cancer Biology & Therapy* **10,** 33–37 (2014).
10. O'Hayre, M. *et al.* The emerging mutational landscape of G proteins and G-protein-coupled receptors in cancer, *Nat. Rev. Cancer* **13,** 412–424 (2013).
11. Landis, C. A. *et al.* GTPase inhibiting mutations activate the alpha chain of Gs and stimulate adenylyl cyclase in human pituitary tumours, *Nature* **340,** 692–696 (1989).

12. Majumdar, S. Ramachandran, S. & Cerione, R. A. Perturbing the linker regions of the alpha-subunit of transducin: a new class of constitutively active GTP-binding proteins, *J. Biol. Chem.* **279,** 40137–40145 (2004).

Conclusion

Knowledge about the function and dysfunction of cellular signal transduction is at the very heart of biomedical research since every physiological and pathophysiological process is intimately associated with functional or defective signaling, respectively. The advent of innovative methodological techniques paved the way for major breakthroughs in deciphering cell signaling in the life sciences. Granting this, it is not technology *per se* but proactive adjustment and attentive implementation of the various methodological approaches that lay the foundation for rewarding research efforts. It is becoming increasingly clear that data obtained from a single assay readout are generally insufficient to mirror the multidimensionality of biological signaling networks. Thus, it was an aim of this thesis by synopsis of different technological, biochemical and pharmacological approaches to provide new insights into the anatomy of signaling events.

G protein-coupled receptors (GPCRs) do not only represent the largest group of drug targets but are also prototype microprocessing units in the cellular signaling machinery and therefore ideally suited to study the biology of signal transduction. This class of receptors represents a cornucopia of signaling diversity since a plethora of signal transduction concepts are mirrored herein. Hence, GPCRs are supremely favored research objects and examined in the majority of the publications communicated in this thesis.

Section I explained the principle of dynamic mass redistribution (DMR). The optical biosensor-based technique allows the detection of cellular events as an integrated whole-cell readout and its label-free nature is capable to reflect signaling events in a non-invasive fashion without using any interfering labels. A set of different cellular backgrounds was used to demonstrate the versatility and applicability of the assay. The integration of recombinant, native and primary cells highlighted the potential of this technique to glean *in vivo* relevant biological information about investigated substances already in early stages of the drug discovery process. Since DMR provides unbiased insights into cell activation, the testimony of multiple concurrent pathways triggered by a stimulus is accessible and helps to understand the underlying biology. The first chapter described the possibility to untangle the GPCR signaling repertoire by means of selective pathway modulators and explained why the real time measuring mode allows the exploration of kinetic aspects in the cell response.

Chapter 2 opens section II of this thesis, in which the biology of the G protein-coupled free fatty acid receptor FFA2 is detailed. With a multifaceted approach exploiting the advantages of holistic label-free readouts, it was possible to uncover an unprecedented mode-of-action of a GPCR modulating ligand. 4-CMTB previously classified as positive allosteric modulator and allosteric agonist (ago-PAM) at the FFA2 receptor was disclosed as the first *sequentially activating ligand (SEAL)* reported so far.

This ligand binds and activates a first recognition site of the receptor before it is also recognized by a further receptor site, where a second signaling impulse is generated. Thus, the association of multiple binding events with multiple signaling events therein is a key difference between *SEALs* and classical *bitopic ligands* that simultaneously bind the receptor. In the concept of *SEALs*, GPCRs could function as transceivers that de- and encode the information in an adjustable manner by extending the possibility to encrypt biological information by a temporal dimension.

Correlating certain signaling events and the resulting phenotype rationally within a complex biological environment remains a prime challenge in signal transduction research. The invention of designer receptors bettered the prospects to approach this question. By isolating a certain receptor signaling behavior and introduce this signaling machinery into an *in vivo* context, scientists might be able to assess the relevance of a certain activation pattern for the individual phenotype. Chapter 3 reports on a strategy how to design and generate a designer FFA2 receptor on a rational basis. A receptor form activated solely by a synthetic ligand (RASSL) of FFA2 was designed based on species differences in agonist selectivity between the human and bovine FFA2 receptor and consequently did not respond to the endogenous short-chain fatty acid ligands anymore but was selectively activated by stimulation with sorbic acid. Future studies involving designer receptors can help elucidating the *in vivo* role of the FFA2 receptor, since the ubiquitous availability of fatty acids in the body and overlap in ligand recognition as well as in the expression patterns of FFA2 and FFA3 challenged a clear definition of FFA2-mediated phenotypes so far.

Section III deals with the human G protein-coupled free fatty acid receptor FFA1 and begins with Chapter 4 that presents a study that investigated the interplay between FFA1 and non-esterified fatty acids (NEFAs) in a diabetes type 2 (TD2) disease context. The deleterious effects of NEFAs on pancreatic β-cell function and survival were claimed to be dependent of FFA1 activation by previous reports. In the present study, however, the activation of FFA1 with a selective small molecule agonist proved even beneficial, while antagonists deteriorated β-cell health, a finding that is also corroborated by other studies. Furthermore, a single nuclear polymorphisms (SNP) in the gene of the FFA1 was identified to modulate the sensitivity against (gluco)lipotoxic effects of fasting levels of non-esterified fatty acids (NEFA) in humans confirming a modulatory role of FFA1 in the pathophysiology of TD2. The second publication in chapter 4 focused on a methodological issue and notes the importance to diligently validate the experimental tools used to determine localization and amount of protein expression, a prerequisite of reliable data acquisition. In doing so, several inconsistent results in the literature of FFA1 receptor biology must be questioned.

In Chapter 5, the chemistry and optimization of synthetic FFA1 ligands is presented. Because of the aim to develop highly selective and potent FFA1 agonists, the unbiased DMR assay proved valuable

to interrogate potential off-target effects of the investigated compounds, as well as confirmed their competence to activate the receptor with appropriate potency and efficacy. The three publications within this chapter present different chemical strategies to tailor the structures for their employment as pharmacologically validated substances. The availability of those ligands is indispensable to study receptor biology and was thus a prerequisite to conduct biological research as depicted in the other chapters.

In the last part of the thesis, section IV, two chapters describe the analysis of signal transduction at a *post*-receptor level. Chapter 6 provides further evidence for a bona fide *second messenger* role of the non-canonical cyclic nucleotides cCMP and cUMP by delineating the biological effectors. The label-free DMR assay disclosed cNMP target proteins and shed light into the signal transduction network of cNMPs in human cells, thereby emphasizing the applicability of this technique that is not restricted to the analysis of signal transduction generated from cell surface receptors but also at the *post*-receptor level. Chapter 7, finally, characterized and defined the mode-of-action of a previously published pan-G protein inhibitor (BIM-46187). By stabilizing the empty-pocket conformation of Gα subunits BIM46187 is the first reported GTP entry inhibitor and was furthermore redefined as a compound that selectively targets $G\alpha_q$ proteins in a cell-type dependent manner.

In conclusion, this thesis comprises several studies covering multiple aspects of cellular signal transduction providing a range from biological-pharmacological, technological and chemical perspectives on the subject. The bulk of the publications deals with the analysis of GPCR biology, especially the exploration of the free fatty acid receptors FFA1 and FFA2. A technology-centered, conceptual section and a section analyzing signal transduction at the *post*-receptor level complement the overall focus on receptor biology.

Publications

Research articles and reviews

1. Christiansen E, Watterson KR, Stocker CJ, Sokol E, Jenkins L, Simon K, **Grundmann M**, Petersen RK, Wargent ET, Hudson BD, Kostenis E, Ejsing CS, Cawthorne MA, Milligan G, Ulven T. Activity of dietary fatty acids on FFA1 and FFA4 and characterisation of pinolenic acid as a dual FFA1/FFA4 agonist with potential effect against metabolic diseases. Br J Nutr. 2015 Jun;113(11):1677-88
2. **Grundmann M**, Kostenis E. Label-free biosensor assays in GPCR screening. Methods Mol Biol 2015;1272:199-213
3. Beckert U, **Grundmann M**, Wolter S, Schwede F, Rehmann H, Kaever V, Kostenis E, Seifert R. cNMP-AMs mimic and dissect bacterial nucleotidyl cyclase toxin effects. Biochem Biophys Res Commun. 2014 Sep 5;451(4):497-502
4. Schmitz AL, Schrage R, Gaffal E, Charpentier TH, Wiest J, Hiltensperger G, Morschel J, Hennen S, Häußler D, Horn V, Wenzel D, **Grundmann M**, Büllesbach KM, Schröder R, Brewitz HH, Schmidt J, Gomeza J, Galés C, Fleischmann BK, Tüting T, Imhof D, Tietze D, Gütschow M, Holzgrabe U, Sondek J, Harden TK, Mohr K, Kostenis E. A cell-permeable inhibitor to trap Gαq proteins in the empty pocket conformation. Chem Biol. 2014 Jul 17;21(7):890-902.
5. Teutsch CA, Panse M, **Grundmann M**, Kaiser G, Kostenis E, Häring HU, Ullrich S. Detection of free fatty acid receptor 1 expression: the critical role of negative and positive controls. Diabetologia 2014 Apr;57(4):776-80
6. Christiansen E, Hansen SV, Urban C, Hudson BD, Wargent ET, **Grundmann M**, Jenkins L, Zaibi M, Stocker CJ, Ullrich S, Kostenis E, Kassack MU, Milligan G, Cawthorne MA, Ulven T. Discovery of TUG-770: A Highly Potent Free Fatty Acid Receptor 1 (FFA1/GPR40) Agonist for Treatment of Type 2 Diabetes. ACS Med Chem Lett. 2013 May 9;4(5):441-445.
7. Wagner R, Kaiser G, Gerst F, Christiansen E, Due-Hansen ME, **Grundmann M**, Machicao F, Peter A, Kostenis E, Ulven T, Fritsche A, Häring HU, Ullrich S. Reevaluation of fatty acid receptor 1 as a drug target for the stimulation of insulin secretion in humans. Diabetes. 2013 Jun;62(6):2106-11
8. Christiansen E, Due-Hansen ME, Urban C, **Grundmann M**, Schmidt J, Hansen SV, Hudson BD, Zaibi M, Markussen SB, Hagesaether E, Milligan G, Cawthorne MA, Kostenis E, Kassack MU, Ulven. Discovery of a potent and selective free fatty acid receptor 1 agonist with low lipophilicity and high oral bioavailability. J Med Chem. 2013 Feb 14;56(3):982-92
9. Hudson BD, Christiansen E, Tikhonova IG, **Grundmann M**, Kostenis E, Adams DR, Ulven T, Milligan G. Chemically engineering ligand selectivity at the free fatty acid receptor 2 based on pharmacological variation between species orthologs. FASEB J. 2012 Dec;26(12):4951-65
10. Christiansen E, Due-Hansen ME, Urban C, **Grundmann M**, Schröder R, Hudson BD, Milligan G, Cawthorne MA, Kostenis E, Kassack MU, Ulven T. Free fatty acid receptor 1 (FFA1/GPR40) agonists: mesylpropoxy appendage lowers lipophilicity and improves ADME properties. J Med Chem. 2012 Jul 26;55(14):6624-8

11. Schröder R, Schmidt J, Blättermann S, Peters L, Janssen N, **Grundmann M**, Seemann W, Kaufel D, Merten N, Drewke C, Gomeza J, Milligan G, Mohr K, Kostenis E. Applying label-free dynamic mass redistribution technology to frame signaling of G protein-coupled receptors noninvasively in living cells. Nat Protoc. 2011 Oct 20;6(11):1748-60

12. Christiansen E, Urban C, **Grundmann M**, Due-Hansen ME, Hagesaether E, Schmidt J, Pardo L, Ullrich S, Kostenis E, Kassack M, Ulven T. Identification of a potent and selective free fatty acid receptor 1 (FFA1/GPR40) agonist with favorable physicochemical and in vitro ADME properties. J Med Chem. 2011 Oct 13(54(19):6691-703

13. Schmidt J, Liebscher K, Merten N, **Grundmann M**, Mielenz M, Sauerwein H, Christiansen E, Due-Hansen ME, Ulven T, Ullrich S, Gomeza J, Drewke C, Kostenis E. Conjugated linoleic acids mediate insulin release through islet G protein-coupled receptor FFA1/GPR40. J Biol Chem. 2011 Apr 8;286(14):11890-4

14. Schmidt J, Smith NJ, Christiansen E, Tikhonova IG, **Grundmann M**, Hudson BD, Ward RJ, Drewke C, Milligan G, Kostenis E, Ulven T. Selective orthosteric free fatty acid receptor 2 (FFA2) agonists: identification of the structural and chemical requirements for selective activation of FFA2 versus FFA3. J Biol Chem. 2011 Mar 25;286(12):10628-40

Poster presentations and talks

- Christiansen E, Due-Hansen M.E, Urban C, **Grundmann M**, Schmidt J, Kassack M, Kostenis E, Ulven T. (2012) Discovery of potent and selective free fatty acid receptor 1 (FFA1/GPR40) agonists. *American Chemical Society´s (ACS) 243rd National Meeting*, San Diego, USA
- Ullrich S, Schmidt J, Merten N, **Grundmanm M,** Mielenz M, Sauerwein H, Christiansen E, Due-Hansen M.E, Ulven T, Gomeza J, Drewke C, Häring H.U, Kostenis E. (2011) Konjugierte Linolsäuren stimulieren die Insulinsekretion über den Fettsäurerezeptor FFA1. Jahrestagung der der Deutschen Diabetes-Gesellschaft (DDG), Leipzig, Germany, *Diabetologie und Stoffwechsel* (Supplement)
- Ullrich S, Schmidt J, Liebscher K, Merten N, **Grundmann M**, Mielenz M, Sauerwein H, Ulven T, Gomeza J, Drewke C, Kostenis E. (2011) Conjugated linoleic acids stimulate insulin secretion through G-protein coupled receptor FFA1/GPR40. *American Diabetes Association's* (ADA) 71st *Scientific Session*, San Diego, USA
- **Grundmann M**, Kostenis E. Label-free technology platforms to resolve integrated cellular signaling of 7TM receptors (2013) European Revolutionaries Global Health Summit, Bruxelles, Belgium
- **Grundmann M**, Kostenis E. Holistic assays for the analysis of cell activation by cCMP, 2nd Symposium for cCMP research, Hannover, Germany
- **Grundmann M**, Kostenis E. Discovering the Unknown – Label-free analysis of signal transduction at receptor and postreceptor level (2014), Epic User Group Meeting, Heidelberg, Germany

- Schmidt J, Schröder R, **Grundmann M**, Drewke C, Mohr K, Kostenis E. (2011) Holistic DMR recordings uncover signaling promiscuity of the free fatty acid receptor FFA1. Jahrestagung der Deutschen Gesellschaft fur Experimentelle und Klinische Pharmakologie und Toxikologie (DGPT), Frankfurt a. M., Germany, *Naunyn-Schmiedeberger's Archives of Pharmacology* 383 (Supplement 1), 46
- **Grundmann M**, Due-Hansen ME, Christiansen E, Ulven T, Ullrich S, Kostenis E. Reevaluation of fatty acid receptor 1 (FFA1/GPR40) as drug target for the stimulation of insulin secretion in humans (2013) Annual meeting of the Germany Pharmaceutical Society in Freiburg, Germany

Danksagung

Zunächst richtet sich mein besonderer Dank an Frau Prof. Dr. Evi Kostenis: Danke, für die Möglichkeit meine Doktorarbeit in deiner Arbeitsgruppe anfertigen zu können und deine Einführung in die faszinierende Welt der G-Protein gekoppelten Rezeptoren, sowie deine Sichtweise auf Wissenschaft und Forschung im Allgemeinen. Ich danke Dir für deine Bereitschaft, deine Erfahrungen auf diesem Gebiet zu teilen und die Schaffung einer besonders guten Arbeitsatmosphäre, die wesentlich zum Gelingen der Arbeit beigetragen hat. Des Weiteren möchte ich mich für dein in mich gesetztes Vertrauen und dein ständiges Engagement, wissenschaftliche Fragstellungen zu erörtern, bedanken.

Herzlich bedanken möchte ich mich auch bei Herrn Prof. Dr. Klaus Mohr für die gute Zusammenarbeit und die Übernahme des Koreferates.

Herrn Prof. Dr. Gerd Bendas und Herrn Prof. Dr. Hanns Häberlein danke ich für die Begutachtung der Arbeit und die Mitwirkung in der Prüfungskommission.

Ein besonderer Dank gilt meinen Kollegen aus dem Arbeitskreis Kostenis, die die Grundlage für das außerordentlich angenehme Arbeitsklima sind und die den Alltag mit Leben ausgefüllt haben. Ich möchte insbesondere Ulrike Rick und Seda Hild danken für die tatkräftige Unterstützung bei vielen Experimenten. Für eine tolle Zeit möchte ich Johannes Schmidt und Lucas Peters danken. Für die schönen Momente danke ich allen jetzigen und ehemaligen Mitgliedern des Arbeitskreises Kostenis: Julia Morschel, Nina Heycke, Katrin Büllesbach, Anne-Lena Schmitz, Lena Vogel, Nicole Merten, Nina-Katharina Schmitt, Katharina Simon, Jesús Gomeza, Christel Drewke, Ralf Schröder, Harald Dargatz, Philip Preis, Marianne Vasmer-Ehses, Irene Loef, Suvi Annala, Stefanie Blättermann, Stephanie Hennen, Daniel Schulz und Waltraud Läer.

Christel Drewke, Johannes Schmidt, Ralf Schröder, Stephanie Hennen und Nina-Katharina Schmitt möchte ich darüber hinaus danken für die gute Zusammenarbeit bei der Studentenbetreuung im Bio III Praktikum.

Darüber hinaus danke ich allen weiteren Angehörigen des Institutes für Pharmazeutische Biologie der Universität Bonn.

Ich möchte mich außerdem bei meinen Kooperationspartnern im In- und Ausland bedanken, ohne die zahlreiche Publikationen nicht möglich gewesen wären. Insbesondere danke ich hier Trond Ulven, Graeme Milligan, Terry Kenakin, Roland Seifert, Akos Heinemann, Susanne Ullrich und Eugen Proschak.

Meiner Frau Marie danke ich zutiefst für die Unterstützung auf allen Ebenen während meiner Promotion: für deine Geduld, Nachsicht und Zuversicht zu jedem Zeitpunkt und besonders während manchmal unübersichtlichen Zeiten.

Zum Schluss möchte ich meinen Eltern danken: für eure Liebe und Unterstützung in meinem ganzen Leben. Diese Arbeit ist euch gewidmet.